Dissertation

submitted to the

Combined Faculty of Natural Sciences and Mathematics

of the Ruperto Carola University Heidelberg, Germany

for the degree of

Doctor of Natural Sciences

presented by
Hannah Fleckenstein (M. Sc.)
born in Offenbach am Main, Germany

Oral examination: ....

Exploring decreased cytoadhesion

in asymptomatic *Plasmodium falciparum* infections

during the dry season

Referees: Prof. Dr. Michael Lanzer

Dr. Silvia Portugal

Ich erkläre hiermit, dass ich die vorliegende Doktorarbeit selbstständig unter Anleitung verfasst und keine anderen als die angegebenen Quellen und Hilfsmittel benutzt habe.

Ich erkläre hiermit, dass ich an keiner anderen Stelle ein Prüfungsverfahren beantragt bzw. die Dissertation in dieser oder anderer Form bereits anderweitig als Prüfungsarbeit verwendet oder einer anderen Fakultät als Dissertation vorgelegt habe.

Die vorliegende Arbeit wurde in der Zeit von September 2017 bis April 2021 unter Anleitung von Dr. Silvia Portugal ausgeführt

……………………………   …………………………………………….

Datum   Hannah Fleckenstein

Summary

In many malaria endemic regions *Plasmodium falciparum* is seasonally transmitted, since parasite transmission is interrupted by the absence of anopheline mosquitoes during the dry season. *P. falciparum* persists at low parasitaemia during the dry season months through mechanisms involving longer time in circulation within each replicative cycle of infected erythrocytes without adhering to the endothelium, compared to clinical cases in the wet season. Cytoadhesion of infected erythocytes is mediated by parasite ligands trafficked via de-novo formed sorting organelles (Maurer's cleft) to the surface of infected erythrocytes and anchored in knob structures. The adhesion ligands bind to endothelial cell receptors, sequestering infected erythrocytes in the vasculature and thus protecting parasites from splenic clearance.

This thesis aimed to understand the mechanisms leading to decreased cytoadhesion of infected erythrocyte, as altered formation of knobs, impaired trafficking of adhesion molecules through the host iRBC, or reduced presentation of adhesion molecules on the iRBC surface, as well as the possible contribution of the host environment. Additionally, it investigates whether, as a consequence of deceased adhesion, the longer-circulationg iRBC are at higher risk of splenic clearance. To address this, we collected infected erythrocytes from asymptomatic individuals at the end of the dry season and from individuals at their first febrile malaria episode during the transmission season. Using an artificial spleen, we found that circulating iRBCs during the dry season are more efficiently filtered in the spleen.

Erythrocyte remodeling and knob density were analyzed by transmission and scanning electron microscopy in developmental stage-matched samples from asymptomatic individuals at the end of the dry season and from individuals at their first febrile malaria episode during the transmission season. Knobs on the surface of the infected erythrocyte were detected at equal densities in both groups but with slightly smaller diameter in the dry season. Maurer's clefts were formed in the host cells in all samples, but were found more frequently in infected erythrocytes in the dry season and were localized at slightly higher distance to the erythrocyte plasma membrane. However, the differences found were small and of unknown biological significance. Further, we quantified the transcription of parasite genes involved in host cell remodeling by qRT-PCR found differential expression of three genes coding for Maurer's cleft proteins which are involved in adhesin trafficking, however possibly as a result of imperfect developmental stage matching. Hence, to

test whether low parasite adhesion during the dry season stems from decreased expression of parasite ligands on the surface of erythrocytes, we used flow cytometry to compare the binding of hyperimmune plasma to the surface of *P. falciparum*-infected erythrocytes. We did not observe different labeling efficiencies in infected erythrocytes collected from asymptomatic individuals during the dry season vs. individuals presenting with acute febrile malaria during the rainy season. On the host side, we investigated how different inflammatory states in asymptomatic and clinical malaria cases alter the availability of host adhesion receptors on endothelial cells. Compared to plasmas from clinical malaria cases, we found lower levels of endothelium-stimulating cytokines and soluble adhesion receptors in plasmas of donors in the dry season, independent of if they carried asymptomatic *P. falciparum* infection or not. We explored whether this difference in endothelial receptor expression affected cytoadhesion efficiency, but in a preliminary test we found no differences in cytoadhesion of infected erythrocytes to endothelial cells stimulated with plasmas from donors with clinical malaria in the transmission season or asymptomatic donors or healthy controls in the dry season.

In summary, the presence of only minor differences in the ultrastructure and no differential labeling by hyperimmune pooled plasma suggests that the contribution of altered host cell remodeling to decreased cytoadhesion in the dry season is only minimal. However, we have first indications that the host environment in the dry season provides less receptors for adhesion. Further, through more efficient splenic clearance of longer-circulating infected erythrocytes, parasitemias are maintained low in asymptomatic infections in the dry season, allowing *P. falciparum* to persist for several months.

Zusammenfassung

In vielen malaria-endemischen Gebieten wird der Malariaerreger *Plasmodium falciparum* saisonal übertragen, da in der Abwesenheit von *Anopheles* Mücken während der Trockenzeit die Parasitenübertragung unterbrochen ist. In dieser Zeit überdauert *P. falciparum* bei niedriger Parasitämie in seinem Wirt durch einen Mechanismus, der beinhaltet, dass infizierte Erythrozyten innerhalb jedes Replikationszyklus länger im Blut zirkulieren ohne am Endothel anzuhaften, im Vergleich zu klinischen Fällen in der Regenzeit. Die Zellanhaftung infizierter Erythrozyten wird durch Parasitenliganden vermittelt, die durch de-novo gebildete Sortierorganelle (Maurersche Spalten) hindurch an die Oberfläche infizierter Erythrozyten transportiert und dort in Knubbelstrukturen verankert werden. Sie binden an Rezeptoren auf Endothelzellen und erwirken, dass infizierte Erythrozyten sich im Gefäßsystem festsetzen und so vor einer Aussortierung in der Milz geschützt sind.

Ziel dieser Arbeit war es, die Mechanismen zu verstehen, die in der Trockenzeit zu einer verminderten Zytoadhäsion infizierter Erythrozyten führen, etwa die veränderte Bildung von Knubbeln, ein beeinträchtigter Transport von Adhäsionsliganden durch die Wirtszelle oder die verminderte Oberflächenpräsentation von Adhäsionsmolekülen auf dem infizierten Erythrozyten, sowie einen möglichen Einfluss des Milieus im Wirt. Zusätzlich wurde untersucht, ob die als Folge der verminderten Adhäsion länger zirkulierenden infizierten Erythrozyten einem höheren Risiko ausgesetzt sind in der Milz aussortiert zu werden.

Dafür sammelten wir infizierte Erythrozyten von asymptomatischen Individuen am Ende der Trockenzeit und von Individuen während ihrer ersten fiebrigen Malariaepisode in der Übertragungszeit. Mithilfe einer künstlichen Milz fanden wir heraus, dass zirkulierende infizierten Erythrozyten während der Trockenzeit effizienter in der Milz gefiltert werden. Der Umbau der Erythrozyten und die Knubbeldichte auf ihrer Oberfläche wurden durch Transmissions- und Rasterelektronenmikroskopie in Proben mit übereinstimmenden Entwicklungsstadien des Parasiten von asymptomatischen Individuen am Ende der Trockenzeit und von Individuen bei ihrer ersten fiebrigen Malariaepisode während der Übertragungszeit untersucht. Knubbel auf der Oberfläche der infizierten Erythrozyten wurden in beiden Gruppen in gleicher Dichte nachgewiesen, jedoch mit etwas kleinerem Durchmesser in Proben aus der Trockenzeit. Alle

Proben wiesen Maurersche Spalten in den Wirtszellen auf, in der Trockenzeit traten sie allerdings häufiger auf und befanden sich in etwas größerem Abstand zur Plasmamembran des Erythrozyten. Die gefundenen Unterschiede waren jedoch gering und von unbekannter biologischer Bedeutung. Desweiteren quantifizierten wir die Transkription von Parasitengenen, die am Umbau der Wirtszelle beteiligt sind, mittels qRT-PCR. Wir stellten eine veränderte Expression von drei Genen fest, die für Maurersche Spalten-assoziierte Proteine kodieren und am Transport der Adhäsionsliganden beteiligt sind. Dies könnte jedoch auch darauf zurückzuführen sein, dass die verglichenen Parasiten in ihrem Entwicklungsalter nicht ganz genau übereinstimmten. Um desweiteren zu testen, ob die geringe Zelladhäsion während der Trockenzeit auf eine verminderte Oberflächenpräsentation von Parasitenliganden auf infizierten Erythrozyten zurückzuführen ist, verglichen wir mit Hilfe der Durchflusszytometrie, wie effizient ein Hyperimmunplasmapool an die Oberfläche von *P. falciparum*-infizierten Erythrozyten binden konnte. Wir beobachteten keine unterschiedlichen Bindungseffizienzen in infizierten Erythrozyten von asymptomatischen Individuen während der Trockenzeit und Individuen mit akuter Malaria während der Regenzeit. In Bezug auf den Wirt untersuchten wir, wie unterschiedliche Entzündungszustände bei asymptomatischer und klinischer Malaria die Verfügbarkeit von Adhäsionsrezeptoren auf Endothelzellen im Wirt verändern. Im Vergleich zu Blutplasmen von klinischen Malariafällen fanden wir geringere Konzentrationen von Endothel-stimulierenden Zytokinen und löslichen Adhäsionsrezeptoren in Plasmen von Individuen in der Trockenzeit, unabhängig davon, ob sie *P. falciparum* Parasiten asymptomatisch in sich trugen oder nicht. Wir untersuchten, ob dieser Unterschied in der endothelialen Rezeptorexpression die Zytoadhäsionseffizienz beeinflusst, fanden aber in einem vorläufigen Versuch keine Unterschiede in der Anheftung von infizierten Erythrozyten an Endothelzellen, unabhängig davon, ob das Plasma für die Stimulierung aus individuen mit klinischer Malaria in der Transmissionssaison oder aus asymptomatischen oder gesunden Personen aus der Trockenzeit stammte.

Zusammenfassend lassen die geringen Unterschiede in der Ultrastruktur und die fehlenden Unterschiede in der Markierung von infizierten Erythrozyten durch den Hyperimmunplasmapool darauf schließen, dass der Beitrag eines veränderten Wirtszellumbaus zur verminderten Zytoadhäsion wahrscheinlich nur minimal ist. Allerdings fanden wir erste Hinweise darauf, dass die

die Endothelzellen im Wirt in der Trockenzeit weniger Rezeptoren für die Adhäsion bereitstellen. Zudem wird durch eine effizientere Aussortierung von länger zirkulierenden infizierten Erythrozyten in der Milz die Parasitendichten in asymptomatisches Infektionen in der Trockenzeit niedrig gehalten, und so ist es *P. falciparum* möglich für mehrere Monate zu überdauern.

Statement of contributions

Safiatou Doumbo, Didier Doumtabe, Moussa Niangaly, Hamidou Cisse, Kassoum Kayentao, Aissata Ongoiba, Boubacar Traore (University of Sciences, Techniques and Technologies of Bamako) and Peter D. Crompton (National Institutes of Health) designed, conducted and supervised field work generating the clinical data and samples.

Mario Recker (University of Exeter) performed mathematical modelling of adhesion and splenic clearance

Nikolay Sergeev contributed to electron microscopy sample acquisition and analysis.

Christina Ntalla and Silvia Portugal performed the determination of endothelial receptor expression time course upon TNF stimulation

Nathalia F. Lima contributed to RNA extraction and cDNA generation of field samples

Table of contents

1. Introduction

1.1 Malaria, a major human disease

History

Malaria has plagued humankind for a long time before its causative agent and mode of transmission were described. It was thought to be caused by bad air, ital. "mal aria", as it occurred often close to swamps. In 1880, Alphonse Laveran detected the *Plasmodium* parasite in red blood cells of patients, and in 1897 Sir Ronald Ross found mosquitoes to be transmitting the parasite in birds; in 1898, Giovanni Battista Grassi could confirm this for human malaria (reviewed in Cox 2010). More and more aspects of the life cycle of malaria have been learned since, and the development of an *in vitro* culture system for *Plasmodium falciparum* (Trager and Jensen 1976) enabled scientists around the world to study its biology in greater detail.

Epidemiology

Early efforts to reduce malaria included the drainage of swamps, straightening of rivers and improvement of housing conditions, and malaria could be eliminated in North America, Europe and parts of Asia during the Global Malaria Eradication Programme (1955 – 1968) through treatment and prophylaxis with quinine derivates and the massive use of the insecticide (dichloro-diphenyl-trichloroethane) DDT; However, in endemic regions in Subsaharan Africa, South- and Central America and South-East Asia, with increasing drug and insecticide resistance, and loss of political will, malaria rose to an estimated 238 million cases and 736 000 deaths in 2000 (Greenwood et al. 2008; World Health Organization 2020). While progress has been made since, the decline has stalled in recent years. Today, malaria is still present in 87 countries, with countries in Subsaharan Africa carrying most of the burden. In 2019, it is estimated that it caused ~229 million malaria cases worldwide, and resulted in ~409 000 deaths each year, mostly in children under 5 years old (World Health Organization 2020).

Malaria is caused by *Plasmodium* parasites

Four *Plasmodium* species circulate among humans (*P. falciparum, P. vivax, P. malariae and P. ovale*) and there are also zoonotic infections with *Plasmodia* of monkeys (*P. knowlesi, P. cynomolgi, P. brasilianum* and *P. simium*) (Imwong et al. 2019; Lalremruata et al. 2015; Brasil et

al. 2017). *Plasmodium* parasites are transmitted by the bite of infected female *Anopheles* mosquitoes. The most important *Anopheles* species for transmission within Africa are *A. gambiae, A. arabiense* and *A. funestus* (Sinka 2013). *Plasmodium* parasites are single-celled eukaryotes and belong to phylum of Apicomplexa. All Apicomplexa share a parasitic lifestyle and are characterized by the apical complex, a unique organelle used to invade host cells (Gubbels and Duraisingh 2012). Other members in this group comprise *Toxoplasma*, which can cause damage to the fetus during pregnancy or to immuno-compromised individuals, *Theileria, Babesia* and *Eimeria*, which cause disease in livestock, and *Cryptosporidium*, that leads to diarrhea.

The *Plasmodium* lifecycle
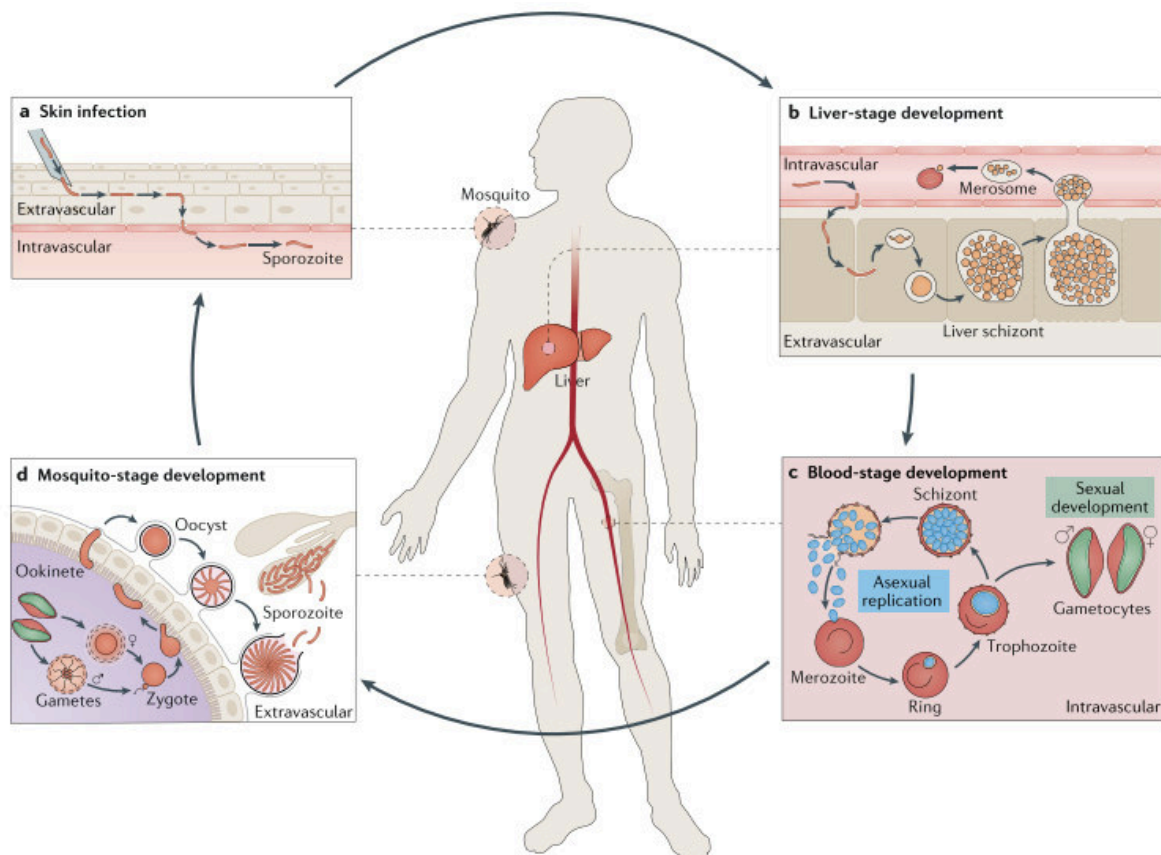
Figure 1: Life cycle of Plasmodium falciparum parasites within the human and the mosquito

Illustration of the Plasmodium life cycle in human malaria. Shown are the exo-erythrocytic stage in the skin (a) and the liver (b) as well as the intra-erythrocytic development in the blood (c) and the development within the mosquito (d). The crescent-shaped gametocytes are characteristic for *P. falciparum*. From Venugopal et al. 2020.

Plasmodium parasites have a very intricate lifecycle (Figure 1). When an infected female *Anopheles* mosquito takes a blood meal around 10-100 sporozoites, the infectious stage of *Plasmodium*, are deposited into the skin with the saliva of the mosquito (Frischknecht et al. 2004) (Figure 1a). The sporozoites then move through the skin and enter a blood vessel. With the blood stream, they travel to the liver (Figure 1b), where they cross the sinusoidal barrier through Kupffer cells or endothelial cells (Tavares et al. 2013) and transverse hepatocytes, before they develop within a hepatocyte (Mota 2001). Within 6 - 8 days in the case of *P. falciparum*, the parasite grows and forms thousands of daughter cells, the merozoites (reviewed in Prudêncio, Rodriguez, and Mota 2006). To do so, it undergoes schizogony, a form of mitosis with multiple rounds of nuclear division without cytoplasmic division. The merozoites are released into the blood stream within merozoite-filled vesicles (merosomes) (Sturm et al. 2006). Moreover, *P. vivax* and *P. ovale* can form dormant liver stages that cause relapses long after infection. During the asexual development in the blood stage (Figure 1c), merozoites rapidly invade erythrocytes, growing within a parasitophorous vacuole and forming new daughter merozoites, which are released upon rupture of the infected red blood cell (iRBC). The blood stage is also the time when the clinical symptoms of malaria appear. Depending on the species, one cycle takes ~24 h (*P. knowlesi*), ~48h (*P. falciparum*, *P. vivax* and *P. ovale*), or ~ 72 h (*P. malariae)*. Within one cycle, the parasite first forms the ring stage, followed by the trophozoite and the schizont stages, all of which show a characteristic morphology on Giemsa-stained thin blood smears (Figure 2). The hemoglobin in the RBC is digested by the parasite in a food vacuole and the toxic byproduct free heme is crystallized into hemozoin (reviewed in Goldberg 2013). In each round of replication, a small subset of merozoite commits to develop into sexual stages, the male and female gametocytes. Nutrient availability and parasite density can influence the rate of sexual commitment (Brancucci et al. 2017; Regev-Rudzki et al. 2013). While the immature stage I-IV gametocytes sequester in the bone marrow (Joice et al. 2014), mature stage V gametocytes circulate in the blood and can infect the next mosquito during a blood meal. The part of the life cycle in the mosquito again comprises several developmental stages and takes approximately 3 weeks (reviewed in Singh et al. 2021) (Figure 1d). Within the gut of the mosquito, the gametocytes develop into male microgametes and female macrogametes, and fuse to a zygote. The zygote then develops into a motile ookinete, which traverses the midgut

wall of the mosquito to form an oocyst at the outer midgut wall. Sporozoites form within the oocyst, and are then released in the hemolymph and migrate into salivary glands, ready to be transmitted during the next blood meal.
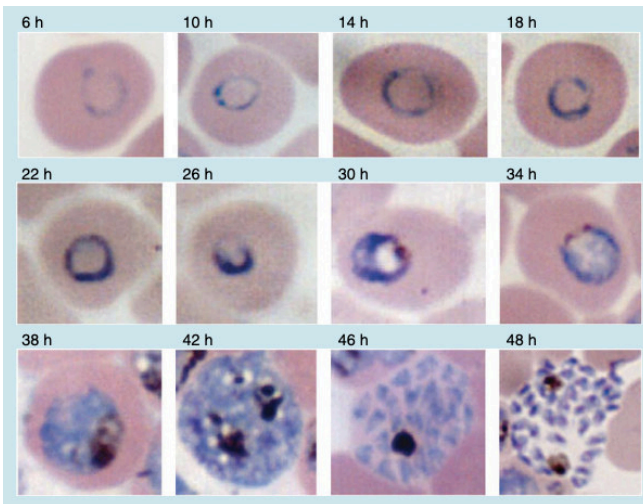
Figure 2: Giemsa-stained thin smears of P. falciparum iRBCs

P. falciparum iRBCs on Giemsa-stained thin blood smear from a synchronous culture, shown as time since invasion (h). In Giemsa staining, nuclei appear red and cytoplasm stains blue. The dark pigments in schizont stages (38 – 48 h) are hemozoin crystals. Individual merozoites are distinguishable in the segmented schizont stages (46 and 48 h). Figure from (Radfar et al. 2009)

Malaria pathology

Malaria can manifest with different symptoms. The most characteristic are fever paroxysm, attacks of fevers and chills that come in periodic waves every 3 or 4 days, reflected in their names: malaria tertiana (caused by *P. vivax* and *P. ovale* species) and malaria quartana (caused by *P. malariae*), respectively. The fevers are also present in malaria tropica caused by *P. falciparum*, although they appear less periodic.

The following section will focus on *Plasmodium falciparum*, which causes the most severe forms of malaria. Still, most infections are classified as mild or uncomplicated malaria, and besides fever paroxysms, symptoms can include headaches, general malaise, muscle pain, fatigue, vomiting and diarrhea. However, severe disease in endemic areas is especially prevalent in young children under 5 years old, pregnant women or malaria-naïve travelers. Severe malaria in children mostly manifests either as cerebral malaria, metabolic acidosis or severe malarial anemia, while adults tend to develop cerebral malaria in combination with pathology of the lungs or the kidneys (Moxon et al. 2020). Cerebral malaria (CM) is a severe complication of infection with *Plasmodium falciparum* characterized by deep coma. A hallmark of CM is sequestration of iRBCs in blood

vessels in the brain (Taylor et al. 2004) and recent findings implicate brain swelling and breakdown of the blood-brain-barrier in CM pathogenesis (Seydel et al. 2015; Dorovini-Zis et al. 2011). The diagnosis of CM was found to be more precise when morphological changes in the retina, caused by iRBC sequestration, were included (Taylor et al. 2004). Pregnancy malaria mostly affects woman in their first pregnancy and can lead to severe maternal anemia, miscarriage or low birthweight of the child (Fried and Duffy 2017).

Uncomplicated malaria is treated with a 3-day course of artemisinin-based combination therapy; for severe malaria, artesunate is recommended (WHO 2021). The fast-acting artemisinins are active against asexual and sexual blood stage parasites, and are combined with a slower-acting partner drug to increase efficiency and reduce the development of drug resistance; however, parasites with reduced artemisinin sensitivity are emerging, resulting in some areas in a slower rate of parasite clearance (reviewed in Tilley et al. 2016). Other parts of the strategy to reduce malaria is the prophylactic treatment of young children during times of high transmission, and of pregnant women (WHO 2021). Progress has been made towards a vaccine against malaria, although its development it is more complicated than a vaccine against viral diseases. The vaccine candidate that has been furthest developed, RTS,S, has a ~30% efficiency against clinical disease (RTSS Clinical Trials Partnership 2015) and is currently under pilot introduction in parts of Malawi, Kenya and Ghana (World Health Organization 2020).

<u>Asymptomatic malaria</u>
Not all *P. falciparum* infections become symptomatic. A person can harbor *P. falciparium* parasites without presenting with the typical symptoms of malaria, which is hence termed subclinical or asymptomatic infection (reviewed in Bousema et al. 2014; Galatas, Bassat, and Mayor 2016; Kimenyi, Wamae, and Ochola-Oyier 2019). The prevalence of subclinical malaria in a population varies, but was on average ~5% in low transmission areas to ~ 50 % in high transmission areas, making up ~ 60 % (low transmission area) to almost all (high transmission area) of all malaria infections in the respective study populations, as summarized by Lindblade et al. 2013.

The detection method determines how many asymptomatic infections can be identified. Rapid diagnostic tests (RDTs) can detect >100 parasites/µl (Ratsimbasoa et al. 2008), microscopy of thick blood smears >10 parasites/µl (Bejon et al. 2006), polymerase chain reaction (PCR) >1 parasites/µl

(Snounou et al. 1993), and some ultrasensitive real-time PCR methods can detect even lower parasite densities (Bourgeois et al. 2010). Loop-mediated isothermal amplification (LAMP) methods, with a similar sensitivity to PCR, are also increasingly used in field settings to detect low-density parasitemias (e.g. Sattabongkot et al. 2018).

Asymptomatic infections are in general associated with lower parasite densities than clinical malaria, and are often not detected on blood smears by microscopy, hence referred to as "submicroscopic". The term "asymptomatic" has been criticized, as carrying parasites can come with negative health impacts, such as anemia and immune system dysregulation (I. Chen et al. 2016). Additionally, chronic parasite carriage could contribute to the risk for malaria-associated endemic Burkitt lymphoma (Redmond et al. 2020). Asymptomatic malaria also poses a risk for blood transfusions, even after several years (up to 12 years documented) (reviewed in Ashley and White 2014).

How asymptomatic infections develop and are maintained is not completely understood. On an individual level, having asymptomatic malaria once infected is more likely with increasing age and exposure to *P. falciparum*, as an effect of acquired immunity (Mosha et al. 2013). On a population level however, in highly endemic areas, it is often school-age children and young adults who harbor most asymptomatic infections (Felger et al. 2012; Marsh and Kinyanjui 2006; Portugal et al. 2017) (Figure 3). This could be a result of several overlapping factors: older children have acquired immunity that protects them from severe disease (Tessema et al. 2019), but not sufficiently anti-parasite immunity to suppress parasite growth as in adults, while tolerating higher parasite densities before developing fever than adults (Rogier, Trape, and Commenges 1996; Filipe et al. 2007). The development of immunity to malaria is reviewed in (Crompton et al. 2014; Gonzales et al. 2020).

Subclinical infections are an important reservoir for malaria transmission. Even very low numbers of gametocytes (down to 0.25- 0.3 gametocytes/µl) can be infectious to mosquitoes (Schneider et al. 2007). Using direct blood feedings of mosquitoes on humans or membrane feeding assays using infected blood, around a quarter of infected individuals without gametocytes in blood smears still were able to infect mosquitoes, although less efficiently than donors with high gametocyte levels (Bousema et al. 2012). In a setting with many (asymptomatic) low gametocyte density carrying

individuals, they contribute largely to overall transmission (Stone et al. 2015), and hence pose a challenge to malaria elimination. Mass screening and treating (MSAT) of asymptomatic individuals could deplete this reservoir, however a high sensitivity of the diagnostic and coverage of the population is crucial in this approach (Cook et al. 2015). Another concern is that treating asymptomatic individuals may increase their subsequent risk of clinical malaria, as it was suspected that maintaining low-level chronic parasitemia protects from clinical malaria episodes, a concept termed "premunition" (T. Smith et al. 1999). However, it was demonstrated that treatment of asymptomatic infections at the end of the dry season does not lead to more episodes of clinical malaria (Portugal et al. 2017).

Still, the association between asymptomatic malaria and risk of febrile disease is not completely understood. In high transmission settings, asymptomatic malaria was associated with a lower subsequent risk of febrile malaria (Sonden et al. 2015; Portugal et al. 2017; Wamae et al. 2019). This could reflect higher levels of immunity in these children, possibly due to higher exposure, which suppresses parasitemia and hence prevents symptoms and results in asymptomatic infections. In low transmission settings however, asymptomatic parasitemia correlated with a higher risk of clinical malaria (Wamae et al. 2019; Slater et al. 2019), possibly also reflecting higher exposure of these individuals in the absence of high levels of immunity against the parasite. In general, many open questions remain regarding (chronic) asymptomatic malaria (Nyarko and Claessens 2020).
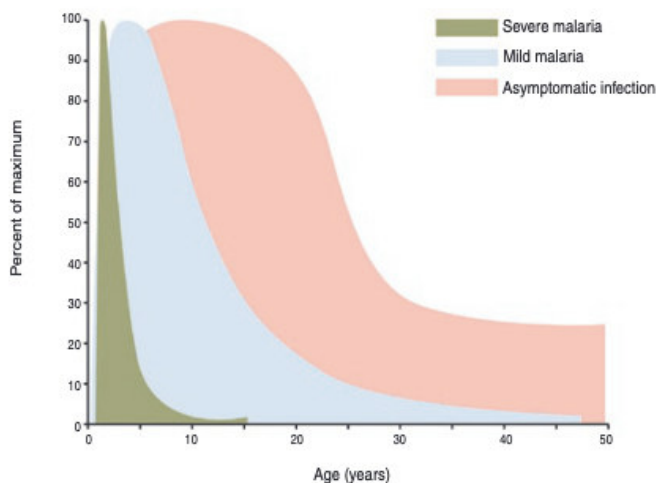
Figure 3: Manifestations of P. falciparum infections by age in endemic areas

The illustration is based on prevalence data in Kilifi, Kenya, with prevalence by age shown as percent of maximum of the respective manifestation of infection. In endemic areas, severe malaria is rare in children > 5 years old. The prevalence of symptomatic disease decreases with age, as well as the prevalence of asymptomatic infections. Peak of asymptomatic malaria are in children > 5 years to young adults. From (Langhorne et al. 2008) based on (Marsh and Kinyanjui 2006).

P. falciparum infections in the dry season

Long-term asymptomatic malaria plays an important role in areas of seasonal transmission, which have pronounced dry seasons. This is the case in many parts of Africa (Figure 4). As *Anopheles* mosquitoes only have a short live span of up to 2 months and depend on water for their larval development, mosquito populations plummet during the dry season (Lehmann et al. 2010) and transmission is interrupted. However, mosquito populations and malaria cases surge again with the arrival of the rains (Lehmann et al. 2010). While mosquitoes survive the dry season possibly by aestivation (Lehmann et al. 2010), or long distance migration with the wind (Dao et al. 2014; Huestis et al. 2019), *P. falciparum* survives by remaining within a part of the population as a subclinical infection (Babiker et al. 1998; Portugal et al. 2017). These form an infectious reservoir from which transmission restarts upon the return of the mosquitos in the following dry season (Ouédraogo et al. 2009). Survival in the dry season poses a challenge for the parasite, because it requires the parasite to remain alive and transmissible in its host for up to several months, while not triggering clearance by the immune system or causing excessive disease that would lead to death, or to treatment.
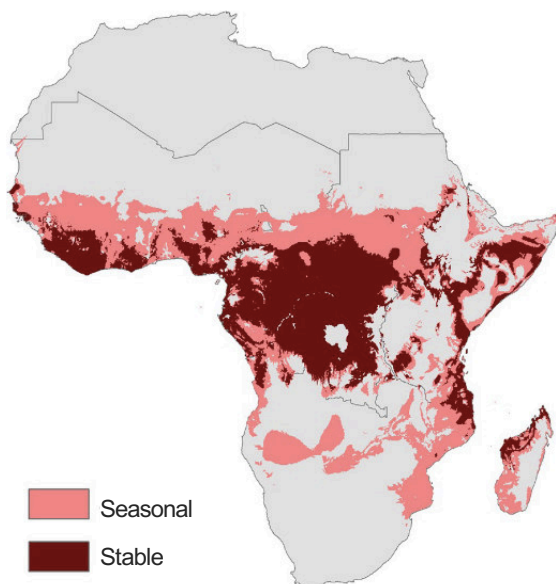
Figure 4: Malaria transmission in Africa is often seasonal

Modelled malaria transmission suitability based on temperature data. Seasonal describes 7-9 months of transmission while stable here refers to 10 – 12 months of transmission per year. Modified from Ryan, Lippi, and Zermoglio 2020.

1.2 Cytoadhesion as a survival strategy

Cytoadhesion is the ability of iRBCs to bind to other cells. Binding to endothelial cells allows iRBCs to adhere to tissues and is also referred to as sequestration. Binding to uninfected RBCs is termed rosetting, and adhesion to other iRBCS is referred to as agglutination. It is considered an important virulence factor, as it helps the parasite to avoid clearance in the spleen, and contributes to the obstruction of microcapillaries and strong local inflammation that can be life-threatening to the infected individual (Louis H Miller et al. 2002).

Brief history of the research on *P. falciparum* cytoadhesion

In 1894, when Marchiafava and Bignami investigated the brains of fatal malaria cases, they observed an accumulation of mature stage iRBCs in brain vessels and first postulated that this could be related with disease (commented in White et al. 2013). Adhesion of iRBCs to endothelial cells was first observed by electron microscopy in 1969 in infected Aotus monkeys (Louis H Miller 1969). It appeared that the mature iRBC attached to the endothelium via protrusions on its surface (Luse and Miller 1971) that had earlier been observed on mature stage iRBCs isolated from a Liberian child with malaria (Trager, Rudzinska, and Bradbury 1966), and that were absent in uninfected erythrocytes or ring stage iRBCs. There protrusions were termed "knobs" and found to contain a knob associated histidine rich protein (KAHRP), which builds the knob structure (Kilejian 1979; Leech et al. 1984; Pologe et al. 1987).
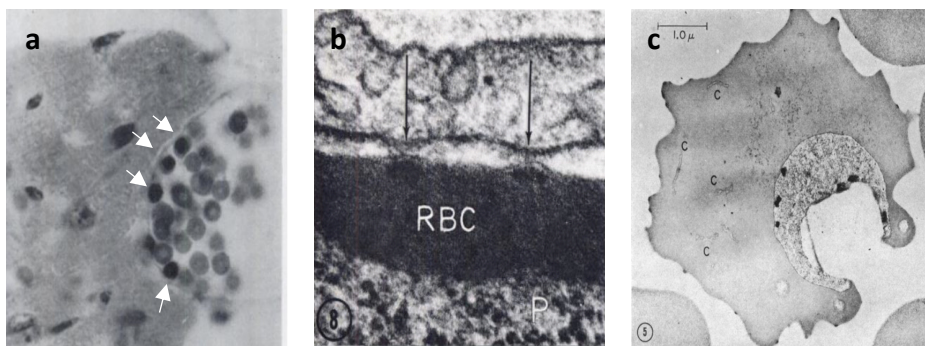
Figure 5: First histological and electron microscopy images of adhesion and host cell remodeling by P. falciparum

a) Histological section showing adhesion of *P. falciparum* iRBCs (arrow) to the endothelium of the cardiac vein in an Aotus monkey (from Miller 1969). **b)** Transmission electron micrograph of an iRBC (P indicates parasite) with electron-dense protrusions that appear to be the site of adhesion to an endothelial cell (arrows). Isolated from heart tissue of a *P. falciparum* infected Aotus monkey (from Luse and Miller 1971). **c)** Transmission electron microscopy image of a *P. falciparum* infected RBC isolated from a 12 year old Liberian girl, showing knobs on the surface and Maurer's clefts in the cytoplasm (Trager, Rudzinska, and Bradbury 1966).

The parasite adhesion ligand PfEMP1

Another breakthrough was the identification of the members of the *var* gene family, coding for the *P. falciparum* exported membrane protein 1 (*Pf*EMP1) protein that serves as the adhesion ligand (Baruch et al. 1995; Su et al. 1995; J. D. Smith et al. 1995). PfEMP1 is anchored in knobs (Baruch et al. 1995), which provide an elevated platform that increases efficiency of adhesion under flow conditions (Crabb et al. 1997). *Var* genes contain 2 exons, the first encoding the variable extracellular domain and the transmembrane domain and exon 2 encoding the conserved intracellular acidic terminal segment (ATS). *Var* genes can be grouped based on their chromosomal location, upstream sequence and direction of transcription. Group A, B and A/B are located in the subtelomeric region, with group A *var* genes being transcribed to the telomers and group B and A/B transcribed to the centromere. Group C and B/C *vars* are located closer to the centromere (Lavstsen et al. 2003). The PfEMP1 extracellular region contains several cysteine-rich interdomain regions (CIDR) and Duffy-binding-like (DBL) domains, and each of them are further divided into subclasses based on their sequence. Tandem arrangements of CIDRs and DBLS are termed domain cassettes. Commonly found in group B and C are CIDRα2-6 that bind to CD36 (Robinson, Welch, and Smith 2003). Binding to intercellular adhesion molecule 1 (ICAM1) is conferred by DBL-β domains, which are found across group B and C as well as A (Howell et al. 2008; Bengtsson et al. 2013). CIDRα1 domains found in DC13 in group A and DC8 in group A/B bind endothelial protein C receptor (EPCR) and are enriched in severe malaria (L. Turner et al. 2013). And *var2csa*, the only member of group E *var* genes, is enriched in pregnancy-related malaria (Salanti et al. 2003).

Var gene transcription levels as determined by nuclear run-on analysis were highest in *P. falciparum* strain FCR3 iRBCs at 4-10 hpi (Schieck et al. 2007). Similarly, var mRNA levels measured by Northern Blot in A4 iRBCs peaked around 6 - 12 hpi and decreased at 18 hpi (S. Kyes, Pinches, and Newbold 2000). From around 16 hpi on, PfEMP1 was detected on the surface of the A4 iRBCs by flow cytometry using a monoclonal anti-PfEMP1 antibody or pooled immune sera (Kriek et al. 2003). Adhesion of A4 iRBC to purified receptors was observed from 14-16 hpi onwards (Gardner et al. 1996). As a result, ring stage iRBCs are circulating, while mature parasite stages are absent from the circulation as they adhere to the endothelium and hence sequester in the tissues. Using transcriptomics, the average age of circulating iRBCs, computed as maximum likelihood estimation, was 8 – 12 hpi (Lemieux et al. 2009), and in another study, transcripts of parasites

above 22 hpi were absent in the circulating parasite population (Pelle et al. 2015), suggesting that iRBCs are able to sequester before this age.

Switching between PfEMP1 genes and antigenic variation of iRBCs

The repertoire of var genes is highly polymorphic within one organism, but also between parasites, creating great variability of sequences and binding phenotypes. Each genome contains close to 60 *var* genes. However, only one *var* gene is expressed at a time (Scherf et al. 1998) and this mutually exclusive expression is regulated epigenetically (reviewed in Deitsch and Dzikowski 2017). The switching occurs at a low frequency of ~ 2% per generation in vitro (Roberts et al. 1992) but may be substantially higher with ~ 16% per generation in vivo during acute infection (Peters et al. 2002).
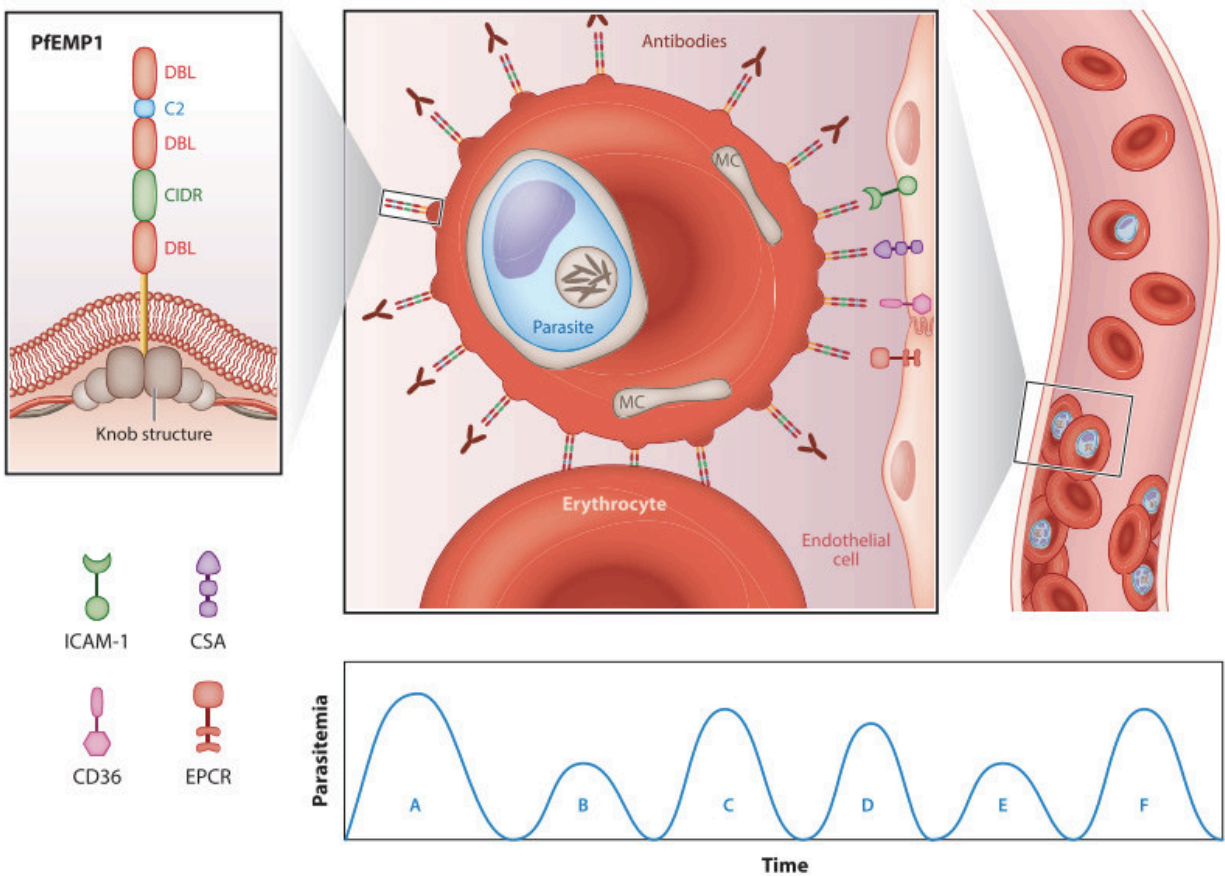
Figure 6: Antigenic variation of PfEMP1 proteins contributes to immune evasion by P. falciparum.

At a time, only one variant of the large polymorphic repertoire of PfEMP1 proteins is presented on the iRBC surface at a time. Different variants can bind to different endothelial cell receptors such as ICAM-1, CD36, CSA or EPCR and mediate binding to the inner lining of blood vessels. In the course of an infection, an antibody response is mounted against the PfEMP1 variant exposed on the surface, inhibiting cytoadhesion and mediating the destruction of the iRBCs. Only iRBCs that have switched to another variant (from PfEMP1 A to PfEMP1 B, or B to C, …) are able to multiply, until they are again targeted by antibodies. In individuals without prior immunity, this can lead to wave-like episodes of parasite expansion and persistent infections. Illustration from (Deitsch and Dzikowski 2017).

It follows a loose hierarchy (Recker et al. 2011), avoiding to present the entire repertoire of PfEMP1s too rapidly. By switching to another variant, *P. falciparum* can evade the mounting antibody response and persist in the host for a longer time (see Figure 6). Antibodies against variant surface antigens like PfEMP1 have also been linked to the gradual acquisition of anti-disease immunity in children in highly endemic regions (reviewed in Jensen, Adams, and Hviid 2020). With repeated exposure, the plasma of children can recognize more parasite isolates, meaning that their immunity covers more variants of the surface antigens (Bull et al. 1998).

Besides PfEMP1: Small variant adhesion molecules are exposed on the iRBC surface

Besides *vars*, other major variant surface antigen gene families are *rifins* and *stevors* (Cheng et al. 1998), with 149 and 28 members in the *P. falciparum* 3D7 genome, respectively (M. J. Gardner et al. 2002). They are referred to as small variant surface antigens due to their lower molecular weight compared to PfEMP1 (reviewed in Wahlgren, Goel, and Akhouri 2017). In asexual stage iRBCs, *rifin* genes are transcribed at 18-23 hpi and exposed on the iRBC surface (S. A. Kyes et al. 1999). The RIFINs comprise A-RIFINs that are exported to the host cell surface and B-RIFINs that remain in the parasite (Petter et al. 2007). At least two different RIFINs, from the same and from different groups, have been observed to be expressed in the same cell (Petter et al. 2007), suggesting that RIFINs are not under monoallelic expression regulation. Unlike *var* genes, *rifin* genes are also expressed in gametocytes, with A-RIFINs localizing to the RBC membrane in stage III gametocytes (Petter, Bonow, and Klinkert 2008), although it is unclear whether they are exposed on the host cell surface. The expression of a subset of *stevor* genes peaks at 16-24 hpi, as determined by RNA sequencing of a synchronous *P. falciparum* 3D7 population, while other *stevor* genes are highly expressed in merozoites (Wichers et al. 2019). Multiple *stevor* genes can be expressed at the same time in one iRBCs (Kaviratne et al. 2002). Some STEVORs play a role during merozoite invasion (Wichers et al. 2019). STEVORs are also expressed in gametocytes and alter the deformability of the host cell (Naissant et al. 2016). *Rifins* and *stevors* are expressed in clinical isolates at even higher levels than in 3D7, suggesting that they are important for *in vivo* survival of iRBCs (Bachmann et al. 2012). Regarding their functions, it was found that A-RIFINs mediate rosetting, the binding of iRBC to multiple uninfected RBCs, via the blood group A antigen and, to a

lower extent, to group O RBCs via glycophorin A (Goel et al. 2015), while STEVORs can bind glycophorin C on RBCs, thereby also contributing to rosetting (Niang et al. 2014). Rosetting was shown to limit the accessibility of anti-PfEMP1 antibodies if the binding occurred to blood group A but not group O RBCs (Moll et al. 2015), and this may contribute to the reduced risk of severe malaria in individuals with blood group O (J. A. Rowe et al. 2007). Furthermore, RIFINs can mimic ligands for inhibitory receptors on immune cells that are used to avoid autoimmune reactions and thereby dampen an immune reaction towards iRBCs (Saito et al. 2017). Interestingly, antibodies with insertions of these inhibitory receptors have been identified in malaria-exposed individuals (Pieper et al. 2017; Y. Chen et al. 2021). STEVOR also has a role in RBC deformability in asexual RBCS (Sanyal et al. 2012).

Given that these gene families are surface exposed, *rifins* and *stevors* elicit antibody responses in their hosts, which have recently been reviewed (Gonzales et al. 2020). Semi-immune individuals harbored antibodies that recognize recombinant RIFIN in a study in Gabon (Abdel-Latif et al. 2002) and Cameroon (Quintana et al. 2018). Similarly, semi-immune individuals in a study in Gabon contained antibodies that recognized few to multiple STEVOR proteins (Schreiber et al. 2008). In a study in Uganda, it appears that almost all RIFINS, even the intracellular B-RIFINs, and STEVORs are immunogenic (Kanoi et al. 2020). However, no clear overall association of these multigene families with clinical presentation was found in these studies (Quintana et al. 2018; Abdel-Latif et al. 2004), but antibodies against some members of them may be associated with disease severity (Travassos et al. 2018; Kanoi et al. 2020).

Still, PfEMP1 appears to be the main variant surface antigen targeted by antibodies against mature-stage parasites in plasmas from semi-immune individuals, as the extend of iRBC labeling is reduced in *var* knockdown parasite lines (Chan et al. 2012) or skeleton binding protein 1 (SBP1) knockout lines that have impaired PfEMP1 surface trafficking (Chan et al. 2016) or a chromosome 9 deletion mutant not expressing PfEMP1 (Piper, Roberts, and Day 1999), even though members of RIFINs and STEVORs on their surface were still present on the iRBC surface (Chan et al. 2012; Chan et al. 2016).

P. falciparum extensively remodels its host erythrocyte for survival and cytoadhesion

Inside the RBC, _P. falciparum_ resides in a vacuole formed at the time of invasion through invagination of the RBC membrane. To be able to cytoadhere, and also to gain access to nutrients and to dispose waste, _P. falciparum_ needs to modify the surrounding RBC (reviewed in Maier et al. 2009). To do so, the parasite exports hundreds of proteins from its vacuole into the host cell and establishes a _de novo_ trafficking and sorting pathway including membranous trafficking organelles called Maurer's clefts. This process includes the crossing of two membranes and directing proteins to their correct location in an environment that lacks trafficking components. All this is taking place in the first half of the intraerythrocytic cycle (Figure 7).
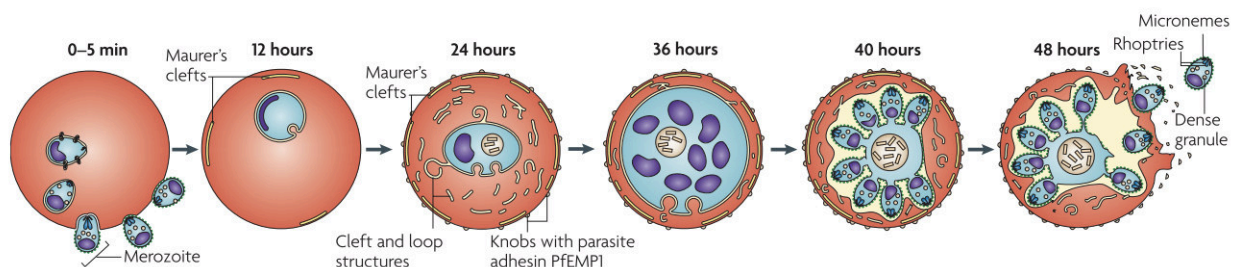
Figure 7: Erythrocyte remodeling by P. falciparum

P. falciparum merozoites invade a red blood cell by pushing inside the cell and wrapping its membrane around itself, creating the parasitophorous vacuole (PV). From there, it exports proteins into the red blood cell. These forms membranous trafficking organelles termed Mauer's clefts in the host cell as well as loop structures connected to the PV membrane termed tubovesicular network (TVN). Furthermore, it exports adhesins as PfEMP1 to the RBC membrane and displays them in knob-like protrusions. To grow within the vacuole, the parasite takes up and digests hemoglobin from the host cell. New daughter merozoites are formed and released by iRBC rupture. Illustration from Maier et al. 2009.

Plasmodium protein export into the host erythrocyte

As protein export is a prerequisite for host cell remodeling, the following section outlines the steps involved (see Figure 8). Proteins are synthesized in the endoplasmatic reticulum of the parasite, and targeted for export by a specific signal sequence, a conserved pentameric motif termed plasmodium export element (PEXEL) (Marti et al. 2004; Hiller et al. 2004). Some known exported proteins lack this signal sequence (PEXEL-negative exported proteins (PNEPs)). In the *P. falciparum* 3D7 strain, apart from 59 *var* genes, 396 genes were predicted to encode an exported protein based on the presence of a signal sequence and the PEXEL sequence (Sargeant et al. 2006), containing many members of multigene families. The real number is likely even higher, as this prediction excludes PNEPs. Cleavage of the PEXEL motif by the protease plasmepsin V then targets the proteins for export (Boddey et al. 2010; Russo et al. 2010). The proteins are brought to the parasite plasma membrane (PPM) via transport vesicles and exocytosed into the parasitophorous vacuole (PV). The vacuolar space is the interface of the parasite to the RBC and highly organized, with contact sites between PPM and parasitophorous vacuole membrane (PVM) separating zones of protein export (Garten 2020). Once in the PV, proteins are transported over the PVM through the *Plasmodium* translocon for exported proteins (PTEX) (de Koning-Ward et al. 2009). The pore is formed by the PTEX component EXP2 (Garten et al. 2018), while structural work using cryo electron microscopy showed that HSP101 provides the treading to move proteins across the translocon (Ho et al. 2018). In the cytosol, the proteins are refolded by parasite chaperones in complexes termed J-dots (Külzer et al. 2010). Exported proteins then either remain in the cytosol,
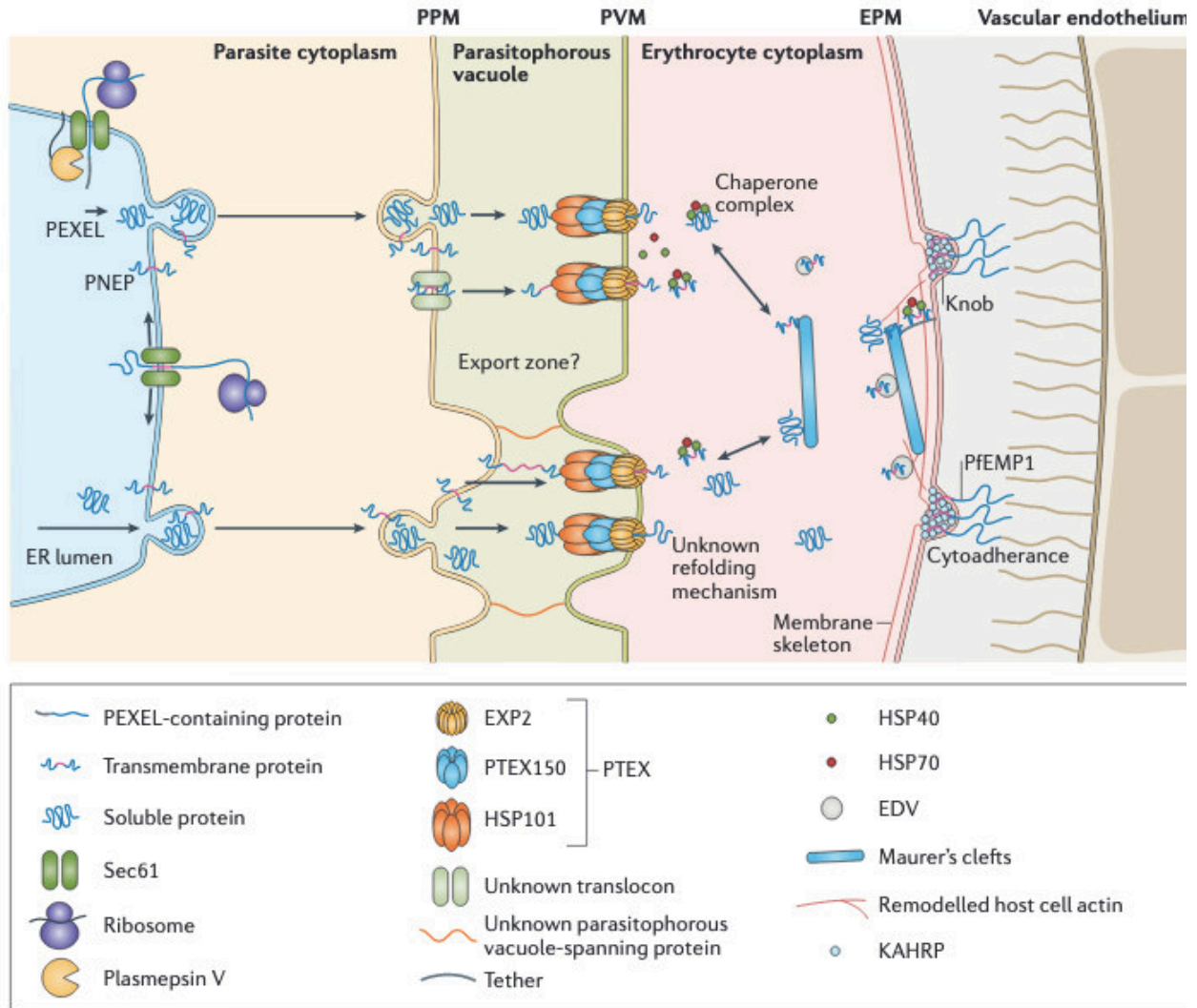
Figure 8: Protein export and trafficking within the host erythrocyte

Proteins are synthesized into the ER lumen (for soluble proteins) or inserted into the ER membrane (for transmembrane proteins). Via the secretory pathway, trafficking through the parasite Golgi apparatus (not shown), the proteins are brought to the parasite plasma membrane (PPM) and released into the parasitophorous vacuole (PV). The proteins are transported over the parasitophorous vacuole membrane (PVM) via the PTEX translocon, where chaperone complexes help refolding. In these chaperone complexes, a subset of proteins is trafficked to the Mauer's cleft. Proteins with transmembrane domains, such as PfEMP1, are membrane inserted here and are brought to the erythrocyte plasma membrane (EPM) via electron dense vesicles (EDV). Figure from de Koning-Ward et al. 2016.

Maurer's clefts are an important intermediate trafficking compartment

As Maurer's clefts (MCs) play a central role in protein trafficking to the surface, this section gives an overview of the formation of MCs and the role of specific MC proteins in enabling cytoadhesion. Mauer's clefts are parasite induced, flat, disc-shaped membrane compartments within the RBC cytosol. MCs derive from the PVM, which during the intra-erythrocytic growth develops into an elaborate membranous structures (reviewed in Matz, Beck, and Blackman 2020); while extrusions of the PVM are termed tubovesicular network and present with a different protein composition as MCs (Hanssen et al. 2010), MCs are discontinuous with the PVM, as shown in photobleaching experiments (Spycher et al. 2006). The first MCs are formed very early, within 2-4 hpi. Interestingly, the number of MCs seem to be stable from initial formation until the end of the cycle (Grüring et al. 2011). Mauer's clefts move freely within the RBC cytoplasm in ring stage iRBCs, but become arrested and docked to the RBC membrane at around 24 hpi (Grüring et al. 2011; Mcmillan et al. 2013). The tether is formed by membrane-associated histidine-rich protein 2 (MAHRP2) (Pachlatko et al. 2010). Additionally, cryo-EM tomography experiments have shown that tethering of MCs requires milling of actin filaments from the RBC membrane cytoskeleton (Cyrklaff et al. 2011). Several proteins are classified as MC resident proteins, such as skeleton binding protein 1 (SBP1) (Blisnick et al. 2000), ring exported protein 1 (REX1) (Hawthorne et al. 2004) and ring exported protein 2 (REX2) (Spielmann et al. 2006), MAHRP1 (Spycher et al. 2003), while others only associate transiently with MCs as they travel to the RBC membrane.

Protein knockouts and interaction studies have shed some light on the function of Maurer's cleft proteins, for review refer to (Maier et al. 2009; de Koning-Ward et al. 2016; Warncke and Beck 2019). The single lamellae architecture of Maurer's clefts is shaped by REX1 and Pf332, whose knockout leads to stacked MCs, i.e. several discs of MCs layered over each other instead of the single lamella phenotype (Hanssen, Hawthorne, et al. 2008; Glenister et al. 2009). REX1 locates to the outer edges of MCs (Hanssen, Hawthorne, et al. 2008). As Pf332 is a very large protein, it was proposed to act as a spacer between MC lamellae during MC generation.

Besides the tether structures formed by MAHRP2 (Pachlatko et al. 2010), Maurer's clefts are connected to the RBC cytoskeleton via remodeled actin filaments. PfEMP1 trafficking protein1 (PTP1) and Pf332 were suggested to mediate attachment of MCs to actin as they were shown experimentally to bind and organize actin (Waller et al. 2010; Rug et al. 2014). Additionally, SBP1

was suggested to be involved in MC connection to tethers as i) it interacts with components of the RBC cytoskeleton, protein 4.1R and spectrin (Kats et al. 2015), ii) it was found associated with tether structures (Hanssen, Sougrat, et al. 2008) and iii) in a SBP1 knockout line MCs showed a higher distance to the plasma membrane (Cooke et al. 2006). SBP1, PTP1 and Pf332 were also suggested to form a complex (Rug et al. 2014). Pf332 lacks a transmembrane domain but may be attached to Maurer's cleft through its interaction with PIESP2 (M. Zhang et al. 2018). SBP1, PTP1 and Pf332 are essential to traffic PfEMP1 to the surface and for adhesion (Cooke et al. 2006; Maier et al. 2007, 2008a; Rug et al. 2014; Glenister et al. 2009). Interestingly, RIFIN and STEVOR proteins were still exposed on the surface of a SBP1 knockout parasite line, suggesting that the trafficking of at least some of their members is independent of SBP1 (J. A. Chan et al. 2016)

Another group of Maurer's cleft proteins, MAHRP1 and gametocyte exported protein 7 (GEXP07), have been suggested to form part of a loading hub for proteins in, especially PfEMP1, into MCs (McHugh et al. 2020). PfEMP1 is inserted into MCs with the later RBC surface-exposed N-terminus inside the cleft (Kriek et al. 2003). MAHRP1 and GEXP07 are located centrally in the MC disc and their knockouts, while also destabilizing Maurer's clefts, leads to the absence of PfEMP1 from MC (Spycher et al. 2008; McHugh et al. 2020). In knockout strains of MAHRP1 and GEXP07 (Spycher et al. 2008; McHugh et al. 2020), and also of PTP1 (Rug et al. 2014), PfEMP1 accumulates in the PV, which cannot be explained by a mere loading function. It was therefore suggested that they also support PfEMP1 trafficking from the PVM to the MC. GEXP07 knockout iRBCs also display aberrant knobs, thus it is likely also involved in the trafficking of knob components (McHugh et al. 2020).

REX1 interacts and shares its localization on the outer edge of Maurer's cleft discs with PfEMP1 trafficking protein 5 and 6 (PTP5 and PTP6) (Hanssen, Hawthorne, et al. 2008; McHugh et al. 2020). The knockout of REX1, PTP5 and PTP6 reduces PfEMP1 trafficking to the RBC (Dixon et al. 2011; Maier et al. 2008a), and PfEMP1 accumulates in the MCs. They were therefore suggested to function in unloading PfEMP1 from MCs for further trafficking (McHugh et al. 2020). Additionally, KAHRP is not trafficked correctly in the absence of REX1 (Dixon et al. 2011), thus it is likely also trafficked by REX1.

Trafficking from MCs to the RBC surface was associated with electron-dense vesicles of 80 nm observed by serial section electron tomography (Hanssen et al. 2010). These vesicles contain PfEMP1 (Mcmillan et al. 2013; Sampaio et al. 2018) and are decorated with PfEMP1 trafficking protein 2 (PTP2), and PfEMP1 transfer to the surface is inhibited in a PTP2 knockout strain (Maier et al. 2008a). Interestingly, beyond cargo transport, the vesicles were shown to be released from iRBCs and function in cell-cell communication, leading to increased gametocytogenesis (Regev-Rudzki et al. 2013).

Knob formation in *P. falciparum*

Another important aspect of cytoadhesion is the presentation of adhesion molecules in knobs. The main component of knobs is the KAHRP protein, and its knockout leads to the absence of knobs and the loss of adhesion under flow conditions (Crabb et al. 1997). In STORM microscopy, tagged KAHRP appears on the membrane as punctae at 16 hpi and from 20-30 hpi assembles into ring structures under the knob, into which at the same time PfEMP1, after appearing on the RBC membrane, are laterally inserted (Looker et al. 2019). Based on structural and protein interaction data, Cutts et al have developed a model of the knob (see Figure 9). The number of PfEMP1 molecules per knob has been studied in *var2csa* expressing parasites by super-resolution microscopy, and found to be 3-4 PfEMP1 molecules per knob (Sanchez et al. 2019).

Knob density and diameter vary by iRBC stage and strain (see Table 1). Over the course of one asexual cycle, knob density increases as the parasite becomes mature (Nagao, Kaneko, and Dvorak 2000; Quadt et al. 2012) while knob diameter has been reported to decrease (Gruenberg, Allred, and Sherman 1983) or to remain stable in most strains analyzed (Quadt et al. 2012). Additionally, knob density can vary depending on the PfEMP1 type expressed, as observed for iRBCs expressing *var2csa* and two other selected *var* genes (Subramani, Quadt, Jeppesen, Hempel, Petersen, et al. 2015).

Table 1: Knob densities and diameters of P. falciparum iRBCs

Study	Parasite line	Method	Knob density (knobs / μm2)	Knob diameter (nm)
Gruenberg et al. 1983	FCR3 trophozoites	SEM	$10 - 35$	$110 - 150$
Gruenberg et al. 1983	FCR3 schizont	SEM	45 - 75	70 - 100
Nagao et al. 2000	A4 trophozoites	AFM	10	
Nagao et al. 2000	A4 Schizonts	AFM	50	
Quadt et al. 2012	Clinical isolates trophozoites	AFM	9 - 32	64 ± 12
Quadt et al. 2012	Various strains expressing *var2csa* trophozoites	AFM	2-8	80 ± 25
Subramani et al. 2015	FCR3/IT4 *var32b*	AFM	16.4 ± 8.8	
Subramani et al. 2015	FCR3/IT4 *var04* (CSA binding)	AFM	2.9 ± 1.6	
Batinovic et al. 2017	3D7 trophozoite	SEM		95 ±2
Sanchez et al. 2019	FCR3 (CSA binding)	SEM	24 ± 6	79 ± 14

SEM: scanning electron microscopy; AFM: Atomic force microscopy;
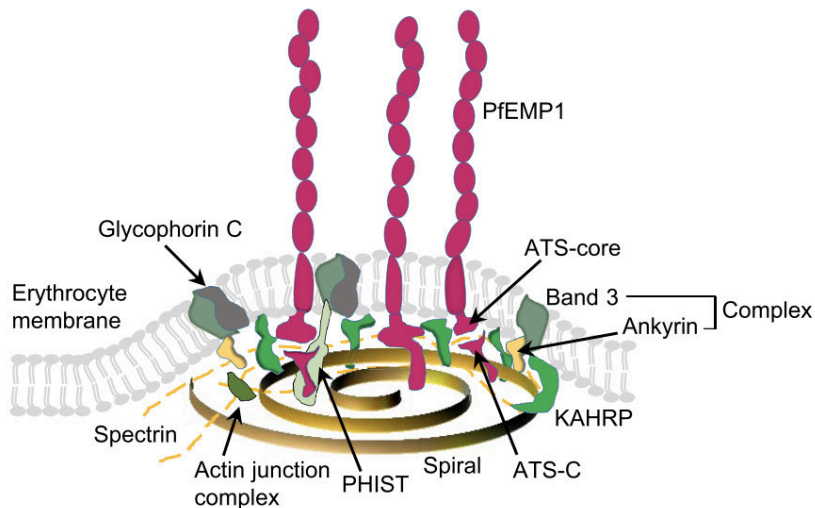
Figure 9: Plasmodium falciparum proteins remodel the RBC cytoskeleton to form knob structures

The RBC cytoskeleton consists of a spectrin-actin network that is linked to the RBC membrane proteins Band3 and glycophorin C via ankyrin. The parasite protein KAHRP interacts with spectrin-ankyrin complexes and self-multimerizes to form a ring (Oh et al. 2000), while the conserved ATS domain of PfEMP1 binds to spectrin and to band 3 via the parasite PHIST protein LyMP (Oberli et al. 2014). The knobs are underlayed by a spiral structure of yet unknown composition (Watermeyer et al. 2016; Looker et al. 2019). Illustration from Jensen, Adams, and Hviid 2020 based on Cutts et al. 2017.

1.3 The role of the spleen in *P. falciparum* infections

The spleen plays a crucial role in the pathophysiology of malaria, with protective and detrimental aspects (Henry et al. 2020). While it removes mature stage or drug-treated infected erythrocytes from circulation, splenic over-activity can lead to splenomegaly and contribute to anemia.

The structure of the spleen

The different functions of the spleen are reflected in its structure (reviewed in Mebius and Kraal 2005). The spleen is located in the left side of the abdomen next to the stomach. The largest part consists of the red pulp, in which the filtration of the RBC takes place, and the white pulp with the follicles (Figure 10a). Not every erythrocyte that enters the spleen gets filtered. Ninety percent of the blood enters the fast closed circuit, transitioning from arterioles to venules trough capillaries, while the remaining 10 % enter the slow circuit (Groom, Schmidt, and MacDonald 1991). Here, the arterioles end in the cords, a microvasculatory bed not lined with endothelial cells and with slower blood flow. To enter the lumen of the venous sinus, RBCs have to squeeze through the interendothelial slits (Figure 10b), with their narrow diameter representing the "quality control" filter for RBCs in the spleen. The average dimensions of the slits as determined by electron microscopy were 1.89 µm (range 0.25 – 1.2 µm) in length and 0.65 µm (0.9 -3.2 µm) in width (Deplaine et al. 2011). RBCs unable to cross are phagocytosed by resident macrophages. Buffet et al. calculated that with 5 liters of blood pumped through the heart every minute, 5% of the blood circulating through the spleen, and 10-20% entering the slow circulation, each RBC would pass through the splenic filter on average every 100-200 minutes. Considering the typical life span of an erythrocyte of around 120 days (Allison 1960), an erythrocyte may pass the spleen filter over 1000 times before it gets sorted out.

Clearance of infected erythrocytes by the spleen

Similarly to uninfected RBCs (Figure 11a), ring stage iRBCs are deformable enough to squeeze through the inter-endothelial slits and are hence found circulating in the peripheral blood, while mature stage infected RBCs are mechanically retained in the spleen because they are less deformable than uninfected RBCs (Figure 11b). Reduced deformability of iRBCs was first demonstrated for *P. knowlesi* (L. H. Miller, Usami, and Chien 1971), and later for *P. falciparum*

(Cranston et al. 1984), and iRBC retention in the spleen was first observed in rats infected with *Plasmodium berghei* (Quinn and Wyler 1979). The increased rigidity of the membrane is thought to enhance cytoadhesion efficiency by distributing the tension forces on adhesion receptors over the cytoskeleton (Y. Zhang et al. 2015). The decreased deformability is conferred by the remodeling of the erythrocyte cytoskeleton by parasite proteins (Mills et al. 2007; Maier et al. 2008a; Glenister et al. 2009), the formation of knobs (Y. Zhang et al. 2015) and the decreased surface-to-volume ratio (Safeukui et al. 2013; Namvar et al. 2020) inherent to the growth of the parasite within the RBC (Hanssen et al. 2012). The rigidity of infected erythrocytes starts to increase at around 8- 16 hpi and is maximal in schizonts (Deplaine et al. 2011). Also a small fraction of ring stage parasite is retained in the spleen, numbered to 10 % per passage observed by ultrasonography in malaria patients and ex vivo spleen perfusions with cultured RBCs (Safeukui et al. 2008).
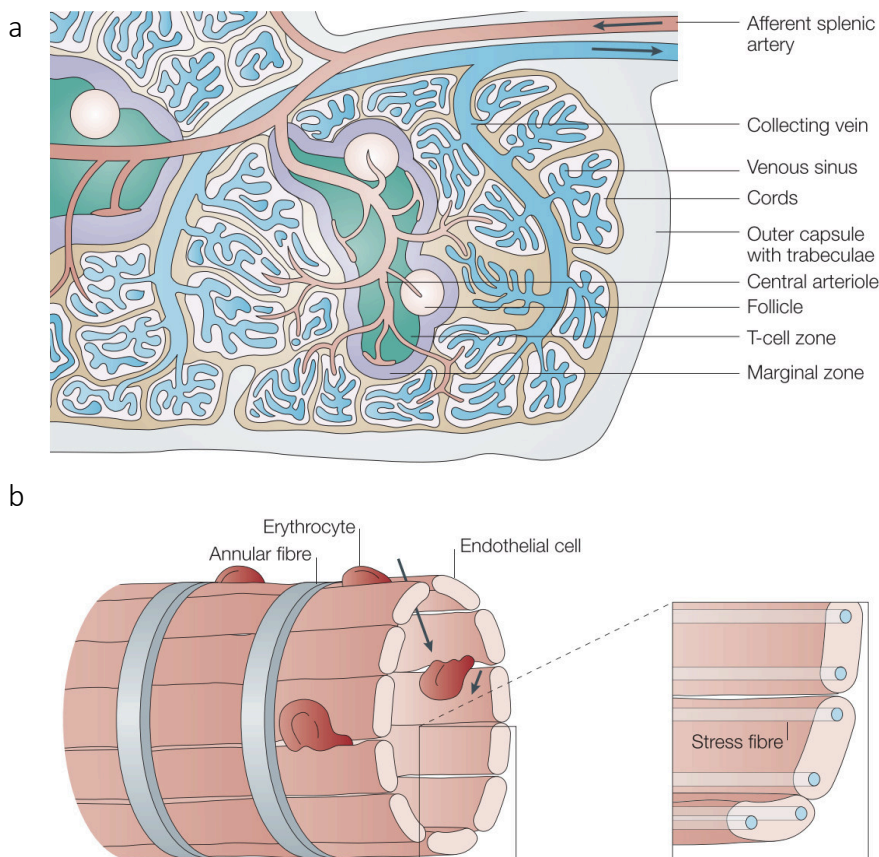
Figure 10: Structure and organization of the spleen

a) The immune function of the spleen is carried out in the white pulp, to which follicles, T-Cell zone and marginal zone belong. The filtration of the blood happens in the red pulp, where arterioles end openly in the cords, where splenic macrophages are located, and RBCs re-enter the blood stream through the venous sinus with their fenestrated endothelium. **b)** Illustration of the venous sinus wall, build of parallel endothelial cells strengthened by stress fibres, and bundled through ring fibres (annular fibre). To enter the lumen, RBCs have to squeeze through the spaces between the endothelial cells, the inter-endothelial slits. Graph modified after Mebius and Kraal 2005.

Regarding the mechanism of splenic clearance, infected RBCs that are retained in the spleen are then phagocytized by splenic macrophages. While some of these iRBCs are taken up completely by macrophages, for others it was observed that the parasite-containing part is separated from the RBC, either by mechanical force at the inter-endothelial slits or with support from macrophages (Schnitzer et al. 1972), and the residual part of the erythrocyte is pinched off and continues to circulate (Figure 11c). This process is termed "pitting", and as these pitted RBCs have a shorter life span than uninfected RBCs (Chotivanich et al. 2000), they can contribute to post-malaria anemia after artesunate treatment, as regularly observed in malaria-naïve travelers (Jauréguiberry et al. 2014) and after severe malaria episodes (Scheu et al. 2019), but was observed less frequently (~5% of patients) after treatment of uncomplicated malaria (Fanello et al. 2017). In addition to the mechanical retention, erythrocytes marked with IgG antibodies are recognized and phagocytosed by splenic macrophages (May Ho et al. 1990), likely also increasing splenic clearance in semi-immune individuals.

Besides the removal of mature asexual parasites, immature gametocytes of stage II – IV are also very stiff (Tibúrcio et al. 2012) and hence their sequestration and development in the bone marrow (Smalley, Abdalla, and Brown 1981; Venugopal et al. 2020) protects them from splenic clearance (Figure 11d). In contrast, stage V gametocytes are deformable again (Tibúrcio et al. 2012), allowing them to circulate and to be accessible to mosquitoes during a blood meal. An interesting approach to reducing gametocyte transmission is to treat them with drugs that increase their stiffness (Ramdani et al. 2015).

The spleen modulates adhesion: insights from infections in splenectomized individuals

The importance of the spleen in iRBC clearance is underlined by studies in splenectomized humans or animals, i.e. from which the spleen had been surgically removed, as these have a greater risk of developing febrile and asymptomatic malaria (Bach et al. 2005). Furthermore, studies in splenectomized individuals have contributed to our understanding of the interplay of adhesion, splenic clearance and adhesion receptor expression. When intact monkeys were infected with *P. falciparum*, only erythrocytes with young stages were found in circulation, while in splenectomized monkeys, mature stages were circulating and had lost the ability to adhere (David et al. 1983). Similarly, iRBCs obtained from a semi-immune splenectomized human patient did not

adhere to endothelial receptors or express *var*, A-type *rif* or *stevor* genes (Bachmann et al. 2009). This is illustrated in Figure 11e and suggests that the spleen, besides removing mature stages from circulation, could also (indirectly) influence the iRBC's cytoadhesive properties. In contrast, iRBCs isolated from another splenectomized human donor contained knobs and were able to cytoadhere (M. Ho et al. 1992). It is likely that the loss of cytoadhesion ligands and knobs within splenectomized hosts is a gradual process, as illustrated by the loss of sequestration and in vitro cytoadhesion of *P. falciparum* parasites in the first passage in splenectomized monkeys and partial loss of knobs in the 4th passage (Barnwell, Howard, and Miller 1983). The capacity to cytoadhere can also be regained by these iRBCs, eg. after 2 weeks of in vitro culture without active selection for cytoadhesion (Bachmann et al. 2009), or as in the case of repeated passage in splenectomized monkeys, after re-introduction in an intact monkey (Barnwell, Howard, and Miller 1983). While the Barnwell, Howard, and Miller 1983 suspected a specific stimulus in the spleen that must be present to induce surface antigen expression, it is also possible that in the absence of a spleen, there is no more evolutionary pressure to adhere in order to avoid splenic clearance, allowing for multiplication of less cytoadhesive iRBC. Additionally, as cytoadhesion ligands are immunogenic, they may be gradually selected against, resulting in adhesion-deficient antigen-less iRBCs.

Furthermore, it appears that the spleen modulates the switch of surface antigens of iRBCs; when a parasite line that was maintained in a splenectomized monkey was transferred to an intact monkey, 2-3 weeks post transfer it changed the expression of surface antigen, but if transferred from an intact to a splenectomized monkey, this switch took place much slower (Hommel, David, and Oligino 1983). Hence, presence of the spleen may be necessary to mount an antibody response against iRBC surface protein, creating sufficient immune pressure to induce switching to a different antigen variant.

Cryptic niches: Hidden replication of *P. falciparum* in the spleen?

As early as 1950, it has been speculated that the spleen is a location for a parasite development in asymptomatic infection (Figure 11f) (discussed in Monteiro et al. 2020). The idea of a hidden pool of iRBC, replicating within an organ and not circulating in the peripheral blood stream, is referred to as a "cryptic cycle" and has been suggested for replication of asexual blood stage parasites as well as the initiation and development of sexual stages in the bone marrow (reviewed

in (Venugopal et al. 2020). Furthermore, accumulation of iRBCs of all stages and uninfected RBCs in the spleens of Thai adults who died from malaria have been observed (Prommano et al. 2005). Additionally, a recent study in Papua New Guinea investigating adults who had their spleen removed after trauma injury, found a high density of all stage P. *falciparum* and/or *P. vivax* iRBCs in their spleens, and inferred that this could represent a niche for reinvasion and development (S. Kho, unpublished, presentation at GRS Malaria Conference 2019). A cryptic cycle in the spleen has also been proposed for *P. berghei* infections in mice (Lee, Waters, and Brewer 2018), however the application to human infection is limited as in mice, the spleen is also a hematopoietic niche. In general, it remains to be demonstrated that an accumulation of asexual stages in the spleen is a result of specific sequestration and not of unspecific retention.

Detrimental role of the spleen in malaria: splenomegaly and malarial anemia

While splenic clearance is important to limit parasite multiplication, it can lead to enlarged spleens (splenomegaly), and in rare cases proceed to hyper-reactive malarial splenomegaly (Leoni et al. 2015). In fact, the prevalence of splenomegaly is correlated with the prevalence of malaria parasites so that the spleen rate, i.e. the percentage of a population with enlarged spleens, was used by the WHO to classify the degree of endemicity of malaria (Baird et al. 2002).

Splenomegaly is frequently associated with cases of severe malarial anemia, as observed in children in Sudan (Giha et al. 2009), Uganda (Kotlyar et al. 2014) and Mali (Ranque et al. 2008). The mechanistic link here is that enlarged spleens have a higher filtration rate that also filters uninfected RBCs, as observed in Thai adults with acute malaria and splenomegaly using labeled uninfected RBCs (Looareesuwan et al. 1987). Compatible with this, decreased deformability of uninfected RBCs during acute malaria also contributes to malarial anemia (Dondorp et al. 1999). However, even asymptomatic parasite carriage can correlate with enlarged spleens, as seen in children in Ghana (Crookston et al. 2010), Côte d'Ivoire (Bassa et al. 2016), Guinea (Beavogui et al. 2020) and Kenya (Idris et al. 2016) but not in a study in Nigerian children (Nwaneri et al. 2020). In highly endemic areas like Mali, severe malarial anemia is more prevalent in very young children (1-2 years) and later CM is more prevalent (3-6 years) (Ranque et al. 2008); hence it has been suggested that higher splenic filtration activity protects from the development of cerebral malaria, but increases their risk of anemia, as discussed in Henry et al. 2020.
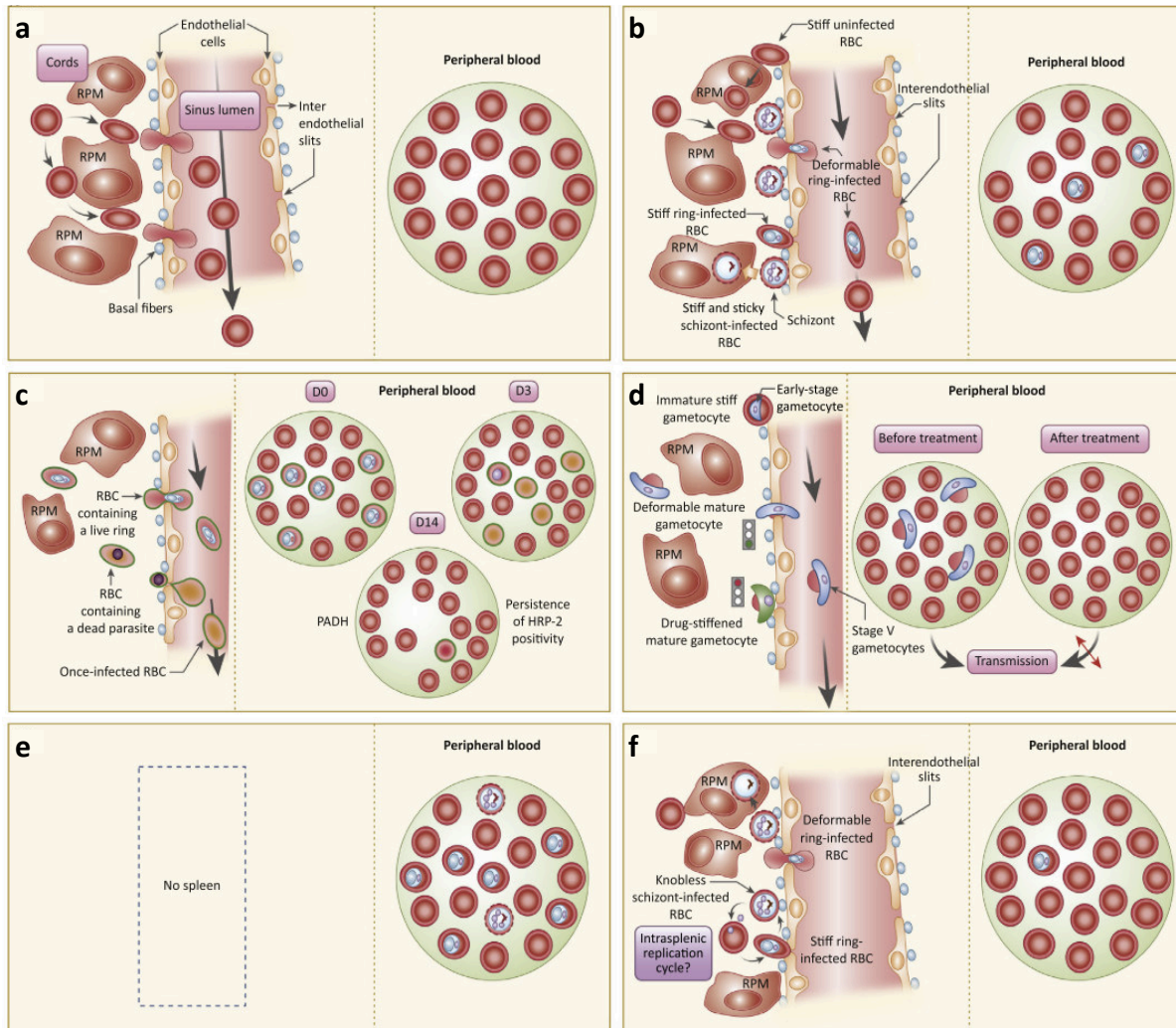
Figure 11: The spleen in P. falciparum malaria: Retention and clearance of mature asexual, drug treated and immature sexual iRBCs

a) The spleen is a quality control filter, removing red blood cells (RBC) that are too stiff to squeeze through the inter-endothelial slits by uptake by red pulp macrophages (RPM). **b)** During *P. falciparum* replication in the blood, mature stage iRBCs are retained in the red pulp and cleared by red pulp macrophages (RPM), while ring stage iRBCs (unless they become stiff) can cross the inter-endothelial slits and hence circulate in the peripheral blood. **c)** Artesunate-treated iRBCs die and the parasite-containing part of the RBC can be severed from the rest of the RBC plasma ("pitting"), which then continues to circulate, but with a shorter lifespan. This can result in post-artesunate delayed hemolysis (PADH) or the persistence of P. falciparum antigens, e.g histidine rich protein II (HRP) used for detection of *P. falciparum*. **d)** Early gametocytes are stiff and hence retained in the spleen, while the infective stage V mature gametocytes are deformable and can pass through the splenic filter. Hence, drug treatment of mature gametocyte that renders them stiffer could prevent the circulation of mature gametocytes and prevent their transmission. **e)** In splenectomized host, mature stage iRBCs are not filtered out by the spleen and hence can be circulating, if not cytoadhering. **f)** High densities of all stage iRBCs in the spleen could be part of an intra-splenic replication cycle, leading to high total iRBC densities while peripheral parasitemia would stay low. Modified after Henry et al 2020.

1.4 Looking at the host side: Endothelial activation and *P. falciparum* iRBC cytoadhesion

Host adhesion receptors and endothelial activation

Through *Pf*EMP1 molecules exposed on the RBC surface, *P. falciparum*-infected erythrocytes can bind to a variety of receptors on endothelial cells: CD36 (C. Ockenhouse et al. 1989), ICAM-1 (Berendt et al. 1989), VCAM-1 and E-Selectin (C. F. Ockenhouse et al. 1992), P-Selectin (Udomsangpetch et al. 1997), PECAM-1 (Treutiger et al. 1997), integrin $\alpha_5\beta_3$ (Siano et al. 1998), gC1qR/HABP1/p32 (Biswas et al. 2007), EPCR (L. Turner et al. 2013), integrin $\alpha_5\beta_1$ (in cooperation with CD36) (Davis et al. 2013) and integrin $\alpha3\beta1$, VE-cadherin, ICAM-2, JAM-A, JAM-B, laminin, cellular fibronectin and vitronectin (Mahamar et al. 2017). Most of these receptors, especially the cellular adhesion molecules (CAMs) and Selectins, are involved in recruiting leukocytes to sites of inflammation through increased receptor expression in response to cytokines. The concerted upregulation of these endothelial receptors supports the tethering and rolling of leukocytes on the endothelium, followed by stable adhesion and the subsequent transmigration into the tissue and to the site of inflammation (reviewed in Ley et al. 2007). The process of endothelial cells changing their function during inflammatory responses is called endothelial activation (reviewed in Pober and Sessa 2007). Skin graft experiments have shown that *P. falciparum* also uses a cascade of rolling and adhesion behaviours (May Ho et al. 2000), although with different dynamics (Helms et al. 2016). Changes in the expression of endothelial adhesion receptors can affect iRBCs adhesion, rendering adhesion susceptible to the effects of proinflammatory cytokines. The following paragraph will give an overview of the interplay of endothelial activation and iRBC cytoadhesion.

As a fast response to inflammatory stimuli, endothelial cells release the contents of small storage granules called Weibel-Palade bodies, secreting von Willebrand Factor (vWF), and within minutes bring P-Selectin to the surface (Murphy and Weaver 2018). A slower, more sustained reaction, is mediated by the leukocyte-produced cytokines TNF and IL-1 via NF-kB and AP1 transcription factors, leading to expression of E-Selectin and VCAM-1 and upregulation of ICAM-1 on the endothelium (Murphy and Weaver 2018). These receptors are expressed with different dynamics: E-Selectin is presented on the cell surface early with a peak after 4 – 6 h stimulation, while ICAM-1 appears on the surface from 4 h onward, gradually increasing until 24 h (Pober, Bevilacqua, et

al. 1986; Pober, Gimbrone, et al. 1986); VCAM-1 levels peak after 6 h and persist until 72 h (Swerlick et al. 1992). Upregulation of these receptors allows for rolling and adhesion of leukocytes to the endothelium, followed by the traversal of the endothelium by opening PECAM-cell-cell connections with leukocyte-bound PECAM (Muller et al. 1993). TNF stimulation does not alter PECAM-1 expression, but induces its relocation away from the inter-endothelial location (Romer et al. 1995). The upregulation of endothelial receptors goes along with increased shedding of receptors during endothelial activation, with regulatory functions in deadhesion, soluble adhesion antagonists and rolling velocity regulation (Garton, Gough, and Raines 2006).

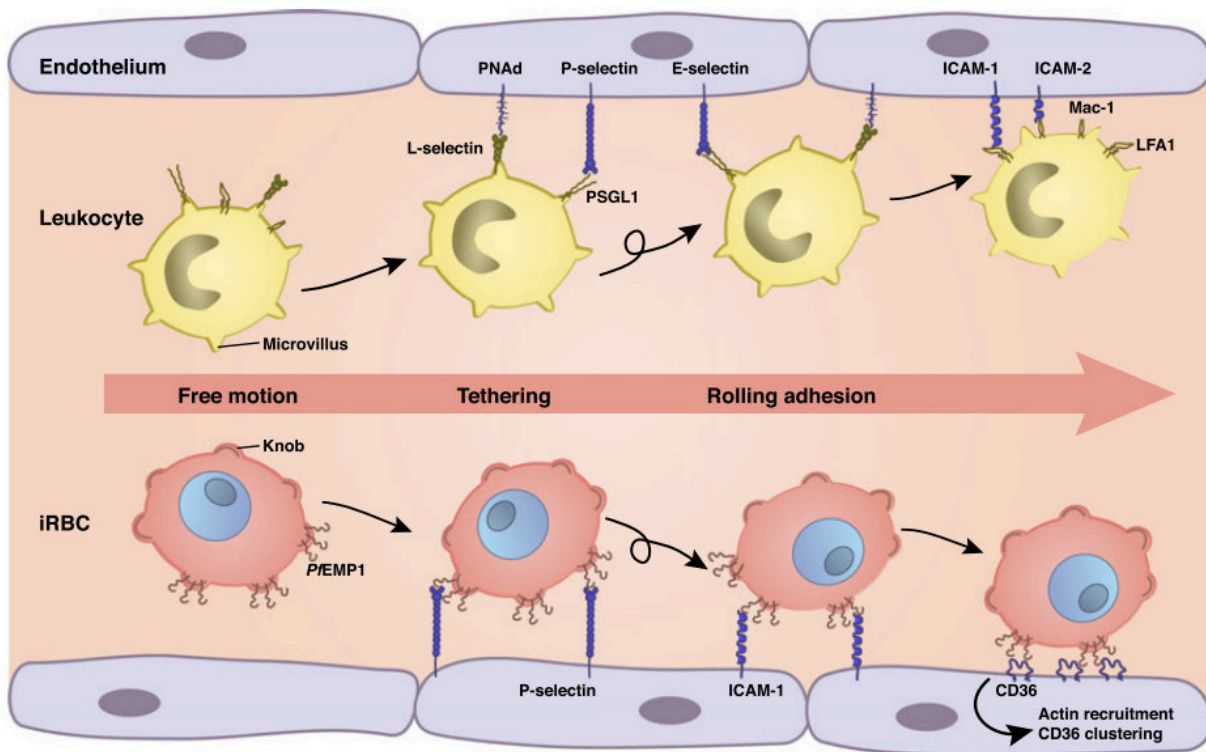*Figure 12: P. falciparum adhesion and leukocyte migration share similar receptors on endothelial cells*

In a simplified view, the adhesion cascade of leukocytes involves tethering to and rolling on Selectins, and firm adhesion to ICAM-1, while iRBCs tether to the endothelium via the Selectins, interact with ICAM-1 during rolling adhesion and use CD36 for static adhesion. From Helms et al. 2016.

28

<u>Endothelium-activating cytokines TNF and IL-1 are produced during *P. falciparum* infections</u>
As TNF and IL-1 play an important role in endothelial activation, and in inflammation in general, they have been extensively studied in clinical malaria. TNF is a pyrogen and its association with fever in malaria is underlined by the observations that in *P. vivax* infections the TNF levels peak with maximal fever (Karunaweera et al. 1992), and that inhibition of TNF by antibodies can lower fever (Kwiatkowski et al. 1993). TNF levels have been associated with malaria severity, but there is still conflicting evidence on the role of TNF in cerebral malaria (Leão et al. 2020) even when retinopathy is used as a diagnostic criterium for CM (Feintuch et al. 2016; Villaverde et al. 2020). Multiple reports have showed increased TNF levels (some also IL-1 levels) in children with uncomplicated malaria compared to healthy controls, e.g. in children in Mali (Lyke et al. 2004), Gambia (Kwiatkowski et al. 1990), Malawi (Mandala et al. 2017), Burkina Faso (Kaboré et al. 2020) and St. Tomé (Baptista et al. 1997), or in adults from India (Prakash et al. 2006). Other studies have not found elevated TNF levels in uncomplicated malaria, e.g. in Gambian children (Jakobsen, McKay, et al. 1994), or only when uncomplicated malaria was accompanied by high parasite density, as observed in Kenyan children (Othoro et al. 1999). The association with asymptomatic parasite carriage is even less consistent, with studies reporting differences in TNF levels between microscopy-positive asymptomatic individuals and compared to the healthy control group, e.g in studies in children in The Gambia (Frimpong et al. 2020) or children in Burkina Faso (Kaboré et al. 2020), while other studies did not observe a difference (Jakobsen, McKay, et al. 1994; Othoro et al. 1999). Our lab has previously reported comparable IL-1β levels in children with asymptomatic infection at the end of the dry season and healthy age-matched controls (Andrade et al. 2020).

What triggers the production of proinflammatory cytokines in malaria? A study in the late 90s showed that the rupture of schizonts coincides with the release of proinflammatory cytokines during infection in vivo, and can trigger TNF release from PBMCs in vitro (Kwiatkowski et al. 1989). Since then, specific pathogen-associated patterns (PAMPs) of malaria parasites and their effect on innate immune cells have been a focus of research. It was found that glycosylphosphatidylinositol (GPI) anchors that are common at the surface of merozoites released by rupturing schizont trigger IL-1 and TNF release from macrophages in vitro (Schofield et al. 1996). AT-rich motifs of *P. falciparum* DNA trigger the release of IFN-b, TNF and IL-6 from macrophages (Sharma et al. 2011), CpG domains on malaria DNA activate NfkB in dendritic cells via TLR9 (Parroche et al. 2007),

and hemozoin leads to release of IL-1β in monocytes (Tiemi Shio et al. 2009) and heme induces TNF release from macrophages (Figueiredo et al. 2007) and iRBC derived microvesicles taken up by macrophages stimulate them to release TNF and IL-10 (Mantel et al. 2013).

Besides acting on endothelial cells through cytokines, *P. falciparum* iRBCs and released molecules can also directly activate endothelial cells. Cytoadhesion of *P. falciparum* itself triggers endothelial activation (Esslinger, Picot, and Ambroise-Thomas 1994; Viebig et al. 2005). GPI anchors were for example shown to activate HUVEC cells directly via the NFkB pathway (Schofield et al. 1996). Additionally, stimulation of brain microvascular endothelial cells with HRPII leads to upregulation of ICAM-1 and VCAM-1 in vitro (Pal et al. 2016).

Endothelial activation contributes to malaria pathogenesis

The first notion that iRBC binding to endothelial receptors could be involved in malaria pathogenesis and disease severity came with the discovery of ICAM-1 as an adhesion molecule (Berendt et al. 1989). Experimental hints found in the brain of a fatal CM case, in which ICAM-1 was strongly upregulated in brain vessels, as well as E-Selectin and VCAM-1 to a lesser extent, and that parasite sequestration correlated with ICAM-1 and E-Selectin expression on the vessels (G. D. H. Turner et al. 1994). Similarly, ICAM-1, VCAM-1 and E-Selectin expression correlated with sequestration in the brain of Ghanaian children who succumbed to malaria (Armah et al. 2005). Later it has been shown that endothelial activation also takes place in uncomplicated malaria, as skin biopsies from Vietnamese adults with uncomplicated malaria showed an increase in VCAM-1 and E-Selectin expression (ICAM-1 was constitutively high) compared to control donors without infections (G. D. H. Turner et al. 1998). Accordingly, adults with mild malaria in Mozambique expressed higher levels of ICAM-1 and P-Selectin and induced VCAM-1 and E-Selectin expression, although these differences were much less pronounced than in the CM cases analyzed in the same study (García et al. 1999).

As biopsy studies are technically and ethically difficult, other studies have assessed endothelial activation through quantification of shed soluble endothelial cell receptors in plasmas. This has been shown to correlate with the upregulation of endothelial receptors in vivo, as plasma sVCAM-1 and sE-Selectin levels correlated with the expression of the respective adhesion molecule on dermal microvessels from skin biopsies in Vietnamese adults (G. D. H. Turner et al. 1998).

In the same line, several studies report increased levels of soluble endothelial cell receptors in uncomplicated malaria versus healthy controls, e.g with increased levels of sICAM-1, sVCAM-1 and sE-Selectin in Cameroonian children (Tchinda et al. 2007) and malaria-naïve Europeans (Jakobsen, Morris-Jones, et al. 1994); or increased levels of ICAM-1 and E-Selectin in Sudanese adults (Hviid et al. 1993) and Malawian children (Moxon et al. 2014); higher levels of sICAM-1 and sVCAM-1 in Ugandan children (Park et al. 2012); or of sICAM-1 only in Brazilian adults (Graninger et al. 1994) or Gambian children (McGuire et al. 1996). A small study that measured sP-Selectin levels also found increased levels in adults with uncomplicated malaria compared to uninfected controls (Facer and Theodoridou 1994). Less data is available regarding the effect of asymptomatic malaria on endothelial activation and shedding of receptors. In asymptomatic Ugandan children, there was a trend to higher sICAM-1 and sVCAM-1 levels if children were smear-positive compared to PCR-positive infections, although the difference between smear-positive and aparasitemic children was not significant (Park et al. 2012).

1.5 Scope and aim of the study

We have studied subclinical *P. falciparum* infections during the dry season in a cohort study in Kalifabougou, Mali (Tran et al. 2013). In a recent publication (Andrade et al. 2020), we showed that at this study site, new infections and clinical cases are strongly restricted to the wet season from June to December (Figure 13a). During the dry season, from January until May, 10-20% of the study participants remained subclinically infected (Figure 13b). Throughout the dry season, parasites persisted in asymptomatic individuals at very low parasitemias compared to those of clinical malaria cases in the transmission season (Figure 13c). Interestingly, the iRBCs that circulated in the blood at the end of the dry season in May were more developed within the 48h-asexual cycle, as observed by morphology in thick smears (Figure 13d), transcriptome analysis (Figure 13e), and time to parasitemia increase (Figure 13f). The presence of iRBC stages that are more developed within the 48h-asexual cycle in circulation suggests that these iRBCs are less capable to cytoadhere and sequester in the deep vasculature, and that they could be at higher risk of splenic clearance.

The thesis addresses these three questions:

1. Are iRBCs during the dry season at higher risk of splenic clearance and does this contribute to maintain low parasitemia during the dry season?

We mimicked the retention of iRBC from asymptomatic donors at the end of the dry season and from donors with clinical malaria during the transmission season using a spleen-like filter, and assessed the impact of increased splenic clearance on parasitemia growth using a mathematical model. Results of these experiments have also been published in Andrade et al. 2020.

2. How does the parasite become less adhesive during the dry season? Is the formation of knobs, the trafficking of adhesion molecules through the host iRBC, or the presentation of adhesion molecules on the iRBC surface altered in iRBCs at the end of the dry season (see Figure 14)?

We isolated and enriched iRBCs from asymptomatic donors at the end of the dry season and from donors with clinical malaria during the transmission season, and analyzed knob formation and host cell remodeling by electron microscopy in developmental stage matched parasites.
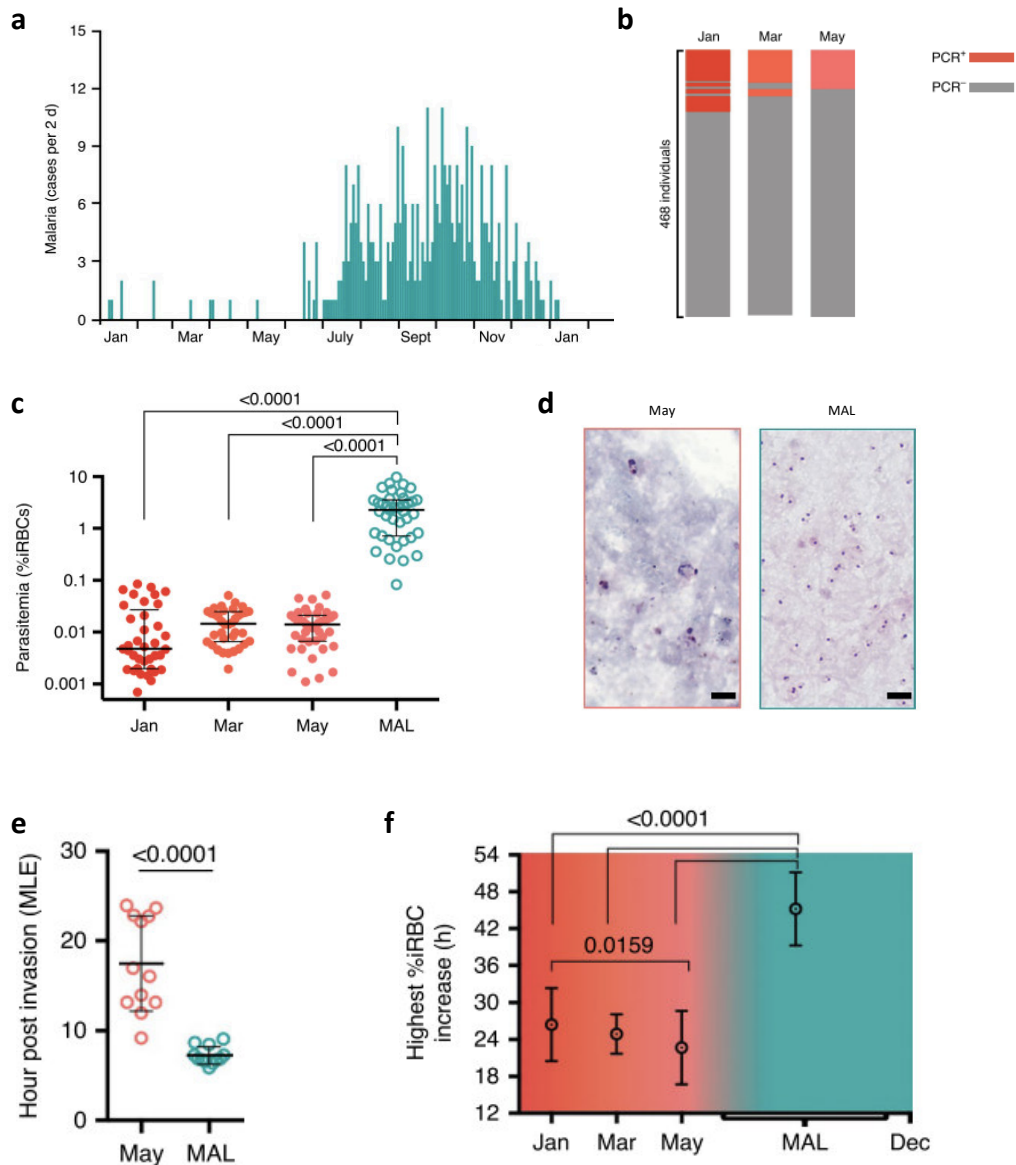
Figure 13: Dry season P. falciparum iRBC in circulation are more advanced within the intra-erythrocytic lifecycle

a) Clinical malaria frequency in a cohort of ~600 individuals aged 3 months to 45 years measured every 2 days. Clinical malaria diagnosed by axillary temperature ≥37.5 °C and ≥2,500 asexual parasites per μl of blood and no other apparent cause of fever. **b)** Prevalence of subclinical P. falciparum determined by PCR in paired individuals (rows) at the beginning (January), middle (March) and end (May) of the dry season in 2017. Columns are sorted to have the same individual represented in a single row at the three time points in each dry season. **c)** Parasite load detected by flow cytometry of RDT+ subclinical children at the beginning (January), mid (March) and end (May) of the dry season and children with their first clinical malaria episode (MAL) in the wet season. Parasitemia data represented as median ± IQR; Kruskal–Wallis test with multiple comparisons. IQR, interquartile range. **d)** Giemsa-stained thick blood films of P. falciparum parasites collected straight from the arms of children at the end of the dry season (May) and at their first clinical malaria (MAL). Scale bar, 5 μm. **e)** Maximum likelihood estimation (MLE) of the hpi of dry season (May, n = 12) and clinical malaria (MAL, n = 12) parasites. Data indicate mean ± s.d.; two-tailed Mann–Whitney test. **f)** Time of highest increase in parasitemia detected during in vitro culture of P. falciparum parasites from children in January (n = 39), March (n = 42) and May (n = 40) during the dry season, and clinical malaria cases (MAL, n = 27). Data indicate mean ± s.d.; one-sided Dunn's Kruskal–Wallis multiple comparisons test.

We determined the expression of adhesin-trafficking related genes of circulating and in short-term cultured parasites from dry season asymptomatic donors and from clinical malaria cases in the transmission season. Using flow cytometry, we compared the presentation of surface antigens, including adhesins, on the iRBCs from asymptomatic donors at the end of the dry season and from donors with clinical malaria during the transmission season.

3. Can the host environment in the dry season contribute to decreased adhesion in the absence of clinical symptoms, by providing less adhesion receptors as result of reduced endothelial activation?

We quantified the levels of endothelium-stimulating cytokines and soluble adhesion receptors in the plasmas of asymptomatic donors at the end of the dry season and of donors with clinical malaria during the transmission season. Additionally, we stimulated endothelial cells with plasmas of asymptomatic donors at the end of the dry season and of donors with clinical malaria during the transmission season and quantified adhesion receptor expression.
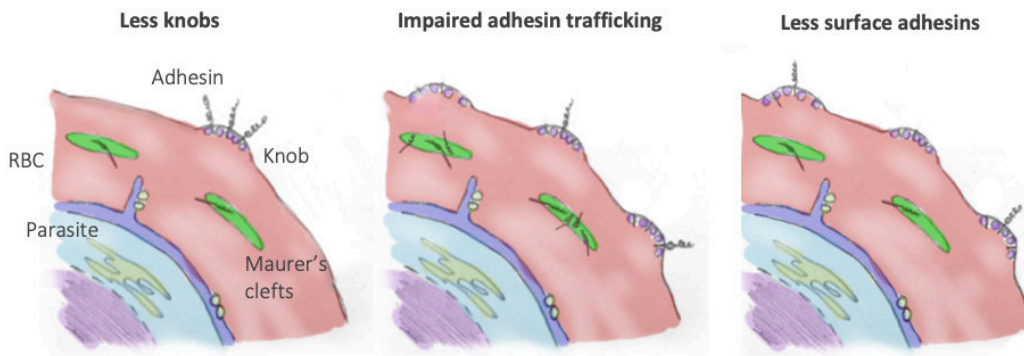
Figure 14: Alterations in host cell remodeling could reduce cytoadhesion

To be able to adhere, *P. falciparum* establishes a traffics parasite adhesins to the RBC surface and presents them on knobs. Illustration shows three ways how cytoadhesion could be reduced in iRBC in asymptomatic donors at the end of the dry season.

2. Materials and methods

2.1 Materials

<u>Equipment</u>

Equipment	Brand / Company
Aqualine waterbath	Lauda
Axio Lab.A1 light microscope	Zeiss
Bio-Plex 200 System	BioRad
Biometra Thermocycler	Analytik Jena
CO2 Incubator Heracell 150i	Thermo Scientific™
Copper grids (G2410C)	PLANO
Cover slips for SEM 12 mm (DRK1)	A. Hartenstein
Critical point dryer EM CPD300	Leica
CryoCube F570 Freezer	Eppendorf
Cytation3 Plate Reader	BioTek
Diamond knive 35 °	Diatome
Diamond knive 45°	Diatome
Digital Microscope Camera Axiocam 305	Zeiss
EM tweezer (72700-D)	Dumont
FACS Canto II	BD Biosciences
FACS LSR II	BD Biosciences
Grid box (G276N)	PLANO
Heraeus™ Fresco™ 21 microcentrifuge	Thermo Scientific™
Heraeus™ Multifuge™ X3 Centrifuge	Thermo Scientific™
Herasafe KS 15 Safety cabinet	Thermo Scientific™
MiniSpin® centrifuge	Eppendorf
Pipetus® Pipetboy	Hirschmann
qTower³ Thermocycler	Analytik Jena
QuadroMACS™ separator	Miltenyi Biotec
Scanning electron microscope Leo 1530	Zeiss
SU1550 centrifuge	Sunlab
Syringe pump AL-4000	World Precision Instruments
ThermoMixer® F1.5	Eppendorf
Titramax 100 Shaker	Heidolph Instruments GmbH & CO
Transmission electron microscope JEM1400	Jeol
UV2 Sterilizing PCR Workstation	UVP
Vacuum coater EM ACE200	Leica

Disposables

Disposables	Brand / Company
0.22 µm filters	Whatman
24-well plates, sterile	Greiner Bio-One
48-well plates, sterile	Greiner Bio-One
96-well PCR Plate	Analytik Jena
96-well plates for ELISA (Immunoplates, Maxisorp F)	Fischer Scientific
96-well plates, flat bottom with lid	Corning
96-well plates, round bottom	Greiner Bio-One
Aspiration pipettes, 2ml unplugged	Carl Roth
Counting slides Glasstic™ 10 with Grids	Kova
Cryotubes	Greiner Bio-One
CultureWell™ removable chambered coverglass	Grace Bio-Labs
DNA LoBind tubes	Eppendorf
EASYseal™ sealing film	Greiner Bio-One
Eppendorfs, 1.5ml	Sarstedt
FACS tubes,	Sarstedt
Falcon tubes, 15ml	Greiner Bio-One
Falcon tubes, 50ml	Sarstedt
Filter tips	Greiner Bio-One
Filter tips (732–0534) (for microsphiltration assay)	VWR
Glass slides	A.Hartenstein
Latex gloves	Semperguard
LS/LD collumns	Miltenyi Biotec
Malaria Ag P.f test of histidine-rich protein II	SD BIOLINE
MicroAmp Optical Adhesive Film	Thermo Scientific™
Needles	Becton Dickinson
Nunc™ EasYFlask™ Cell Culture Flasks	Thermo Scientific™
Optical sealing foil	Analytik Jena
Pipetting reservoir	Bio-Pure
Pipetting reservoir, sterile	VWR
Plate sealers, adhesive	Sigma
Protein Saver 903 Filter paper	Whatman

Puradisc 13 syringe filter 1.2 µm	Whatman
Serological pipettes	Greiner Bio-One
Serological pipettes	Sarstedt
Steri Cups, 0.22µm	Millipore
Steri-Flip vacuum filtration system	Millipore
Syringes, Luer-Lock	Becton Dickinson
Tips	Sarstedt
Tips	Greiner Bio-One
TouchNTuff Nitril gloves	Ansell
Vacutainer CPT Tubes	Becton Dickinson

Chemicals and reagents

Chemicals / Reagents	Brand / Company
10 nM dNTPs	Invitrogen
10 x PBS	Carl Roth
10x PBS for molecular biology	Invitrogen™
96% Ethanol	Zentrallager Universiät Heidelberg
Accutase solution	Promocell
Acetone, dry	AppliChem
Agarose Low Melt, 5 g	Carl Roth
Albumax II	Gibco
BSA	Carl Roth
Chloroform	Sigma-Aldrich
CryoSFM	Promocell
D-sorbitol	Sigma-Aldrich
Detach kit (trypsin, trypsin inhibitor, HBSS)	Promocell
DMSO	Sigma-Aldrich
Ethanol absolut	Sigma Aldrich
FBS, South American, 500ml	Gibco
Gelafundin	
Gentamycin, 20ml (50mg/ml)	Carl Roth
Giemsa	Merck
Glutaraldehyde 25 % in water, for electron microscopy	Carl Roth
Glycerol	Honeywell
GlycoBlue Coprecipitant	ThermoFisher
Growth medium MV2 (Ready-to-use or kit)	Promocell
Heparin-sodium 5000 IU/ml	Ratiopharm
HEPES	Gibco

Human AB+ serum (H4522)	Sigma-Aldrich
Hypoxanthine, 100x	CC Pro
Lead nitrate $Pb(NO_3)_2$	Merck
Low-melting agarose	
Methanol	Sigma-Aldrich
Microspheres (Sn96.5% tin, 3% silver, 0.5% copper), 15 - 25 µm diameter	Industrie des Poudres Sphériques
Microspheres (Sn96.5% tin, 3% silver, 0.5% copper), 5-10 µm diameter	Industrie des Poudres Sphériques
MitoTracker Deep Red	Applied Biosystems
Nuclease-Free Water	Invitrogen
O+ plasma	Blutbank Universitätsmedizin Mannheim
Oligo(dT) 20-Primers	Invitrogen
Osmium tetroxide, 4%	Science Services
Paraformaldehyde, 16% (w/v)	Thermo Scientific
Pioloform	PLANO
Pioloform F	PLANO
Poly-L-lysine 0.01%	Merck Millipore
RAL 555 Kit	BioRepair GmbH
Razor Blades	PLANO
RPMI 1640 w/25mM HEPES	Gibco
Sodium bicarbonate, 7.5%	Gibco
Sodium Citrat	Riedel de Haen
Spurr's embedding medium ERL 4221 D	Serva
SYBR Green I	Invitrogen
TNF recombinant protein (#PHC3015)	Gibco
TRIzol LS	Ambion
Trypan Blue Stain	Gibco
Tween 20	AppliChem
Uranyl Acetate	Serva

Kits

Kit	Brand / Company
7-plex Luminex Human Magnetic Assay (LXSAHM-07) for human ICAM-1, VCAM-1, PECAM-1, E-Selectin, P-Selectin, IL-1α and IL-1β	R&D systems
Detach kit (trypsin, trypsin inhibitor, HBSS)	Promocell
DNaseI Amplification Grade set	Invitrogen

EasySep CD45 Depletion Kit	Stemcell Technologies
Power SYBR Green PCR Master Mix	Applied Biosystems
SuperScript IV VILO Master Mix with ezDNase	Invitrogen
SuperScript VILO cDNA Synthesis	Invitrogen
SuperScript™ IV Reverse Transkriptase	Invitrogen
TNF-alpha DuoSet ELISA (DY210)	R&D systems

Antibodies

Antibody	Brand / Company
anti-human CD36 (clone FA6-152)	abcam
anti-human E-Selectin (clone BBIG-E1)	R&D systems
anti-human ICAM-1 (clone 15.2)	Invitrogen
anti-human IgG-APC (Biolegend)	Biolegend
anti-human VCAM-1 (clone BBIG-V1)	R&D systems
anti-mouse IgG (H+L) - Alexa Fluor 488	Invitrogen

Primers

Gene	Gene ID	forward (3' to 5')	reverse (3' to 5')
GEXP07	PF3D7_1301700	TCACAACGATCTCAATGCACTC	CCAAGAGCACCAACTCCTGC
GlyRS	PF3D7_1420400	TGAGTGATATGGATAATATAAAGGAACAAA	GGATGATATTTCACAAACGTATCTTTCT
HGPRT	PF3D7_1012400	ACCAAATAATCCAGGAGCTGGT	AGGTCATAACCATCGTCATCCT
HGPRT	PF3D7_1012400	ACCAAATAATCCAGGAGCTGGT	AGGTCATAACCATCGTCATCCT
KAHRP	PF3D7_0202000	AGAAAGAAGGCTTTCCCTGTT	GAAATCGAAGGAGTCACCGGA
MAHRP1	PF3D7_1370300	CGCCTTCTTATACCACTCAATCA	AAGTTCATGAGCGTGTGCAG
OAT	PF3D7_0608800	AGGCTCTTTCTGGAGGTCACT	ACCGTGTTCTCCTGGTTTCAA
OAT	PF3D7_0608800	AGGCTCTTTCTGGAGGTCACT	ACCGTGTTCTCCTGGTTTCAA
PF332	PF3D7_1149000	AAGAAGATGTGGGATGTGTTCCA	CATTTTCATTATCCAACCTTTCCAT
PTP1	PF3D7_0202200	ACCACCTGCTTCTGCTTCAG	ACGATTCCTTTGGTACCGTTT
SBP1	PF3D7_0501300	TAGCCGACGAACCAACACAA	ATCCGAAACTACTTCGGCCA
SDH4	PF3D7_1010300	GGTATGTCTAATTGGTTTTGCCGT	TCACATCTAGTGGCGAGTTGC
SDH4	PF3D7_1010300	GGTATGTCTAATTGGTTTTGCCGT	TCACATCTAGTGGCGAGTTGC

Software

Software	Developer / Company
EM-Menu	TVIPS GmbH
FACS Diva	BD Biosciences
FlowJo	Tree Star
GraphPad	Prism
ImageJ	NIH
Mendeley Desktop	Mendeley Ltd
SmartSEM	Zeiss
Zen2 core v2.4	Zeiss

Organisms and cells

Organisms and cells	Origin
Human dermal microvascular endothelial cells (HDMEC) (C-12210)	Promocell
Plasmodium falciparum FCR3	(J. B. Jensen and Trager 1978)
Plasmodium falciparum M2K1	Malian blood donors, Portugal lab
O^{Rh+} erythrocyte concentrate	Blood donors, Blutbank Universitätsmedizin Mannheim

2.2 Methods

P. falciparum field samples

Study design, participants and Ethical approvals

Samples and clinical data for this work were obtained between 2018 and 2019 in a cohort study conducted in the Kalifabougou, Mali, a village of approximately 5,000 inhabitants located 48 km northwest of Bamako, the capital of Mali. The study is ongoing since 2011 and is an observational study of malaria immunity in cooperation between Dr. Peter Cromptons group at the NIH, and the team of Prof. Boubacar Traoré at the University of Bamako, Mali and has been described elsewhere before (Tran et al. 2013; Portugal et al. 2017). Participants aged between 3 months and 45 years were enrolled from an age-stratified, random sample of the village population. Enrollment exclusion criteria were hemoglobin concentration <7 g/dL, axillary temperature ≥ 37.5°C, acute systemic illness, pregnancy, and use of antimalarial or immunosuppressive

medications in the preceding 30 days. Written informed consent was obtained from all participants or the parents/guardians of participating children. The Ethics Committee of Heidelberg University Hospital, the Faculty of Medicine, Pharmacy and Odontostomatology (FMPOS) at the University of Bamako, and the National Institute of Allergy and Infectious Diseases of the National Institutes of Health Institutional Review Board approved this study. The study is registered at ClinicalTrials.gov (identifier NCT01322581).

Clinical malaria episodes were detected prospectively by passive surveillance and were defined by an axillary temperature of ≥ 37.5°C, ≥ 2500 asexual parasites per microliter of blood, and no other cause of fever on physical examination. Malaria episodes were treated with a 3-day course of artemether/lumefantrine according to Malian national guidelines. The health center and pharmacy in the village provided the only access to antimalarial drugs. Additionally, cross-sectional clinical visit and blood draws were performed at the beginning (January), mid (March) and end (May) of each dry season.

Blood sample collection

Samples were collected during passive surveillance from individuals presenting with their first febrile malaria episode in a given transmission season, or during cross-sectional visits from all enrolled participants. From each individual a thick smear, dried blood spots and venous blood (4 or 8 ml depending if donor age was below or above 4 years old) drawn into sodium citrate-containing cell preparation tubes (CPT tubes) were prepared. The venous blood samples were transported to the laboratory in Bamako and PBMCs, plasma and RBC pellet were separated by centrifugation. The plasma was immediately stored at −80°C. RBCs pellets were washed twice in PBS and used freshly or stored at −80°C within three hours. RBC pellets for thawing were mixed with 1.5 x pellet volumes heat-inactivated human AB+ serum and 2.5 x pellet volume glycerolyte or freezing solution.

Detection of clinical malaria and subclinical *P. falciparum* infection

To identify clinical malaria cases, thick smears of all symptomatic participants presenting to the study clinic were stained with Giemsa and parasite densities were determined by the study team

as the number of parasites per microliter of whole blood (based on a mean leukocyte count of 7500 cells/µL) by counting the number of parasites against 300 leukocytes. Two expert microscopists evaluated each smear separately, and a third resolved discrepancies. At cross-sectional timepoints, subclinical infections were detected by rapid diagnostic tests of *P. falciparum* histidine-rich protein II (RDT) with a sensitivity of ~100 parasites/µl (Ratsimbasoa et al. 2008) once the blood arrived in the laboratory.

<u>Laboratory strains of *P. falciparum*</u>

P. falciparum laboratory strains culture
FCR3 *P. falciparum* parasites were cultured in complete RPMI medium (RPMI 1640 medium with L-glutamine and HEPES, 7.4% Sodium Bicarbonate, 100µM Hypoxanthine and 25 mg/ml gentamycin) supplemented with 0.25% Albumax II at 5% haematocrit in human O^{Rh+} erythrocytes at 37 °C either in the presence of a gas mixture containing 5% O_2, 5% CO_2 and 90% N_2 or using the candle jar system previously described by Trager and Jensen 1976. FCR3 iRBCs cultured to use in cytoadhesion assays were maintained in complete RPMI medium supplemented with 0.25% Albumax II and 10 % pooled O^{Rh+} plasma.

Infected RBCs were cryopreserved as 200 µl pellet, 300 µl heat inactivated O^+ plasma pool and 500 µl freezing solution. Blood pellets were thawed at 37 °C, pellet volume was determined and mixed with 0.1x pellet volume 12% NaCl solution while pipetting very slowly and shaking the tube. After 5 min incubation, 10x pellet volume 1.6% NaCl solution was slowly added. The iRBCs were centrifuged and washed in 10x pellet volume complete RPMI volume.

P. falciparum laboratory strain synchronization

Synchronization of culture was carried out by repeated rounds of magnetic enrichment of mature iRBCs(Ribaut et al. 2008), inhibition of invasion by 30 IU/ml heparin, and enrichment of ring stage iRBCs by sorbitol lysis of mature iRBC stages (Radfar et al. 2009).

P. falciparum panning for high-binding profile

To select for binding to human primary endothelial cells, a near-confluent culture of human primary endothelial cells was stimulated with 10 ng/ml TNF in MV2 medium without hydrocortisone for 16-24 h. FCR3 iRBCs were enriched by gelafundin floatation, by mixing the iRBC pellet with 1.4 x pellet volume complete RPMI medium and 2.4x pellet volume gelafundin, mixing, incubation at 37 °C for 15 min and isolation of the non-pellet fraction, followed by 2x washes in complete medium. Infected erythrocytes were then allowed to bind to HDMEC cells in 0.5% BSA supplemented RPMI 1640 medium with L-glutamine and HEPES, pH 6.8, for 30-60 min, with gentle rotation of the flask every 15 min. Unbound cells were removed and the endothelial cells washed 5x wash in 2%FCS/PBS. Complete malaria culture medium with 5% fresh RBCs, and after reinvasion (mostly overnight), iRBCs were transferred to a fresh flask continued to be cultured.

Primary human endothelial cells

Endothelial cell culture

Human microvascular dermal endothelial cells (HDMEC) at passage 2 were purchased from Promocell and thawed according to the manufacturer's instructions. Cells were grown in T25 or T75 flasks in MV2 medium. Before seeding, flasks were incubated with 0.3 ml / cm^3 of MV2 medium to coat the growth area. Cells were split when 90% confluent using the DetachKit. In short, cells were washed in 0.1 ml/cm^3 HBSS, detached with 0.1 ml/cm^3 trypsin solution for 2-5 min at RT while monitoring the cells in an inverted microscope before stopping detachment with 0.1 ml/cm^3 trypsin inhibitor. Cells were pelleted for 3 min at 200 g, resuspended in 2-5 ml MV2 medium and counted as 1:2 dilution in TrypanBlue solution in Kova counting slides. Cell densities in cells per ml was calculated from the average of 3 large squares *2 (dilution factor) * 10. Cells were seeded at minimum 10,000 cells per cm^3 as recommended by the manufacturer and medium was changed every 2-3 days. For cryopreservation, 2.5, 5 or 7.5 * 10^5 cells were taken up in CryoSFM solution and frozen in cryovials in a Styrofoam box at -80 °C. For storage, cells were transferred to the liquid nitrogen tank.

Cytoadhesion assay

Primary human dermal microvascular endothelial cells (HDMEC) were thawed and cultured according to the manufacturer's instructions in MV2 medium and used until passage 8-9. For static assays, HDMEC were seeded and grown to confluency on gelatin-coated coverslips in a 24 well plate format. Infected RBCs at 1-5% parasitemia were washed in binding buffer (0.5% BSA in RPMI pH 6.8) and for binding, 1 µl iRBC pellet was added in 500 µl binding buffer on the cells for 20 min. Coverslips were washed 2x 10 min upside-down in PBS/2%FCS to remove unbound cells. Bound cells were fixed in 1% GA for 30 min at RT or 4 °C overnight, stained in RAL, mounted in DPX and quantified by counting the number of parasite in 10 fields taken using the 10x objective. Inhibition by antibodies was carried out as pre-incubation in 10 µg/ml anti-human CD36 mAbs for 30 min at 37 °C.

Microsphiltration assay

Sample preparation

RBC pellets isolated from CPT tubes of RDT⁺ samples in the dry season and of malaria cases samples in the transmission season were leucocyte depleted using the EasySep CD45 Depletion Kit, according to the manufacturer's instructions. iRBCs were cultured in complete RPMI medium supplemented with Albumax II. To maximize growth potential, iRBCs from clinical cases were diluted 1:10, 1:20 or 1:25 in uninfected RBCs. Microsphiltration was performed as previously described (Deplaine et al. 2011), in duplicates or triplicates at 0, 6, 18 and 30h in culture (and 48h for iRBCs from clinical cases).

Microsphiltration tips preparation

Briefly, calibrated microspheres of 5–15µm and 15–25µm in diameter were mixed at 4g each in 12ml of complete RPMI medium supplemented with Albumax II (no plasma). Filter tips (732–0534, VWR) were cut diagonally on the tip and wet by pushing 200 µl of complete medium through the filter. The bead suspension was vortexed, and 400µl was loaded onto the filter tips, yielding a 1.5-mm layer of microsphere beads. The tips were then filled up with medium and connected to a three-way stopcock. Microsphiltration tips were used within 12h of preparation.

Microsphiltration assay

At each time point, 600 μl of the 2% hematocrit culture was loaded onto the microbead layer and perfused with 5 ml of complete medium at 1 ml min^{-1} using a syringe pump. The upstream and downstream samples were collected at the different time points and stained for *P. falciparum* quantification by flow cytometry. Samples in which parasitemia increased (fold change > 1) between 0 and 30 h (May) or 0 and 48 h (MAL) were included in the analysis.

Electron microscopy

P. falciparum field isolates short term culture for electron microscopy

For culture over one cycle, RBC pellets isolated from CPT tubes in the dry season and of malaria cases' samples in the transmission season were cultured at 1 - 5% haematocrit in complete RPMI 1640 (complete medium with L-glutamine and HEPES, added 7.4% sodium bicarbonate, 100 μM hypoxanthine, 25 mg / ml gentamycin) supplemented with 0.25% Albumax II, at 37 °C in a candle jar until parasites reached young schizont stage (12-18 h for dry season samples and 26-42 h for malaria cases). Malaria cases' samples were cultured undiluted or at 1:10 dilution with non-infected O^{Rh+} erythrocytes, to provide optimal growth conditions. The parasites were then enriched by MACS using LD columns or LS columns with a 27 G needle and to achieve high yields were loaded twice on the column. For washes and elution complete RPMI supplemented with 0.25% Albumax II was used. Pellets were fixed in 4% paraformaldehyde, 0.016% glutaraldehyde in Cacodylate buffer (0.1 M Cacodylate in H$_2$O, pH 7.2) at 4 °C overnight in a low bind Eppendorf tube and stored in 1% PFA and 0.016% GA in Cacodylate buffer at 4 °C.

Transmission electron microscopy

For embedding, pellets were used directly or embedded in 3% low-melt agarose in Cacodylate buffer. Therefore, the agarose solution (3% low-melt agarose in 0.1 M Cacodylate buffer) was dissolved at 80 °C and kept at 37 °C. The sample was pelleted in a 0.5 % BSA coated 0.1 ml tube for 1 min at 2,000 rpm, overlayed with 100 μl agarose solution, infiltrated for 1 min at 37 °C, hardened on ice for 15 min, and then placed in another 0.1 μl tube with 50 μl agarose solution,

infiltrated for 1 min at 37 °C, hardened on ice for 15 min, and cut into cubes using with 1-2 mm edges using razor blades. The following procedure was carried out in 1.5 ml tubes and using 500 µl volume. After 2x 5 min washes in 0.1 M Cacodylate buffer, the pellets were stained with 1% OsO_4 solution for 1h at RT, washed 2x in 0.1 M Cacodylate buffer and 2x in H_2O, stained in 1% Uranylacetat in H_2O over night at 4 °C. Following 2x 5 min washes in H_2O, the samples were subjected to an acetone dehydration series (10 min each in 30, 50, 70, 90 % Acetone in H_2O and 2x 100 % Acetone at RT) and resin infiltrated in 25, 50, 75% Spurr's resin in acetone for 45 min at RT, followed by 100% in Spurr's resin over night at 4 °C. For hardening, the pellet was embedded in ca. 400 µl fresh Spurr's and hardened at 60 °C for 24-48 h. The blocks were trimmed using razor blades and glass knives, and ultrathin sections (70 nm) were retrieved with a diamond knife on an ultramicrotome onto copper grids coated with pioloform film. To obtain more sections of different iRBCs, after a few section 4-5 µm were removed from the block and new 70 nm sections obtained from that area. The sections were contrast stained with 2% uranyl acetate in H_2O and lead citrate solution (1.33 g Pb $(NO_3)_2$ and 1.76 g sodium citrate in 50 ml H_2O) for 3 min each and washed in H_2O. Sections were imaged in a JEOL JEM1400 transmission electron microscope at 12,000 kV and 2x2 fields were stitched to one image. Per donor ~ 20 iRBC were recorded.

Scanning electron microscopy

For scanning electron microscopy, 12 mm round coverslips were thoroughly cleaned by two sonication steps in H_2O, 1h incubation on an orbital shaker in 0.1 N HCl for 1h, 3 washes in H_2O, 1h in 96% EtOH on an orbital shaker followed by 2 washes in H_2O, and storage until use in 96% EtOH. The coverslips were then coated with 0.01% Poly-L-lysine for 15 min and RBC pellets stored in 1% PFA 0.016 % GA in 0.1 M Cacodylate buffer were allowed to settle for 15 min at room temperature. The density of RBCs on the coverslip was monitored through an inverted microscope. After 2x washes in 500 µl Cacodylate buffer, the samples were stained with 500 µl 1% OsO_4 solution for 1h at RT, washed 1x in Cacodylate buffer and 1x in H_2O and subjected to an acetone dehydration series (10 min each in 30, 50, 70, 90 % acetone in H_2O and 2x 100 % acetone at RT, with fast pipetting to prevent drying. The coverslips were then subjected to critical point drying in a critical point dryer, mounted on pins with silver glue and sputtered with a 10 nm film

of palladium gold in a vacuum coater. Images were acquired in a Zeiss Leo 1530 at 2 kV accelerating voltage at 4-6 mm working distance at 12,000 x magnification using the SE2 detector at 3000x2000 image setting in scanning speed 3.

Image analysis

Images were analyzed in Image J. Before analysis, we randomized the image names using the Randomizer macro (https://imagej.nih.gov/ij/macros/Filename_Randomizer.txt). To determine stages, the area of RBC and parasite was measured manually but images were presented using the MeasureAreas macro in batch mode. Scoring for number of nuclei and presence of rhoptries or segmentation was done using EMimages_scoring macro. In TEM images, knob density was determined by counting the number of knobs on the iRBC surface and dividing by the circumference of the iRBC. In SEM images, knobs were counted in a selected plane area of the iRBC, using the KnobDensity macro. For obtaining cropped images of the same size and scalebar, the CropImage macro was used.

Transcription analysis

RNA extraction and cDNA generation

To extract the RNA, up to 250 µl of RBC pellet was taken up in 750 µl Trizol LS, incubated for 10 min at RT and vortexed for 15s to dissolve the RBC pellet. After addition of 200 µl chloroform and a 15 min centrifugation at 12,000 g, the upper organic phase is recovered and nucleic acids are precipitated in 500 µl isopropanol mixed with 2 µl GlycoBlue at -20 °C overnight. After a 60 min centrifugation at 12,000 g at 4 °C, the pellet was washed in 500 µl 70% ethanol, air-dried and resuspended in 18 µl RNase-free water. Remaining DNA was removed using the Invitrogen DNaseI Amplification Grade set according to the manufacturer's instructions. To synthesize cDNA, the SuperScript IV VILO Master Mix with ezDNase or the SuperScript™ IV Reverse Transcriptase in combination with 10 nM dNTPs and Oligo(dT) 20-Primers was used. RNA content was quantified on a Cytation3 reader at 260 nm and sample purity was assessed using the 260:280 nm and 260:230 nm ratios, respectively.

Quantitative RT-PCR

For qPCR reactions, 0.5 µl of cDNA was mixed with each 0.5 µl 100 µM primer, 8 µl DEPC-treated water and 10 µl Power Sybr Green PCR Master Mix (applied biosystems) in 96 well optical plates covered with optical foil and run on a qTower with the following settings: 10 min at 95 °C and 40 cycles of 15 s at 95 °C and 60 s at 60 °C, followed by a melting curve. Expression values were normalized to the *P. falciparum* reference gene glycine-tRNA ligase GlyRS (PF3D7_1420400).

Surface antigen quantification

Surface recognition assay using FCR iRBCs

Plasmas from study participants > 14 years were pooled according to blood type (only Rh$^+$ donors included) (n = 90 (A$^+$), n = 112 (B$^+$), n = 25 (AB$^+$), n = 159 (O$^+$))to obtain a hyperimmune plasma pools. AB+ Serum or O+ plasma pools from 3 malaria-naïve German donors obtained from the blood bank were used as controls. All pools were heat inactivated for 30 min at 56 °C. For the surface recognition assay, based on (Attaher et al. 2019), pellet volumes were 2 µl for the pre-tests and 0.5 µl for field samples. The iRBC pellets were incubated in 50 µl of a 1:10 hyperimmune plasma dilution of the respective blood group at 4 °C overnight. The cells were washed 3x in 200 µl PBS with 1 min centrifugation steps at 1500 rpm and stained in 1:50 anti-human IgG-APC (Biolegend, cat# 409306) in PBS/2%FCS and 1:2000 SybrGreen for 30 min at RT in the dark, followed by 3x washes in 200 µl PBS. For the trypsin control, the iRBC pellet was incubated with 100 µl trypsin solution (Promocell Detach kit) for 30 min at 37 °C and inactivated with 100 trypsin inhibitor, prior to hyperimmune plasma pool binding. The cells were then read in the FITC and APC channel of a flow cytometer and analyzed by FlowJo software.

Surface recognition assay of Malian field samples

Cryopreserved blood samples were thawed as described above. Infected erythrocytes were cultured in complete RPMI with Albumax II at 1 % hematocrit. Blood samples from malaria cases were diluted 1:10 in uninfected RBCs. Per timepoint, 2 µl of blood pellet were stained as described above, using the blood group specific hyperimmune plasma pool. Donors with unknown blood group were labeled with AB$^+$ plasma pool. As not all samples had a malaria-naïve plasma control,

we were not able to correct for unspecific binding in all samples. However, the unspecific binding in the 2 blood samples of donors with clinical malaria was reflected on the flow cytometry plots also in a higher nonspecific binding on the uninfected RBCs (Supplemental figure 3). We therefore screened the samples that didn't have a malaria-naïve serum control for this morphology and identified one other sample with this pattern among the samples without naïve serum control, which was excluded from further analysis (Supplemental figure 3).

Assessment of endothelial activation

Quantification of Inflammation markers in patient plasmas

Levels of TNF were detected in undiluted plasma using the Human TNF-alpha DuoSet ELISA (DY210, R&D systems) according to the manufacturer's instructions and read on a plate reader at 450 and 570 nm. To remove optical imperfections of the plate, the absorbances at 570 nm were deducted from the 450 nm absorbances. The standard was diluted 10-fold, and an asymmetric sigmoidal standard curve was calculated using the 5PL method in Graph Pad Prism, resulting in a range of 1 ng – 1.95 pg/ml TNF. A 7-plex Luminex Human Magnetic Assay (LXSAHM-07, R&D systems) was used to detect soluble plasma levels of ICAM-1, VCAM-1, PECAM-1, E-Selectin, P-Selectin, IL-1α and IL-1β. Plasmas were diluted 2-fold (additional 4-fold duplicate for 4 samples from malaria cases with high TNF levels) and the standards were diluted 8x in 2-fold dilution steps. The assay was carried out according to the manufacturer's instructions, and read on a Luminex 200 device (Bio-Rad) and standard curves were calculated using the 5PL method.

Adhesion receptor expression by flow cytometry

To measure endothelial activation, HDMEC cells at passage 6-9 were seeded on 96 well plates at 10^4 cells/well and grown for 2 days. The cells were then washed in 200 µl Hank's balanced salt solution (HBSS) and incubated with 70 µl 50 % plasma in MV2 medium without hydrocortisone supplemented with 90 µg/ml heparin for 24h. TNF stimulations were performed with 10 ng/ml TNF in MV2 medium without hydrocortisone supplemented with 90 µg/ml heparin (Lansche et al. 2018). To quantify ICAM-1, VCAM-1 and E-Selectin receptor expression, HDMEC cells were washed in HBSS, detached with 70 µl Accutase solution for 2-5 min, followed by addition of 150 µl 2% FBS

in PBS , resuspension of cells before transfer to 96-well round bottom staining plate. The cells were pelleted at 300g for 2 min and incubated with 50 µl 1:200 anti-human ICAM-1 antibody (1µg/µl), 1:200 E-Selectin (1µg/µl), 1:200 VCAM-1 (0.5 µg/µl)or 1:200 mouse isotype control in 2% FCS in PBS for 30 min at 4 °C followed by 3 washes in 200 PBS and incubation with 50 µl 1:200 anti-mouse IgG -AF488 in 2% FCS in PBS. FACS analysis was carried out with a FACS Canto II using the HTS loader and FlowJo software.

P. falciparum adhesion assay on plasma-stimulated endothelium

Multiwell chambered coverslips (CultureWells) were gelatin coated by incubating for 1h at 37 °C in 70 µl autoclave-sterilized 1% gelatin solution, followed by removal of the supernatant and air-drying in the sterile hood. HDMEC cells at passage 6-8 were seeded as 10^4 cells per well in 200 µl MV2 medium by pipetting the cell suspension in the well and allowing the cells to settle for 10 min in the hood without shaking, before transfer to the incubator and incubated for 2 days. The cells were washed in 200 µl PBS and incubated for 4 h with 60 µl of 50% plasma in MV2 medium without hydrocortisone supplemented with 90 µg/ml heparin to prevent clotting of the plasma. For the assay, it is very important to avoid sudden temperature drops or too harsh pipetting, as the cells will detach. Therefore, all reagents were prewarmed to 37 °C, handled only shortly at RT and the chambered coverslips were placed on a prewarmed cool pad in the hood. Cells were washed gently in 200 µl cytoadhesion buffer and then incubated with 0.2 µl FCR3 parasite pellet (44 % parasitemia, ca 35 - 40 hpi) in 100 µl cytoadhesion buffer for 30 min at 37 °C without shaking. To remove unbound RBCs, the wells were washed 4x in 100 µl 1% FCS in PBS, removing all the liquid from the well in each washing step, but proceeding quickly to avoid drying of the cells. The cells were then fixed in 1% glutaraldehyde in PBS for 30 min at RT, the casket removed and the coverslip washed in PBS and stained in May-Grünwald Giemsa solutions (RAL 555 kit) before mounting on coverslips using DPX mounting medium. Images of bound RBCs were acquired with a 40x objective. For quantification, the macro "CountAdhesion" was run as a batch process in ImageJ, which sequentially opens the images, projects a grid onto it. Of each image, 4 squares were counted and the number of adhered RBCs per image was recorded in a separate excel file (the macro does not

save it automatically). Output files were saved as .tif for later reference. The data was then analyzed and plotted in Graph Pad Prism.

3. Results

3.1 *P. falciparum* iRBCs in circulation in the dry season are at higher risk of splenic clearance

To better understand what happens to the more developed iRBC in circulation in the dry season when they pass through the spleen, we implemented a spleen-like filtration assay that uses metal microbeads of different sizes to mimic the geometry of the spleen, termed microsphiltration assay (Deplaine et al. 2011). The assay was first tested with synchronized laboratory strain parasites (FCR3), and then applied to ex vivo and in vitro cultured blood samples from Malian donors.

Stage-dependent retention of *P. falciparum* FCR3 iRBCs in a spleen-like filter

To prepare the spleen-like filters, a suspension of metal beads of 5-15 μm and 15-25 μm diameter was layered onto a filter tip and connected to a syringe pump (Figure 15a). Synchronized FCR3 iRBCs at 2% hematocrit were then loaded on the filter and a constant flow of medium was applied for 5 min. The downstream filtered blood pellet was collected and together with a sample of the unfiltered iRBCs stained with SybrGreen and analyzed by flow cytometry to determine the parasitemia. The gating strategy is shown in Fig. Supplemental figure 1. The % flow-through of filtered samples was calculated as ($\%iRBC_{(downstream)}$ / $\%iRBC_{(upstream)}$ x 100 %) . Using this assay, parasite strain FCR3 ring stage iRBCs (8 and 14 hours post invasion (hpi)) could flow through the filter, while trophozoite stages were increasingly retained (flow through 51.2 % at 20 hpi and 19.7 % at 26 hpi), and of the schizonts stages at 38 hpi, only 15.3 % were able to pass the filter (Figure 15b). In the flow cytometry plots, ring stage iRBCs as present at 8 hpi were still found in the filtered sample, while schizont stage iRBCs (characterized by stronger SybrGreen signal) at 38 hpi were retained in the spleen-like filter and hence not found in the flow-through (filtered sample) (Figure 15c). The flow-through of the 38 hpi schizont stage sample contains almost only ring stages iRBCs (Figure 15c), suggesting that these make up the residual 15.3 % of flow through in the 38 hpi schizont stage sample.
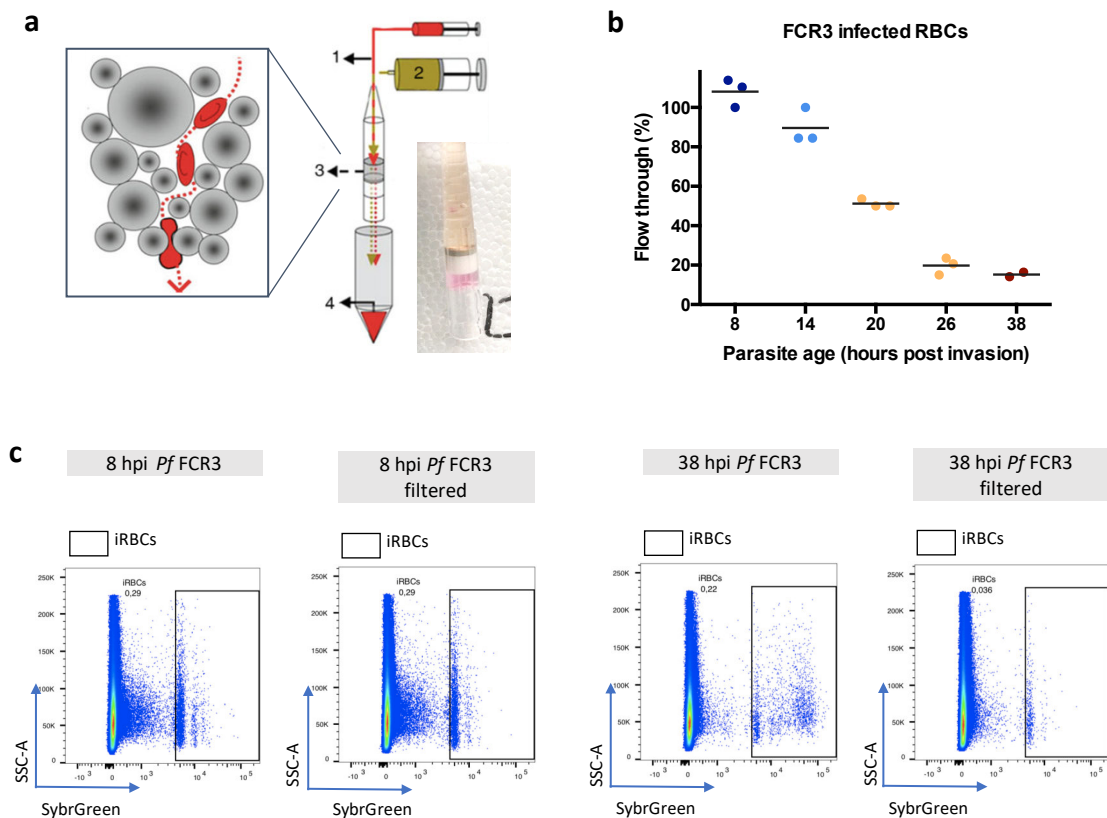
Figure 15: A microsphere-based filtration assay mimics iRBC filtration in the spleen

a) The setup of the spleen-like filter in the microsphiltration assay. Microbeads of 5-25 μm diameter mimic the geometry of the interendothelial slits. An iRBC suspension at 2 % hematocrit is loaded onto the filter (1) and then connected to a syringe pump for continuous flow (2). The bead suspension forms a thin filter layer on the filter of the tip (3). The flow through is then collected (4). Modified from (Lavazec et al. 2012). Inserted photo shows the microsphere layer inside the tip. **b)** *P. falciparum* strain FCR3 iRBCs synchronized to a 3 h window were subjected to microsphiltration. Line indicates mean, triplicates of one experiment are shown, 38 h timepoint only performed in duplicates. **c)** Flow cytometry graphs of selected timepoints of the microsphiltration experiment showing the RBC population with a gate on the iRBCs population, for blood samples before and after passage through the spleen-like filter (filtered).

Circulating iRBC at the end of the dry season are at increased risk of splenic clearance

We then aimed to apply the microsphiltration method in Mali to iRBCs obtained from infected individuals with asymptomatic malaria at the end of the dry season in May (May), or with their first clinical malaria episode in the transmission season (MAL) (Figure 16a).
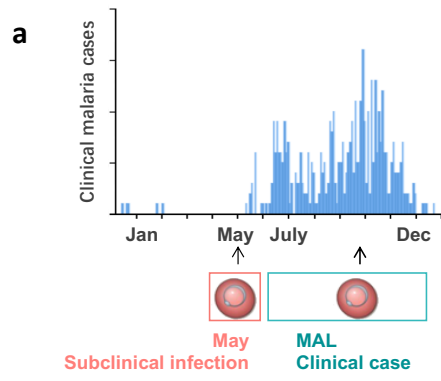
We hypothesized that iRBCs collected at the end of the dry season should be retained in the spleen at higher rates than those collected from malaria cases in the wet season, based on their estimated average age (hpi) within the 48 h development cycle: Parasites from asymptomatic donors at the

end of the dry season (May) were predicted to have an average age of 17 hpi, compared to 7 hpi of iRBCs from clinical cases in the wet season (MAL), based on their transcription profile (Figure 16b) (Andrade et al. 2020). We calculated the averages ages (hpi) of both samples after additional 6, 18 and 30 h of in vitro culture and compared it with the observed filtration rates of FCR3 at different ages (Figure 15b). We expected that most iRBC from clinical malaria cases would be able to pass the filter after 0 and 6 h of in vitro culture, and would start to be retained after 18h of culture, while dry season parasites would already be increasingly retained after 6 h of culture (Figure 15b). We then proceeded to test this experimentally. During the cross-sectional study timepoint in May and at the first febrile malaria episode during the ensuing transmission season, each study participant donated 4-8 ml of blood, which was transported to the laboratory, separated from plasma and white blood cells by centrifugation, washed and tested for *P. falciparum* by rapid diagnostic test (RDT). Blood of RDT+ individuals was depleted of CD45+ cells to remove residual leukocytes, and subjected to short-term culture (n= 16) (May) and 19 (MAL). Because parasite density of malaria cases was much higher than RDT+ individuals at the end of the dry season, we diluted blood samples of malaria cases up to 25-fold. We filtered samples after 0, 6, 18 and 30 h of in vitro culture, with an additional timepoint at 48 h of culture for samples in the transmission season (MAL). Parasitemias were determined by flow cytometry (see Fig. Supplemental figure 1. for the gating strategy), and the blood samples were flown through the spleen-like filter. We excluded 3 end of the dry season samples in May due to extremely low parasitemia (< 0.001), and 1 sample (May) and 5 samples (MAL) for incomplete timepoints. As samples which did not adjust to culture present very high levels of dying parasites that could confound the analysis, we only included samples in the final analysis which showed increased parasitemia (P) within the cycle in culture ($P_{(last\ timepoint)} / P_{(0h)}$) > 1) (Figure 16c) .Eight samples from *P. falciparum* infected asymptomatic donors at the end of the dry season (May) and 8 samples of donors with their first clinical malaria episode in the transmission season (MAL) (Figure 16d) fulfilled the criteria. When filtered through the artificial spleen, iRBCs isolated from clinical cases (MAL) could pass through the filter and this capacity was barely reduced after 6 and 18 h in culture (Figure 16e). However, at 30 and 48 hpi, iRBCs were significantly less able to pass through the filter, as only 24.6 and 43% of iRBC loaded on the filter were found in the flow through, respectively

(Figure 16e). At the end of the dry season however, a third of iRBCs isolated from asymptomatic donors (May) were already retained in the spleen, and already after 6 and 18 h in culture only ~50 % of iRBCs could pass the spleen-like filter (Figure 16e). This corresponds to the significantly higher percentage of non-ring stage iRBCs at 0h in samples obtained at the end of the dry season (Figure 16f), as these stages were expected to have a higher risk of splenic retention. Furthermore, the times of highest retention in both in the dry and the transmission season were paralleled by high levels of schizonts in the culture (Figure 16g). We also analyzed the retention of rings, trophozoite and schizont stage iRBC and observed an overall decrease in the percentage of iRBCs able to flow though the filter as the iRBCs matured (Figure 16h) for iRBCs in the dry season and in the transmission season. However, ring stage iRBCs from asymptomatic donors in the dry season were significantly less able to flow through the filter than ring stage iRBCs from clinical donors in the transmission season, while there was no significant difference in trophozoite or schizont stage iRBC (Figure 16h).
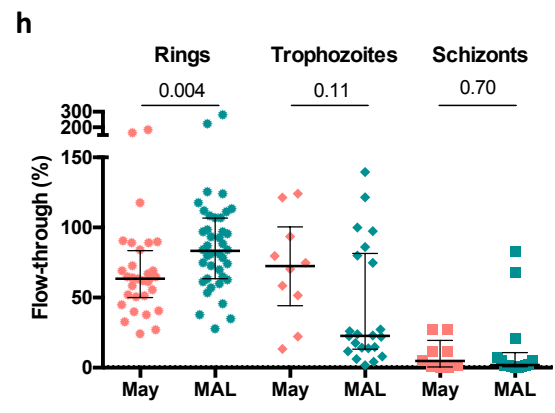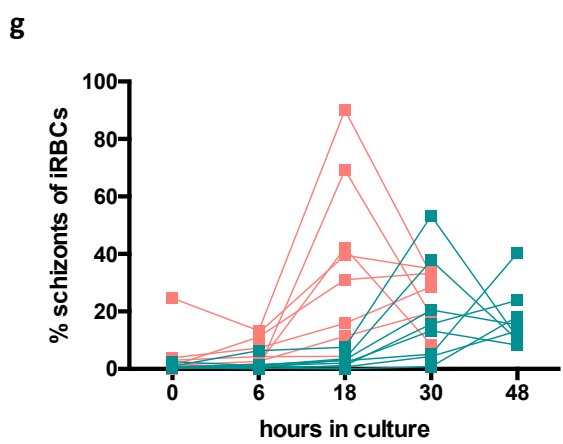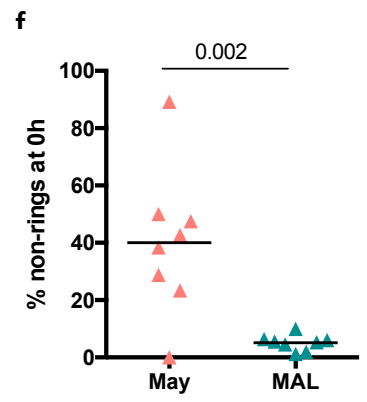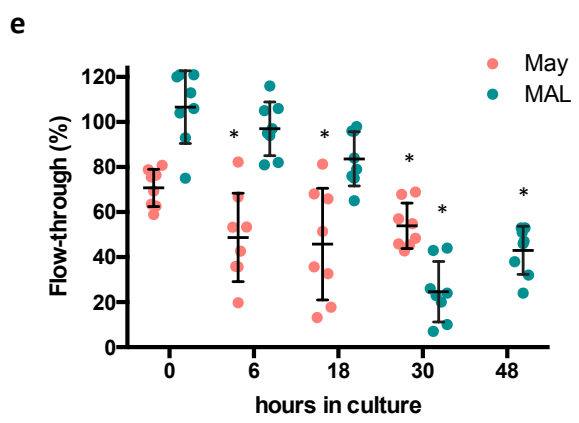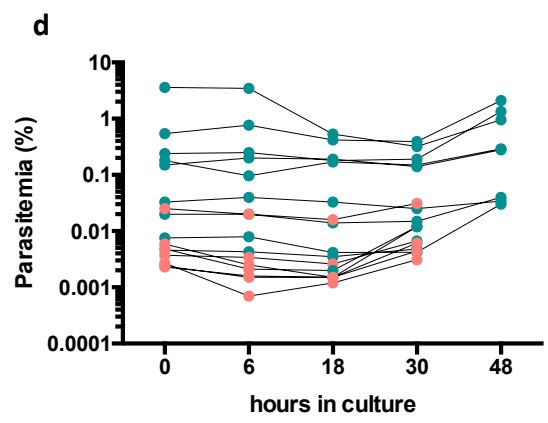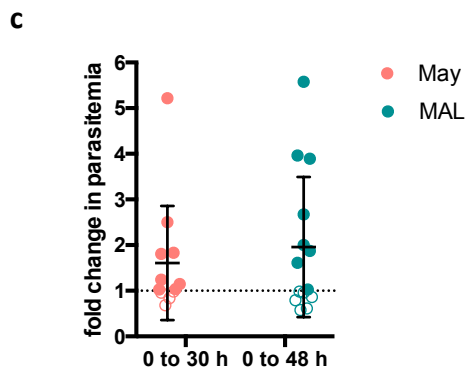
Figure 16: Circulating P. falciparum iRBC at the end of the dry season are at higher risk of splenic clearance

a) Blood samples from subclinically infected donors at the end of the dry season were obtained during the cross-sectional study timepoint in May 2019, while blood samples of donors with their first febrile malaria episode (MAL) were obtained in the transmission season, in August and October 2019. Figure modified after Portugal et al. 2017. **b)** Calculation of parasite age in hpi (hours post invasion) at 0 – 30 hours in culture. Ages at 0h from parasite age estimation based on the transcriptome profile (Andrade et al. 2020). The colors refer to the estimated % of iRBCs in the flow-through after filtration in the artificial spleen, based on the filtration of synchronized FCR iRBC (see Fig b). **c)** Growth of parasitemia in culture was assessed by the increase of parasitemia between start of culture and the last timepoint in culture. Dashed line indicates fold change of 1, al datapoints below did not increase parasitemia and are shown as open circles. n = 14 (MAL) and 12 donors (May). **d)** Delevelopment of parasitemia of all samples that increased parasitemia in culture and were included in the subsequent analysis. Parasitemia were determined by flow cytometry after staining with SybrGreen and MitoTracker. n = 8 (MAL) and 8 (May). **e)** Filtration of P. falciparum iRBC of subclinical donors at the end of the dry season (n = 8, May) and with clinical malaria during the transmission season (n = 8 MAL). Flow-through percentage is defined as (average of triplicate downstream %iRBCs/upstream %iRBCs) × 100. Data indicate mean ± SD; Dunn's multiple comparisons test of the mean rank of each condition compared to 0-h MAL; * shows $P < 0.001$. **f)** Percentage of non-ring stage iRBCs circulating at the end of the dry season and during malaria cases (n = 8 May, 8 MAL) determined by flow cytometry. Line indicates the mean; unpaired t-test. **g)** Percentage of schizont stage iRBCs during one cycle of in vitro culture at the end of the dry season and during malaria cases (n = 8 May, 8 MAL) as determined by flow cytometry. **h)** Filtration rates of ring, trophozoite and schizont stage iRBC, calculated as (average of triplicate downstream % of RBCs/upstream % of RBC) × 100. For trophozoite and schizont stages, only timepoints with n = ≥ 20 iRBCs of the respective stage. Rings: n= 31 (May) and 40 (MAL), trophozoites n = 10 (May) and 22 (MAL), and schizonts n = 9 (May) and 14 (MAL). Line at median ± IQR. P-values of Mann-Whitney test shown.

Reducing cytoadhesion is sufficient to cause longer circulation and increased risk of splenic retention

The increased risk of retention and clearance in the spleen of iRBC during the dry season could be the result of a difference in adhesion, leading to iRBCs in circulation that are more developed within the 48 h cycle. In collaboration with Dr. Mario Recker at the University of Exeter, we explored these data in a mathematical model (see also Andrade et al, 2020). The model follows the within-host growth and removal of iRBCs from circulation through cyto-adhesion in the vasculature and through splenic retention. In the model setup, young iRBCs were assumed not to cytoadhere and not to be removed by the spleen, while mature-stage infected RBCs that cytoadhered were counted as replicating and mature non-adhering iRBCs as eliminated in the spleen. With these assumptions, we modeled the growth of parasitaemia in the host with low- or high-cytoadhering iRBCs for 5 intra-erythrocytic development cycles (Figure 17a). As high-cytoadhering iRBCs were already adherent by the time they would be filtered in the spleen, they could replicate and hence strongly increased parasite density. In contrast, a fraction of the low-adhering iRBCs did not adhere and were removed by the spleen, leading to a reduced effective growth rate and population size after 5 cycles (Figure 17a). To see the effect of different cytoadhesion efficiencies on the length of time in circulation, we retrieved the iRBC age distribution of the low- and high-cytoadhering populations (averaged over multiple sampled timepoints) from the simulated developmental cycles, similar to blood sampling from a population, and observed a narrow age range of high-cytoadhering iRBCs but a broader range for low-adhering iRBCs (Figure 17b). This was a result of the high-cytoadhering iRBCs leaving circulation early by cytoadhesion, while low-adhering iRBCs remained in circulation longer and were removed from circulation with a higher age by the spleen (compare with Figure 17a). These age patterns were also observed on thick blood smears from iRBCs at the end of the dry season (broad age range) and in clinical cases (narrow age range) (Figure 13). We also modeled how these sampled iRBC populations, with an age-dependent retention profile, would be susceptible to splenic clearance over the course of their development, much like the microsphiltration experiment described in Figure 16e. In this simulation, high-cytoadhering iRBCs initially passed the spleen-like filter and were increasingly retained as they matured, while low-cytoadhering iRBCs were retained earlier in the spleen, but flow-through varied less over the timecourse due to the

lower synchronicity of the iRBC population. Again, the simulation matched well with the experimental data (Figure 16e). Altogether, it suggests that a difference adhesion efficiency is sufficient to produce the difference in time in circulation, rendering these more mature iRBCs in circulation at higher chance to be cleared by the spleen.
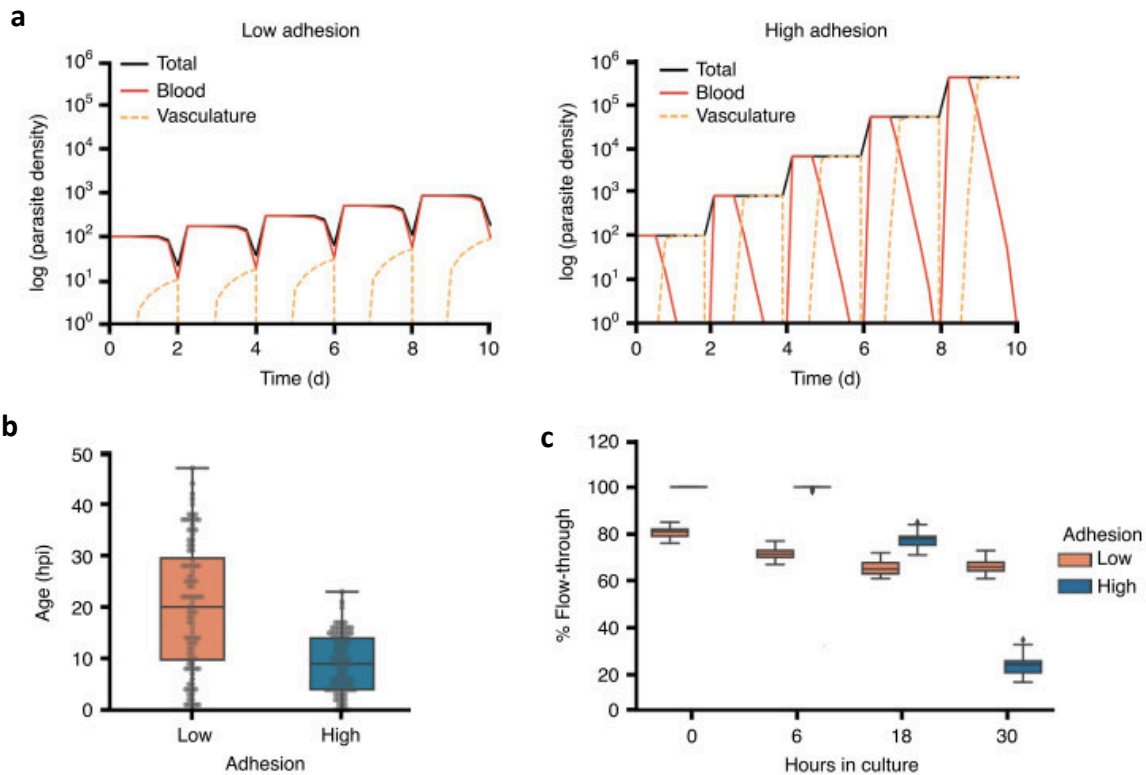
Figure 17: Mathematical model of the interplay of cytoadhesion, time in circulation and splenic retention

a) Within-host dynamics simulation of growth rates and population sizes over five replication cycles of low-cyto-adhering (left) and high-cyto-adhering (right) parasites, stratified as circulating (red lines), cyto-adhering (orange dashed lines) and total biomass (black lines). **b)** Simulation of circulating parasite age distribution over two replication cycles after repeated sampling of low-cyto-adhering parasites (Low, n = 100) and high-cyto-adhering parasites (High, n = 100). **c)** Simulation of circulation and passage through the spleen of independently sampled parasites aging over time, with low-cyto-adhering (Low, n = 50) and high-cyto-adhering (High, n = 50) parasites. Figure from Andrade et al. 2020, mathematical model by Mario Recker.

Subclinical *P. falciparum* carriage in the dry season does not lead to splenomegaly

Grade 0: Normal, impalpable spleen

Grade 1: Spleen palpable only on deep inspiration

Grade 2: Spleen palpable on mid clavicular line, half way between umbilicus and costal margin

Grade 3: The spleen expands towards the umbilicus

Grade 4: The spleen goes past the umbilicus

Grade 5: The spleen expands towards the symphisis pubis

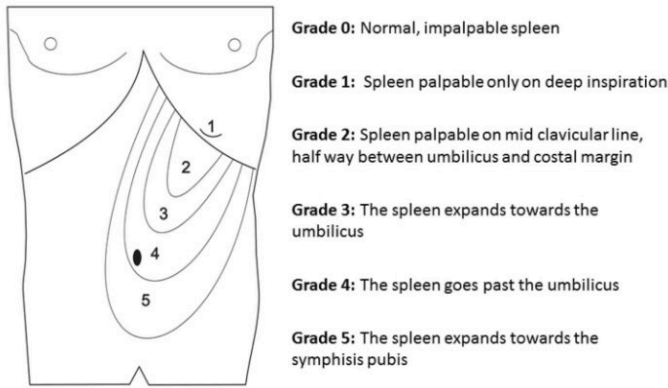*Figure 18: Hackett's grading system for palpable splenomegaly*

Illustration from Laman et al. 2015, based on Hackett 1944.

We then wondered whether the prominent role of the spleen during the dry season would manifest in a higher prevalence of enlarged spleens in asymptomatic *P. falciparum* carriers compared to uninfected individuals at the end of the dry season. At study enrollment and each cross-sectional timepoint, the study participants were examined by study doctors and spleen size was recorded using the Hackett's score, with 0 for no enlargement, and 1-5 representing increasing levels of enlargement as determined by palpation (Figure 18) (Hackett 1944). At enrollment in 2011, 14.5% of study participants presented with enlarged spleen, representing 5.6 % of uninfected individuals (Pf⁻) and 25.2 % of *P. falciparum* infected individuals (Pf⁺) as detected by PCR (Table 2). The association with infection status was significant (χ^2 (4, N = 695) = 56.9, p < 0.001). In the following dry seasons however, enlarged spleens were a rarely diagnosed in both asymptomatically infected (Pf⁺) and uninfected children (Pf⁻) (as determined by PCR) with only 1.3 and 3.4 % of infected children presenting with enlarged spleens (Table 2). This suggests that carrying *P. falciparum* parasites during the dry season doesn't lead to increased spleen size.

Table 2: Spleen sizes at the end of the dry season in May

		2011		2012		2013	
		Pf -	Pf +	Pf -	Pf +	Pf -	Pf +
	n	378	317	426	154	404	178
Hackett score	0	357	237	426	152	401	172
	1	1	2	-	1	-	2
	2	15	55	-	1	2	4
	3	4	23	-	-	1	-
	4	1	-	-	-	-	-
	5	-	-	-	-	-	-
% splenomegaly		5.6	25.2	0.0	1.3	0.7	3.4

Blood samples taken in May of indicated year. Pf +: *P. falciparum* infected donors; Pf -: uninfected donors. Infection status was determined based on thick smears (2011) and PCR (2012 and 2013).

3.2 Host cell remodeling is not strongly altered in dry season *P. falciparum* iRBCs

To better understand how *P. falciparum* iRBCs in the dry season circulate longer, we questioned if host cell remodeling, which allows the parasite to traffic adhesion ligands to the iRBC surface and present them in knobs, is less efficient or altered in the dry season. We therefore analyzed the parasite's ultrastructure, looking for differences in the morphology, density and positioning of knobs and Maurer's clefts. We compare these features in stage-matched iRBC as identified by morphology in the ultrastructure. This was important, as the dynamics of host cell remodeling are iRBC stage dependent, but iRBCs from the dry season and clinical cases in circulation differ in their mean developmental age and synchrony. We aimed to investigate late trophozoites/young schizonts, as they have already substantially remodeled their host cell and can be enriched by magnetic cell sorting (MACS).

Isolating iRBC from low-parasitemia asymptomatic donors for electron microscopy

To study differences in host cell remodeling by electron microscopy, we collected parasites from subclinically infected donors at the end of the dry season (May) which were identified by rapid diagnostic test, and from malaria cases in the wet season from age-matched individuals (MAL). The RBCs were cultured until the mature trophzoite/schizont stage and iRBCs were enriched magnetically. The workflow is shown in Figure 19a. As dry season parasites in circulation were more developed, they were cultured for 12 or 18 h, while parasites from clinical cases after 18 hours in culture still contained mostly young stages and hence required further culturing until similar developmental stages as those in May samples were observed on Giemsa-stained smears, resulting in culture times of 26 - 32 or 42 h. Representative images of isolated Giemsa-stained iRBC are shown in in Figure 19b.

Table 3: Demographic data of donors of electron microscopy samples

Visit	n	age (years, 95% CI))	% female	time in culture (h, 95% CI)
May	13	16.3 (15.9 − 16.8)	30.8	14.8 (12.9 − 16.7)
MAL	10	13.0 (10.2 − 15.6)	50.0	32.5 (28.0 − 37.0)
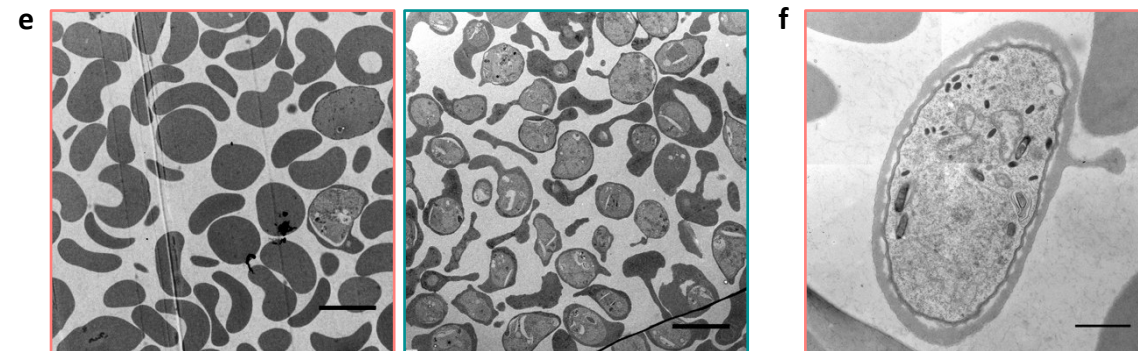
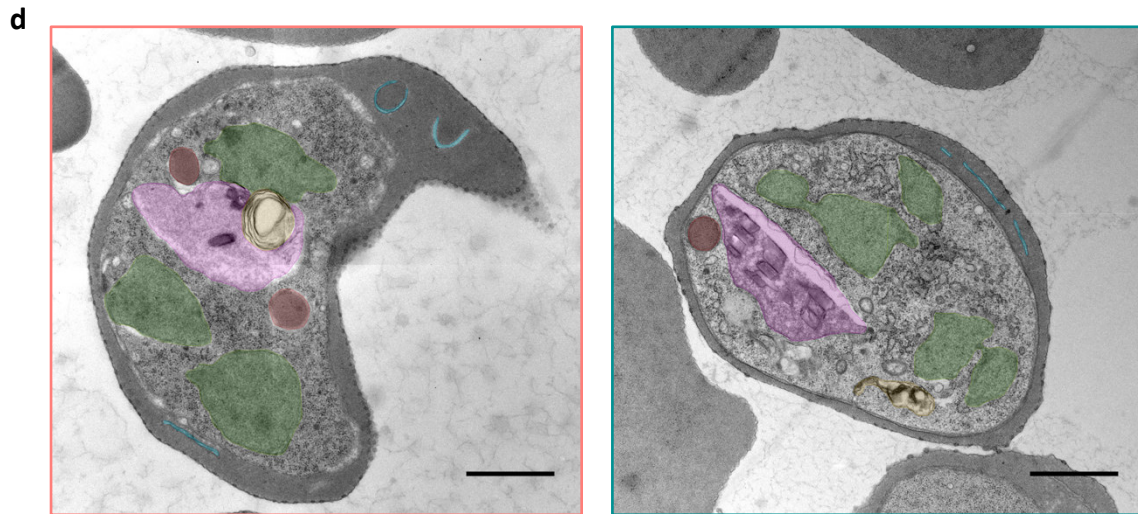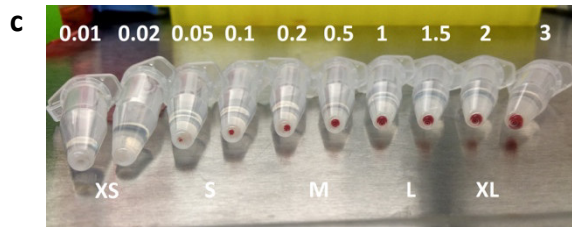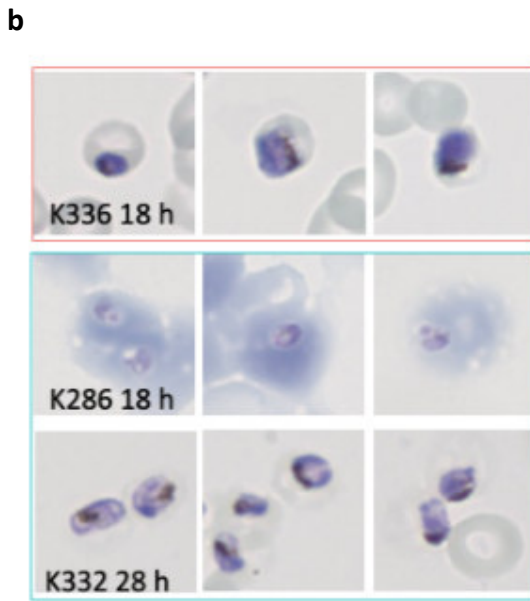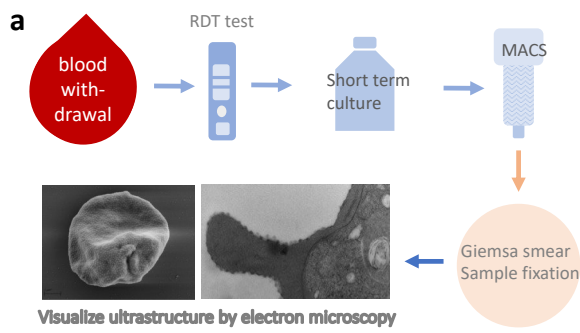*Figure 19: Ex vivo culture and sample preparation of iRBCs for electron microscopy*

a) Workflow of sample processing for electrion microscopy. During the May cross-sectional timepoint, or when a study participant had a malaria episode, 4-8 ml of blood was drawn and, in the case of May samples, tested for P. falciparum parasites by rapid diagnostic test (RDT). The blood samples were then cultured until they reached a young schizont stage, magnetically enriched (MACS) and a thin smear was prepared, and the samples were fixed for subsequent electron microscopy analysis. **b)** Giemsa smears of donor K0336 in May after 18h of culture and magnetic enrichment, or of iRBCs isolated from donor K286 during the first febrile malaria episode of the season (MAL) after 18 and 28 h in culture. **c)** Example of pellet sized as listed in Table X. The tubes contain the amount of RBCs (in µl) as indicated above, and on this basis pellet sizes of enriched mature stage iRBCs were classified from XS to XL. **d)** Two examples of iRBCs isolated during the dry season (May, salmon color) or a clinical case (MAL, aqua frame). A few characteristic ultrastructural details are highlighted in color. The parasites contain several nuclei (green) and takes up RBC cytosol in food vesicles, which will be transported to the food vacuole (violet) and metabolized to hemozoin crystals. The apicoplast is visible as multi-membrane organelle, tho not well preserved here. The parasite cytosol is packed with ribosomes and rough endoplasmatic reticulum can be observed. In the RBC cytosol, Maurer's cleft are found (blue) and on the RBC surface many knobs are found. Scale bars 1 µm. **e)** Overview images of a TEM section of May (salmon) and MAL (aqua) samples. Scale bar 5 µm. **f)** Infrequently, gametocytes are found, here in a May sample. Scale bar 1 µm

Parasitemias in the dry season are very low, and even after enrichment parasitemia varied but could be below 1%. To be able to image sufficient iRBCs in one sample, the a minimal parasitemia of 0.5 % was set to proceed for electron microscopy analyses. Additionally, the total volume of pellet varied from ca. 5 µl down to barely visible pellets, and was classified to size XS to XL. To visualize how small pellets could be, a serial dilution of RBC pellet and their grouping to the respective categories is shown in Figure 19c. Of each sample, images of ~20 parasites were acquired by transmission electron microscopy (TEM). An example of iRBCs from both seasons and the ultrastructural features observed is shown in Figure 19d. In general, imaging May samples was tedious as finding iRBCs under the electron microscope took longer than for MAL samples (Figure 19e). Occasionally, a gametocyte was detected under the electron microscope (Figure 19f).

Aligning parasites from dry and transmission season to similar developmental stages

The host cell is increasingly remodeling as the parasite matures, building the trafficking machinery and placing more and more knobs on the iRBC surface (Grüring et al. 2011; Quadt et al. 2012). We therefore sought to match the samples by iRBC stage and categorized each iRBC image obtained by TEM to one of five groups from young trophozoites to segmented schizonts based on their size within the RBC, the presence of multiple nuclei, rhoptries and signs of segmentation (Figure 20a). When comparing the composition of all parasite stages, we found them to vary between donors (Figure 20b).
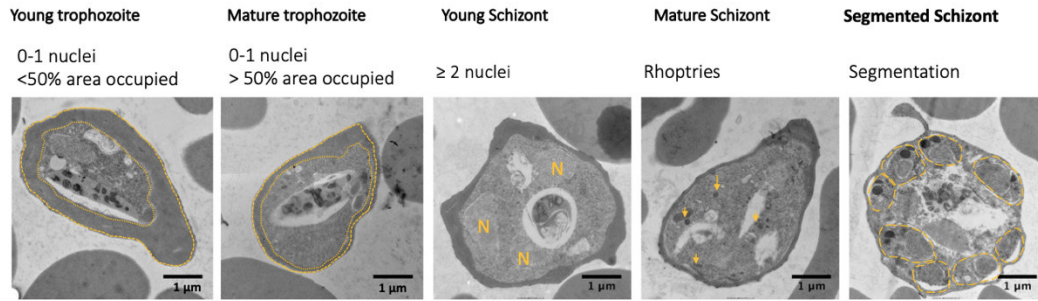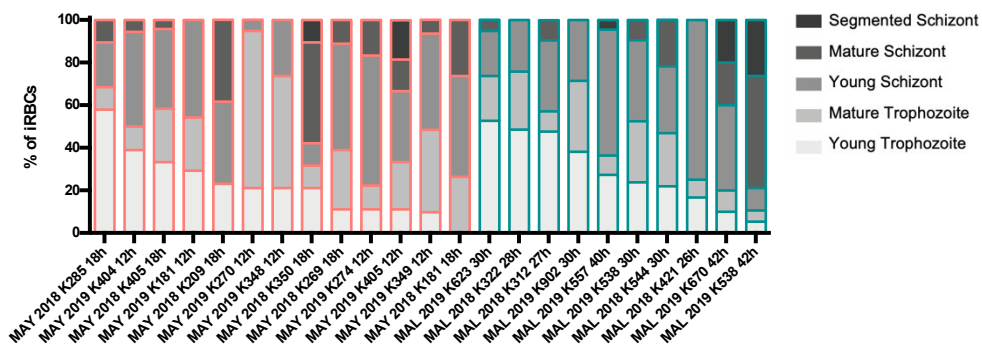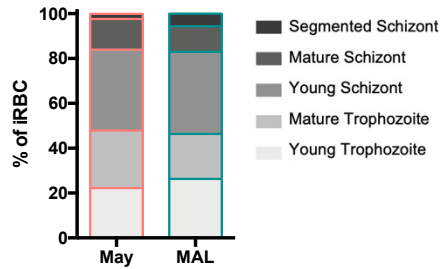
Figure 20: Identifying samples with similar stage composition

a) TEM images of iRBCs were categorized into the indicated stages from young trophozoite to segmented schizont based on the relative size (area parasite/area RBC), number of nuclei (N) and presence of rhoptries (arrows) or segmentation (dotted lines circling individual merozoites within a schizont). b) Categorizing each iRBC results in a unique stage distribution of iRBCs per individual donors at the end of the dry season (May, salmon color) or with the first febrile malaria episode in the transmission season (MAL, aqua color). For each donor, the year of collection, the donor ID and the time in culture is indicated. As many MAL donors contained iRBC with mostly young schizonts, all donors with more than 60 % young trophozoites (dotted line) were excluded from the analysis (x). c) The iRBC stage composition of the combined donors with asymptomatic infection at the end of the dry season (May, n = 13 donors and 268 images) or clinical malaria (MAL, n = 10 donors and 220 images).

As expected, longer time in culture also led to more mature stages. Culturing samples for different lengths of time allowed obtaing equivalent stage compositions between samples of the dry and transmission seasons. As many of the blood samples from clinical cases contained mainly early stages which appeared to not have developed well in culture and could disturb our analysis, we decided to exclude all MAL donors with > 60 % young trophozoite stages. All considered, we gathered a collection of donors with similar iRBC stage composition between May and MAL, that allowed us to compare host cell remodeling between the seasons. (Figure 20c). The dataset consisted of 240 images from 13 asymptomatic donors from the end of the dry season (May) and 202 images from 10 donors with clinical malaria (MAL) and demographic data is given in Table 3. Data on the individual donors is shown Supplemental table 1.

Knob density is not altered during the dry season

As the presentation of PfEMP1 in knob structures is essential for adhesion under flow conditions (Crabb et al. 1997), we determined the knob density first using transmission electron micrographs of iRBCs from asymptomatic carriers at the end of the dry season (May) and clinical cases in the wet season (MAL) (Figure 21a). We found variability in knob density between individual donors within May and within MAL samples (Figure 21b) and observed that the mean knob density increased as parasites matured, but found no significant difference between paired parasite developmental stage of the seasons (Figure 21c). Also, when measurements from all donors of each season were combined, the mean density was not significantly different (Figure 21d). Knob density was also determined on scanning electron microscopy images (Figure 21e) of samples from the same donors. Again, knob density in iRBCs from May and from clinical cases (MAL) vary within and between donors (Figure 21f), but were not significantly different between the seasons, with knob densities of 52.4 ± 24.6 (May, mean± SD) and 50.1 ± 19.0 knobs/μm^2 (MA, mean± SD), respectively (Figure 21g).
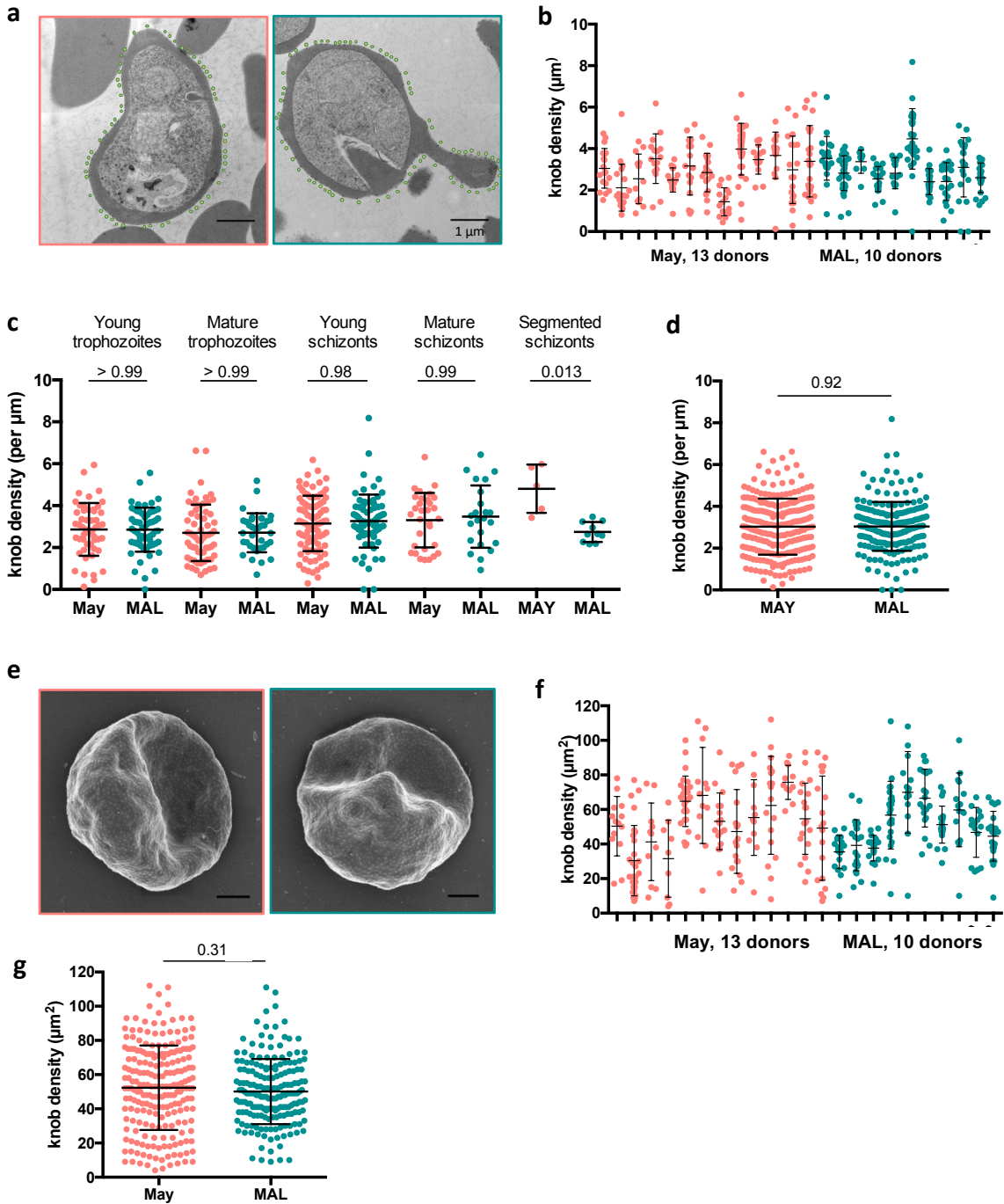
Figure 21: Similar knob density between May and MAL iRBCs as quantified on TEM and SEM images

a) Knob density was determined on transmission micrographs of iRBCs obtained at the end of the dry season in May (salmon) or of clinical cases during the wet season (MAL, aqua) by assessing the number of knobs relative to the RBC circumference (knobs/μm) (knobs marked by green dots). Scale bar 1 μm. **b)** Knob density of iRBCs by donor. Each dot represents one iRBC image. Mean ± SD. **c)** Knob density per iRBC separated by iRBC stage categories. Mean ± SD, Sidak's multiple comparisons test. **d)** Combined comparison of the knob density of all iRBCs from 13 donors asymptomatically infected at the end of the dry season (May, 240 images) and 10 donors with clinical malaria in the transmission season (MAL, 202 images). Mean ± SD, unpaired t-test. **e)** Scanning electron micrographs of iRBCs obtained from asymptomatically infected donors at the end of the dry season in May (salmon) or of clinical cases during the wet season (MAL, aqua). Scale bar 1 μm. **f)** Knob densities as measured by SEM, shown by donor. Mean ± SD. **g)** Combined knob densities of all iRBCs from 13 donors asymptomatically infected at the end of the dry season (May
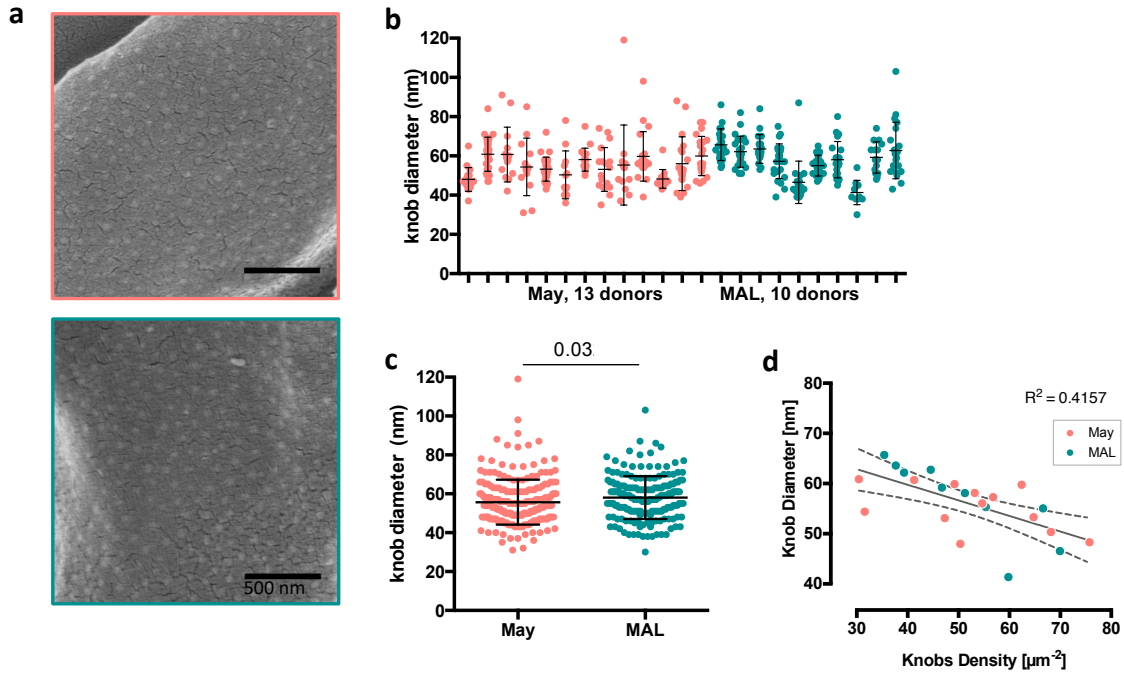
Figure 22: Quantification of knob diameters by scanning electron microscopy

a) Scanning electron micrographs of knob structures on iRBCs obtained from asymptomatically infected donors at the end of the dry season in May (salmon) or of clinical cases during the wet season (MAL, aqua). Scale bar 500 µm. **b)** Knob diameters as determined by SEM, by individual donors. Each dot represents an image of an iRBC. Mean ± SD. **c)** Knob diameters of 233 iRBCs of 13 donors (May) and 191 iRBCs of 10 donors (MAL). Mean ± SD, unpaired t-test. **d)** Correlation of mean knob diameter and mean knob density as determined on SEM images of iRBC from asymptomatic Pf carriers at the end of the dry season (salmon) or clinical cases in the transmission season (aqua). Each dot represents a donor. Line shows linear regression, dotted line marks the 95% confidence interval.

Knob diameter is slightly reduced in the dry season

We then measured knob diameter in the scanning electron micrographs (Figure 22a) from asymptomatic carriers at the end of the dry season (May) and clinical cases in the wet season (MAL). We observed that knob diameters ranged between 30 and 119 nm, with mean knob diameters between 41 and 66 nm in different donors (Figure 22b). Overall, the average diameter in samples from May was 55.7 ± 11.6 nm and 58.0 ± 11.0nm (mean ± SD) in iRBCs from clinical cases (MAL), presenting a small but significant difference (p = 0.032) (Figure 22c). In general, we observed that the knob diameter and knob density, as measured on SEM images, were inversely correlated in our samples (Figure 22d).

Maurer's clefts morphology is slightly altered in dry season parasites

Knocking-out of genes coding for Maurer's cleft proteins like Pf332 (Glenister et al. 2009), SBP1 (Cooke et al. 2006) or PTP1 (Rug et al. 2014) have been reported to lead to loss of iRBCs adhesion as well as aberrant Mauer's cleft morphology. Thus, we analyzed Mauer's cleft number, length and position in transmission electron images (Figure 23a) from asymptomatic carriers at the end of the dry season (May, n = 13) and clinical cases in the wet season (MAL, n = 10). When we determined the number of MCs present on a iRBC section, we found 3 (2-5) (median and IQR) Maurer's clefts in samples from the end of the dry season (May) and 2 (1-4) (median and IQR) in samples from donors with their first clinical episode in the transmission season (Figure 23b). Maurer's clefts were similar in length with median 274 (152 – 448, IQR) nm (May) and 309 (168 – 477, IQR) nm (MAL) (Figure 23c). In trophozoites and schizonts iRBCs, Maurer's clefts are tethered to the erythrocyte membrane (Grüring et al. 2011). To test whether tethering was equally efficient in May and MAL samples, we measured the distance from the closest point of erythrocyte membrane to Maurer's clefts and found that iRBCs in the dry season present with the Maurer's cleft slightly more distant to the PM (May: media 184 (153 – 214, IQR) nm and MAL: 160 (135 – 188, IQR) nm). In May samples, the average distance was 184 nm, compared to 160 nm in MAL samples. While small, the difference was statistically significant ($p < 0.001$). (Figure 23d). We also quantified stacked Maurer's clefts that can appear when separation of the clefts is impaired (Hanssen, Hawthorne, et al. 2008; Glenister et al. 2009). Most iRBCs had only unstacked Maurer's clefts (Figure 23e), and the few iRBCs showing stacked Maurer's clefts cluster more with individual donors than between seasons (Figure 23f).

In summary, the ultrastructure analyses of iRBCs show that typical features of host cell remodeling as knobs and Maurer's clefts are also found in dry season iRBCs and appear highly similar to iRBCs from malaria cases, with only very small differences in knob diameter and MC number and positioning.
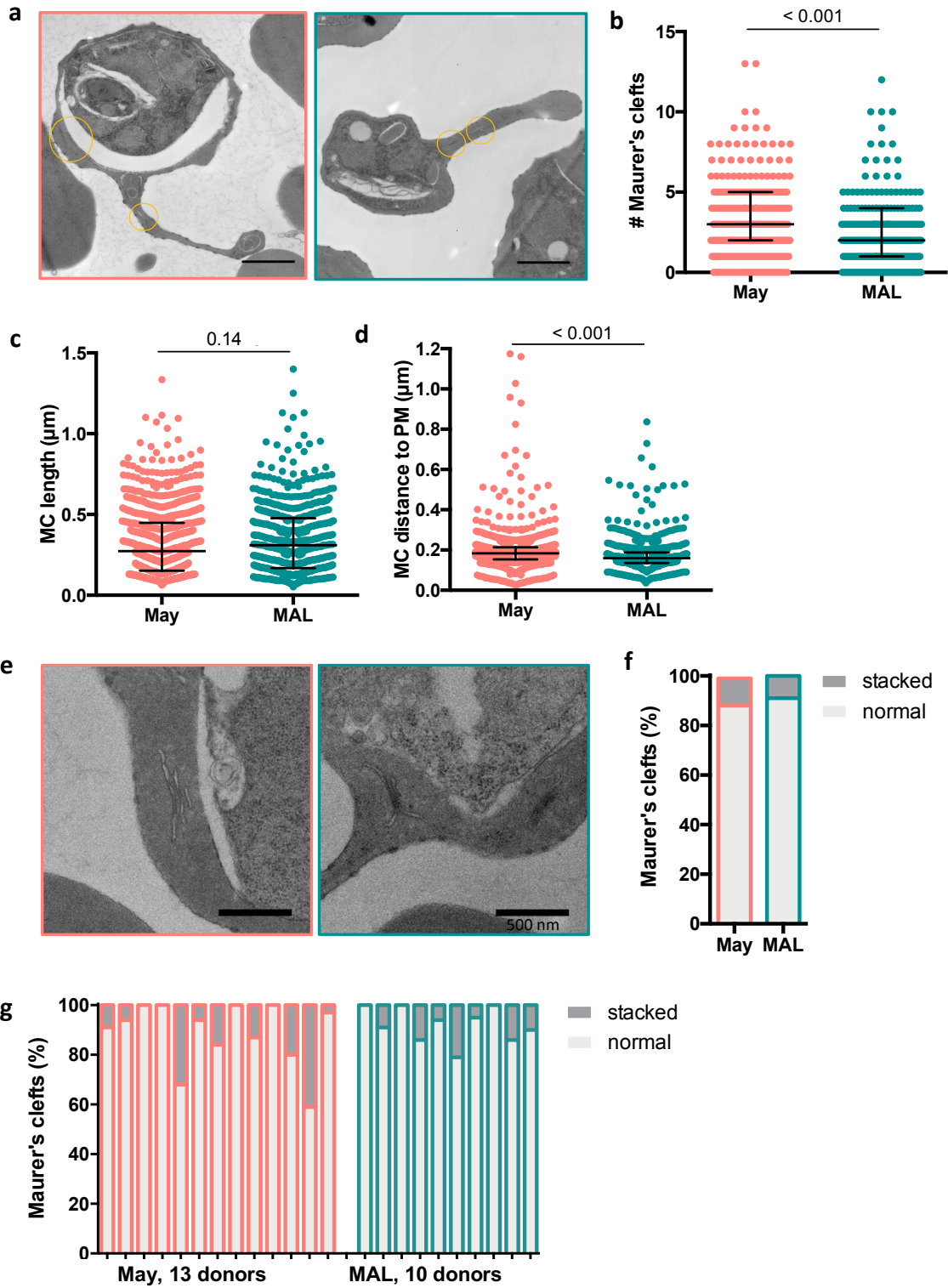
Figure 23: Morphology and quantification of Maurer's clefts in transmission electron micrographs

a) Transmission micrographs of iRBCs obtained from asymptomatic individuals at the end of the dry season in May (salmon) or of clinical cases during the wet season (MAL, aqua) with Maurer's clefts circled in yellow. **b)** Number of Maurer's clefts per iRBC. Each dot represents one iRBC. N = 271 of 13 donors (May) and n = 227 of 10 donors (MAL). Bar shows median ± IQR. Significance test by Mann-Whitney test. **c)** Length of Maurer's clefts. Each dot represents a Maurer's cleft, n = 881 of 13 donors (May) and n = 578 of 10 donors (MAL). Bar shows median + IQR, Mann Whitney test. **d)** Closest distance of Maurer's clefts to the RBC membrane. Each dot represents a Maurer's cleft, n = 881 of 13 donors (May) and n = 578 of 10 donors (MAL). Bar shows median + IQR, Mann-Whitney test. **e)** Examples of stacked Maurer's clefts as observed on TEM images of asymptomatic individuals at the end of the dry season in May (salmon) or of clinical cases during the wet season (MAL, aqua) . **f)** Percentage of unstacked (light grey) and stacked (grey) Maurer's clefts in iRBCs of asymptomatic *Pf* carriers in May (n = 271 of 13 donors) and clinical malaria cases (MAL, n = 227 of 10 donors). **g)** Percentage of unstacked (light grey) and stacked (grey) Maurer's clefts in iRBCs shown by donor, of asymptomatic *Pf* carriers in May (n = 13) and clinical malaria cases (MAL, n = 10).

Analyzing expression of host cell remodeling related genes

To better understand if these small differences in host cell remodeling might impact iRBC circulation time, and whether parasites adhesion ligands may not be properly transported to the iRBC surface, we investigated the expression levels of genes involved in host cell remodeling and adhesion ligand trafficking.

In iRBCs of subclinically infected donors from the dry season (May) and clinical cases during the wet season (MAL), we analyzed five genes which previous knockouts led to the absence of PfEMP1 surface expression and adhesion, and also included the knob protein KAHRP in the analysis (Table 3). Expression levels of each gene were first quantified in synchronized M2K1 iRBCs, a clonal culture-adapted parasite strain derived from Malian blood donors, along the 48h cycle at 2, 9, 18, 25, 33 and 41 h post invasion (Figure 24a and d). KAHRP was expressed throughout the cycle and showed very high levels at 25 hpi. Expression of MAHRP1 and GEXP07 gradually increased until 25h hpi, while PTP1 expression peaked very early at 2 hpi, and SBP1 expression was more stable between 2 and 25 hpi;. Pf332 however was only expressed in the second half of the cycle and peaked at 33 hpi.

Table 4: Characteristics of qRT-PCR samples

Visit	n (all)	n (complete timepoints)	Age (years, 95% CI)	% Female	% hemotype AA
May	15	10	15.8 (14.1 – 17.6)	13.3	100.0
MAL	13	9	14.2 (12.8 – 15.5	38.5	92.3

We then quantified the transcription of these six genes in iRBCs from donors at the end of the dry season (May, n= 15) and with the first febrile malaria case in the transmission season (MAL, n = 13) (Table 5) (see Table 4 and Supplemental table 2 for data on all included donors). The expression levels in parasite freshly collected from the donors and during the first cycle in culture are shown in Figure 24b and e. Expression levels varied strongly between donors, and iRBCs samples from clinical cases (MAL) recapitulated the rise and fall of expression of KAHRP, MAHRP1 and GEXP07 as observed in synchronized ring-stages of M2K1 iRBCs (Figure 24b) and also the expression patterns of PTP1, SBP1 and Pf332 (Figure 24e). The iRBCs collected in May, on the other hand showed a distinct pattern and the difference between highest and lowest expression was less pronounced, possibly due to a more mixed population. Independent of the timepoint, the maximal expression levels in May samples compared to MAL in the donors at any time within the time course were similar in KAHRP, GEXP07, Pf332 and PTP1 but significantly lower in MAHRP1 ($p <$ 0.001) and SBP1 ($p = 0.008$) (Figure 24c and f).

Table 5: Host cell remodeling genes analyzed by qRT-PCR

Gene name	Localisation	Adhesion under flow	Surface PfEMP1 on host RBC	PfEMP1 localisation	Reference
PTP1	MC, RBC cytoplasm	None	None	PVM	Maier et al 2008
SBP1	MC	None	Partial	PVM/MC	Maier et al 2008
MAHRP1	MC	(no adhesion in static assay)	None	PVM	Spycher et al 2008
Pf332	MC/RBC skeleton	Partial	Partial	MC	Glennister et al 2009
GEXP07	MC / RBC surface	None	None	PVM/MC	McHugh et al 2019

MC: Maurer's cleft, PVM: parasitophorous vacuole membrane
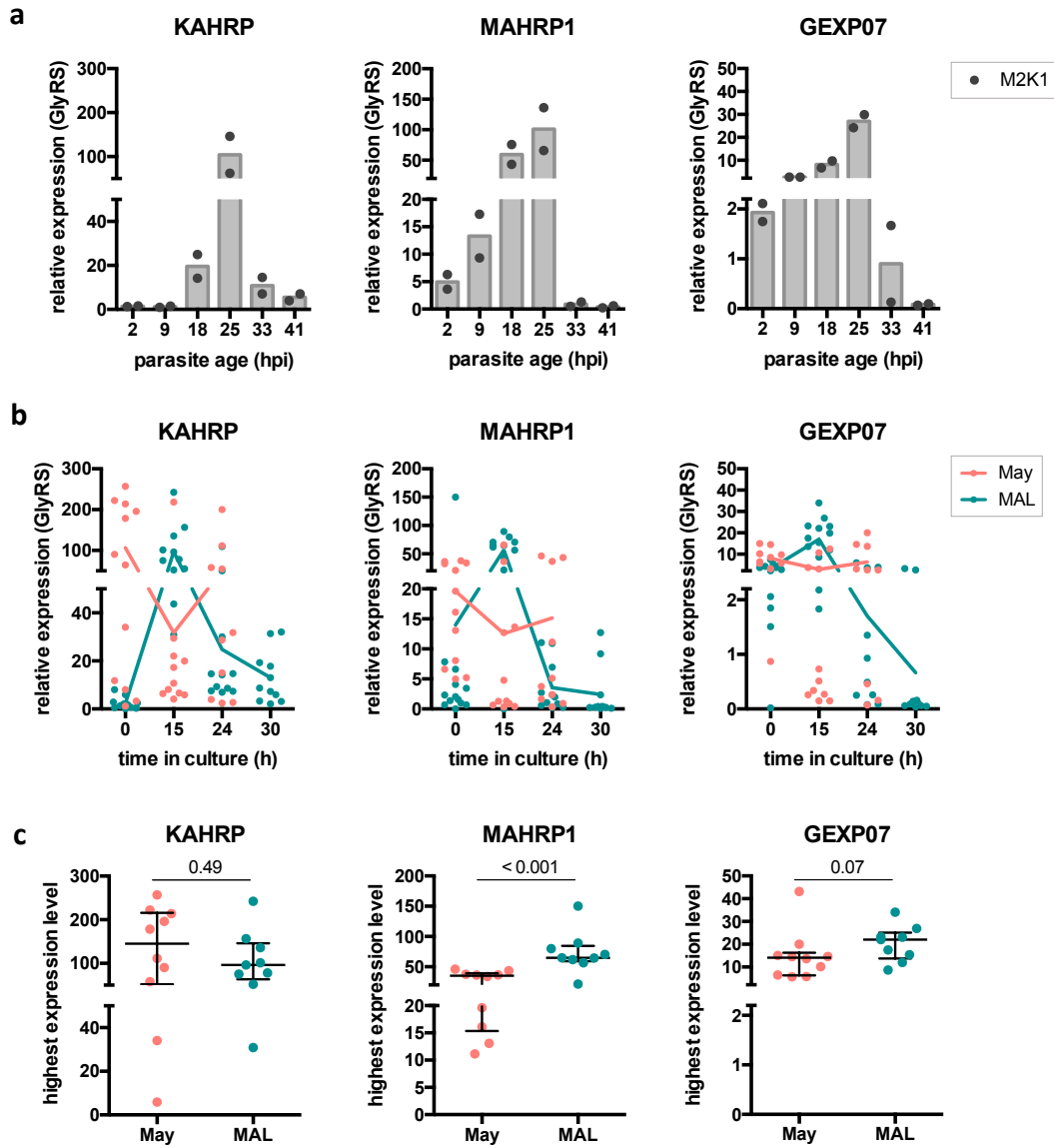
Figure continued on next page
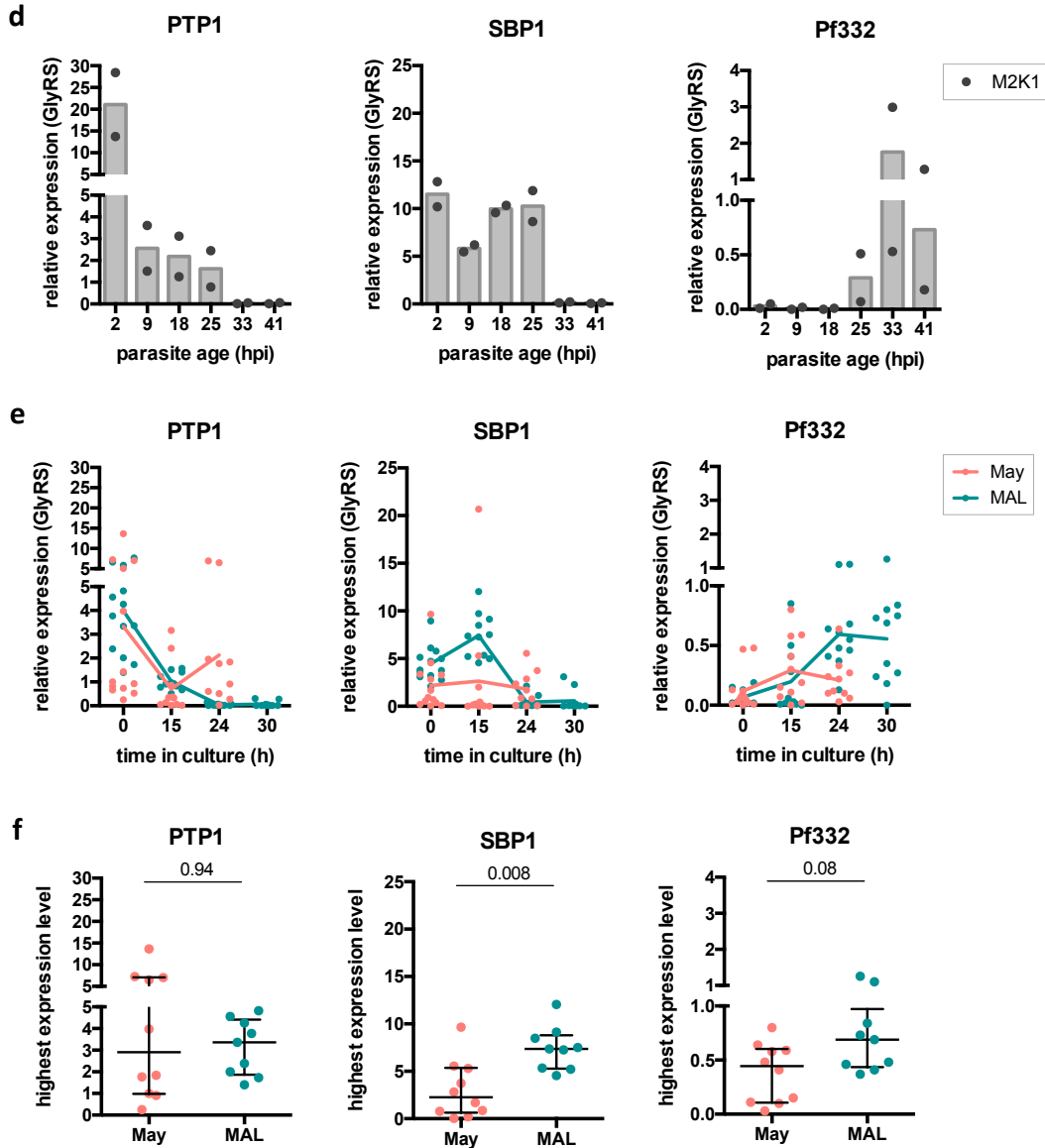
Figure 24: Expression of genes involved in knob formation and PfEMP1 trafficking

a, d) Gene expression time course of the indicated genes in 4 h synchronized M2K1 laboratory parasites, relative to a housekeeping gene (GlyRS). The two dots show expression in two qRT-PCR runs, the grey bars indicate the mean. **b, e)** Gene expression time course of the indicated genes. iRBCs isolated from asymptomatically infected donors at the end of the dry season (May, n= 15 and n= 10 with coverage of all timepoints (0 – 24h)) and with the first febrile malaria case in the transmission season (MAL, n = 13, 9 all timepoints) directly after blood drawal (0h) or after 15, 24 or 30 h of in vitro culture. Each dot represents a one donor. Lines connect the mean expression levels. **c, f)** Gene expression time course of the indicated genes in May and MAL samples relative to a housekeeping gene (GlyRS). Each dot is a donor, at the maximal expression of the respective gene during the 0 – 30 h timecourse. Mean ± ICR, Mann-Whitney test.

<u>Identifying stage normalizer genes</u>

To better understand the gene expression patterns, we wanted to directly compare expression levels between iRBCs from the dry season (May) and clinical malaria cases (MAL). As gene expression in *P. falciparum* is tightly controlled (Bozdech et al. 2003), we needed to compare parasites of the same developmental stage. As iRBCs circulating in the dry season are older within the 48h cycle than iRBCs in clinical cases (Figure 13) we could not just match by equal culture time, but had to find the timepoints where the proportion of ring, trophozoite and schizont stages was similar. To determine these proportions by qPCR, we first identified genes that were exclusively expressed in the ring, trophozoite or schizont stage and include them in the analysis (Bozdech et al. 2003). This allowed us to compare similar parasite stages and question whether host cell remodeling-related genes were differentially expressed in asymptomatic infections in the dry versus clinical cases in the wet season.

To identify these developmental stage marker genes, we screened the 3D7 transcriptome published by Bozdech et al. 2003 for genes that were exclusively expressed in rings, late trophozoites and schizonts. The expression of a few candidate genes was quantified in M2K1 parasite, a clonal culture-adapted parasite strain derived from Malian blood donors. As an additional criterion, exported genes were removed from the list of candidates to avoid misclassification of stages in the hypothetical case of a protein export deficit in iRBCs in the dry season. We found succinate dehydrogenase subunit 4 (SDH4, PF3D7_1010300) to be highly expressed rings between 2 and 9 hpi and in late schizonts, hypoxanthine-guanine phosphoribosyltransferase (HGPRT, PF3D7_1012400) in trophozoites and young schizont stages between 25 and 41 hpi with a peak at 33hpi, and ornithine aminotransferase (OAT, PF3D7_0608800) in schizonts with a peak at 41 hpi. (Figure 25a). We next quantified the expression of these stage marker genes in blood samples isolated from asymptomatic children at the end of the dry season (May) or children with their first clinical malaria episode in the transmission season (MAL), at the time of blood draw (0h) or after 15, 24 or 30h of in vitro culture (Figure 25b-c). May samples appeared more advanced in the cycle than MAL samples, with relatively low expression of the ring-specific gene SDH4 at the 0h timepoint.
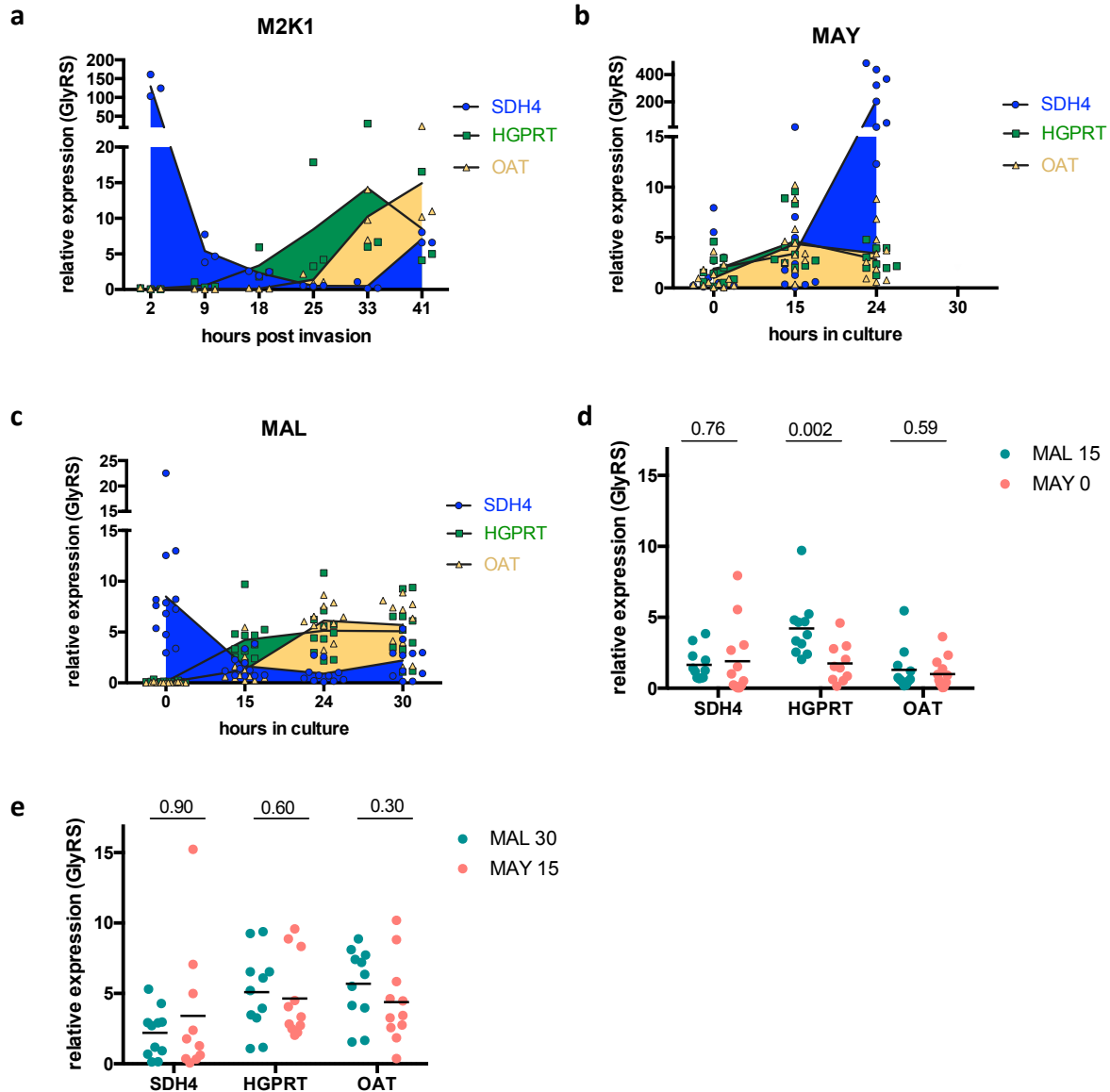
Figure 25: Stage-matching of iRBCs using marker genes of ring, trophozoite and schizont stages

a) In 4 h synchronized M2K1 laboratory parasites, a gene expression time course was generated by qRT-PCR of ring stage marker SDH4 (succinat hedydrogenase 4), trophozoite marker gene HGPRT (hypoxanthine-guanine phosphoribosyltransferase) and schizont marker gene OAT (ornithine aminotransferase). Gene expression is relative to a housekeeping gene (GlyRS). The dots show expression in three qRT-PCR runs, lines indicate the mean. **b, c)** Gene expression time course of the stage marker genes in iRBCs isolated from asymptomatically infected donors at the end of the dry season (May) **(b)** or clinical cases (MAL) **(c)** directly after blood drawal (0h) or after 15, 24 or 30 h of in vitro culture. Each dot represents a one donor. Lines connect the mean expression levels. **d, e)** Comparing the stage marker gene expression in May samples with to MAL samples with additional 15 h in culture, for earlier stages (May 0h vs MAL 15h **(d)**) and later stages (May 15h vs MAL 30 h **(e)**). Each dot is a donor. Line indicates mean, significance level determined using Mann-Whitney test.

This is in line with the average age of 17 hpi for iRBCs isolated from May samples predicted from their transcriptome (Andrade et al. 2020). Accordingly, by stage normalizer gene expression iRBCs from the dry season (May) were more similar to iRBC samples from clinical malaria (MAL) of the respective next timepoint, i.e. that had been cultured an additional 15 h. We hence compared "intermediate stages" (MAY 0h vs MAL 15h), corresponding roughly to ~20 hpi to 20 hpi iRBs, and "late stages" (MAY 15h vs MAL 30h), corresponding to ~ 35 hpi iRBCs, respectively (see Figure 25d and e). Expression of all 3 stage markers in the later stages (MAY 15h vs MAL 30h) was similar, while in the intermediate stages comparison (MAY 0h vs MAL 15h), the trophozoite marker gene HGPRT was significantly different between MAY and MAL. This suggests that the matching of intermediate stages and late stages was good, but not perfect.

Analysis of host cell remodeling related genes in age matched samples

With the stage-matched samples, where MAY 0h and MAL 15h should corresponded to ~20 hpi iRBCs, and May 15h and MAL 30h) to ~ 35 hpi iRBCs (see Figure 25d and e), we compared gene expression of HCR related transcripts. In this stage-matched comparison we found no significant difference between the iRBC samples from subclinically infected donors in the dry season (May) and clinical cases (MAL) in KAHRP or Pf332 expression. PTP1, expressed early in the IDC, showed similar expression in the earlier stages at May 0h in culture and MAL 15 h in culture, but we found a significant difference in the late stage comparison, with slightly higher expression levels in May 15 h in culture (relative expression 0.33 (May 15) and 0.01 (MAL), p = 0.003). MAHRP and GEXP07, which peaked in expression at 25 hpi in M2K1 iRBCs, had reduced expression levels in May 0h compared to MAL 15h in culture samples, but higher expression levels May 15 h versus MAL 30h in culture samples. Finally, SBP1 expression was significantly reduced in May 0h compared to MAL 15h in culture samples (relative expression 0.92 (May 0h) and 7.36 (MAL 15h), p < 0.001).

In summary, three of the analyzed six genes (MAHRP1, GEXP07 and SBP1) showed reduced expression in iRBCs obtained at the end of the dry season (May) compared to clinical malaria cases (MAL) in ~20 hpi iRBCs, corresponding to peak expression times of these genes within the 48h asexual cycle. However, this could also be linked with the lower presence of trophozoites in the May 0h in culture sample, as indicated by the reduced trophozoite stage marker HGPRT expression.
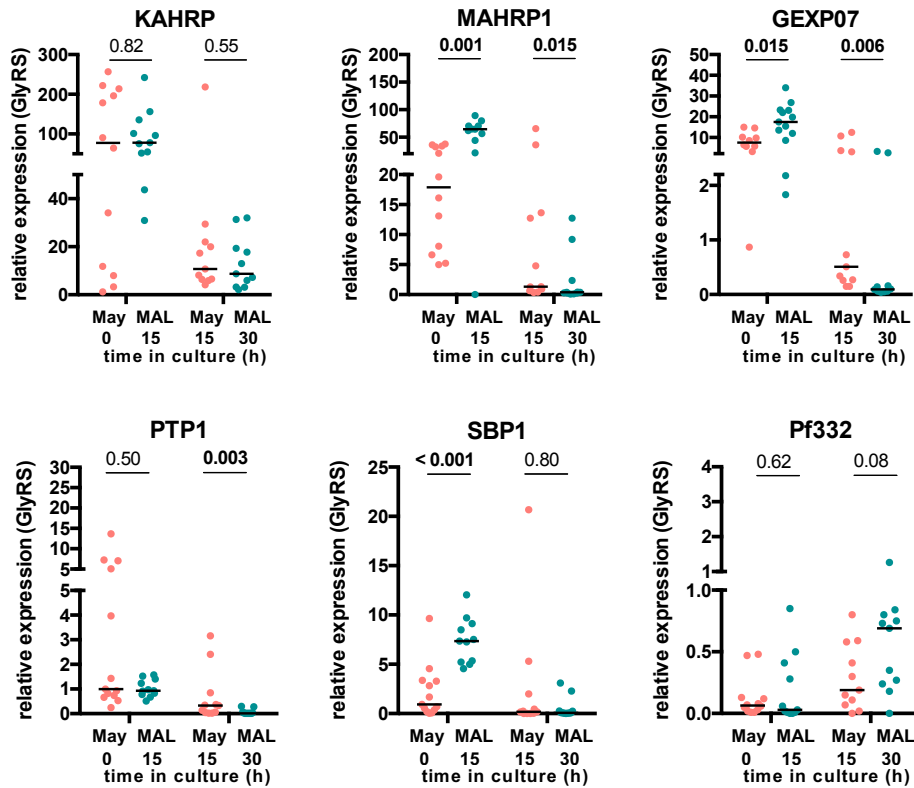
Figure 26: Host cell remodeling related gene expression in stage-matched iRBC samples from May and MAL donors

Expression of the indicated genes as determined by qRT-PCR relative to a house keeping gene (GlyRS). Gene expression was compared between stage-matched samples, i.e. May samples to MAL samples with additional 15 h in culture, for earlier stages (May 0h vs MAL 15h) and later stages (May 15h vs MAL 30 h). Each dot is a donor. Line indicates median, significance level determined using Mann-Whitney test.

3.3 Presentation of *P. falciparum* surface antigens is not reduced in the dry season

Adhesion efficiency in the dry season could be decreased through less parasite adhesion ligands expressed on the iRBC surface. In the absence of knowledge of which adhesin variants are presented on the iRBC surface, we used blood group specific hyperimmune plasma pools to detect a broad range of antigens on the surface of infected RBCs from asymptomatic carriers at the end of the dry season (May) and clinical cases in the transmission season (MAL).

Detecting surface antigens on *P. falciparum* strain FCR3 iRBC using hyperimmune plasma pool and flow cytometry

Initially, we pooled plasmas of 22 individuals that were collected during the October 2017 cross-sectional timepoint. To test how well this pool could detect *P. falciparum* antigens, we performed an ELISA assay on lysed *P. falciparum* parasites (Figure 27a). Detection levels were similar to a Kenyan hyperimmune plasma pool provided by the Osier lab (Plasma pool Osier) and higher than of German individuals (DE #1 and #2). Also, the plasma pool showed higher recognition levels than plasmas of five individual Malian donors (OCT17 #1-5), indicating that the pool covered a broader range of antigens. We then tested how well this plasma pool recognized mature stage *P. falciparum* strain FCR3 parasites. The principle of the assay is shown in Figure 27b. RBCs were incubated with different concentrations of hyperimmune plasma and then labeled with an anti-human IgG-APC coupled secondary antibody, and iRBCs were stained with SybrGreen. The gating strategy is shown in Supplemental figure 2. The FCR3 parasite strain was cultured in blood group O$^+$ RBCs, however to be able to use the hyperimmune plasma pool on the field samples with different ABO blood groups, we created blood-group specific pools. For negative control staining with malaria-naïve plasma, we used a commercial AB$^+$ serum. To determine the optimal labeling condition, we tested different plasma pool concentrations and incubation times, and found that labeling overnight with 10% plasma at 4°C recognized 54 % of mature-stage iRBCs (Figure 27c). The labeling was also specific for parasite surface antigen, as close to 70 % of mature-stage iRBCs were labeled, while ring stage parasites or trypsin-treated iRBCs were not labeled (Figure 27d).
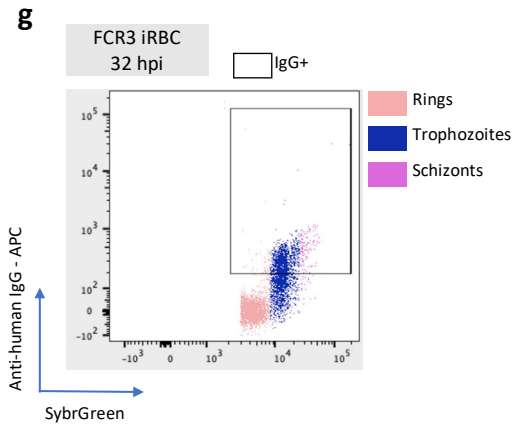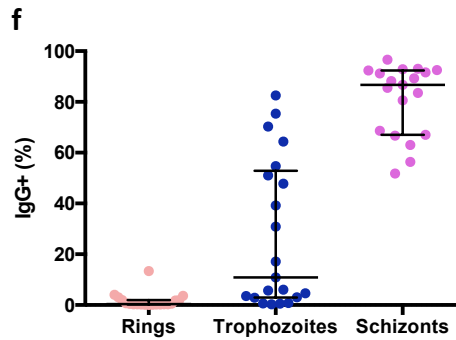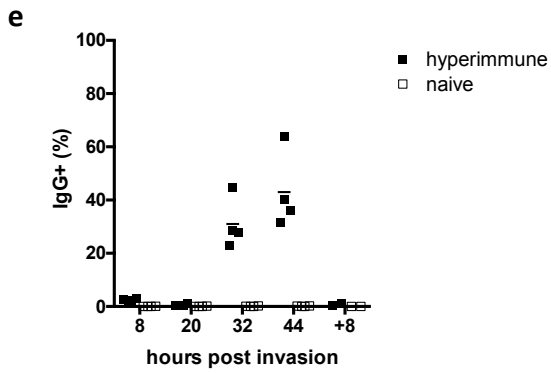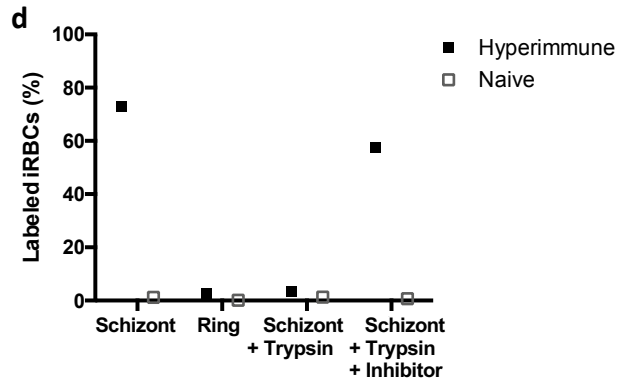
a) ELISA of plasma containing antibodies detecting Pf lysate coated on the plate. Pre-test of a plasma pool from 22 individuals (Plasma pool OCT17) compared to a different hyperimmune plasma pool from Kenyan donors (provided by AG Osier) and to individual plasmas contributing to the hyperimmune pool (OCT #1-5) or to malaria-naïve German plasma donors (DE #1-2). **b)** Principle of the Pf surface antigen recognition assay. Antigens on the surface of iRBCs are bound by antibodies contained in the plasma, which are detected by APC-labeled anti-human IgG secondary antibodies. Infected RBCs are detected by SybrGreen staining. **c)** Detection of surface antigens on mature stage, MACS purified FCR3 parasites incubated with 5, 10 and 20% of plasma for 30 min at RT or overnight at 4 °C. **d)** FCR3 parasites synchronized to schizonts or rings were labeling by hyperimmune plasma as detected by flow cytometry. Surface antigens were cleaved by trypsin treatment for 30 min, also in the presence of a trypsin inhibitor. **e)** Synchronized FCR3 iRBCs were labeled with hyperimmune plasma or naïve plasma every 12 h within one cycle. Data from 4 independent experiments. Line indicates median. **f)** Labeling of indicated stages of FCR3 iRBC during the 48h development in culture. Each dot represents one timepoint of one of 4 replicates. Line indicates median ± ICR**. g)** Representative flow cytometry plot of FCR3 iRBCs at 32 hpi. Ring, trophozoite and schizont stages are indicated by color, hyperimmune plasma labeled iRBC found in IgG+ gate.

This assay was also used to analyze the dynamics at which antigens appear on the surface. We used synchronized cultures of FCR3 iRBCs, which were labeled and analyzed every 12 hours over one replicative cycle. We observed labeling of the population at 32 and 44 hpi, with ring, trophozoite and schizont stages increasingly labeled by the hyperimmune plasma pool (median 0.4 %, 10.9 % and 86.7 %, respectively) but not by the naive plasma pool (Figure 27e). Furthermore, when gating on ring, trophozoite and schizont stage iRBCs regardless of the time in culture, we observed that the fraction of iRBCs recognized by IgG in the hyperimmune plasma pool was only 0.4 % of rings, but increased to median 10.9 % of trophozoites and 86.7 % of schizonts (Figure 27f). This stage-specific increase was also clear in the flow cytometry plots (Figure 27g). We established that the surface labeling, and hence the expression of surface antigens, increased during the trophozoite stage.

Detection of surface antigen expression in iRBCs of asymptomatic carriers at the end of the dry season is not different to iRBCs from clinical cases

We next applied this surface antigen recognition assay to field samples. Decreased levels of recognition of surface antigens would hint to lower levels of adhesins on the surface, which in turn could render the iRBCs less adhesive. Cryopreserved blood samples from asymptomatic donors at the end of the dry season (May, n = 11) and from clinical cases in the wet season (MAL, n = 10) (Table 6) were thawed and cultured in vitro for one replicative cycle (36 h in culture for dry season samples (May), and 48 h in culture for samples from clinical cases (MAL)), giving each group time to complete the cycle. To provide optimal growth conditions, samples from clinical cases (MAL)

were diluted in uninfected RBCs upon thawing. Every 12 hours, a fraction of the samples was labeled with hyperimmune plasma, stained and analyzed on a flow cytometer. The growth of parasitemia in culture is presented in Figure 28a. Infected RBCs from clinical cases (MAL) all increased parasitemia in culture , while of iRBCs from the dry season didn't increase parasitemia within 36 h in culture, only a subset with an additional timepoint at 48h showed an increase of parasitemia within 48h (Figure 29a). This is in contrast to our observations of the development of dry season iRBCs in culture using freshly collected samples (Andrade et al. 2020) (Figure 13). We also failed to find a substantial fraction of non-rings in the culture at 0h (Figure 29b) in contrast to earlier observations with ex vivo iRBCs (Figure 13)), suggesting that only ring stage iRBCs survived the freeze-thaw cycle. Furthermore, in blood samples of donors with clinical malaria (MAL), the prevalence of schizonts peaked at 36 h in culture (making up 7 − 30 % of iRBCs), but in blood samples in the dry season schizont development peaked at 24 or 36 hpi, appearing overall still not as synchronous as iRBCs obtained from clinical malaria cases (Figure 28b).

We analyzed the labeling of surface antigens over the development of the parasite in culture. We therefore substracted the background staining with naïve plasma from each available timepoint and excluded from the analysis a sample with unspecific staining without naïve plasma control and a timepoint in one batch with technical difficulties (see Methods). We observed that peak surface labeling occurred at 24-36 h in culture in iRBC from donors with clinical malaria (MAL) and up to ~20 % of iRBCs were labeled with the hyperimmune plasma pool (Figure 28d). Infected RBCs from the dry season also exhibited a peak at 24-36 hours in culture with average labeling of ~20 % of iRBCs (Figure 28d). However, this analysis only shows the detection of surface antigens across all iRBCs in one sample, regardless of parasite stage.

Table 6: Demographic and hemological data of field sample donors

Season	n	Mean age (95% CI)	% female	% hemotype AA
MAL	10	11.0 (8.2 - 13.8)	40	100
MAY	11	16.5 (15.8 - 17.2)	36	100
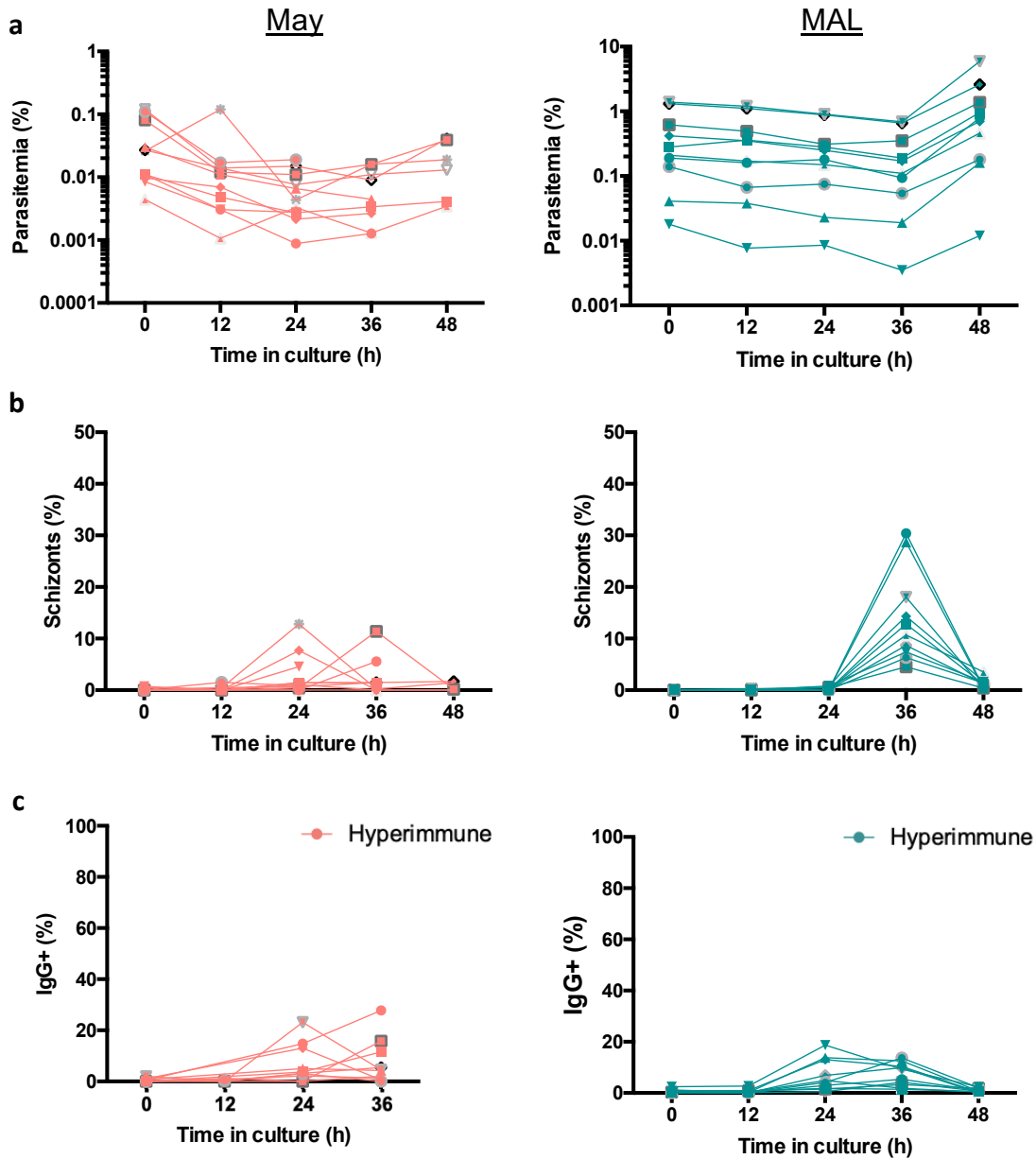
Figure 28: Detection of surface antigens on field sample iRBCs using a hyperimmune plasma pool

a) Cryopreserved blood samples of 11 donors with subclinical malaria at the end of the dry season in May (May) and of 10 donors at their first febrile malaria in the transmission season (MAL) were thawed and cultured for one cycle. Each 12 hours, the parasitemia was determined by flow cytometry after SybrGreen staining. Note the different scales from 0.0001 – 1% (May) and 0.001 – 10 % (MAL). **b)** The appearance of schizont stage iRBC (shown as % of iRBC) in blood samples of 11 donors with subclinical malaria at the end of the dry season in May (May) and of 10 donors at their first febrile malaria in the transmission season (MAL). **d)** Infected RBCs at each timepoint of the growth in culture were incubated with 10 % hyperimmune plasma pool (pool matched to ABO blood group of donor) and detected with anti-human IgG –APC labeled secondary antibody and on a flow cytometer. n = 10 (May) and 10 (MAL).

To better understand in which stages surface antigens become detectable, and whether there are differences between the seasons, we explored the labeling of ring, trophozoite and schizont stage iRBCs by the hyperimmune plasma pool, independent of the time cultured. We observed that ring stage iRBCs from clinical malaria cases were barely labeled by hyperimmune plasma, and the same applied to ring stage iRBCs from the dry season (with the exceptions mainly attributable to the 12h timepoint in one batch) (Figure 29c). Of trophozoite stage iRBC, median 4.7 and 2.9 % were labeled in blood samples from asymptomatic donors at the end of the dry season (May) and clinical cases from the transmission season (MAL). We could only measure the surface antigen density on schizont stage iRBC in very few samples of the dry season, limiting the accuracy of this result, but we observed also a broad range (0 – 95%) of labeling intensities of schizonts in the dry season (May) similar to schizonts from clinical cases (range 1 – 83 %, median 28.5 %) in clinical cases (MAL) (Figure 29c). The overall labeling pattern of ring, trophozoite and schizont stages is also reflected in the density plots of iRBC from one donor of the dry season and one donor with clinical malaria (Figure 29d).

Altogether, we observed that we could not investigate the non-ring population typically found in circulation in asymptomatic donors in the dry season, due to the freeze-thaw procedure of the used blood samples. However, the remaining iRBCs, when analyzed overall or separately by iRBC stage, were similarly labeled by the hyperimmune plasma pool in asymptomatic individuals at the end of the dry season and clinical cases in the transmission season.

Figure 29: Quantification of iRBC stages and stage-specific detection of surface antigens on iRBC

a) The proportion of non-rings in iRBC directly after thawing of blood samples of 11 donors with asymptomatic malaria at the end of the dry season in May (May) and 10 donors with clinical malaria in the transmission season (MAL), calculated as sum of %trophozoites of iRBC and % schizonts of iRBC in one sample. Line indicates median, statistical testing by Mann-Whitney test. **b)** The growth of iRBCs in culture over one cycle was calculated as the fold change between the last and the first timepoint in culture. Dotted line at fold change 1, values > 1 indicate overall multiplication in culture. We analyzed 10 donors with asymptomatic malaria at the end of the dry season in May (May) and 10 donors with clinical malaria in the transmission season (MAL). Line indicates median. **c)** Hyperimmune plasma labeling of iRBC separated by iRBC stages (ring, trophozoites and schizonts). We analyzed blood samples of 10 donors with asymptomatic malaria at the end of the dry season in May (May) and 10 donors with clinical malaria in the transmission season (MAL). For each iRBC sample and timepoint that n ≥ 10 iRBCs of the respective stage were observed, the percentage of IgG+ cells was included in the analysis. Rings: n = 36 (10 donors May) and 50 (10 donors MAL), n = 17 (7 donors May) and 43 (10 donors MAL), n = 8 (3 donors May) and 21 (9 donors MAL). **d)** Representative flow cytometry plot of one donor with asymptomatic malaria at the end of the dry season (May donor k274) and with clinical malaria in the transmission season (MAL donor K557), both cultured for 36 hours. Ring, trophozoite and schizont stages are indicated by color, hyperimmune plasma labeled iRBC fall in IgG+ gate.

a

% non-rings at 0h

0.48

May   MAL

b

Fold change parasitemia

● 0 to 48 h
◐ 0 to 36 h
○ 0 to 24 h

May   MAL

c

IgG+ (%)

Rings   Trophozoites   Schizonts
0.77   0.50   0.70

May MAL   May MAL   May MAL

d

MAL k557
36 h   IgG+

Anti-human IgG - APC

IgG+iRBCs
1,33

SybrGreen

May k274
36 h   IgG+

Anti-human IgG - APC

IgG+iRBCs
3,92

SybrGreen

■ Rings
■ Trophozoites
■ Schizonts
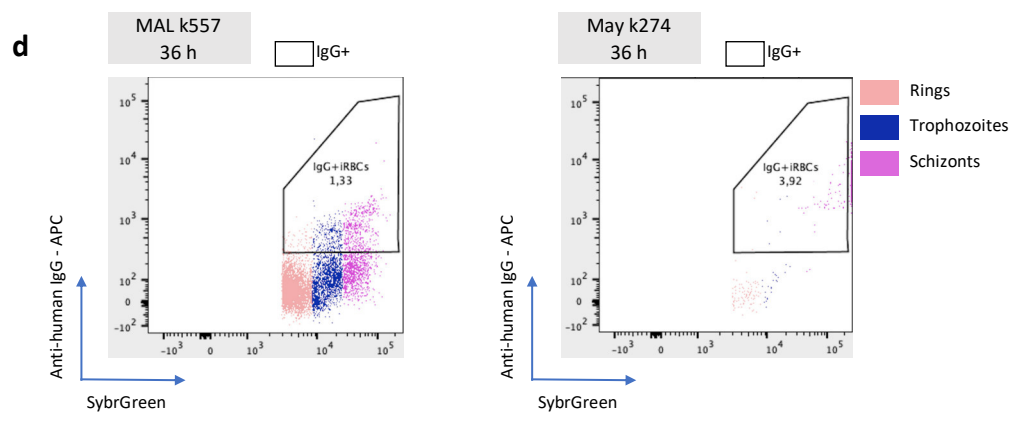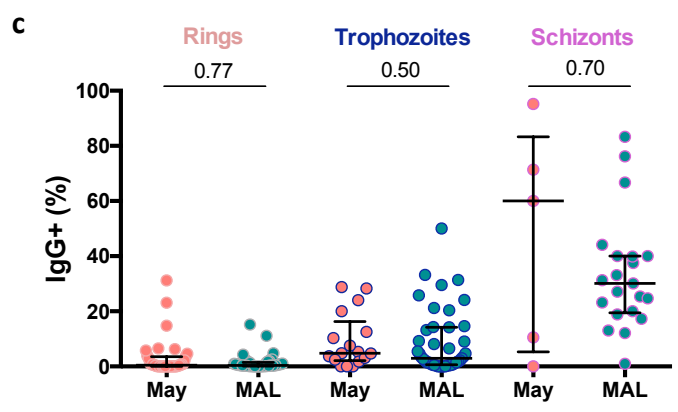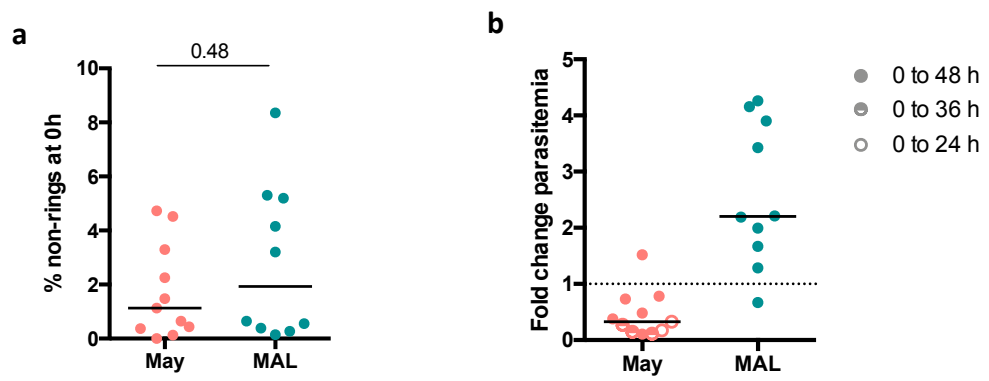
<u>3.4 Low levels of endothelial activation in the dry season could contribute to decreased adhesion</u>

The efficiency of iRBC adhesion to endothelial cells depends on, beside the presentation of parasite adhesion ligands on the iRBC suface, the density of adhesion receptors on endothelial cells. This density increases during inflammation, when endothelial cells become "activated" to allow leukocyte migration to the site of inflammation (Murphy and Weaver 2018). *P. falciparum* also triggers a pro-inflammatory response during clinical malaria episodes, especially in severe malaria cases (Wassmer et al. 2015), while asymptomatic parasite carriage during the dry season barely triggers an immune response (Andrade et al. 2020). It is hence possible that cytoadhesion efficiency during the dry season is negatively impacted by a lower density of adhesion receptors on endothelial cells in the subclinically infected hosts. To assess this hypothesis, we characterized and compared asymptomatic carriers at the end of the dry season and clinical malaria cases in the wet season regarding i) plasma levels of pro-inflammatory cytokines that trigger endothelial activation, ii) cellular adhesion molecules soluble in the plasma, and iii) the effect on endothelial recptors following in vitro stimulation of endothelial cells with donors' plasmas; and finally whether vi) parasites bind differently to these endothelial cells after plasma stimulation.

<u>Proinflammatory cytokines are not upregulated in the dry season</u>

The pro-inflammatory cytokines tumor necrosis factor (TNF), interleukin 1 α (IL-1α) and IL-1β can activate endothelial cells leading to higher expression levels of endothelial cell receptors (Pober, Gimbrone, et al. 1986; Pober, Bevilacqua, et al. 1986; Swerlick et al. 1992). We quantified TNF, IL-1α and IL-1β concentrations in plasmas of individuals during their first malaria episode during the wet season (MAL, n = 18), and of subclinical individuals that carried parasites (May[+], n = 20) or not (May-, n = 20) at the end of the dry season . We observed that TNF levels were elevated in malaria cases (MAL) (median 9.2 (6.8 − 16.9 IQR) pg/ml), while low TNF levels were found in individuals at the end of the dry season independently of the donor's infection status (May[+]: 4.1 (3.2 − 6.4 IQR) and May[−]: 2.81 (2.5 − 4.8 IQR) pg/ml) (Figure 30a). A similar pattern was observed for IL-1α (MAL: 56.6 ± 13.5 pg/ml, May[+]: 44.5 ± 16.7, May-: 43.2 ± 12.8; mean ± SD), and IL-1β (MAL: 62.8 ± 14.8, May[+]: 40.1 ± 11.4, May-: 44.0 ± 10.2; mean ± SD) (Figure 30a). These data suggest that subclinical low-density parasitemias did not trigger the release of cytokines as it occurred in malaria cases.
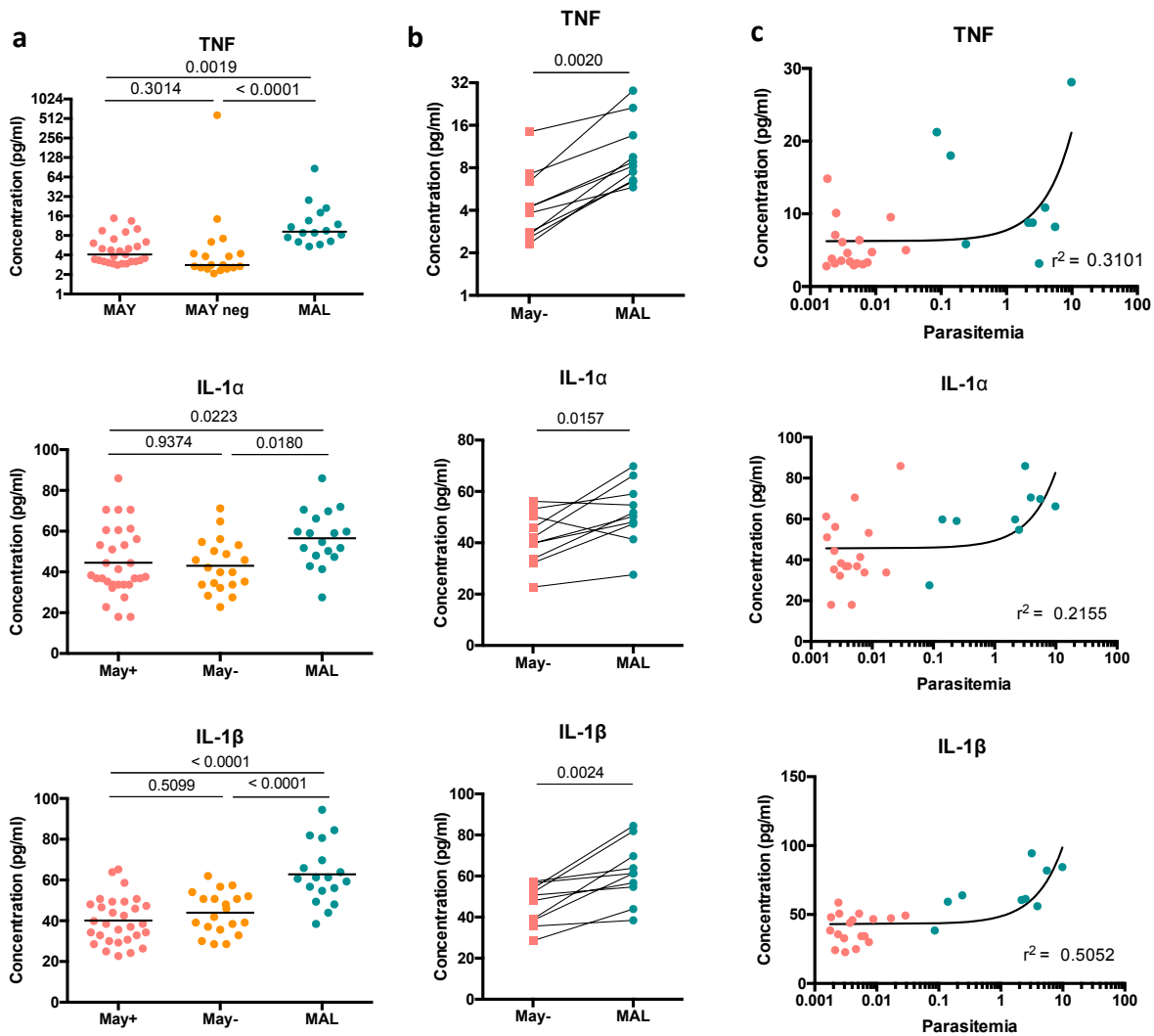
Figure 30: Asymptomatic parasite carriage during the dry season doesn't induce endothelial-activating cytokines

a) Quantification of plasma levels of TNF, IL-1α and IL-2b from the end of the dry season in donors subclinically carrying *P. falciparum* (May+) and uninfected donors (May-) and in donors with clinical malaria (MAL). TNF measurements performed by ELISA (n = 27 (May+), 18 (May-) and 16 (MAL). Line indicates median, statistical testing by Dunn's multiple comparisons. IL-1α and IL-1β quantified by Luminex assay (n = 30 (May+), 20 (May-) and 18 (MAL). Line indicates mean, statistical testing by Tukey's multiple comparisons test. **b)** Paired analysis of plasma levels of TNF, IL-1α and IL-1β of 10 donors that were uninfected at the end of the dry season in May (May-) and during their first febrile malaria episode in the ensuing transmission season (MAL). Statistical analysis by Wilcoxon matched-pairs signed rank test (TNF) and paired t-test (IL-1α and IL-1β). **c)** Correlation of plasma levels of TNF, IL-1α and IL-2b from donors with asymptomatic *P. falciparum* infection in the dry season (May+) and donors with clinical malaria (MAL). TNF: n = 27 (May+) and 16 (MAL), IL-1α and IL-1β n = 30 (May+) and 18 (MAL). The linear regression was performed to determine r2 values.

Table 7: Demographic data of Malian plasma donors

	n	mean age (years)	(95% CI)	%Female
MAL	18	9.9	(7.7 – 12.2)	50
May+	30	14.2	(12.4-16.0)	30
May-	20	11.9	(9.6 – 14.1)	35

Nevertheless there was substantial overlap in cytokine levels between the dry season and clinical cases, however in paired samples of 10 donors we observed a significant increase in levels of TNF, IL-1α and IL-1β upon development of clinical malaria compared to baseline (uninfected) levels at the end of the previous dry season (Figure 30b). Further, we found a linear relationship between parasitemia and TNF ($r^2 = 0.31$), IL-1α ($r^2 = 0.22$) and IL-1β ($r^2 = 0.51$) levels with parasitemia, which appear mainly to be driven by the plasmas from malaria cases (Figure 30c).

Shedding of adhesion molecules as proxy for in vivo endothelial activation

Next, we assessed whether increased cytokine levels as observed in malaria cases were sufficient to induce the upregulation of adhesion receptors on endothelial cells in vitro. The response to proinflammatory cytokines includes the protease-mediated shedding of the ectodomains of adhesion molecules, which then circulate in soluble forms in the plasma (Garton, Gough, and Raines 2006). Hence, we measured the levels of soluble (s)ICAM-1, sVCAM-1, sPECAM-1, sE-Selectin and sP-Selectin in plasmas collected from subclinical individuals carrying *P. falciparum* at the end of the dry season (May[+], n = 30), uninfected individuals (May[-], n = 20) and from donors with clinical malaria in the ensuing transmission season (MAL, n = 18) using a Luminex assay. Plasma levels of sVCAM-1, sE-Selectin and sP-Selectin were significantly higher in donors with clinical malaria (MAL) compared to those of plasmas collected in the dry season (May[+] and May[−]), and we found no significant difference in sVCAM-1, sE-Selectin and sP-Selectin plasma levels between subclinical carriers (May[+]) and healthy control individuals (May[−]) in the dry season (Figure 31a). Furthermore, individuals with clinical malaria (MAL) had significantly increased levels of sVCAM-1, sE-Selectin and also sICAM-1, but not sP-Selectin compared to their own paired plasma taken in the preceding dry season when they were uninfected (May[-]) (Figure 31b). Again, parasitemia showed a linear relationship with plasma levels of sVCAM-1 ($r^2 = 0.90$), sE-Selectin ($r^2 = 0.53$) and sP-Selectin ($r^2 = 0.29$) (Figure 31c). In contrast, sICAM-1 and sPECAM-1 levels were similar in all three groups and were not associated with parasitemia (Figure 31a and c), and sPECAM-1 levels were not different in paired plasma samples (May[−] vs MAL) (Figure 31b).
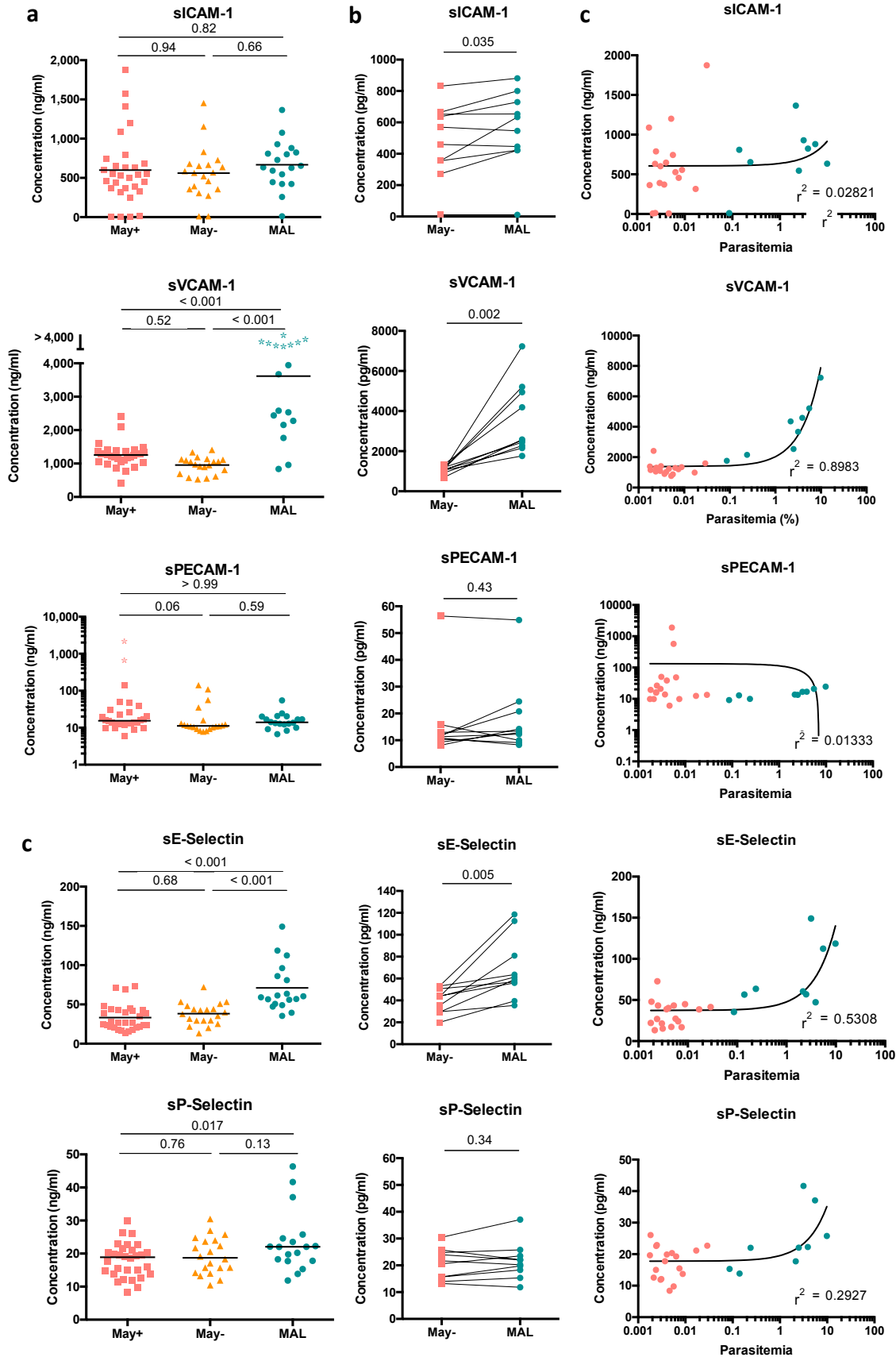
Figure 31: Soluble endothelial cell adhesion receptor concentrations in the plasmas of study participants

a) Quantification of soluble endothelial cell adhesion receptors in plasmas of donors at the end of the dry season in with asymptomatic P- falciparum infected (May+, n = 30) or uninfected (May-, n = 20) and from the transmission season in donors with clinical malaria (MAL, n = 18) using a Luminex assay. sVCAM-1 and sPECAM-1: stars indicate values above the dynamic range of detection. Line indicates mean (sPECAM-1: median), statistical testing by Tukey's multiple comparisons test (sPECAM-1: Dunn's multiple comparisons test). **b)** Paired analysis of plasma levels of soluble endothelial cell adhesion receptors in donors (n=10) at the end of the dry season in May when they were uninfected (May-) and during their first febrile malaria episode in the ensueing transmission season (MAL). Statistical analysis by paired t-test, and Wilcoxon matched-pairs signed rank test (sPECAM-1). **c)** Correlation of plasma levels of soluble endothelial cell adhesion receptors from donors with asymptomatic P- falciparum infected at the end of the dry season (May+, n = 18) and donors with clinical malaria (MAL, n = 9). Linear regression was performed to determine r^2 values.

Based on the cytokine and soluble receptor concentrations and parasitaemia data of asymptomatic carriers at the end of the transmission season (May$^+$) and clinical cases in the following transmission season (MAL), a correlation matrix was created to identify connections between the endothelium-stimulating cytokines and the soluble endothelial cell adhesion receptors found in the plasmas of in total 68 plasma donors (Table 8). It showed that IL-1β correlated positively with IL-1α and TNF (r = 0.76, p < 0.001 and 0.45, p = 0.018) but TNF and IL-1α did not correlate (r = 0.17). Except for PECAM-1, all soluble adhesion receptors positively correlated with IL-1α and IL-1β plasma levels, with the strongest correlation between sE-Selectin and IL-1β (r = 0.96, p < 0.001). TNF correlated moderately with E-Selectin (r = 0.47, p = 0.014), but not with other adhesion receptors. All measured analytes except PECAM-1 and sICAM-1 correlated significantly with parasitemia.

	TNF	IL-1a	IL-1b	sICAM-1	sVCAM-1	sPECAM-1	sP-Selectin	sE-Selectin	Parasitemia
TNF		0.412	0.018	0.916	0.067	0.869	0.126	0.014	0.041
IL-1a	0.165		<0.001	<0.001	0.014	0.138	<0.001	<0.001	0.010
IL-1b	0.451	0.767		0.007	0.009	0.651	<0.001	<0.001	<0.001
sICAM-1	-0.021	0.838	0.510		0.186	0.105	0.067	0.031	0.061
sVCAM-1	0.365	0.474	0.501	0.268		0.289	0.046	0.020	0.002
sPECAM-1	0.034	0.299	0.093	0.325	-0.221		0.347	0.401	0.923
sP-Selectin	0.302	0.676	0.769	0.358	0.395	0.192		<0.001	0.084
sE-Selectin	0.468	0.709	0.969	0.416	0.454	0.172	0.727		<0.001
Parasitemia	0.395	0.486	0.646	0.366	0.584	-0.020	0.339	0.600	

Table 8: Correlation matrix of plasma levels of endothelialium-activating cytokines and soluble endothelial adhesion receptors

Correlation matrix showing in the lower left corner the Spearman correlation from high positive (r = 1, red) to uncorrelated (r = 0, white) to negatively correlated (r = -1, blue) and in the upper right corner the p-value, with green shading indicating p < 0.05.

Endothelial cell receptors are not upregulated upon dry season plasma stimulation

To better understand whether adhesion receptors are present at lower densities on endothelial cells in asymptomatic individuals in the dry season, compared to clinical malaria cases in the transmission season, we tested how plasmas from these donors could activate endothelial cells to express adhesion receptors on the surface.
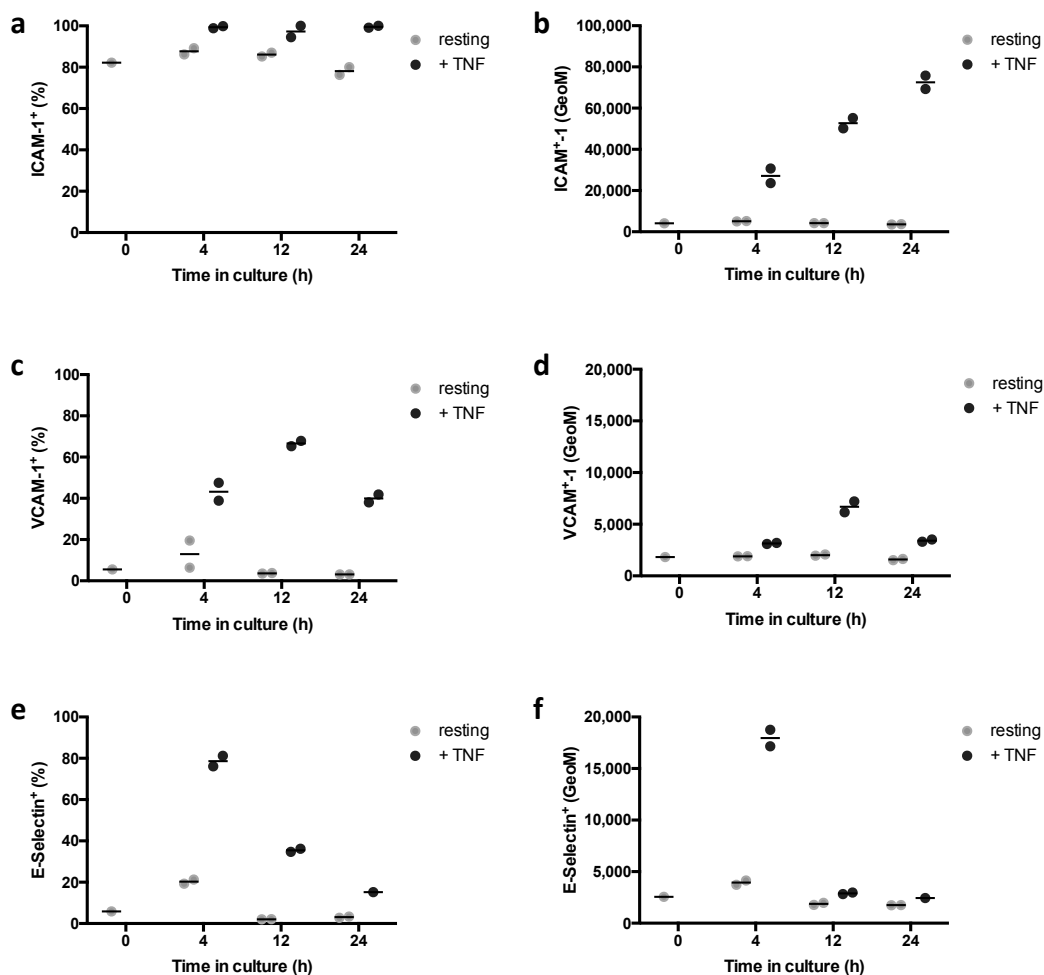
Figure 32: Endothelial adhesion receptor expression time course after TNF stimulation

Endothelial adhesion receptor expression was quantified by flow cytometry on human dermal endothelial cells (HDMEC) following TNF stimulation (black) or unstimulated (grey). a) Percentage of HBMEC gated positive for each adhesion receptor. b) Geometric mean of HBMEC gated positive for each adhesion receptor. Note the different scales (0 – 100,000 for ICAM-1, 0-20,000 for VCAM-1 and E-Selectin).

First, we analyzed the dynamics of ICAM-1, VCAM-1 and E-Selectin expression on cultured human endothelial cells in response to supra-physiological concentrations of TNF as are commonly used in vitro (Viebig et al. 2005). The three adhesion receptors were selected for further analysis for the differential expression profile of sVCAM-1 and sE-Selectin described above, and the prominent role together with ICAM-1 in fatal malaria (Turner et al. 1994, 1998; Armah et al. 2005). We cultured primary human endothelial cells (human dermal microvascular endothelial cells, HDMEC) in medium alone (resting) or in medium supplemented with 10 ng/ml TNF (TNF) and analyzed the expression of ICAM-1, VCAM-1 and E-Selectin on the cell surface after 4, 12 and 24 h by flow cytometry (see Supplemental figure 4 for the gating strategy). In the resting condition, ~80 % expressed intermediate levels of ICAM-1 (Figure 32a), while addition of TNF stimulated HDMECs to express ICAM-1 on all cells with increasing intensity over the time course (Figure 32b). VCAM-1 and E-Selectin were barely expressed in unstimulated HDMEC cells, but could be induced by TNF to be expressed in 67% and 79 % of cells, respectively (Figure 32c and e), with E-Selectin detected with a higher geometric mean than VCAM-1 (Figure 32d and f). We concluded that the expression of E-Selectin and VCAM-1 is best determined at 4-12 h of HDMEC stimulation, while ICAM-1 can be analyzed at all timepoints but reaches highest adhesion receptor density at 24 h. We therefore proceeded to analyze the expression of adhesion receptors after stimulation with plasmas from donors with subclinical *P. falciparum* infection (May$^+$, n = 15) or uninfected (May$^-$, n = 13) at the end of the dry season, and with their first clinical malaria episode in the transmission season (MAL, n = 15). After 6 h of incubation with 50% plasma, we did not observe a significant difference in the percentage of cells expressing ICAM-1, VCAM-1 or E-Selectin (Figure 33a-c) or the geometric mean signal intensity (Figure 33d-f). However, we observed significantly higher ICAM-1 and E-Selectin levels on HDMEC after stimulation with plasmas from uninfected donors at the end of the dry season (May$^-$), compared to asymptomatic or clinical cases (Figure 33a, c, d and f).

Additionally, we quantified ICAM-1 expression on HDMECs after 24 h of stimulation with the abovementioned plasmas. Endothelial cells stimulated with plasmas of donors with clinical malaria (MAL) exhibited significantly increased ICAM-1$^+$ percentages than cells stimulated with dry season plasmas (53 ± 9 (MAL) vs 38 ± 6 (May$^+$) and 38 ± 4 (May$^-$)) (Figure 33g). Likewise, the geometric

mean signal of the ICAM-1^{+} cell population in HDMECs stimulated with plasmas of clinical cases (MAL) showed a significant increase compared to the other groups (May[+] and May[-]), suggesting also an increased receptor density. Of note, the ICAM-1 expression on plasma-stimulated cells was even higher than after stimulation with super-physiological TNF concentrations (10 ng/ml) after 24h but not after 6h (data not shown) (Figure 33a,d,g,h).
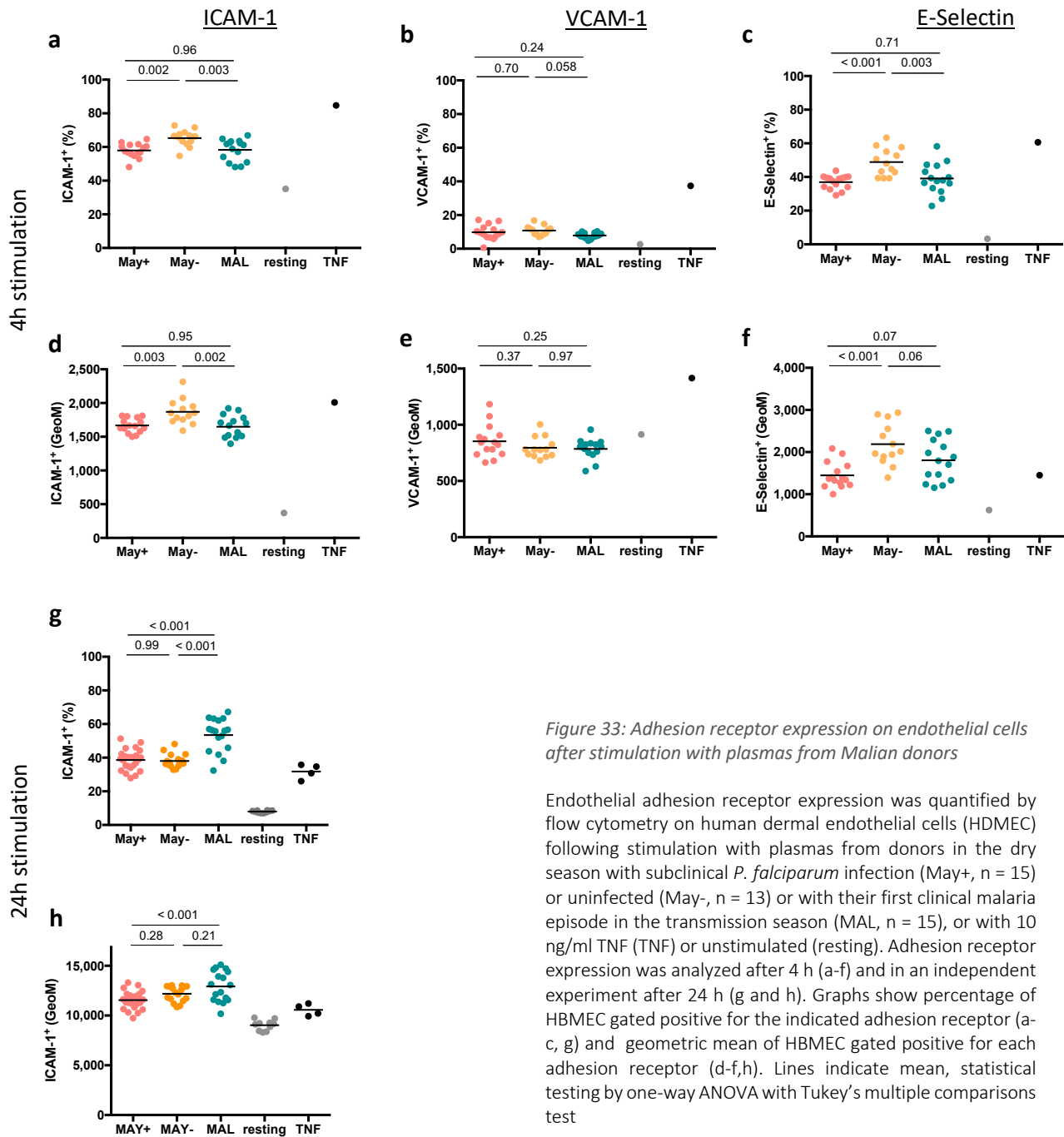
Figure 33: Adhesion receptor expression on endothelial cells after stimulation with plasmas from Malian donors

Endothelial adhesion receptor expression was quantified by flow cytometry on human dermal endothelial cells (HDMEC) following stimulation with plasmas from donors in the dry season with subclinical *P. falciparum* infection (May+, n = 15) or uninfected (May-, n = 13) or with their first clinical malaria episode in the transmission season (MAL, n = 15), or with 10 ng/ml TNF (TNF) or unstimulated (resting). Adhesion receptor expression was analyzed after 4 h (a-f) and in an independent experiment after 24 h (g and h). Graphs show percentage of HBMEC gated positive for the indicated adhesion receptor (a-c, g) and geometric mean of HBMEC gated positive for each adhesion receptor (d-f,h). Lines indicate mean, statistical testing by one-way ANOVA with Tukey's multiple comparisons test

Endothelial cell adhesion after dry and wet season plasma's activation

Finally, we aimed to assess the binding capacity of a *P. falciparum* parasite line on endothelial cells previously stimulated by plasmas of malaria cases in the transmission season (MAL) and donors carrying or not parasites at the end of the dry season (May$^+$ and May$^-$). With a static binding assay, we showed that *P. falciparum* strain FCR3 parasites, but not uninfected RBCs, adhered to HDMECs and that binding of iRBCs could be reduced to half by pre-incubating the cells with monoclonal antibodies against CD36 and ICAM-1 (Figure 34a). Even at low parasitemia of ~1%, adhesion of FCR3 iRBCs could be quantified in this assay, and we observed that stimulation of HDMEC cells with TNF for 24 h prior to the adhesion assay lead to increased binding of iRBCs (Figure 34b).

We then analyzed the binding capacity of FCR3 iRBCs to HDMEC cells stimulated for 4 h with plasmas of individuals at the end of the dry season subclinically carrying *P. falciparum* (May$^+$) or uninfected (May$^-$) and in donors with clinical malaria in the ensuing transmission s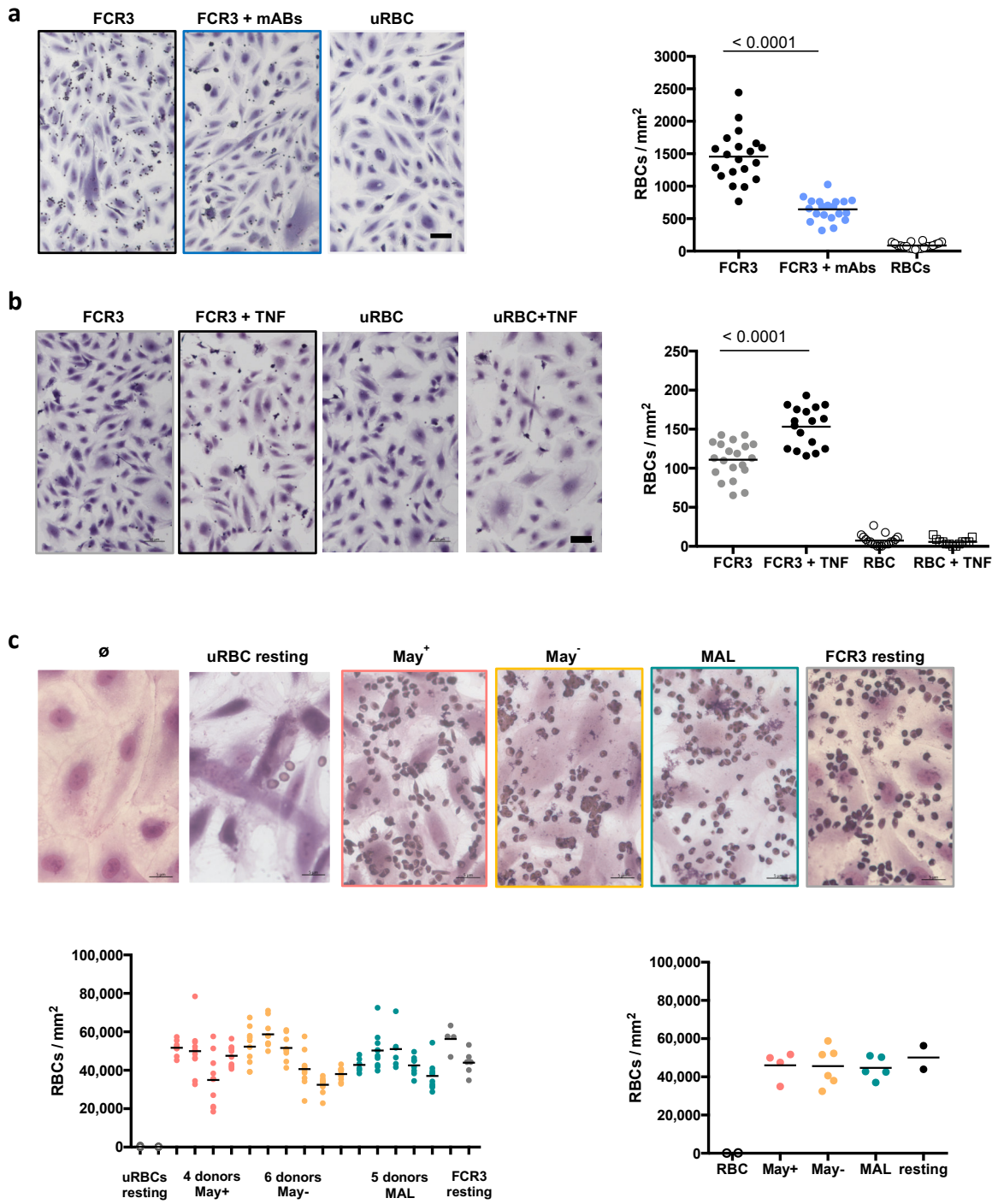eason (MAL) and then allowed FCR3 iRBCs to cytoadhere. The assay was carried out in parallel to the detection of endothelial adhesion receptors after 4h stimulation by plasma (Figure 33 a-f). Samples of 15 donors could be analyzed (May$^+$: n = 4, May$^-$: n = 6, MAL: n = 5) and we observed that iRBCs bound well to plasma-stimulated HDMEC and to the untreated control HDMECs (resting). There was variation in adhesion efficiency between donors within each group of samples, but overall FCR3 iRBCs adhesion to 4h plasma-stimulated HDMEC cells was not significantly different than that seen to non-stimulated HDMEC cells and did not vary between the seasons or infection status (Figure 34c).

Figure 34: Static adhesion assay of FCR3 iRBCs on HDMEC cells after stimulation with Malian plasmas

a) HDMEC cells were stimulated with 10 ng/ml TNF for 16 h and then pre-incubated with monoclonal antibodies (mABs) against CD36 (10 μg/ml) and ICAM-1 (5 μg/ml) for 15 min. Trophozoite-stage FCR3 iRBCs (panned for HDMEC adhesion for 4 rounds) at 25 % parasitemia were allowed to bind for 30 min, washed, fixed and stained with May-Grünwald giemsa. The experiment was carried out in duplicates and of each well 5-10 images were recorded at 100X magnification. A representative images is shown for each condition. Scale bar 50 μm. Each dot in the graph represents an image of HDMEC cells. Line shows mean, statistical test by unpaired t-test. **b)** HDMEC cells were stimulated with 10 ng/ml TNF for 24 h and then FCR3 iRBCs at 1 % parasitemia were added for 30 min, washed, fixed and stained with May-Grünwald giemsa. The experiment was carried out in duplicates, of each well 5-10 images were recorded in 100x magnification. A representative images is shown for each condition. Scale bar 50 μm. Each dot in the graph represents an image of HDMEC cells. Line shows mean, statistical test by unpaired t-test. **c)** HDMEC cells were stimulated for 4 h with 50% plasmas of donors with asymptomatic malaria at the end of the dry season (May+) or uninfected (May-) or of donors with clinical malaria during the transmission season. Plasmas were then washed off and young schizont-stage FCR3 iRBC (panned for HDMEC binding for 8 rounds) at 44% parasitemia were allowed to bind for 30 min, washed, fixed and stained with May-Grünwald giemsa and imaged at 400x magnification. Of each sample, ~10 images were recorded. Dots in graph represent one image (left side graph) or one mean value of one donor of the respective group (right side graph).

a FCR3 | FCR3 + mABs | uRBC

b FCR3 | FCR3 + TNF | uRBC | uRBC+TNF

c ø | uRBC resting | May⁺ | May⁻ | MAL | FCR3 resting

4. Discussion

During the dry season, *P. falciparum* remains asymptomatically in individuals without being cleared and without making its hosts sick, ensuring its survival for several months until mosquitoes return in the rainy season and transmission restarts. In these dry season hosts, *P. falciparum* iRBCs were found to circulate longer in the blood stream within its 48 h asexual cycle without sequestering in the deep vasculature (Andrade et al. 2020).

First, we addressed whether the circulating iRBCs during the dry season were at higher risk of splenic clearance and how this contributed to maintain low parasitemia during the dry season. We therefore mimicked the retention of iRBC from asymptomatic donors at the end of the dry season and from donors with clinical malaria during the transmission season using a microsphiltration assay (Andrade et al. 2020). We found that circulating iRBCs collected from clinical cases and subjected to filtration could pass through the filter, while about one third of circulating iRBCs from the dry season were retained in the filter, and this corresponded well with the higher percentage of non-ring iRBCs in blood samples from asymptomatic donors in the dry season as determined by flow cytometry (Figure 16). Furthermore, iRBCs could mature in culture for 18h until they were retained in the spleen-like filter, while iRBCs in the dry season were already unable to pass the filter after 6h in culture (Figure 16). Hence, the higher risk of splenic clearance is a result of mature stages not adhering and hence passing more through the spleen in the dry season, while iRBCs in clinical malaria are sequestered away before becoming mature enough to be susceptible to splenic filtration. Infected RBCs in the dry season additionally could be less deformable and hence more likely to be retained in the spleen. We have analyzed this in the microsphiltration assay by gating on ring, trophozoite and schizont stages and found that ring stages in the dry season were retained in the spleen-like filter at higher rates (Figure 16). Besides a true decrease in deformability, it could also reflect the higher presence of older, less deformable, ring stages in this gate in the dry season. Differences in deformability could be studied better in tightly synchronized parasite populations, or by single-cell based methods as e.g. micropipette aspiration (Nash et al. 1989). The deformability of iRBCs was suggested by a modeling study to also depend on the density of knobs (Zhang et al. 2015). Given that knob densities and KAHRP expression were similar in stage-matched

iRBCs from the dry season compared to iRBCs from clinical cases, we have no evidence to support that iRBC deformability is altered between the seasons.

To better understand whether the higher risk of splenic clearance in the dry season is an effect of reduced cytoadhesion, we modeled the within-host growth for low and high cytoadhering iRBCs populations (Figure 17). We found that low cytoadhesion led to a broad age composition of the circulating iRBC population, which in a modeled microsphiltration assay showed this iRBC population to be filtered at higher efficiencies. These results matched well the observed age range and filtration rates in the dry season in the experimental setting. Thus, we have good evidence that lower adhesion efficiency drives the observed longer circulation time and the higher risk of splenic clearance. The mathematical model also suggests that iRBCs in clinical cases leave the circulation by adhesion. The estimated age of iRBCs in individuals with clinical malaria was ~7 hpi (Andrade et al. 2020), and in line with the abovementioned hypothesis this is younger than what would be expected if iRBCs were only removed by the spleen starting at 16-20 hpi (Figure 15) (Deplaine et al. 2011). Cytoadhesion, in turn, observed in vitro as A4 strain iRBC adhesion to purified receptors, was observed to start at 14-16 hpi (Gardner et al. 1996). This is compatible with an average age of 7 hpi, however as they are also highly synchronous (Andrade et al. 2020), it's also conceivable that adhesion could start earlier, around 10-12 hpi. Febrile temperatures increased the efficiency of adhesion in adhesion experiments with FCR3 iRBCs under flow (Lubiana et al. 2020), possibly by increasing phosphatidyl serin presentation on the RBC surface that strengthens binding to CD36 (Zhang et al. 2018). For circulating iRBCs during the dry season, the results of the model suggest that a higher fraction is removed from circulation by the spleen. Given that laboratory strain *P. falciparum* iRBCs are starting to be filtered in an artificial spleen from 16-20 hpi (Figure 15), (Deplaine et al. 2011), it is remarkable that ~17 hpi is the average age of iRBCs found in circulation in the dry season; iRBCs of up to 32- 36 hpi are probably circulating in the dry season, as after 12 h of culture occasionally segmented schizonts were found and increase in parasitemia could be observed after 16 h in culture (Andrade et al. 2020). It is also possible that the artificial spleen is a stricter filter than the real spleen. These mature iRBCs in vivo likely did not pass through the spleen for a few hours, which is possible in principle, as RBCs are estimated to only pass through the splenic filter every ~100 − 200 minutes (Buffet et al. 2011). It also highlights

that probably many more iRBCs in the dry season could be able to circulate this long, but were caught in the spleen. In accordance to that, the within-host growth model also showed lower parasite levels at the end of 5 replicative cycles in the low-cytoadhering iRBC population due to increased splenic filtration of iRBCs (Figure 17). Taken together, our data supports that low adhesion and resulting elimination in the spleen maintains low parasitemia during the dry season, allowing *P. falciparum* to survive the lengthy dry season.

We also explored whether the constant splenic clearance leads to splenomegaly in the dry season (**Error! Reference source not found.**). On the first year of the study in May 2011, ~15 % of study participant showed splenomegaly at enrollment (and associated with asymptomatic parasitemia, as has been described before (Crookston et al. 2010; Bassa et al. 2016; Beavogui et al. 2020; Idris et al. 2016). In the following years however, the overall prevalence of splenomegaly at the end of the dry season strongly declined, suggesting that the easily accessible and free-of-cost treatment of febrile malaria that came with the implementation of the clinical study had a large effect to reduce spleen size. A shift of asymptomatic infections to higher age groups likely contributed to decreased the prevalence of splenomegaly at the end of the dry season, as splenomegaly is more frequent in younger children (Kotlyar et al. 2014), and in May 2011 the age groups of ≤ 5 years showed infection rates of ~10 – 40 %, but in the following years they were barely *P. falciparum* positive at the end of the dry season (Portugal et al. 2017). The low levels of splenomegaly also argue against the hypothesis that a more strongly filtering spleen maintains low parasitemia in the dry season, as higher filtration rates were rather observed in clinical cases with splenomegaly (Looareesuwan et al. 1987). In summary, carrying low-density parasitemia throughout the dry season did not lead to splenomegaly in our study population.

Next, we sought to understand how iRBCs in asymptomatic individuals during the dry season become less adhesive compared to iRBCs from clinical malaria cases. We hypothesized that iRBC adhesion efficiency could be reduced through fewer knobs on the iRBC surface and/or a defect in trafficking of parasite adhesion ligands to the surface, or a lower density of parasite adhesion ligands on the iRBC surface. We therefore isolated and enriched iRBCs from asymptomatic individuals at the end of the dry season and from clinical malaria cases, and analyzed the iRBC ultrastructure by transmission and scanning electron microscopy in iRBC stage matched samples.

Stage matching was important as host cell remodeling and the formation of knobs is a dynamic process (Quadt et al. 2012; Mcmillan et al. 2013; Grüring et al. 2011). The validity of our interpretation and conclusions drawn over the electron microscopy data depend on how good the matching of equivalent developmental stages was. We imaged ~20 iRBCs per donor, resulting in 268 images iRBCs in 13 donors with asymptomatic malaria in the dry season and 220 iRBC images from 10 donors with clinical malaria in the transmission season. The number of donors and iRBC images was limited by the low parasitaemia in samples in the dry season, resulting in very small pellet volumes after magnetic enrichment, which still showed very low parasitaemias, limiting how many iRBCs could be imaged. In general, due to the different developmental age of the parasites within the 48 h asexual cycle and differences in synchrony (Andrade et al. 2020), stage matching between dry and transmission season iRBCs was challenging. We excluded images of iRBCs with < 5 μm^2 area to make sure we were analyzing a rather central section of the iRBC. The categorization of iRBCs images into developmental stages based on the relative size of the iRBC within the RBCs and organelle presence is intrinsically imperfect, as not all organelles can be captured in a 70 nm section, nevertheless we achieved a sufficiently precise categorization to identify similar iRBC stages that then could be systematically compared (Figure 20). We quantified knob density by transmission and scanning electron microscopy (Figure 21). Knob density varied between individual donors within the dry and the wet season, probably due to multiple factors as different *P. falciparum* strains (Subramani, Quadt, Jeppesen, Hempel, Vang, et al. 2015) and individual differences in RBC properties. As hemoglobinopathies such as the sickle cell trait and hemoglobin C affect knob density (Cholera et al. 2008; Fairhurst et al. 2005), donors with these traits were not included in the analysis. Mechanistically, the HbS and HbC interfere with the actin remodeling in iRBC and lead to distorted Maurer's cleft and the lack of trafficking vesicles, hence reducing PfEMP1 trafficking to the iRBC surface (Cyrklaff et al. 2011).

In alignment with earlier studies in laboratory strain iRBCs and clinical isolates (Nagao, Kaneko, and Dvorak 2000; Quadt et al. 2012), our data shows that schizont stage iRBCs presented higher mean knob densities. Comparing iRBCs from asymptomatic donors in the dry season to donors with clinical malaria, we found no significant difference between paired parasite developmental stage and overall between the samples, by transmission and scanning electron microscopy. While

both methods yielded the same result, the knob density measurements between the two method did not correlate particularly well, possibly reflecting high variability within donors. We also measured knob diameters on SEM images and found a significantly reduced knob size albeit a very small difference (May 55.7 ± 11.6 nm and MAL: 58.0 ± 11.0 nm) and also substantial overlap in knob diameters on iRBCs between the seasons, leaving it open how biologically meaningful this difference is (Figure 22).

Compared to knob densities reported in the literature (Table 1), we observed knob densities by SEM (mean 52.4 ± 24.6 (May) and 50.1 ± 19.0 knobs/μm^2 (MAL) are similar to knob density determined by SEM in FCR3 iRBCs schizonts ($45-50$ knobs/μm^2) (Gruenberg, Allred, and Sherman 1983) and A4 iRBC schizonts by atomic force microscopy (AFM) (~50 knobs/μm^2), but higher than on FCR3 or other *P. falciparum* laboratory strain iRBCs measured in other studies (Subramani, Quadt, Jeppesen, Hempel, Vang, et al. 2015; Sanchez et al. 2019; Quadt et al. 2012), especially when iRBCs were panned to bind to CSA. The knob densities reported here were also higher than those measured by AFM on iRBCs from Ghanaian children (9-32 knobs/μm^2) that were isolated and cultured for one cycle (Quadt et al. 2012). It's possible that the differences are due to methodology, as the dehydration step during sample processing for electron microscopy can induce shrinkage. However, the knob diameters we observed in the analyzed field isolates were similar to knob diameters on iRBCs of Ghanaian clinical isolates (64 ± 12 nm), while the other studies report higher knob diameters of up to 110 nm (Table 1) (Gruenberg, Allred, and Sherman 1983; Quadt et al. 2012; Sanchez et al. 2019). This difference could also be an effect of the measurement type used. We measured knob diameters manually after a pre-test of using an intensity plot to determine where a knob started and ended led to more variable and less reproducible results between two independent readers measuring the images. Quadt et al. also described that knob density would decrease on iRBCs at the end of the asexual cycle. We didn't observe this on the few segmented schizonts available in our dataset. The loss of knob density in mature schizonts has been proposed to occur due to "sloughing" of knob material (Langreth et al. 1978), which has not been experimentally demonstrated or molecularly defined, but of note we have observed similar structures in a few of our samples. Taken together, it appears that *P. falciparum* iRBCs from asymptomatic donors at the end of the dry season and from clinical cases

in the transmission season are equally capable of forming knobs on iRBCs, suggesting that PfEMP1 molecules can be properly presented on iRBCs.

We next analyzed the ultrastructure of Maurer's clefts in search of possible perturbations that could indicate reduced adhesion or ligand trafficking in dry season iRBCs. Such phenotypes have been described in several knock out studies of Maurer's cleft proteins whose absence led to a defect in trafficking PfEMP1 to the surface, e.g. stacked Maurer's clefts observed in REX1 or Pf332 knockouts (Hanssen, Hawthorne, et al. 2008; Glenister et al. 2009), increased distance of Maurer's clefts to the RBC membrane In SBP1 KO lines (Cooke et al. 2006), fragmented Maurer's clefts in the absence of MAHRP1 or GEXP07 (Spycher et al. 2008; McHugh et al. 2020) or aggregated Maurer's clefts in the PTP1 knockout iRBCs ((Rug et al. 2014). When comparing iRBCs from asymptomatic donors in the dry season compared to iRBCs from clinical cases in the transmission season, we found on average more Maurer's clefts on sections of dry season iRBCs, but no difference in the average length (Figure 23). This suggests that iRBCs could be slightly more frequent in dry season iRBCs. Furthermore, Maurer's clefts in iRBCs of asymptomatic donors in the dry season were located slightly further away from the RBC membrane (May: 184 nm (153 − 214 nm IQR) and MAL: 160 (135 − 188 nm IQR)). It's unclear how strongly a 24 nm difference affects PfEMP1 trafficking, however, the knockout of Maurer's cleft protein SBP1 disrupts PfEMP1 trafficking and also causes MCs located further away from the RBC membrane ((139 ± 12 nm in wildtype gene vs 160 ± 15 nm in the knockout, mean ± SEM) (Cooke et al. 2006). Hence, it is possible that this small phenotype hints to a reduced efficiency of Maurer's cleft tethering to the RBC membrane. While we performed a thorough analysis, it could also be that we missed to observe more subtle phenotypes. The Maurer's cleft gene MAHRP1 for example, when knocked out abolished cytoadhesion in a static adhesion assay, but changes in ultrastructure were only observed in iRBCs when hemoglobin was removed from the host cell after permeabilization by Equinatoxin II treatment (Spycher et al. 2008). In conclusion, the analysis of Maurer's clefts revealed that these structured present with the typical morphology in iRBCs collected during the dry season and from clinical cases during the transmission season, with mild differences in MC number and tethering. Still, it is possible that the host cell remodeling and adhesin trafficking are

altered in the dry season, but in a way that does not promote ultrastructural phenotypes as distinctive as knockout phenotypes do.

We also considered the possibility that host cell remodeling related genes could be downregulated and traffic less PfEMP1 to the RBC surface, without majorly disrupting the ultrastructure. We therefore analyzed the expression of five MC genes that were shown previously to be essential for PfEMP1 trafficking to the surface and adhesion: SBP1 (Cooke et al. 2006), MAHRP1 (Spycher et al. 2008), PTP1 ((Maier et al. 2008a), Pf332 (Glenister et al. 2009) and GEXP07 (McHugh et al. 2020) (Figure 26). While this list is not exhaustive, as at least seven other genes were shown to be essential for cytoadhesion and PfEMP1 trafficking (Maier et al. 2008a), these are among the best described. Additionally, we analyzed the expression of the knob protein KAHRP. As the parasite age within the 48 h asexual cycle greatly influences which genes are expressed (Bozdech et al. 2003), and circulating iRBCs in the dry season were more developed in the asexual cycle as observed by morphology on Giemsa stains, time to increase of parasitemia in culture and transcription profile (Andrade et al. 2020), again we first needed to align iRBCs by stage to be able to detect differences in the gene expression in iRBCs collected from asymptomatic donors at the end of the dry season compared to clinical cases during the transmission season. To this end, we established a qRT-PCR assay quantifying genes that are specifically expressed in ring stage iRBCs (SDH4), trophozoites (HGPRT) and schizonts (OAT), to indicate the presence of the respective stage in the analyzed sample (Figure 25). Interestingly, OAT was also suggested as a marker gene in a recent study that developed a mathematical tool to predict the mean age of a parasite population based on qRT-PCR data, but is limited to the first 23 hours of the intraerythrocytic lifecycle (Ciuffreda et al. 2020). Using these three stage marker genes, we could match iRBCs freshly collected from asymptomatic donors in May (May 0h) to iRBC samples from clinical cases samples that had grown additional 15 hours in culture (MAL 15h). The matching was not exactly perfect, as the trophozoite marker gene HGPRT was expressed significantly lower in iRBCs in the dry season without culture (May 0h) than in iRBCs from clinical cases with 15h of culture (MAL 15h), however it is impossible to perfectly match iRBCs from the dry and the wet season for their large difference in mean age and synchronicity when collected from donors (Andrade et al. 2020). The lower expression of the trophozoite marker gene in iRBCs from the dry season could reflect less

trophozoite iRBCs in these samples, less synchronicity or also that HGPRT is expressed less in trophozoites in the dry season. In these stage-matched samples from the dry season and from clinical cases, we found similar expression levels of KAHRP and Pf332 (Figure 26). In contrast, MAHRP and GEXP07 were downregulated in freshly collected iRBCs May samples at the May 0h vs MAL 15h comparison, but upregulated in the May 15h MAL 30 h comparison. PTP1 was found downregulated in the May 15h vs MAL 30h comparison, while SBP1 was downregulated in May 0h samples compared to MAL 15h in culture samples.

It is possible that the expression of these genes is differentially regulated at the respective timepoints. However, it is possible that a remaining difference in age or synchrony in the matched samples could lead to this effect. Ultimately, gene expression will have to be analyzed by single cell RNA sequencing to be able to draw more reliable conclusions about the expression of these and other host cell remodeling-related genes, and this is currently ongoing in the lab. For now, we can speculate on how a difference in age or synchrony in the matched samples could affect gene expression. First, May samples could be slightly younger after matching. Given that at 0h, the average iRBC was estimated to be 17 hpi old in May samples, while MAL samples were 7 hpi old (Andrade et al. 2020). Additional 15h of culturing MAL samples leads to 17 hpi (May) and 23 hpi (MAL). This would be in line with reduced expression of the trophozoite marker HGPRT in May 0h samples than MAL15h samples, as HGPRT expression increased until 33 hpi in M2K1 iRBCs. Given that expression of MAHRP1 was shown to increase until 25 hpi in M2K1 iRBCs, it is possible that this is an effect of a slightly older iRBC population in the sample obtained from clincal malaria (MAL). However, in this scenario we would expect KAHRP and Pf332 to be differentially expressed as well, and SBP1 should be up – and not downregulated in May 0h vs MAL 15h samples. Second, the observed differences could be attributed to decreased synchrony of the iRBC population in May donors. This would be in line with less pronounced peaks and dips of gene expression when observed in the time course in May samples compared to MAL samples. Also, the lower maximal expression levels of SBP1 and MAHRP1 could be attributed to this, as well as the altered expression of MAHRP1 and GEXP07, and the higher levels of PTP1 in May 15h vs MAL 30 h samples. Still, we would expect KAHRP to also be differentially expressed.

All in all, it is hard to draw definite conclusions about the expression levels of these genes from the bulk qRT-PCR analysis, as the iRBC samples are likely not perfectly matched in age, and the measured expression levels are, beside differences in gene expression between the season, influenced by a multifactor mix of iRBC age at start of culture, level of synchrony, individual differences by donors, efficiency of in vitro growth, and others. Still, it is interesting that SBP1 may be downregulated in iRBCs at the end of the dry season, as observed in the matched timepoints and also the maximal expression level, possibly leading to the small difference observed in MC tethering to the membrane and reducing PfEMP1 surface trafficking and thereby ability to cytoadhere; suggesting further analysis of this gene.

Adhesion efficiency in the dry season may be decreased through less parasite adhesion ligands expressed on the iRBC surface. In the absence of knowledge of which adhesin variants are presented on the iRBC surface, we used blood group specific hyperimmune plasma pools to detect a broad range of antigens on the surface of thawed iRBC samples from asymptomatic carriers at the end of the dry season (May, n = 10) and clinical cases in the transmission season (MAL, n = 10). Upon thawing, in blood samples from the dry season we failed to find a substantial fraction of non-rings in the culture (Figure 27) in contrast to earlier observations with freshly collected iRBCs in May (Figure 16), suggesting that only ring stage iRBCs survived the freeze-thaw cycle. Hence, we could not directly study this interesting population, and also it prolonged the time-to increase in culture, suggesting that we should have implemented a 48 h in culture timepoint also for all iRBC samples of the dry season to be able to evaluate the growth in culture. Furthemore, this has implications for other assays using cryopreserved dry season iRBC samples and needs to be considered in the experimental design. We then analyzed the labeling of surface antigens by a blood-group specific hyperimmune pool over the development of the parasite in culture (Figure 28). As a control, we used pooled serum from malaria-naïve donors, which revealed unspecific labeling iRBCs and uRBCs in a few donors with increasing intensity as the parasites matured in culture, possibly reflecting the release of *P. falciparum* proteins from dying iRBCs that then attached to the cells in culture. The hyperimmune plasma pool similarly labeled up to ~20 % the iRBC population at 24 – 36 h in culture in samples from asymptomatic donors in the dry season

and clinical malaria cases in the wet season, and also when we compared the labeling of ring, trophozoite and schizont stages, we observed no significant differences between the seasons. However, we only observed schizonts in very few samples and at low density; an additional 48 h in culture timepoint with hyperimmune plasma labeling would have been useful here.

From similar levels of iRBC surface labeling by the hyperimmune pool, we deduct that these iRBCs have a similar density of surface antigens on the surface. Further, there is evidence that PfEMP1 is the dominant antigen in mature iRBCs recognized by pooled immune plasmas, as the extend of iRBC labeling is reduced in *var* knockdown parasite lines (Chan et al. 2012) or skeleton binding protein 1 (SBP1) knockout lines that have impaired PfEMP1 surface trafficking (J. A. Chan et al. 2016) or a chromosome 9 deletion mutant not expressing PfEMP1 (Piper, Roberts, and Day 1999), even though members of RIFINs and STEVORs on their surface were still present on the iRBC surface (Chan et al. 2012; Chan et al. 2016). Complementary, immuno-EM with plasma from infected monkeys showed specific labeling at the knobs (Langreth and Reese 1979). However, several studies detected antibodies against RIFINs (Abdel-Latif et al. 2002) or an A-type RIFIN (Quintana et al. 2018) or STEVOR proteins (Schreiber et al. 2008) or almost all RIFINS, even the intracellular B-RIFINs, and STEVORs (Kanoi et al. 2020) in the plasma of semi-immune individuals. Hence, these antibodies could also bind to iRBC surface antigens when labeled with a hyperimmune pool.

Further, we assume that the hyperimmune plasma pool recognizes surface antigens on iRBCs from asymptomatic donors or clinical malaria cases with equal efficiency. However, there is evidence for differences in recognition of iRBCs by disease severity: a study in Kenyan children showed that iRBCs isolated from children with severe malaria was recognized by plasmas of more children than iRBCs from uncomplicated malaria (Bull et al. 1999). The same was demonstrated in Ghanaian children, with iRBCs from children younger than 5 years old detected more frequently (Nielsen et al. 2002). This is thought to be linked to the acquisition of antibodies against very virulent *P. falciparum* variants early in life (Cham et al. 2010). However, this might not necessarily apply to our data for several reasons: the malaria cases analyzed in this studies were all categorized as mild malaria and obtained from children of 5 years or older (11.0 years (8.2 − 13.8 95% CI)). Additionally, the plasma pools used for recognition were combined from 25 − 159 donors

(depending on the blood group) of at least 15 years old, increasing the likelihood that antibodies against almost all of the circulating PfEMP1 variants were covered. On the other hand, in vitro culture of iRBCs represents a strong change of environment and removes the selection pressure for adhesion. It has also been suggested that culture in RPMI medium supplemented with Albumax II is inferior to supplementation with human plasma, with less PfEMP1 expression after three cycles (Ribacke et al. 2013) or already after 15 h (Frankland et al. 2007). Loss of knobs however occurs more slowly, as observed after 3 months (Tilly et al. 2015). To provide optimal growth conditions, we previously tried to culture iRBC in 10% plasma of the respective donor, but found that most donor's iRBC did not tolerate this well and died (data not shown). It is possible that the iRBCs grown in Albumax II do not reach their full potential regarding PfEMP1 surface expression. However, we assume that this similarly affects dry and wet season parasites and still allows us to detect differences between them. As we did not observe significant differences between the labeling of iRBCs from asymptomatic donors in the dry season and clinical malaria cases in the wet season, we conclude that they are equally able to place surface antigens, among them PfEMP1 molecules, on the surface, allowing them to cytoadhere. It remains still the possibility that PfEMP1 molecules are presented on the surface at different densities, and as soon as we have identified the most common types, we may be able to quantify them directly with specific antibodies.

In summary, it appears that the three mechanisms to render an iRBCs less adhesive that were studied in this thesis (reduced knob density, impaired adhesin trafficking, reduced surface presentation) are not or only minimally altered in dry season iRBCs. It is therefore still unclear how *P. falciparum* iRBCs become less adhesive in the dry season.

An alternative hypothesis is the expression of less adhesive PfEMP1 variants during the dry season. Investigating PfEMP1 type in malaria field samples is not trivial, as it requires the establishment of a pipeline to predict PfEMP1 sequences and binding types from qPCR data from field samples, adjustment of sequencing protocols to very low parasitemias and the mapping to a collection of reference PfEMP1s that are present in the local parasite population or *de novo* assemblies. These tasks are underway in our lab and will give valuable insights into the PfEMP1 types during the dry and the transmission season. So far, *var* gene expression in asymptomatic individuals has been

addressed by a number of studies. Asymptomatic infections have been associated with var group C expression (Kaestli et al. 2006; Falk et al. 2009; Gupta et al. 2019). A study in Tanzanian children found lower group A and B var gene expression in asymptomatic donors using *var* group specific primers in qRT-PCR, but no group of *var* genes that were expressed at higher levels (Rottmann et al. 2006), also opening to the possibility that *var* gene expression is reduced in asymptomatic infections. In contrast, a study in Kenyan children found a smaller range of different *var* genes expressed in the parasite population of asymptomatic individuals than clinical malaria cases, but the overall distribution of group A and non-group A var appeared to vary more between individuals than between symptomatic or asymptomatic infection (Warimwe et al. 2013). Similarly, a CHMI study in semi-immune individuals compared individuals who controlled parasite growth (and stayed asymptomatic) or not and found differences in the breadth of var genes expression but no strong differences in the var type, with mostly B and B/C var genes expressed (Bachmann et al. 2019). It is possible that upon infection, existing immunity against EPCR binding var groups in group A (Turner et al. 2015) drives down these PfEMP1, forcing the parasite to express other non-A types to survive immune clearance. To be able to persist for at least 6 months, it is necessary that the parasite has sufficient low binding PfEMP1 variants to switch between during the dry season. If we assume that it needs to switch every 2 weeks, that would be at least 13 variants, and this is only counting one person in one year. Alternatively, it may be that these PfEMP1 variants are less immunogenic than other variants, either intrinsically, or as a result of the limited multiplication of the respective iRBCs.

Finally, we investigated whether the host environment in the dry season also contributes to decreased adhesion. We hypothesized that in the absence of clinical symptoms, the host provides less adhesion receptors on endothelial cells as result of reduced endothelial activation.

We first compared asymptomatic carriers at the end of the dry season and clinical malaria cases in the wet season regarding the expression of the pro-inflammatory cytokines tumor necrosis factor (TNF), interleukin 1 α (IL-1α) and IL-1β (Figure 30), which can activate endothelial cells leading to higher expression levels of endothelial cell receptors (Pober, Gimbrone, et al. 1986; Pober, Bevilacqua, et al. 1986; Swerlick et al. 1992). We observed that TNF levels were elevated in

malaria cases (MAL) (9.1 (6.8 – 16.9) pg/ml), while low TNF levels were found in individuals at the end of the dry season independently of the donor's infectious status (median (IQR): May$^+$, 4.1 (3.2 – 6.4) and May$^-$, 2.81 (2.5 – 4.8) pg/ml). Compared to the literature, in the groups of uncomplicated malaria cases vs. uninfected controls, some studies have reported higher mean: 31 pg/ml compared to 10 pg/ml (Shaffer et al. 1991), 24 pg/ml compared to < 10 pg/ml (Kwiatkowski et al. 1990), while other studies measured similarly low values (8.8 pg/ml and 7.7 pg/ml (Lyke et al. 2004)) or even lower values (2.12 pg/ml and 1.4 pg/ml (Mandala et al. 2017)). In general, the amount of TNF may depend on the method and the sensitivity of the measurement. We did not observe differences in TNF, IL-1α and IL-1β between asymptomatic and aparasitemic children, in contrast to previous reports (Kaboré et al. 2020; Frimpong et al. 2020). The asymptomatic group in this study possibly contained pre-clinical infections. Additionally, we know that parasitemia can decrease over the dry season (Andrade et al. 2020), so possibly the parasitemia in our asymptomatic group was lower than in other studies.

Next, we assessed whether increased cytokine levels as observed in malaria cases were sufficient to induce the upregulation of adhesion receptors on endothelial cells in vitro. As a surrogate, we measured the levels of soluble adhesion molecules in the plasma (Figure 31). This has been shown to correlate with the upregulation of endothelial receptors in vivo, as plasma sVCAM-1 and sE-Selectin levels correlated with the expression of the respective adhesion molecule on dermal microvessels from skin biopsies in Vietnamese adults (Turner et al. 1998). We measured soluble (s)ICAM-1, sVCAM-1, sPECAM-1, sE-Selectin and sP-Selectin in plasmas collected from subclinical individuals carrying *P. falciparum* at the end of the dry season, uninfected individuals and from donors with clinical malaria in the ensuing transmission season and found higher plasma levels of sVCAM-1, sE-Selectin and sP-Selectin in donors with clinical malaria compared to those of plasmas collected in the dry season (May$^+$ and May$^-$), but not of sICAM-1 and sPECAM-1. The upregulation of sVCAM-1 and sE-Selectin is in agreement with other studies on plasma levels of the respective molecules in uncomplicated malaria versus healthy controls, however typically sICAM-1 was also significantly increased (Tchinda et al. 2007; Jakobsen, Morris-Jones, et al. 1994); others reported only increased levels of ICAM-1 and E-Selectin (Hviid et al. 1993; Moxon et al. 2014) or of sICAM-

1 and sVCAM-1 (Park et al. 2012); For sICAM-1 plasma levels, it is possible that inter-individual differences mask differences between the groups. In paired donors (May⁻ and MAL), sICAM-1 levels were significantly different Possibly the elevated levels of proinflammatory cytokines are sufficient to stimulate E-Selectin and VCAM-1 production, but not ICAM-1. Of course differences could also be linked to different shedding dynamics of different receptors. In an in vitro experiment, HUVEC cells were shown to shed VCAM-1 more strongly than ICAM-1 or E-Selectin (Pigott et al. 1992), which could contribute to the high VCAM-1 levels we observed.

To better understand whether adhesion receptors are present at lower densities on endothelial cells in asymptomatic individuals in the dry season, compared to clinical malaria cases in the transmission season, we tested how plasmas from these donors could activate endothelial cells to express adhesion receptors on the surface (Figure 33). After 4 h of incubation with 50% plasma, we did not observe a significant difference in the expression ICAM-1, VCAM-1 or E-Selectin on endothelial cells stimulated with plasma from donors with subclinical *P. falciparum* infection compared to donors with their first clinical malaria episode in the transmission season, but we found increased ICAM-1 expression after 24 h of stimulation with plasmas from clinical malaria cases compared to subclinically infected donors at the end of the dry season. It is possible that the differences in endothelium-stimulating cytokines are so small that they only manifest in measurable differences of receptor expression after prolonged stimulation. To this end, we also used the high plasma concentrations of 50%. However, the ICAM-1 expression on plasma-stimulated cells was even higher than after stimulation with super-physiological TNF concentrations (10 ng/ml) after 24h, suggesting that prolonged stimulation with 50% plasma may also have adverse effects on endothelial cells. It is interesting that ICAM-1 showed differential expression patterns after stimulation with plasmas of malaria cases in the transmission season (MAL) and donors carrying or not parasites at the end of the dry season (May⁺ and May⁻), but sICAM-1 levels in the plasma did not. The inverse effect was observed for E-Selectin-1 and VCAM-1. This is possibly an effect of higher shedding of E-Selectin and VCAM-1 than ICAM-1, or due to the very high expression levels of ICAM-1 on HDMEC cells especially after 24 h of stimulation, allowing for a higher sensitivity to detect subtle differences.

Lastly, we assess the binding capacity of a *P. falciparum* parasite line on endothelial cells previously stimulated for 4 h by plasmas of malaria cases in the transmission season (MAL, n =5) and donors carrying or not parasites at the end of the dry season (May$^+$, n = 4 and May$^-$, n = 6), in a static binding assay, but we did not observe differences in cytoadhesion to the plasma-stimulated cells between the three groups (Figure 34). It is possible that differences were subtle and would only become significant in a larger dataset, however as we also did not see significant differences in receptor expression after 4h of plasma stimulation (apart from mildly elevated receptor expression levels in May$^-$ plasma stimulated cells, compared to May$^+$ and MAL plasma stimulated cells), it is possible that in all three conditions (stimulated with plasmas of malaria cases in the transmission season (MAL) and donors carrying or not parasites at the end of the dry season (May$^+$ and May$^-$) the same adhesion receptor density led to similar adhesion efficiencies. Third, iRBCs in this static assay may not bind to ICAM-1, VCAM-1 and E-Selectin, as these have been reported to be involved in rolling adhesion if iRBCs and rather bind to constitutively expressed receptors as CD36 (Helms et al. 2016). Besides increasing the number of samples tested and expanding the analysis to the 24 hpi timepoint, it could also be useful to perform this assay under flow conditions. For better comparison of adhesion to the three receptors, the assay could also be performed at ~10-12 h post stimulation when all receptors are expressed at higher levels on the same cell.

Taken together, our preliminary data suggests that during asymptomatic malaria, the endothelium is not or less activated than in malaria cases. It remains to be demonstrated whether this small difference in receptor expression leads lower cytoadhesion of iRBCs during the dry season. If this is the case, it is very interesting, and poses a *hen or egg* problem: Do the parasites inherently adhere less, thereby cause less direct activation of the endothelium as well produce less parasite toxin, triggering the production of TNF and IL-1 to a lesser degree, causing less endothelial activation, and hence adhesion? Or Is the immune system of the individual reacting less to these parasites, and by producing less cytokines and endothelial activation, keeping adhesion down, preventing parasites from reaching a fever threshold?

Further, it would be interesting to understand the absence of endothelial activation in the dry season. Possibly, it is an effect of disease tolerance. After a febrile malaria episode, upon iRBC stimulation PBMCs exhibited downregulated gene expression of proinflammatory cytokines like

IL-1β and IL-6, although this could not be observed on the protein level (Portugal et al. 2014). However, in the same cohort, a recent pre-print reports that isolated monocytes from adults produced less TNF, IL-1β and other proinflammatory cytokines upon iRBC stimulation than children or malaria-naïve adults, suggesting that malaria episodes attenuate the proinflammatory response at reinfection (Guha et al. 2020). Similarly, an association between decreased TNF-producing CD4+ T cells with asymptomatic infection was described in Ugandan children (Jagannathan et al. 2014) and in the same cohort it was reported that high rates of malaria episodes in children led to fewer γδ2 T cells, and that these produced less TNF and INFγ (Farrington et al. 2017). A follow up study added that individuals with low γδ 2 T cells were more likely to have asymptomatic infections, while those with higher γδ 2 T cells were less likely to be asymptomatic, but more likely to fall sick once infected (Jagannathan et al. 2017). It is hence possible that the first febrile malaria case in the season attenuates the induction of a proinflammatory, endothelium-activating immune response in later infections in the season. When a new clone arrives, the immune system could be more tolerant of infection, keeping endothelial receptor density low and hence providing less optimal opportunities for adhesion, limiting parasite growth, but not directly eliminating the parasite, hence allowing for asymptomatic infections.

5. References

Abdel-Latif, Mohamed S., Ayman Khattab, Christoph Lindenthal, Peter G. Kremsner, and Mo Quen Klinkert. 2002. "Recognition of Variant Rifin Antigens by Human Antibodies Induced during Natural Plasmodium Falciparum Infections." *Infection and Immunity* 70 (12): 7013–21. https://doi.org/10.1128/IAI.70.12.7013-7021.2002.

Abdel-Latif, Mohamed S, Gerardo Cabrera, Carsten Köhler, Peter G Kremsner, Adrian J F Luty, and 1-95/C Study Team. 2004. "Antibodies to Rifin: A Component of Naturally Acquired Responses to Plasmodium Falciparum Variant Surface Antigens on Infected Erythrocytes." *The American Journal of Tropical Medicine and Hygiene* 71 (2): 179–86. https://doi.org/10.4269/ajtmh.2004.71.2.0700179.

Allison, A. C. 1960. "Turnovers of Erythrocytes and Plasma Proteins in Mammals." *Nature* 188 (4744): 37–40. https://doi.org/10.1038/188037a0.

Andrade, Carolina M., Hannah Fleckenstein, Richard Thomson-Luque, Safiatou Doumbo, Nathalia F. Lima, Carrie Anderson, Julia Hibbert, et al. 2020. "Increased Circulation Time of Plasmodium Falciparum Underlies Persistent Asymptomatic Infection in the Dry Season." *Nature Medicine* 26 (December). https://doi.org/10.1038/s41591-020-1084-0.

Armah, H., A. K. Dodoo, E. K. Wiredu, J. K. Stiles, A. A. Adjei, R. K. Gyasi, and Y. Tettey. 2005. "High-Level Cerebellar Expression of Cytokines and Adhesion Molecules in Fatal, Paediatric, Cerebral Malaria." *Annals of Tropical Medicine and Parasitology* 99 (7): 629–47. https://doi.org/10.1179/136485905X51508.

Ashley, Elizabeth A., and Nicholas J. White. 2014. "The Duration of Plasmodium Falciparum Infections." *Malaria Journal* 13 (1). https://doi.org/10.1186/1475-2875-13-500.

Attaher, Oumar, Almahamoudou Mahamar, Bruce Swihart, Amadou Barry, Bacary S Diarra, Moussa B Kanoute, Adama B Dembele, et al. 2019. "Age-Dependent Increase in Antibodies That Inhibit Plasmodium Falciparum Adhesion to a Subset of Endothelial Receptors." *Malaria Journal* 18 (1): 128. https://doi.org/10.1186/s12936-019-2764-4.

Babiker, H A, A M Abdel-Muhsin, L C Ranford-Cartwright, G Satti, and D Walliker. 1998. "Characteristics of Plasmodium Falciparum Parasites That Survive the Lengthy Dry Season in Eastern Sudan Where Malaria Transmission Is Markedly Seasonal." *The American Journal of Tropical Medicine and Hygiene* 59 (4): 582–90. http://www.ncbi.nlm.nih.gov/pubmed/9790434.

Bach, Olaf, Michael Baier, Annika Pullwitt, Nedson Fosiko, George Chagaluka, Matthew Kalima, Wolfgang Pfister, Eberhard Straube, and Malcolm Molyneux. 2005. "Falciparum Malaria after Splenectomy: A Prospective Controlled Study of 33 Previously Splenectomized Malawian Adults." *Transactions of the Royal Society of Tropical Medicine and Hygiene* 99 (11): 861–67. https://doi.org/10.1016/j.trstmh.2005.03.008.

Bachmann, Anna, Ellen Bruske, Ralf Krumkamp, Louise Turner, J. Stephan Wichers, Michaela Petter, Jana Held, et al. 2019. "Controlled Human Malaria Infection with Plasmodium Falciparum Demonstrates Impact of Naturally Acquired Immunity on Virulence Gene Expression." Edited by Alexandra Rowe. *PLOS Pathogens* 15 (7): e1007906. https://doi.org/10.1371/journal.ppat.1007906.

Bachmann, Anna, Claudia Esser, Michaela Petter, Sabine Predehl, Vera von Kalckreuth, Stefan Schmiedel, Iris Bruchhaus, and Egbert Tannich. 2009. "Absence of Erythrocyte Sequestration and Lack of Multicopy Gene Family Expression in Plasmodium Falciparum from a Splenectomized Malaria Patient." Edited by Volker Theo Heussler. *PLoS ONE* 4 (10): e7459. https://doi.org/10.1371/journal.pone.0007459.

Bachmann, Anna, Michaela Petter, Ann Kathrin Tilly, Laura Biller, Karin A. Uliczka, Michael F. Duffy, Egbert Tannich, and Iris Bruchhaus. 2012. "Temporal Expression and Localization Patterns of Variant Surface Antigens in Clinical Plasmodium Falciparum Isolates during Erythrocyte Schizogony." *PLoS ONE* 7 (11). https://doi.org/10.1371/journal.pone.0049540.

Baird, J. Kevin, Michael J. Bangs, Jason D. Maguire, and Mazie J. Barcus. 2002. "Epidemiological Measures of Risk of Malaria." In *Malaria Methods and Protocols*, 72:13–22. New Jersey: Humana Press. https://doi.org/10.1385/1-59259-271-6:13.

Baptista, João Luís, Guido Vanham, Marc Wéry, and Eric Van Marck. 1997. "Cytokine Levels during Mild and Cerebral Falciparum Malaria in Children Living in a Mesoendemic Area." *Tropical Medicine and International Health* 2 (7): 673–79. https://doi.org/10.1046/j.1365-3156.1997.d01-355.x.

Barnwell, John W., Russell J. Howard, and Louis H. Miller. 1983. "Influence of the Spleen on the Expression of Surface Antigens on Parasitized Erythrocytes." *Ciba Foundation Symposium* 94 (May): 117–36. https://doi.org/10.1002/9780470715444.ch8.

Baruch, Dror I., Britten L. Pasloske, Hardeep B. Singh, Xiahui Bi, Xin C. Ma, Michael Feldman, Theodore F. Taraschi, and Russell J. Howard. 1995. "Cloning the P. Falciparum Gene Encoding PfEMP1, a Malarial Variant Antigen and Adherence Receptor on the Surface of Parasitized Human Erythrocytes." *Cell* 82 (1): 77–87. https://doi.org/10.1016/0092-8674(95)90054-3.

Bassa, Fidèle K., Mamadou Ouattara, Kigbafori D. Silué, Lukas G. Adiossan, Nahoua Baikoro, Siaka Koné, Moussan N'Cho, et al. 2016. "Epidemiology of Malaria in the Taabo Health and Demographic Surveillance System, South-Central CIV." *Malaria Journal* 15 (1): 1–11. https://doi.org/10.1186/s12936-015-1076-6.

Beavogui, Abdoul Habib, Alexandre Delamou, Bienvenu Salim Camara, Daouda Camara, Karifa Kourouma, Robert Camara, Issaka Sagara, Eugene

Kaman Lama, and Abdoulaye Djimde. 2020. "Prevalence of Malaria and Factors Associated with Infection in Children Aged 6 Months to 9 Years in Guinea: Results from a National Cross-Sectional Study." *Parasite Epidemiology and Control* 11: e00162. https://doi.org/10.1016/j.parepi.2020.e00162.

Bengtsson, Anja, Louise Joergensen, Thomas S Rask, Rebecca W Olsen, Marianne A Andersen, Louise Turner, Thor G Theander, et al. 2013. "A Novel Domain Cassette Identifies Plasmodium Falciparum PfEMP1 Proteins Binding ICAM-1 and Is a Target of Cross-Reactive, Adhesion-Inhibitory Antibodies." *The Journal of Immunology* 190 (1): 240–49. https://doi.org/10.4049/jimmunol.1202578.

Berendt, A R, D L Simmons, J Tansey, C I Newbold, and K Marsh. 1989. "Intercellular Adhesion Molecule-1 Is an Endothelial Cell Adhesion Receptor for Plasmodium Falciparum." *Nature* 341 (6237): 57–59. https://doi.org/10.1038/341057a0.

Biswas, Anup Kumar, Abdul Hafiz, Bhaswati Banerjee, Kwang Sik Kim, Kasturi Datta, and Chetan E. Chitnis. 2007. "Plasmodium Falciparum Uses GC1qR/HABP1/P32 as a Receptor to Bind to Vascular Endothelium and for Platelet-Mediated Clumping." *PLoS Pathogens* 3 (9): 1271–80. https://doi.org/10.1371/journal.ppat.0030130.

Blisnick, Thierry, Maria Eugenia Morales Betoulle, Jean Christophe Barale, Pierrick Uzureau, Laurence Berry, Sarah Desroses, Hisashi Fujioka, Denise Mattei, and Catherine Braun Breton. 2000. "Pfsbp1, a Maurer's Cleft Plasmodium Falciparum Protein, Is Associated with the Erythrocyte Skeleton." *Molecular and Biochemical Parasitology* 111 (1): 107–21. https://doi.org/10.1016/S0166-6851(00)00301-7.

Boddey, Justin A., Anthony N. Hodder, Svenja Günther, Paul R. Gilson, Heather Patsiouras, Eugene A. Kapp, J. Andrew Pearce, et al. 2010. "An Aspartyl Protease Directs Malaria Effector Proteins to the Host Cell." *Nature* 463 (7281): 627–31. https://doi.org/10.1038/nature08728.

Bourgeois, N., A. Boutet, P. J. Bousquet, D. Basset, C. Douard-Enault, S. Charachon, and L. Lachaud. 2010. "Comparison of Three Real-Time PCR Methods with Blood Smears and Rapid Diagnostic Test in Plasmodium Sp. Infection." *Clinical Microbiology and Infection* 16 (8): 1305–11. https://doi.org/10.1111/j.1469-0691.2009.02933.x.

Bousema, Teun, Rhoel R. Dinglasan, Isabelle Morlais, Louis C. Gouagna, Travis van Warmerdam, Parfait H. Awono-Ambene, Sarah Bonnet, et al. 2012. "Mosquito Feeding Assays to Determine the Infectiousness of Naturally Infected Plasmodium Falciparum Gametocyte Carriers." *PLoS ONE* 7 (8). https://doi.org/10.1371/journal.pone.0042821.

Bousema, Teun, Lucy Okell, Ingrid Felger, and Chris Drakeley. 2014. "Asymptomatic Malaria Infections: Detectability, Transmissibility and Public Health Relevance." *Nature Reviews Microbiology* 12 (12): 833–40. https://doi.org/10.1038/nrmicro3364.

Bozdech, Zbynek, Manuel Llinás, Brian Lee Pulliam, Edith D Wong, Jingchun Zhu, and Joseph L DeRisi. 2003. "The Transcriptome of the Intraerythrocytic Developmental Cycle of Plasmodium Falciparum." *PLoS Biology* 1 (1): E5. https://doi.org/10.1371/journal.pbio.0000005.

Brancucci, Nicolas M.B., Joseph P. Gerdt, Cheng Qi Wang, Mariana De Niz, Nisha Philip, Swamy R. Adapa, Min Zhang, et al. 2017. "Lysophosphatidylcholine Regulates Sexual Stage Differentiation in the Human Malaria Parasite Plasmodium Falciparum." *Cell* 171 (7): 1532-1544.e15. https://doi.org/10.1016/j.cell.2017.10.020.

Brasil, Patrícia, Mariano Gustavo Zalis, Anielle de Pina-Costa, Andre Machado Siqueira, Cesare Bianco Júnior, Sidnei Silva, André Luiz Lisboa Areas, et al. 2017. "Outbreak of Human Malaria Caused by Plasmodium Simium in the Atlantic Forest in Rio de Janeiro: A Molecular Epidemiological Investigation." *The Lancet Global Health* 5 (10): e1038–46. https://doi.org/10.1016/S2214-109X(17)30333-9.

Buffet, Pierre A, Innocent Safeukui, Guillaume Deplaine, Valentine Brousse, Virginie Prendki, Marc Thellier, Gareth D Turner, and Odile Mercereau-Puijalon. 2011. "The Pathogenesis of Plasmodium Falciparum Malaria in Humans: Insights from Splenic Physiology." *Blood* 117 (2): 381–92. https://doi.org/10.1182/blood-2010-04-202911.

Bull, Peter C., Breit S. Lowe, Moses Kortok, Catherine S. Molyneux, Christopher I. Newbold, and Kevin Marsh. 1998. "Parasite Antigens on the Infected Red Cell Surface Are Targets for Naturally Acquired Immunity to Malaria." *Nature Medicine* 4 (3): 358–60. https://doi.org/10.1038/nm0398-358.

Bull, Peter C., Brett S. Lowe, Moses Kortok, and Kevin Marsh. 1999. "Antibody Recognition of Plasmodium Falciparum Erythrocyte Surface Antigens in Kenya: Evidence for Rare and Prevalent Variants." *Infection and Immunity* 67 (2): 733–39. https://doi.org/10.1128/iai.67.2.733-739.1999.

Cham, Gerald K.K., Louise Turner, Jonathan D. Kurtis, Theonest Mutabingwa, Michal Fried, Anja T.R. Jensen, Thomas Lavstsen, Lars Hviid, Patrick E. Duffy, and Thor G. Theander. 2010. "Hierarchical, Domain Type-Specific Acquisition of Antibodies to Plasmodium Falciparum Erythrocyte Membrane Protein 1 in Tanzanian Children." *Infection and Immunity* 78 (11): 4653–59. https://doi.org/10.1128/IAI.00593-10.

Chan, Jo Anne, Katherine B. Howell, Christine Langer, Alexander G. Maier, Wina Hasang, Stephen J. Rogerson, Michaela Petter, et al. 2016. "A Single Point in Protein Trafficking by Plasmodium Falciparum Determines the Expression of Major Antigens on the Surface of Infected Erythrocytes Targeted by Human Antibodies." *Cellular and Molecular Life Sciences* 73 (21): 4141–58. https://doi.org/10.1007/s00018-016-2267-1.

Chan, Joanne, Katherine B. Howell, Linda Reiling, Ricardo Ataide, Claire L. Mackintosh, Freya J.I. Fowkes, Michaela Petter, et al. 2012. "Targets of Antibodies against Plasmodium Falciparum–Infected Erythrocytes in Malaria Immunity." *Journal of Clinical Investigation* 122 (9): 3227–38. https://doi.org/10.1172/JCI62182.

Chen, Ingrid, Siân E Clarke, Roly Gosling, Busiku Hamainza, Gerry Killeen, Alan Magill, Wendy O'Meara, Ric N. Price, and Eleanor M. Riley. 2016. "'Asymptomatic' Malaria: A Chronic and Debilitating Infection That Should Be Treated." *PLOS Medicine* 13 (1): e1001942. https://doi.org/10.1371/journal.pmed.1001942.

Chen, Yiwei, Kai Xu, Luca Piccoli, Mathilde Foglierini, Joshua Tan, Wenjie Jin, Jason Gorman, et al. 2021. "Structural Basis of Malaria RIFIN Binding by LILRB1-Containing Antibodies." *Nature*, March. https://doi.org/10.1038/s41586-021-03378-6.

Cheng, Qin, Nicole Cloonan, Katja Fischer, Jenny Thompson, Gary Waine, Michael Lanzer, and Allan Saul. 1998. "Stevor and Rif Are Plasmodium Falciparum Multicopy Gene Families Which Potentially Encode Variant Antigens." *Molecular and Biochemical Parasitology* 97 (1–2): 161–76. https://doi.org/10.1016/s0166-6851(98)00144-3.

Cholera, Rushina, Nathaniel J Brittain, Mark R Gillrie, Tatiana M Lopera-Mesa, Séidina A S Diakité, Takayuki Arie, Michael A Krause, et al. 2008. "Impaired Cytoadherence of Plasmodium Falciparum-Infected Erythrocytes Containing Sickle Hemoglobin." *Proceedings of the National Academy of Sciences of the United States of America* 105 (3): 991–96. https://doi.org/10.1073/pnas.0711401105.

Chotivanich, K., R. Udomsangpetch, A. Dondorp, T. Williams, B. Angus, J. A. Simpson, S. Pukrittayakamee, S. Looareesuwan, C. I. Newbold, and N. J. White. 2000. "The Mechanisms of Parasite Clearance after Antimalarial Treatment of Plasmodium Falciparum Malaria." *Journal of Infectious Diseases* 182 (2): 629–33. https://doi.org/10.1086/315718.

Ciuffreda, Laura, Lisa Ranford-Cartwright, Neils Quashie, and Felix Zoiku. 2020. "Estimation of Parasite Age and Synchrony Status in Plasmodium Falciparum Infections." In *EMBL Conference: BioMalPar XVI: Biology and Pathology of the Malaria Parasite*.

Cook, Jackie, Weiping Xu, Mwinyi Msellem, Marlotte Vonk, Beatrice Bergström, Roly Gosling, Abdul Wahid Al-Mafazy, et al. 2015. "Mass Screening and Treatment on the Basis of Results of a Plasmodium Falciparum-Specific Rapid Diagnostic Test Did Not Reduce Malaria Incidence in Zanzibar." *Journal of Infectious Diseases* 211 (9): 1476–83. https://doi.org/10.1093/infdis/jiu655.

Cooke, Brian M., Donna W. Buckingham, Fiona K. Glenister, Kate M. Fernandez, Lawrence H. Bannister, Matthias Marti, Narla Mohandas, and Ross L. Coppel. 2006. "A Maurer's Cleft-Associated Protein Is Essential for Expression of the Major Malaria Virulence Antigen on the Surface of Infected Red Blood Cells." *Journal of Cell Biology* 172 (6): 899–908. https://doi.org/10.1083/jcb.200509122.

Cox, Francis EG. 2010. "History of the Discovery of the Malaria Parasites and Their Vectors." *Parasites & Vectors* 3 (1): 5. https://doi.org/10.1186/1756-3305-3-5.

Crabb, Brendan S, Brian M Cooke, John C Reeder, Ross F Waller, Sonia R Caruana, Kathleen M Davern, Mark E Wickham, Graham V Brown, Ross L Coppel, and Alan F Cowman. 1997. "Targeted Gene Disruption Shows That Knobs Enable Malaria-Infected Red Cells to Cytoadhere under Physiological Shear Stress" 89: 287–96.

Cranston, H., C. Boylan, G. Carroll, S. Sutera, Williamson, I. Gluzman, and D. Krogstad. 1984. "Plasmodium Falciparum Maturation Abolishes Physiologic Red Cell Deformability." *Science* 223 (4634): 400–403. https://doi.org/10.1126/science.6362007.

Crompton, Peter D, Jacqueline Moebius, Michael Waisberg, Lindsey S Garver, Louis H Miller, Carolina Barillas, Susan K Pierce, et al. 2014. "Malaria Immunity in Man and Mosquito: Insights into Unsolved Mysteries of a Deadly Infectious Disease." *Annu Rev Immunol.* 32 (1): 157–87. https://doi.org/10.1146/annurev-immunol-032713-120220.Malaria.

Crookston, Benjamin T, Stephen C Alder, Isaac Boakye, Ray M Merrill, John H Amuasi, Christina A Porucznik, Joseph B Stanford, et al. 2010. "Exploring the Relationship between Chronic Undernutrition and Asymptomatic Malaria in Ghanaian Children." *Malaria Journal* 9 (1): 39. https://doi.org/10.1186/1475-2875-9-39.

Cutts, Erin E., Niklas Laasch, Dirk M. Reiter, Raphael Trenker, Leanne M. Slater, Phillip J. Stansfeld, and Ioannis Vakonakis. 2017. "Structural Analysis of P. Falciparum KAHRP and PfEMP1 Complexes with Host Erythrocyte Spectrin Suggests a Model for Cytoadherent Knob Protrusions." *PLoS Pathogens* 13 (8): 1–28. https://doi.org/10.1371/journal.ppat.1006552.

Cyrklaff, M., C. Bisseye, J. Simpore, F. Frischknecht, N. Kilian, C. P. Sanchez, and M. Lanzer. 2011. "Hemoglobins S and C Interfere with Actin Remodeling in Plasmodium Falciparum-Infected Erythrocytes." *Science* 334 (6060): 1283–86. https://doi.org/10.1126/science.1213775.

Dao, A, A S Yaro, M Diallo, S Timbiné, D L Huestis, Y Kassogué, A I Traoré, Z L Sanogo, D Samaké, and T Lehmann. 2014. "Signatures of Aestivation and Migration in Sahelian Malaria Mosquito Populations." *Nature* 516 (7531): 387–90. https://doi.org/10.1038/nature13987.

David, P. H., M. Hommel, L. H. Miller, I. J. Udeinya, and L. D. Oligino. 1983. "Parasite Sequestration in Plasmodium Falciparum Malaria: Spleen and Antibody Modulation of Cytoadherence of Infected Erythrocytes." *Proceedings of the National Academy of Sciences of the United States of America* 80 (16 I): 5075–79. https://doi.org/10.1073/pnas.80.16.5075.

Davis, Shevaun P, Kristine Lee, Mark R Gillrie, Lina Roa, Matthias Amrein, and May Ho. 2013. "CD36 Recruits A5β1 Integrin to Promote Cytoadherence of P. Falciparum-Infected Erythrocytes." Edited by Joe Smith. *PLoS Pathogens* 9 (8): e1003590. https://doi.org/10.1371/journal.ppat.1003590.

Deitsch, Kirk W, and Ron Dzikowski. 2017. "Variant Gene Expression and Antigenic Variation by Malaria Parasites."

Deplaine, Guillaume, Innocent Safeukui, Fakhri Jeddi, François Lacoste, Valentine Brousse, Sylvie Perrot, Sylvestre Biligui, et al. 2011. "The Sensing of Poorly Deformable Red Blood Cells by the Human Spleen Can Be Mimicked in Vitro." *Blood* 117 (8): e88–95. https://doi.org/10.1182/blood-2010-10-312801.

Dixon, Matthew W.A., Shannon Kenny, Paul J. Mcmillan, Eric Hanssen, Katharine R. Trenholme, Donald L. Gardiner, and Leann Tilley. 2011. "Genetic Ablation of a Maurer's Cleft Protein Prevents Assembly of the Plasmodium Falciparum Virulence Complex." *Molecular Microbiology* 81 (4): 982–93. https://doi.org/10.1111/j.1365-2958.2011.07740.x.

Dondorp, A. M., B. J. Angus, K. Chotivanich, K. Silamut, R. Ruangveerayuth, M. R. Hardeman, P. A. Kager, J. Vreeken, and N. J. White. 1999. "Red Blood Cell Deformability as a Predictor of Anemia in Severe Falciparum Malaria." *American Journal of Tropical Medicine and Hygiene* 60

(5): 733–37. https://doi.org/10.4269/ajtmh.1999.60.733.

Dorovini-Zis, Katerina, Kristopher Schmidt, Hanh Huynh, Wenjiang Fu, Richard O. Whitten, Dan Milner, Steve Kamiza, Malcolm Molyneux, and Terrie E. Taylor. 2011. "The Neuropathology of Fatal Cerebral Malaria in Malawian Children." *The American Journal of Pathology* 178 (5): 2146–58. https://doi.org/10.1016/j.ajpath.2011.01.016.

Esslinger, C. W., S. Picot, and P. Ambroise-Thomas. 1994. "Intra-Erythrocytic Plasmodium Falciparum Induces Up-Regulation of Inter-Cellular Adhesion Molecule-1 on Human Endothelial Cells In Vitro." *Scandinavian Journal of Immunology* 39 (3): 229–32. https://doi.org/10.1111/j.1365-3083.1994.tb03365.x.

Facer, Christine A., and Agapi Theodoridou. 1994. "Elevated Plasma Levels of P-Selectin (GMP-140/CD62P) in Patients with Plasmodium Falciparum Malaria." *Microbiology and Immunology* 38 (9): 727–31. https://doi.org/10.1111/j.1348-0421.1994.tb01848.x.

Fairhurst, Rick M., Dror I. Baruch, Nathaniel J. Brittain, Graciela R. Ostera, John S. Wallach, Holly L. Hoang, Karen Hayton, et al. 2005. "Abnormal Display of PfEMP-1 on Erythrocytes Carrying Haemoglobin C May Protect against Malaria." *Nature* 435 (7045): 1117–21. https://doi.org/10.1038/nature03631.

Falk, Nicole, Mirjam Kaestli, Weihong Qi, Michael Ott, Kay Baea, Alfred Cortés, and Hans Peter Beck. 2009. "Analysis of Plasmodium Falciparum Var Genes Expressed in Children from Papua New Guinea." *Journal of Infectious Diseases* 200 (3): 347–56. https://doi.org/10.1086/600071.

Fanello, C., M. Onyamboko, S. J. Lee, C. Woodrow, S. Setaphan, K. Chotivanich, P. Buffet, et al. 2017. "Post-Treatment Haemolysis in African Children with Hyperparasitaemic Falciparum Malaria; a Randomized Comparison of Artesunate and Quinine." *BMC Infectious Diseases* 17 (1): 1–8. https://doi.org/10.1186/s12879-017-2678-0.

Farrington, Lila, Hilary Vance, John Rek, Mary Prahl, Prasanna Jagannathan, Agaba Katureebe, Emmanuel Arinaitwe, Moses R. Kamya, Grant Dorsey, and Margaret E. Feeney. 2017. "Both Inflammatory and Regulatory Cytokine Responses to Malaria Are Blunted with Increasing Age in Highly Exposed Children." *Malaria Journal* 16 (1): 1–11. https://doi.org/10.1186/s12936-017-2148-6.

Feintuch, Catherine Manix, Alex Saidi, Karl Seydel, Grace Chen, Adam Goldman-Yassen, Neida K. Mita-Mendoza, Ryung S. Kim, Paul S. Frenette, Terrie Taylor, and Johanna P. Daily. 2016. "Activated Neutrophils Are Associated with Pediatric Cerebral Malaria Vasculopathy in Malawian Children." *MBio* 7 (1): 1–12. https://doi.org/10.1128/mBio.01300-15.

Felger, Ingrid, Martin Maire, Michael T. Bretscher, Nicole Falk, André Tiaden, Wilson Sama, Hans Peter Beck, Seth Owusu-Agyei, and Thomas A. Smith. 2012. "The Dynamics of Natural Plasmodium Falciparum Infections." *PLoS ONE* 7 (9): 1–10. https://doi.org/10.1371/journal.pone.0045542.

Figueiredo, Rodrigo T., Patricia L. Fernandez, Diego S. Mourao-Sa, Bárbara N. Porto, Fabianno F. Dutra, Letícia S. Alves, Marcus F. Oliveira, Pedro L. Oliveira, Aurélio V. Graça-Souza, and Marcelo T. Bozza. 2007. "Characterization of Heme as Activator of Toll-like Receptor 4." *Journal of Biological Chemistry* 282 (28): 20221–29. https://doi.org/10.1074/jbc.M610737200.

Filipe, João A.N., Eleanor M. Riley, Christopher J. Drakeley, Colin J. Sutherland, and Azra C. Ghani. 2007. "Determination of the Processes Driving the Acquisition of Immunity to Malaria Using a Mathematical Transmission Model." *PLoS Computational Biology* 3 (12): 2569–79. https://doi.org/10.1371/journal.pcbi.0030255.

Frankland, Sarah, Salenna R Elliott, Francisca Yosaatmadja, James G Beeson, Stephen J Rogerson, Akinola Adisa, and Leann Tilley. 2007. "Serum Lipoproteins Promote Efficient Presentation of the Malaria Virulence Protein PfEMP1 at the Erythrocyte Surface." *Eukaryotic Cell* 6 (9): 1584–94. https://doi.org/10.1128/EC.00063-07.

Fried, Michal, and Patrick E. Duffy. 2017. "Malaria during Pregnancy." *Cold Spring Harbor Perspectives in Medicine* 7 (6): a025551. https://doi.org/10.1101/cshperspect.a025551.

Frimpong, Augustina, Jones Amponsah, Abigail Sena Adjokatseh, Dorothy Agyemang, Lutterodt Bentum-Ennin, Ebenezer Addo Ofori, Eric Kyei-Baafour, et al. 2020. "Asymptomatic Malaria Infection Is Maintained by a Balanced Pro- and Anti-Inflammatory Response." *Frontiers in Microbiology* 11 (November). https://doi.org/10.3389/fmicb.2020.559255.

Frischknecht, Friedrich, Patricia Baldacci, Béatrice Martin, Christophe Zimmer, Sabine Thiberge, Jean Christophe Olivo-Marin, Spencer L. Shorte, and Robert Ménard. 2004. "Imaging Movement of Malaria Parasites during Transmission by Anopheles Mosquitoes." *Cellular Microbiology* 6 (7): 687–94. https://doi.org/10.1111/j.1462-5822.2004.00395.x.

Galatas, Beatriz, Quique Bassat, and Alfredo Mayor. 2016. "Malaria Parasites in the Asymptomatic: Looking for the Hay in the Haystack." *Trends in Parasitology* 32 (4): 296–308. https://doi.org/10.1016/j.pt.2015.11.015.

García, Felipe, Mireia Cebrián, Martinho Dgedge, Jordi Casademont, José Luis Bedini, Otilia Neves, Xavier Filella, Maria Cinta Cid, Manel Corachán, and Josep Maria Grau. 1999. "Endothelial Cell Activation in Muscle Biopsy Samples Is Related to Clinical Severity in Human Cerebral Malaria." *Journal of Infectious Diseases* 179 (2): 475–83. https://doi.org/10.1086/314598.

Gardner, J. P., R. A. Pinches, D. J. Roberts, and C. I. Newbold. 1996. "Variant Antigens and Endothelial Receptor Adhesion in Plasmodium Falciparum." *Proceedings of the National Academy of Sciences of the United States of America* 93 (8): 3503–8. https://doi.org/10.1073/pnas.93.8.3503.

Gardner, Malcolm J., Neil Hall, Eula Fung, Owen White, Matthew Berriman, Richard W. Hyman, Jane M. Carlton, et al. 2002. "Genome Sequence of the Human Malaria Parasite Plasmodium Falciparum." *Nature* 419 (6906): 498–511. https://doi.org/10.1038/nature01097.

Garten, Matthias, Armiyaw S. Nasamu, Jacquin C. Niles, Joshua Zimmerberg, Daniel E. Goldberg, and Josh R. Beck. 2018. "EXP2 Is a Nutrient-Permeable Channel in the Vacuolar Membrane of Plasmodium and Is Essential for Protein Export via PTEX." *Nature Microbiology*. https://doi.org/10.1038/s41564-018-0222-7.

Garton, Kyle J., Peter J Gough, and Elaine W Raines. 2006. "Emerging Roles for Ectodomain Shedding in the Regulation of Inflammatory Responses." *Journal of Leukocyte Biology* 79 (6): 1105–16. https://doi.org/10.1189/jlb.0106038.

Giha, H. A., G. Elghazali, T. M.E. A-Elgadir, I. E. A-Elbasit, and M. I. Elbashir. 2009. "Severe Malaria in an Unstable Setting: Clinical and Laboratory Correlates of Cerebral Malaria and Severe Malarial Anemia and a Paradigm for a Simplified Severity Scoring." *European Journal of Clinical Microbiology and Infectious Diseases* 28 (6): 661–65. https://doi.org/10.1007/s10096-008-0665-5.

Glenister, Fiona K., Kate M. Fernandez, Lev M. Kats, Eric Hanssen, Narla Mohandas, Ross L. Coppel, and Brian M. Cooke. 2009. "Functional Alteration of Red Blood Cells by a Megadalton Protein of Plasmodium Falciparum." *Blood* 113 (4): 919–28. https://doi.org/10.1182/blood-2008-05-157735.

Goel, Suchi, Mia Palmkvist, Kirsten Moll, Nicolas Joannin, Patricia Lara, Reetesh R Akhouri, Nasim Moradi, et al. 2015. "RIFINs Are Adhesins Implicated in Severe Plasmodium Falciparum Malaria." *Nature Medicine* 21 (4): 314–21. https://doi.org/10.1038/nm.3812.

Goldberg, Daniel E. 2013. "Complex Nature of Malaria Parasite Hemoglobin Degradation." *Proceedings of the National Academy of Sciences* 110 (14): 5283–84. https://doi.org/10.1073/pnas.1303299110.

Gonzales, S. Jake, Raphael A. Reyes, Ashley E. Braddom, Gayani Batugedara, Sebastiaan Bol, and Evelien M. Bunnik. 2020. "Naturally Acquired Humoral Immunity Against Plasmodium Falciparum Malaria." *Frontiers in Immunology* 11 (October): 1–15. https://doi.org/10.3389/fimmu.2020.594653.

Graninger, W., J. Prada, G. Zotter, S. Neifer, F. Thalhammer, and P. G. Kremsner. 1994. "Upregulation of ICAM-I by Plasmodium Falciparum: In Vitro and in Vivo Studies." *Journal of Clinical Pathology* 47 (7): 653–56. https://doi.org/10.1136/jcp.47.7.653.

Greenwood, Brian M., David a. Fidock, Dennis E. Kyle, Stefan H I Kappe, Pedro L. Alonso, Frank H. Collins, and Patrick E. Duffy. 2008. "Malaria: Progress, Perils, and Prospects for Eradication." *Journal of Clinical Investigation* 118 (4): 1266–76. https://doi.org/10.1172/JCI33996.

Groom, A. C., E. E. Schmidt, and I. C. MacDonald. 1991. "Microcirculatory Pathways and Blood Flow in Spleen: New Insights from Washout Kinetics, Corrosion Casts, and Quantitative Intravital Videomicroscopy." *Scanning Microscopy* 5 (1): 159–74.

Gruenberg, J., D. R. Allred, and I. W. Sherman. 1983. "Scanning Electron Microscope-Analysis of the Protrusions (Knobs) Present on the Surface of Plasmodium Falciparum-Infected Erythrocytes." *Journal of Cell Biology* 97 (3): 795–802. https://doi.org/10.1083/jcb.97.3.795.

Grüring, Christof, Arlett Heiber, Florian Kruse, Johanna Ungefehr, Tim-Wolf Gilberger, and Tobias Spielmann. 2011. "Development and Host Cell Modifications of Plasmodium Falciparum Blood Stages in Four Dimensions." *Nature Communications* 2: 165. https://doi.org/10.1038/ncomms1169.

Gubbels, Marc Jan, and Manoj T. Duraisingh. 2012. "Evolution of Apicomplexan Secretory Organelles." *International Journal for Parasitology* 42 (12): 1071–81. https://doi.org/10.1016/j.ijpara.2012.09.009.

Guha, Rajan, Anna Mathioudaki, Safiatou Doumbo, Didier Doumtabe, Jeff Skinner, Gunjan Arora, Shafiuddin Siddiqui, et al. 2020. "Plasmodium Falciparum Malaria Drives Epigenetic Reprogramming of Human Monocytes toward a Regulatory Phenotype." *BioRxiv : The Preprint Server for Biology* 21 (1): 1–9. https://doi.org/10.1101/2020.10.21.346197.

Gupta, Himanshu, Beatriz Galatas, Gloria Matambisso, Lidia Nhamussua, Pau Cisteró, Quique Bassat, Aina Casellas, et al. 2019. "Differential Expression of Var Subgroups and PfSir2a Genes in Afebrile Plasmodium Falciparum Malaria : A Matched Case – Control Study." *Malaria Journal* 153: 1–7. https://doi.org/10.1186/s12936-019-2963-z.

Hackett, L. W. 1944. "Spleen Measurement in Malaria." *Journal of the National Malaria Society* 3 (2): 121–33.

Hanssen, Eric, Peter Carlton, Samantha Deed, Nectarios Klonis, John Sedat, Joe DeRisi, and Leann Tilley. 2010. "Whole Cell Imaging Reveals Novel Modular Features of the Exomembrane System of the Malaria Parasite, Plasmodium Falciparum." *International Journal for Parasitology* 40 (1): 123–34. https://doi.org/10.1016/j.ijpara.2009.09.004.

Hanssen, Eric, Paula Hawthorne, Matthew W.A. Dixon, Katharine R. Trenholme, Paul J. McMillan, Tobias Spielmann, Donald L. Gardiner, and Leann Tilley. 2008. "Targeted Mutagenesis of the Ring-Exported Protein-1 of Plasmodium Falciparum Disrupts the Architecture of Maurer's Cleft Organelles." *Molecular Microbiology* 69 (4): 938–53. https://doi.org/10.1111/j.1365-2958.2008.06329.x.

Hanssen, Eric, Christian Knoechel, Megan Dearnley, Matthew W.A. Dixon, Mark Le Gros, Carolyn Larabell, and Leann Tilley. 2012. "Soft X-Ray Microscopy Analysis of Cell Volume and Hemoglobin Content in Erythrocytes Infected with Asexual and Sexual Stages of Plasmodium Falciparum." *Journal of Structural Biology* 177 (2): 224–32. https://doi.org/10.1016/j.jsb.2011.09.003.

Hanssen, Eric, Rachid Sougrat, Sarah Frankland, Samantha Deed, Nectarios Klonis, Jennifer Lippincott-Schwartz, and Leann Tilley. 2008. "Electron Tomography of the Maurer's Cleft Organelles of Plasmodium Falciparum-Infected Erythrocytes Reveals Novel Structural Features." *Molecular Microbiology* 67 (4): 703–18. https://doi.org/10.1111/j.1365-2958.2007.06063.x.

Hawthorne, Paula L., Katharine R. Trenholme, Tina S. Skinner-Adams, Tobias Spielmann, Katja Fischer, Matthew W.A. Dixon, Maria R. Ortega, Karen L. Anderson, David J. Kemp, and Donald L. Gardiner. 2004. "A Novel Plasmodium Falciparum Ring Stage Protein, REX, Is Located in Maurer's Clefts." *Molecular and Biochemical Parasitology* 136 (2): 181–89. https://doi.org/10.1016/j.molbiopara.2004.03.013.

Helms, Gesa, Anil Kumar Dasanna, Ulrich S Schwarz, and Michael Lanzer. 2016. "Modeling Cytoadhesion of Plasmodium Falciparum- Infected Erythrocytes and Leukocytes — Common Principles and Distinctive Features" 590: 1955–71. https://doi.org/10.1002/1873-3468.12142.

Henry, Benoît, Camille Roussel, Mario Carucci, Valentine Brousse, Papa Alioune Ndour, and Pierre Buffet. 2020. "The Human Spleen in Malaria : Filter or Shelter ?" *Trends in Parasitology* 36 (5): 435–46. https://doi.org/10.1016/j.pt.2020.03.001.

Hiller, N. Luisa, Souvik Bhattacharjee, Christiaan Van Ooij, Konstantinos Liolios, Travis Harrison, Carlos Lopez-Estraño, and Kasturi Haldar. 2004. "A Host-Targeting Signal in Virulence Proteins Reveals a Secretome in Malarial Infection." *Science* 306 (5703): 1934–37. https://doi.org/10.1126/science.1102737.

Ho, M., L. H. Bannister, S. Looareesuwan, and P. Suntharasamai. 1992. "Cytoadherence and Ultrastructure of Plasmodium Falciparum-Infected Erythrocytes from a Splenectomized Patient." *Infection and Immunity* 60 (6): 2225–28.

Ho, May, Michael J. Hickey, Allan G. Murray, Graciela Andonegui, and Paul Kubes. 2000. "Visualization of Plasmodium Falciparum - Endothelium Interactions in Human Microvasculature: Mimicry of Leukocyte Recruitment." *Journal of Experimental Medicine* 192 (8): 1205–11. https://doi.org/10.1084/jem.192.8.1205.

Ho, May, Nicholas J. White, Sornchai Looareesuwan, Yupaporn Wattanagoon, Szu Hee Lee, Mark J. Walport, Danai Bunnag, and Tranakchit Harinasuta. 1990. "Splenic Fc Receptor Function in Host Defense and Anemia in Acute Plasmodium Falciparum Malaria." *Journal of Infectious Diseases* 161 (3): 555–61. https://doi.org/10.1093/infdis/161.3.555.

Hommel, B Y Marcel, Peter H David, and A D Lynette D Oligino. 1983. "Surface Alterations of Erythrocytes in *Plasmodium Falciparum* Malaria." *The Journal of Experimental Medicine* 157 (April): 1137–48.

Howell, Dasein P.G., Emily A. Levin, Amy L. Springer, Susan M. Kraemer, David J. Phippard, William R. Schief, and Joseph D. Smith. 2008. "Mapping a Common Interaction Site Used by Plasmodium Falciparum Duffy Binding-like Domains to Bind Diverse Host Receptors." *Molecular Microbiology* 67 (1): 78–87. https://doi.org/10.1111/j.1365-2958.2007.06019.x.

Huestis, Diana L., Adama Dao, Moussa Diallo, Zana L. Sanogo, Djibril Samake, Alpha S. Yaro, Yossi Ousman, et al. 2019. "Windborne Long-Distance Migration of Malaria Mosquitoes in the Sahel." *Nature* 574 (7778): 404–8. https://doi.org/10.1038/s41586-019-1622-4.

Hviid, Lars, Thor G. Theander, Ibrahim M. Elhassan, and James B. Jensen. 1993. "Increased Plasma Levels of Soluble ICAM-1 and ELAM-1 (E-Selectin) during Acute Plasmodium Falciparum Malaria." *Immunology Letters* 36 (1): 51–58. https://doi.org/10.1016/0165-2478(93)90068-D.

Idris, Zulkarnain Md, Chim W. Chan, James Kongere, Jesse Gitaka, John Logedi, Ahmeddin Omar, Charles Obonyo, et al. 2016. "High and Heterogeneous Prevalence of Asymptomatic and Sub-Microscopic Malaria Infections on Islands in Lake Victoria, Kenya." *Scientific Reports* 6 (July): 1–13. https://doi.org/10.1038/srep36958.

Imwong, Mallika, Wanassanan Madmanee, Kanokon Suwannasin, Chanon Kunasol, Thomas J. Peto, Rupam Tripura, Lorenz Von Seidlein, et al. 2019. "Asymptomatic Natural Human Infections with the Simian Malaria Parasites Plasmodium Cynomolgi and Plasmodium Knowlesi." *Journal of Infectious Diseases* 219 (5): 695–702. https://doi.org/10.1093/infdis/jiy519.

Jagannathan, Prasanna, Ijeoma Eccles-James, Katherine Bowen, Felistas Nankya, Ann Auma, Samuel Wamala, Charles Ebusu, et al. 2014. "IFNγ/IL-10 Co-Producing Cells Dominate the CD4 Response to Malaria in Highly Exposed Children." *PLoS Pathogens* 10 (1). https://doi.org/10.1371/journal.ppat.1003864.

Jagannathan, Prasanna, Fredrick Lutwama, Michelle J. Boyle, Felistas Nankya, Lila A. Farrington, Tara I. McIntyre, Katherine Bowen, et al. 2017. "Vδ2+ T Cell Response to Malaria Correlates with Protection from Infection but Is Attenuated with Repeated Exposure." *Scientific Reports* 7 (1): 1–12. https://doi.org/10.1038/s41598-017-10624-3.

Jakobsen, P. H., V. McKay, S. D. Morris-Jones, W. McGuire, M. B. Van Hensbroek, S. Meisner, K. Bendtzen, I. Schousboe, I. C. Bygbjerg, and B. M. Greenwood. 1994. "Increased Concentrations of Interleukin-6 and Interleukin-1 Receptor Antagonist and Decreased Concentrations of Beta-2-Glycoprotein I in Gambian Children with Cerebral Malaria." *Infection and Immunity* 62 (10): 4374–79. https://doi.org/10.1128/iai.62.10.4374-4379.1994.

Jakobsen, P. H., S. Morris-Jones, A. Ronn, L. Hviid, T. G. Theander, I. M. Elhassan, I. C. Bygbjerg, and B. M. Greenwood. 1994. "Increased Plasma Concentrations of SICAM-1, SVCAM-1 and SELAM-1 in Patients with Plasmodium Falciparum or P. Vivax Malaria and Association with Disease Severity." *Immunology* 83 (4): 665–69.

Jauréguiberry, Stéphane, Papa A. Ndour, Camille Roussel, Flavie Ader, Innocent Safeukui, Marie Nguyen, Sylvestre Biligui, et al. 2014. "Postartesunate Delayed Hemolysis Is a Predictable Event Related to the Lifesaving Effect of Artemisinins." *Blood* 124 (2): 167–75. https://doi.org/10.1182/blood-2014-02-555953.

Jensen, Anja Ramstedt, Yvonne Adams, and Lars Hviid. 2020. "Cerebral Plasmodium Falciparum Malaria: The Role of PfEMP1 in Its Pathogenesis and Immunity, and PfEMP1-Based Vaccines to Prevent It." *Immunological Reviews* 293 (1): 230–52. https://doi.org/10.1111/imr.12807.

Jensen, James B., and William Trager. 1978. "Plasmodium Falciparum in Culture: Establishment of Additional Strains *." *The American Journal of Tropical Medicine and Hygiene* 27 (4): 743–46. https://doi.org/10.4269/ajtmh.1978.27.743.

Joice, R., B. Morahan, M. Marti, K. C. Williamson, K. B. Seydel, S. Dankwa, J. Montgomery, et al. 2014. "Plasmodium Falciparum Transmission Stages Accumulate in the Human Bone Marrow." *Science Translational Medicine* 6 (244): 244re5-244re5. https://doi.org/10.1126/scitranslmed.3008882.

Kaboré, Berenger, Annelies Post, Mike L.T. Berendsen, Salou Diallo, Palpouguini Lompo, Karim Derra, Eli Rouamba, et al. 2020. "Red Blood Cell Homeostasis in Children and Adults with and without Asymptomatic Malaria Infection in Burkina Faso." *PLoS ONE* 15 (11 November): 1–19. https://doi.org/10.1371/journal.pone.0242507.

Kaestli, Mirjam, Ian A. Cockburn, Alfred Cortés, Kay Baea, J. Alexandra Rowe, and Hans Peter Beck. 2006. "Virulence of Malaria Is Associated with Differential Expression of Plasmodium Falciparum Var Gene Subgroups in a Case-Control Study." *Journal of Infectious Diseases* 193 (11): 1567–74. https://doi.org/10.1086/503776.

Kanoi, Bernard N., Hikaru Nagaoka, Michael T. White, Masayuki Morita, Nirianne M.Q. Palacpac, Edward H. Ntege, Betty Balikagala, et al. 2020. "Global Repertoire of Human Antibodies Against Plasmodium Falciparum RIFINs, SURFINs, and STEVORs in a Malaria Exposed Population." *Frontiers in Immunology* 11 (May). https://doi.org/10.3389/fimmu.2020.00893.

Karunaweera, Nadira D., G. E. Grau, P. Gamage, R. Carter, and Kamini N. Mendis. 1992. "Dynamics of Fever and Serum Levels of Tumor Necrosis Factor Are Closely Associated during Clinical Paroxysms in Plasmodium Vivax Malaria." *Proceedings of the National Academy of Sciences of the United States of America* 89 (8): 3200–3203. https://doi.org/10.1073/pnas.89.8.3200.

Kats, Lev M., Nicholas I. Proellocks, Donna W. Buckingham, Lionel Blanc, John Hale, Xinhua Guo, Xinhong Pei, et al. 2015. "Interactions between Plasmodium Falciparum Skeleton-Binding Protein 1 and the Membrane Skeleton of Malaria-Infected Red Blood Cells." *Biochimica et Biophysica Acta - Biomembranes* 1848 (7): 1619–28. https://doi.org/10.1016/j.bbamem.2015.03.038.

Kaviratne, M, S M Khan, W Jarra, and P R Preiser. 2002. "Small Variant STEVOR Antigen Is Uniquely Located within Maurer's Clefts in Plasmodium Falciparum-Infected Red Blood Cells." *Eukaryotic Cell* 1 (6): 926–35. https://doi.org/10.1128/EC.1.6.926-935.2002.

Kilejian, Araxie. 1979. "Characterization of a Protein Correlated with the Production of Knob-like Protrusions on Membranes of Erythrocytes Infected with Plasmodium Falciparum." *Proceedings of the National Academy of Sciences* 76 (9): 4650–53. https://doi.org/10.1073/pnas.76.9.4650.

Kimenyi, Kelvin M., Kevin Wamae, and Lynette Isabella Ochola-Oyier. 2019. "Understanding P. Falciparum Asymptomatic Infections: A Proposition for a Transcriptomic Approach." *Frontiers in Immunology* 10 (October): 1–10. https://doi.org/10.3389/fimmu.2019.02398.

Koning-Ward, Tania F. de, Matthew W.A. Dixon, Leann Tilley, and Paul R. Gilson. 2016. "Plasmodium Species: Master Renovators of Their Host Cells." *Nature Reviews Microbiology* 14 (8): 494–507. https://doi.org/10.1038/nrmicro.2016.79.

Koning-Ward, Tania F de, Paul R Gilson, Justin a Boddey, Melanie Rug, Brian J Smith, Anthony T Papenfuss, Paul R Sanders, et al. 2009. "A Newly Discovered Protein Export Machine in Malaria Parasites." *Nature* 459 (7249): 945–49. https://doi.org/10.1038/nature08104.

Kotlyar, Simon, Julius Nteziyaremye, Peter Olupot-Olupot, Samuel O. Akech, Christopher L. Moore, and Kathryn Maitland. 2014. "Spleen Volume and Clinical Disease Manifestations of Severe Plasmodium Falciparum Malaria in African Children." *Transactions of the Royal Society of Tropical Medicine and Hygiene* 108 (5): 283–89. https://doi.org/10.1093/trstmh/tru040.

Kriek, Neline, Leann Tilley, Paul Horrocks, Robert Pinches, Barry C. Elford, David J.P. Ferguson, Klaus Lingelbach, and Chris I. Newbold. 2003. "Characterization of the Pathway for Transport of the Cytoadhereince- Mediating Protein, PfEMP1, to the Host Cell Surface in Malaria Parasite-Infected Erythrocytes." *Molecular Microbiology* 50 (4): 1215–27. https://doi.org/10.1046/j.1365-2958.2003.03784.x.

Külzer, Simone, Melanie Rug, Klaus Brinkmann, Ping Cannon, Alan Cowman, Klaus Lingelbach, Gregory L. Blatch, Alexander G. Maier, and Jude M. Przyborski. 2010. "Parasite-Encoded Hsp40 Proteins Define Novel Mobile Structures in the Cytosol of the P. Falciparum-Infected Erythrocyte." *Cellular Microbiology* 12 (10): 1398–1420. https://doi.org/10.1111/j.1462-5822.2010.01477.x.

Kwiatkowski, D., J. G. Cannon, K. R. Manogue, A. Cerami, C. A. Dinarello, and B. M. Greenwood. 1989. "Tumour Necrosis Factor Production in Falciparum Malaria and Its Association with Schizont Rupture." *Clinical and Experimental Immunology* 77 (3): 361–66.

Kwiatkowski, D., M. E. Molyneux, S. Stephens, N. Curtis, N. Klein, P. Pointaire, M. Smit, R. Allan, D. R. Brewster, and G. E. Grau. 1993. "Anti-TNF Therapy Inhibits Fever in Cerebral Malaria." *QJM: An International Journal of Medicine* 86 (2): 91–98. https://doi.org/10.1093/oxfordjournals.qjmed.a068783.

Kwiatkowski, D., I. Sambou, P. Twumasi, B.M. Greenwood, A.V.S. Hill, K.R. Manogue, A. Cerami, J. Castracane, and D.R. Brewster. 1990. "TNF Concentration in Fatal Cerebral, Non-Fatal Cerebral, and Uncomplicated Plasmodium Falciparum Malaria." *The Lancet* 336 (8725): 1201–4. https://doi.org/10.1016/0140-6736(90)92827-5.

Kyes, S. A., J. A. Rowe, N. Kriek, and C. I. Newbold. 1999. "Rifins: A Second Family of Clonally Variant Proteins Expressed on the Surface of Red Cells Infected with Plasmodium Falciparum." *Proceedings of the National Academy of Sciences* 96 (16): 9333–38. https://doi.org/10.1073/pnas.96.16.9333.

Kyes, Sue, Robert Pinches, and Chris Newbold. 2000. "A Simple RNA Analysis Method Shows Var and Rif Multigene Family Expression Patterns in Plasmodium Falciparum." *Molecular and Biochemical Parasitology* 105 (2): 311–15. https://doi.org/10.1016/S0166-6851(99)00193-0.

Lalremruata, Albert, Magda Magris, Sarai Vivas-Martínez, Maike Koehler, Meral Esen, Prakasha Kempaiah, Sankarganesh Jeyaraj, Douglas Jay Perkins, Benjamin Mordmüller, and Wolfram G. Metzger. 2015. "Natural Infection of Plasmodium Brasilianum in Humans: Man and Monkey Share Quartan Malaria Parasites in the Venezuelan Amazon." *EBioMedicine* 2 (9): 1186–92. https://doi.org/10.1016/j.ebiom.2015.07.033.

Laman, Moses, Susan Aipit, Cathy Bona, Peter M. Siba, Leanne J. Robinson, Laurens Manning, and Timothy M.E. Davis. 2015. "Ultrasonographic Assessment of Splenic Volume at Presentation and after Anti-Malarial Therapy in Children with Malarial Anaemia." *Malaria Journal* 14 (1):

116

1–9. https://doi.org/10.1186/s12936-015-0741-0.

Langhorne, Jean, Francis M. Ndungu, Anne Marit Sponaas, and Kevin Marsh. 2008. "Immunity to Malaria: More Questions than Answers." *Nature Immunology* 9 (7): 725–32. https://doi.org/10.1038/ni.f.205.

Langreth, S G, J B Jensen, R T Reese, and W Trager. 1978. "Fine Structure of Human Malaria in Vitro." *The Journal of Protozoology* 25 (4): 443–52. https://doi.org/10.1111/j.1550-7408.1978.tb04167.x.

Langreth, S G, and Robert T Reese. 1979. "Antigenicity of the Infected-Erythrocyte and Merozoite Surfaces in Falciparum Malaria." *Journal of Experimental Medicine* 150 (5): 1241–54. https://doi.org/10.1084/jem.150.5.1241.

Lansche, Christine, Anil K. Dasanna, Katharina Quadt, Benjamin Fröhlich, Dimitris Missirlis, Marilou Tétard, Benoit Gamain, et al. 2018. "The Sickle Cell Trait Affects Contact Dynamics and Endothelial Cell Activation in Plasmodium Falciparum-Infected Erythrocytes." *Communications Biology* 1 (1). https://doi.org/10.1038/s42003-018-0223-3.

Lavazec, Catherine, Guillaume Deplaine, Innocent Safeukui, Sylvie Perrot, Geneviève Milon, Odile Mercereau-Puijalon, Peter H. David, and Pierre Buffet. 2012. "Microsphiltration: A Microsphere Matrix to Explore Erythrocyte Deformability." In *Malaria: Methods and Protocols, Methods in Molecular Biology*, edited by Robert Ménard, vol. 923, 291–97. Springer Science+Business Media. https://doi.org/10.1007/978-1-62703-026-7_20.

Lavstsen, Thomas, Ali Salanti, Anja T R Jensen, David E Arnot, and Thor G Theander. 2003. "Sub-Grouping of Plasmodium Falciparum 3D7 Var Genes Based on Sequence Analysis of Coding and Non-Coding Regions." *Malaria Journal* 2 (September): 27. https://doi.org/10.1186/1475-2875-2-27.

Leão, Luana, Bruna Puty, Maria Fâni Dolabela, Marinete Marins Povoa, Yago Gecy De Sousa Né, Luciana Guimarães Eiró, Nathália Carolina Fernandes Fagundes, Lucianne Cople Maia, and Rafael Rodrigues Lima. 2020. "Association of Cerebral Malaria and TNF-α Levels: A Systematic Review." *BMC Infectious Diseases* 20 (1): 442. https://doi.org/10.1186/s12879-020-05107-2.

Lee, Rebecca S, Andrew P Waters, and James M Brewer. 2018. "A Cryptic Cycle in Haematopoietic Niches Promotes Initiation of Malaria Transmission and Evasion of Chemotherapy." *Nature Communications* 9 (1): 1689. https://doi.org/10.1038/s41467-018-04108-9.

Leech, J. H., J. W. Barnwell, M. Aikawa, L. H. Miller, and R. J. Howard. 1984. "Plasmodium Falciparum Malaria: Association of Knobs on the Surface of Infected Erythrocytes with a Histidine-Rich Protein and the Erythrocyte Skeleton." *Journal of Cell Biology* 98 (4): 1256–64. https://doi.org/10.1083/jcb.98.4.1256.

Lehmann, Tovi, Adama Dao, Alpha Seydou Yaro, Abdoulaye Adamou, Yaya Kassogue, Moussa Diallo, Traoré Sékou, and Cecilia Coscaron-Arias. 2010. "Aestivation of the African Malaria Mosquito, Anopheles Gambiae in the Sahel." *American Journal of Tropical Medicine and Hygiene* 83 (3): 601–6. https://doi.org/10.4269/ajtmh.2010.09-0779.

Lemieux, J. E., N. Gomez-Escobar, A. Feller, C. Carret, A. Amambua-Ngwa, R. Pinches, F. Day, et al. 2009. "Statistical Estimation of Cell-Cycle Progression and Lineage Commitment in Plasmodium Falciparum Reveals a Homogeneous Pattern of Transcription in Ex Vivo Culture." *Proceedings of the National Academy of Sciences* 106 (18): 7559–64. https://doi.org/10.1073/pnas.0811829106.

Leoni, Stefania, Dora Buonfrate, Andrea Angheben, Federico Gobbi, and Zeno Bisoffi. 2015. "The Hyper-Reactive Malarial Splenomegaly: A Systematic Review of the Literature." *Malaria Journal* 14 (1). https://doi.org/10.1186/s12936-015-0694-3.

Ley, Klaus, Carlo Laudanna, Myron I Cybulsky, and Sussan Nourshargh. 2007. "Getting to the Site of Inflammation: The Leukocyte Adhesion Cascade Updated." *Nature Reviews Immunology* 7 (9): 678–89. https://doi.org/10.1038/nri2156.

Lindblade, Kim A., Laura Steinhardt, Aaron Samuels, S. Patrick Kachur, and Laurence Slutsker. 2013. "The Silent Threat: Asymptomatic Parasitemia and Malaria Transmission." *Expert Review of Anti-Infective Therapy* 11 (6): 623–39. https://doi.org/10.1586/eri.13.45.

Looareesuwan, Sornchai, May Ho, Yupaporn Wattanagoon, Nicholas J. White, David A. Warrell, Danai Bunnag, Tranakchit Harinasuta, and David J. Wyler. 1987. "Dynamic Alteration in Splenic Function during Acute Falciparum Malaria." *New England Journal of Medicine* 317 (11): 675–79. https://doi.org/10.1056/NEJM198709103171105.

Looker, Oliver, Adam J Blanch, Boyin Liu, Juan Nunez-iglesias Id, Paul J Mcmillan, Leann Tilley Id, and Matthew W A Dixon Id. 2019. "The Knob Protein KAHRP Assembles into a Ring-Shaped Structure That Underpins Virulence Complex Assembly" 1: 1–26.

Lubiana, Pedro, Philip Bouws, Lisa Katharina Roth, Michael Dörpinghaus, Torben Rehn, Jana Brehmer, Jan Stephan Wichers, et al. 2020. "Adhesion between P. Falciparum Infected Erythrocytes and Human Endothelial Receptors Follows Alternative Binding Dynamics under Flow and Febrile Conditions." *Scientific Reports* 10 (1): 1–14. https://doi.org/10.1038/s41598-020-61388-2.

Luse, S A, and L H Miller. 1971. "Plasmodium Falciparum Malaria. Ultrastructure of Parasitized Erythrocytes in Cardiac Vessels." *The American Journal of Tropical Medicine and Hygiene* 20 (5): 655–60. https://doi.org/10.11603/1811-2471.2017.v0.i2.7727.

Lyke, K. E., R. Burges, Y. Cissoko, L. Sangare, M. Dao, I. Diarra, A. Kone, et al. 2004. "Serum Levels of the Proinflammatory Cytokines Interleukin-1 Beta (IL-1β), IL-6, IL-8, IL-10, Tumor Necrosis Factor Alpha, and IL-12(P70) in Malian Children with Severe Plasmodium Falciparum Malaria and Matched Uncomplicated Malaria or Healthy Controls." *Infection and Immunity* 72 (10): 5630–37. https://doi.org/10.1128/IAI.72.10.5630-5637.2004.

Mahamar, Almahamoudou, Oumar Attaher, Bruce Swihart, Amadou Barry, Bacary S. Diarra, Moussa B. Kanoute, Kadidia B. Cisse, et al. 2017. "Host Factors That Modify Plasmodium Falciparum Adhesion to Endothelial Receptors." *Scientific Reports* 7 (1): 1–8. https://doi.org/10.1038/s41598-017-14351-7.

Maier, Alexander G., Melanie Rug, Matthew T. O'Neill, James G. Beeson, Matthias Marti, John Reeder, and Alan F. Cowman. 2007. "Skeleton-Binding Protein 1 Functions at the Parasitophorous Vacuole Membrane to Traffic PfEMP1 to the Plasmodium Falciparum-Infected Erythrocyte Surface." *Blood* 109 (3): 1289–97. https://doi.org/10.1182/blood-2006-08-043364.

Maier, Alexander G., Melanie Rug, Matthew T. O'Neill, Monica Brown, Srabasti Chakravorty, Tadge Szestak, Joanne Chesson, et al. 2008a. "Exported Proteins Required for Virulence and Rigidity of Plasmodium Falciparum-Infected Human Erythrocytes." *Cell* 134 (1): 48–61. https://doi.org/10.1016/j.cell.2008.04.051.

———. 2008b. "Exported Proteins Required for Virulence and Rigidity of Plasmodium Falciparum-Infected Human Erythrocytes." *Cell* 134 (1): 48–61. https://doi.org/10.1016/j.cell.2008.04.051.

Maier, Alexander G, Brian M Cooke, Alan F Cowman, and Leann Tilley. 2009. "Malaria Parasite Proteins That Remodel the Host Erythrocyte." *Nature Reviews Microbiology* 7 (5): 341–54. https://doi.org/10.1038/nrmicro2110.

Mandala, Wilson L., Chisomo L. Msefula, Esther N. Gondwe, Mark T. Drayson, Malcolm E. Molyneux, and Calman A. MacLennan. 2017. "Cytokine Profiles in Malawian Children Presenting with Uncomplicated Malaria, Severe Malarial Anemia, and Cerebral Malaria." Edited by David W. Pascual. *Clinical and Vaccine Immunology* 24 (4): 1–11. https://doi.org/10.1128/CVI.00533-16.

Mantel, Pierre Yves, Anh N. Hoang, Ilana Goldowitz, Daria Potashnikova, Bashar Hamza, Ivan Vorobjev, Ionita Ghiran, et al. 2013. "Malaria-Infected Erythrocyte-Derived Microvesicles Mediate Cellular Communication within the Parasite Population and with the Host Immune System." *Cell Host and Microbe* 13 (5): 521–34. https://doi.org/10.1016/j.chom.2013.04.009.

Marsh, K., and S. Kinyanjui. 2006. "Immune Effector Mechanisms in Malaria." *Parasite Immunology* 28 (1–2): 51–60. https://doi.org/10.1111/j.1365-3024.2006.00808.x.

Marti, Matthias, Robert T. Good, Melanie Rug, Ellen Knuepfer, and Alan F. Cowman. 2004. "Targeting Malaria Virulence and Remodeling Proteins to the Host Erythrocyte." *Science* 306 (5703): 1930–33. https://doi.org/10.1126/science.1102452.

Matz, Joachim M., Josh R. Beck, and Michael J. Blackman. 2020. "The Parasitophorous Vacuole of the Blood-Stage Malaria Parasite." *Nature Reviews Microbiology*. https://doi.org/10.1038/s41579-019-0321-3.

McGuire, W., A.V.S. Hill, B.M. Greenwood, and D. Kwiatkowski. 1996. "Circulating ICAM-1 Levels in Falciparum Malaria Are High but Unrelated to Disease Severity." *Transactions of the Royal Society of Tropical Medicine and Hygiene* 90 (3): 274–76. https://doi.org/10.1016/S0035-9203(96)90244-8.

McHugh, Emma, Olivia M S Carmo, Adam Blanch, Oliver Looker, Boyin Liu, Snigdha Tiash, Dean Andrew, et al. 2020. "Role of Plasmodium Falciparum Protein GEXP07 in Maurer's Cleft Morphology, Knob Architecture, and P. Falciparum EMP1 Trafficking." Edited by Thomas E. Wellems. *MBio* 11 (2): 1–22. https://doi.org/10.1128/mBio.03320-19.

Mcmillan, Paul J., Coralie Millet, Steven Batinovic, Mauro Maiorca, Eric Hanssen, Shannon Kenny, Rebecca A. Muhle, et al. 2013. "Spatial and Temporal Mapping of the PfEMP1 Export Pathway in Plasmodium Falciparum." *Cellular Microbiology* 15 (8): 1401–18. https://doi.org/10.1111/cmi.12125.

Mebius, Reina E, and Georg Kraal. 2005. "Structure and Function of the Spleen." *Nature Reviews Immunology* 5 (8): 606–16. https://doi.org/10.1038/nri1669.

Miller, L. H., S. Usami, and S. Chien. 1971. "Alteration in the Rheologic Properties of Plasmodium Knowlesi--Infected Red Cells. A Possible Mechanism for Capillary Obstruction." *The Journal of Clinical Investigation* 50 (7): 1451–55. https://doi.org/10.1172/JCI106629.

Miller, Louis H. 1969. "Distribution of Mature Trophozoites and Schizonts of Plasmodium Falciparum in the Organs of Aotus Trivirgatus, the Night Monkey." *The American Journal of Tropical Medicine and Hygiene* 18 (6): 860–65. https://doi.org/10.4269/ajtmh.1969.18.860.

Miller, Louis H, Dror I Baruch, Kevin Marsh, and Ogobara K Doumbo. 2002. "The Pathogenic Basis of Malaria." *Nature* 415 (6872): 673–79. https://doi.org/10.1038/415673a.

Mills, J. P., M. Diez-Silva, D. J. Quinn, M. Dao, M. J. Lang, K. S.W. Tan, C. T. Lim, et al. 2007. "Effect of Plasmodial RESA Protein on Deformability of Human Red Blood Cells Harboring Plasmodium Falciparum." *Proceedings of the National Academy of Sciences of the United States of America* 104 (22): 9213–17. https://doi.org/10.1073/pnas.0703433104.

Moll, Kirsten, Mia Palmkvist, Junhong Ch'ng, Mpungu Steven Kiwuwa, and Mats Wahlgren. 2015. "Evasion of Immunity to Plasmodium Falciparum: Rosettes of Blood Group A Impair Recognition of PfEMP1." Edited by Érika Martins Braga. *PLOS ONE* 10 (12): e0145120. https://doi.org/10.1371/journal.pone.0145120.

Monteiro, Wuelton, José Diego Brito-Sousa, Aleix Elizalde-Torrent, Camila Bôtto-Menezes, Gisely Cardoso Melo, Carmen Fernandez-Becerra, Marcus Lacerda, and Hernando A. del Portillo. 2020. "Cryptic Plasmodium Chronic Infections: Was Maurizio Ascoli Right?" *Malaria Journal* 19 (1): 1–9. https://doi.org/10.1186/s12936-020-03516-x.

Mosha, Jacklin F., Hugh Jw Sturrock, Bryan Greenhouse, Brian Greenwood, Colin J. Sutherland, Nahla Gadalla, Sharan Atwal, et al. 2013. "Epidemiology of Subpatent Plasmodium Falciparum Infection: Implications for Detection of Hotspots with Imperfect Diagnostics." *Malaria Journal* 12 (1): 1–9. https://doi.org/10.1186/1475-2875-12-221.

Mota, M. M. 2001. "Migration of Plasmodium Sporozoites Through Cells Before Infection." *Science* 291 (5501): 141–44. https://doi.org/10.1126/science.291.5501.141.

Moxon, Christopher A., Ngawina V. Chisala, Samuel C. Wassmer, Terrie E. Taylor, Karl B. Seydel, Malcolm E. Molyneux, Brian Faragher, et al. 2014. "Persistent Endothelial Activation and Inflammation after Plasmodium Falciparum Infection in Malawian Children." *Journal of Infectious Diseases* 209 (4): 610–15. https://doi.org/10.1093/infdis/jit419.

Moxon, Christopher A., Matthew P. Gibbins, Dagmara McGuinness, Danny A. Milner, and Matthias Marti. 2020. "New Insights into Malaria Pathogenesis." *Annual Review of Pathology: Mechanisms of Disease* 15 (1): 315–43. https://doi.org/10.1146/annurev-pathmechdis-012419-032640.

Muller, William A., Susan A. Weigl, Xiaohui Deng, and David M. Phillips. 1993. "PECAM-1 Is Required for Transendothelial Migration of Leukocytes." *Journal of Experimental Medicine* 178 (2): 449–60. https://doi.org/10.1084/jem.178.2.449.

Murphy, Kenneth, and Casey Weaver. 2018. *Janeway Immunologie*. Janeway Immunologie. https://doi.org/10.1007/978-3-662-56004-4.

Nagao, Eriko, Osamu Kaneko, and James A. Dvorak. 2000. "Plasmodium Falciparum-Infected Erythrocytes: Qualitative and Quantitative Analyses of Parasite-Induced Knobs by Atomic Force Microscopy." *Journal of Structural Biology* 130 (1): 34–44. https://doi.org/10.1006/jsbi.2000.4236.

Naissant, Bernina, Florian Dupuy, Yoann Duffier, Audrey Lorthiois, Julien Duez, Judith Scholz, Pierre Buffet, Anais Merckx, Anna Bachmann, and Catherine Lavazec. 2016. "Plasmodium Falciparum STEVOR Phosphorylation Regulates Host Erythrocyte Deformability Enabling Malaria Parasite Transmission." *Blood* 127 (24): e42–53. https://doi.org/10.1182/blood-2016-01-690776.

Namvar, Arman, Adam J. Blanch, Matthew W. Dixon, Olivia M.S. Carmo, Boyin Liu, Snigdha Tiash, Oliver Looker, et al. 2020. "Surface Area-to-Volume Ratio, Not Cellular Viscoelasticity, Is the Major Determinant of Red Blood Cell Traversal through Small Channels." *Cellular Microbiology*, no. September: 1–16. https://doi.org/10.1111/cmi.13270.

Nash, G.B., E O'Brien, EC Gordon-Smith, and JA Dormandy. 1989. "Abnormalities in the Mechanical Properties of Red Blood Cells Caused by Plasmodium Falciparum." *Blood* 74 (2): 855–61. https://doi.org/10.1182/blood.V74.2.855.855.

Niang, Makhtar, Amy Kristine Bei, Kripa Gopal Madnani, Shaaretha Pelly, Selasi Dankwa, Usheer Kanjee, Karthigayan Gunalan, et al. 2014. "STEVOR Is a Plasmodium Falciparum Erythrocyte Binding Protein That Mediates Merozoite Invasion and Rosetting." *Cell Host and Microbe* 16 (1): 81–93. https://doi.org/10.1016/j.chom.2014.06.004.

Nielsen, Morten A., Trine Staalsoe, Jørgen A. L. Kurtzhals, Bamenla Q. Goka, Daniel Dodoo, Michael Alifrangis, Thor G. Theander, Bartholomew D. Akanmori, and Lars Hviid. 2002. " Plasmodium Falciparum Variant Surface Antigen Expression Varies Between Isolates Causing Severe and Nonsevere Malaria and Is Modified by Acquired Immunity ." *The Journal of Immunology* 168 (7): 3444–50. https://doi.org/10.4049/jimmunol.168.7.3444.

Nwaneri, Damian, Olukayode Oladipo, Emeka Ifebi, Omoruyi Oviawe, Osaro Asemota, Bamidele Ogboghodo, Yetunde Israel-Aina, and Ayebo Sadoh. 2020. "Haematological Parameters and Spleen Rate of Asymptomatic and Malaria Negative Children in Edo South District, Nigeria." *Annals of Global Health* 86 (1): 1–12. https://doi.org/10.5334/AOGH.2458.

Nyarko, Prince B., and Antoine Claessens. 2020. "Understanding Host–Pathogen–Vector Interactions with Chronic Asymptomatic Malaria Infections." *Trends in Parasitology* 37 (3): 195–204. https://doi.org/10.1016/j.pt.2020.09.017.

Oberli, Alexander, Leanne M. Slater, Erin Cutts, Françoise Brand, Esther Mundwiler-Pachlatko, Sebastian Rusch, Martin F. G. Masik, Michèle C. Erat, Hans-Peter Beck, and Ioannis Vakonakis. 2014. "A Plasmodium Falciparum PHIST Protein Binds the Virulence Factor PfEMP1 and Comigrates to Knobs on the Host Cell Surface." *The FASEB Journal* 28 (10): 4420–33. https://doi.org/10.1096/fj.14-256057.

Ockenhouse, C., N. Tandon, Cathleen Magowan, G. Jamieson, and J. Chulay. 1989. "Identification of a Platelet Membrane Glycoprotein as a Falciparum Malaria Sequestration Receptor." *Science* 243 (4897): 1469–71. https://doi.org/10.1126/science.2467377.

Ockenhouse, C F, T Tegoshi, Y Maeno, C Benjamin, M Ho, K E Kan, Y Thway, K Win, M Aikawa, and R R Lobb. 1992. "Human Vascular Endothelial Cell Adhesion Receptors for Plasmodium Falciparum -- Infected Erythrocytes: Roles for ELAM-1 and VCAM-1." *J Exp Med* 176 (October): 1183–89.

Oh, S. Steven, Sabine Voigt, Derek Fisher, Scott J. Yi, Patrick J. LeRoy, Laura H. Derick, Shih Chun Liu, and Athar H. Chishti. 2000. "Plasmodium Falciparum Erythrocyte Membrane Protein 1 Is Anchored to the Actin-Spectrin Junction and Knob-Associated Histidine-Rich Protein in the Erythrocyte Skeleton." *Molecular and Biochemical Parasitology* 108 (2): 237–47. https://doi.org/10.1016/S0166-6851(00)00227-9.

Othoro, Caroline, Altaf A. Lal, Bernard Nahlen, Davy Koech, Alloys S.S. Orago, and Venkatachalam Udhayakumar. 1999. "A Low Interleukin-10 Tumor Necrosis Factor-α Ratio Is Associated with Malaria Anemia in Children Residing in a Holoendemic Malaria Region in Western Kenya." *Journal of Infectious Diseases* 179 (1): 279–82. https://doi.org/10.1086/314548.

Ouédraogo, André Lin, Teun Bousema, Petra Schneider, Sake J. de Vlas, Edith Ilboudo-Sanogo, Nadine Cuzin-Ouattara, Issa Nébié, et al. 2009. "Substantial Contribution of Submicroscopical Plasmodium Falciparum Gametocyte Carriage to the Infectious Reservoir in an Area of Seasonal Transmission." Edited by David Joseph Diemert. *PLoS ONE* 4 (12): e8410. https://doi.org/10.1371/journal.pone.0008410.

Pachlatko, Esther, Sebastian Rusch, Anouk Müller, Andrew Hemphill, Leann Tilley, Eric Hanssen, and Hans-Peter Beck. 2010. "MAHRP2, an Exported Protein of Plasmodium Falciparum, Is an Essential Component of Maurer's Cleft Tethers." *Molecular Microbiology* 77 (5): 1136–52. https://doi.org/10.1111/j.1365-2958.2010.07278.x.

Pal, Priya, Brian P. Daniels, Anna Oskman, Michael S. Diamond, Robyn S. Klein, and Daniel E. Goldberg. 2016. "Plasmodium Falciparum Histidine-Rich Protein II Compromises Brain Endothelial Barriers and May Promote Cerebral Malaria Pathogenesis." *MBio* 7 (3): 1–11.

119

https://doi.org/10.1128/mBio.00617-16.

Park, Gregory S., Kathleen F. Ireland, Robert O. Opoka, and Chandy C. John. 2012. "Evidence of Endothelial Activation in Asymptomatic Plasmodium Falciparum Parasitemia and Effect of Blood Group on Levels of von Willebrand Factor in Malaria." *Journal of the Pediatric Infectious Diseases Society* 1 (1): 16–25. https://doi.org/10.1093/jpids/pis010.

Parroche, Peggy, Fanny N. Lauw, Nadege Goutagny, Eicke Latz, Brian G. Monks, Alberto Visintin, Kristen A. Halmen, et al. 2007. "Malaria Hemozoin Is Immunologically Inert but Radically Enhances Innate Responses by Presenting Malaria DNA to Toll-like Receptor 9." *Proceedings of the National Academy of Sciences of the United States of America* 104 (6): 1919–24. https://doi.org/10.1073/pnas.0608745104.

Pelle, Karell G., Keunyoung Oh, Kathrin Buchholz, Vagheesh Narasimhan, Regina Joice, Danny A. Milner, Nicolas M.B. Brancucci, et al. 2015. "Transcriptional Profiling Defines Dynamics of Parasite Tissue Sequestration during Malaria Infection." *Genome Medicine* 7 (1): 1–20. https://doi.org/10.1186/s13073-015-0133-7.

Peters, Jennifer, Elizabeth Fowler, Michelle Gatton, Nanhua Chen, Allan Saul, and Qin Cheng. 2002. "High Diversity and Rapid Changeover of Expressed Var Genes during the Acute Phase of Plasmodium Falciparum Infections in Human Volunteers." *Proceedings of the National Academy of Sciences of the United States of America* 99 (16): 10689–94. https://doi.org/10.1073/pnas.162349899.

Petter, Michaela, Insa Bonow, and Mo Quen Klinkert. 2008. "Diverse Expression Patterns of Subgroups of the Rif Multigene Family during Plasmodium Falciparum Gametocytogenesis." *PLoS ONE* 3 (11). https://doi.org/10.1371/journal.pone.0003779.

Petter, Michaela, Malin Haeggström, Ayman Khattab, Victor Fernandez, Mo Quen Klinkert, and Mats Wahlgren. 2007. "Variant Proteins of the Plasmodium Falciparum RIFIN Family Show Distinct Subcellular Localization and Developmental Expression Patterns." *Molecular and Biochemical Parasitology* 156 (1): 51–61. https://doi.org/10.1016/j.molbiopara.2007.07.011.

Pieper, Kathrin, Joshua Tan, Luca Piccoli, Mathilde Foglierini, Sonia Barbieri, Yiwei Chen, Chiara Silacci-Fregni, et al. 2017. "Public Antibodies to Malaria Antigens Generated by Two LAIR1 Insertion Modalities." *Nature* 548 (7669): 597–601. https://doi.org/10.1038/nature23670.

Pigott, R., L. P. Dillon, I. H. Hemingway, and A. J.H. Gearing. 1992. "Soluble Forms of E-Selectin, ICAM-1 and VCAM-1 Are Present in the Supernatants of Cytokine Activated Cultured Endothelial Cells." *Biochemical and Biophysical Research Communications* 187 (2): 584–89. https://doi.org/10.1016/0006-291X(92)91234-H.

Piper, K. P., D. J. Roberts, and K. P. Day. 1999. "Plasmodium Falciparum: Analysis of the Antibody Specificity to the Surface of the Trophozoite-Infected Erythrocyte." *Experimental Parasitology* 91 (2): 161–69. https://doi.org/10.1006/expr.1998.4368.

Pober, J S, M P Bevilacqua, D L Mendrick, L A Lapierre, W Fiers, and M A Gimbrone. 1986. "Two Distinct Monokines, Interleukin 1 and Tumor Necrosis Factor, Each Independently Induce Biosynthesis and Transient Expression of the Same Antigen on the Surface of Cultured Human Vascular Endothelial Cells." *Journal of Immunology (Baltimore, Md. : 1950)* 136 (5): 1680–87. http://www.ncbi.nlm.nih.gov/pubmed/3485132.

Pober, J S, M A Gimbrone, L A Lapierre, D L Mendrick, W Fiers, R Rothlein, and T A Springer. 1986. "Overlapping Patterns of Activation of Human Endothelial Cells by Interleukin 1, Tumor Necrosis Factor, and Immune Interferon." *Journal of Immunology (Baltimore, Md. : 1950)* 137 (6): 1893–96. http://www.ncbi.nlm.nih.gov/pubmed/3091693.

Pologe, Laura G, Amalia Pavlovec, H. Shio, and Jeffrey V Ravetch. 1987. "Primary Structure and Subcellular Localization of the Knob-Associated Histidine-Rich Protein of Plasmodium Falciparum." *Proceedings of the National Academy of Sciences* 84 (20): 7139–43. https://doi.org/10.1073/pnas.84.20.7139.

Portugal, Silvia, Jacqueline Moebius, Jeff Skinner, Safiatou Doumbo, Didier Doumtabe, Younoussou Kone, Seydou Dia, et al. 2014. "Exposure-Dependent Control of Malaria-Induced Inflammation in Children." *PLoS Pathogens* 10 (4). https://doi.org/10.1371/journal.ppat.1004079.

Portugal, Silvia, Tuan M Tran, Aissata Ongoiba, Aboudramane Bathily, Shanping Li, Safiatou Doumbo, Jeff Skinner, et al. 2017. "Treatment of Chronic Asymptomatic Plasmodium Falciparum Infection Does Not Increase the Risk of Clinical Malaria Upon Reinfection." *Clinical Infectious Diseases* 64 (5): 645–53. https://doi.org/10.1093/cid/ciw849.

Prakash, D., Constantin Fesel, Rajendra Jain, Pierre André Cazenave, Gyan Chandra Mishra, and Sylviane Pied. 2006. "Clusters of Cytokines Determine Malaria Severity in Plasmodium Falciparum-Infected Patients from Endemic Areas of Central India." *Journal of Infectious Diseases* 194 (2): 198–207. https://doi.org/10.1086/504720.

Prommano, Oranan, Urai Chaisri, Gareth D.H. Turner, Polrat Wilairatana, David J.P. Ferguson, Parnpen Viriyavejakul, Nicholas J. White, and Emsri Pongponratn. 2005. "A Quantitative Ultrastructural Study of the Liver and the Spleen in Fatal Falciparum Malaria." *Southeast Asian Journal of Tropical Medicine and Public Health* 36 (6): 1359–70.

Prudêncio, Miguel, Ana Rodriguez, and Maria M Mota. 2006. "The Silent Path to Thousands of Merozoites: The Plasmodium Liver Stage." *Nature Reviews. Microbiology* 4 (November): 849–56. https://doi.org/10.1038/nrmicro1529.

Quadt, Katharina A., Lea Barfod, Daniel Andersen, Jonas Bruun, Ben Gyan, Tue Hassenkam, Michael F. Ofori, and Lars Hviid. 2012. "The Density of Knobs on Plasmodium Falciparum-Infected Erythrocytes Depends on Developmental Age and Varies among Isolates." *PLoS ONE* 7 (9): 1–8. https://doi.org/10.1371/journal.pone.0045658.

Quinn, Thomas C., and David J. Wyler. 1979. "Intravascular Clearance of Parasitized Erythrocytes in Rodent Malaria." *Journal of Clinical Investigation* 63 (6): 1187–94. https://doi.org/10.1172/JCI109413.

Quintana, Maria del Pilar, Jun-Hong Ch'ng, Kirsten Moll, Arash Zandian, Peter Nilsson, Zulkarnain Md Idris, Somporn Saiwaew, Ulrika Qundos, and Mats Wahlgren. 2018. "Antibodies in Children with Malaria to PfEMP1, RIFIN and SURFIN Expressed at the Plasmodium Falciparum Parasitized Red Blood Cell Surface." *Scientific Reports* 8 (1): 3262. https://doi.org/10.1038/s41598-018-21026-4.

Radfar, Azar, Darío Méndez, Carlos Moneriz, María Linares, Patricia Marín-García, Antonio Puyet, Amalia Diez, and José M. Bautista. 2009. "Synchronous Culture of Plasmodium Falciparum at High Parasitemia Levels." *Nature Protocols* 4 (12): 1899–1915. https://doi.org/10.1038/nprot.2009.198.

Ramdani, Ghania, Bernina Naissant, Eloise Thompson, Florence Breil, Audrey Lorthiois, Florian Dupuy, Ross Cummings, et al. 2015. "CAMP-Signalling Regulates Gametocyte-Infected Erythrocyte Deformability Required for Malaria Parasite Transmission." *PLoS Pathogens* 11 (5): 1–20. https://doi.org/10.1371/journal.ppat.1004815.

Ranque, Stéphane, Belco Poudiougou, Abdoulaye Traoré, Modibo Keita, Aboubacar A. Oumar, Innocent Safeukui, Sandrine Marquet, et al. 2008. "Life-Threatening Malaria in African Children: A Prospective Study in a Mesoendemic Urban Setting." *Pediatric Infectious Disease Journal* 27 (2): 130–35. https://doi.org/10.1097/INF.0b013e31815988ed.

Ratsimbasoa, Arsène, Laza Fanazava, Rogelin Radrianjafy, Julien Ramilijaona, Hughes Rafanomezantsoa, and Didier Ménard. 2008. "Short Report: Evaluation of Two New Immunochromatographic Assays for Diagnosis of Malaria." *American Journal of Tropical Medicine and Hygiene* 79 (5): 670–72. https://doi.org/10.4269/ajtmh.2008.79.670.

Recker, Mario, Caroline O. Buckee, Andrew Serazin, Sue Kyes, Robert Pinches, Zóe Christodoulou, Amy L. Springer, Sunetra Gupta, and Chris I. Newbold. 2011. "Antigenic Variation in Plasmodium Falciparum Malaria Involves a Highly Structured Switching Pattern." *PLoS Pathogens* 7 (3). https://doi.org/10.1371/journal.ppat.1001306.

Redmond, Lawrence S., Martin D. Ogwang, Patrick Kerchan, Steven J. Reynolds, Constance N. Tenge, Pamela A. Were, Robert T. Kuremu, et al. 2020. "Endemic Burkitt Lymphoma: A Complication of Asymptomatic Malaria in Sub-Saharan Africa Based on Published Literature and Primary Data from Uganda, Tanzania, and Kenya." *Malaria Journal* 19 (1): 1–14. https://doi.org/10.1186/s12936-020-03312-7.

Regev-Rudzki, Neta, Danny W. Wilson, Teresa G. Carvalho, Xavier Sisquella, Bradley M. Coleman, Melanie Rug, Dejan Bursac, et al. 2013. "Cell-Cell Communication between Malaria-Infected Red Blood Cells via Exosome-like Vesicles." *Cell* 153 (5): 1120–33. https://doi.org/10.1016/j.cell.2013.04.029.

Ribacke, Ulf, Kirsten Moll, Letusa Albrecht, Hodan Ahmed Ismail, Johan Normark, Emilie Flaberg, Laszlo Szekely, et al. 2013. "Improved In Vitro Culture of Plasmodium Falciparum Permits Establishment of Clinical Isolates with Preserved Multiplication, Invasion and Rosetting Phenotypes." *PLoS ONE* 8 (7). https://doi.org/10.1371/journal.pone.0069781.

Ribaut, Clotilde, Antoine Berry, Séverine Chevalley, Karine Reybier, Isabelle Morlais, Daniel Parzy, Françoise Nepveu, Françoise Benoit-vical, and Alexis Valentin. 2008. "Concentration and Purification by Magnetic Separation of the Erythrocytic Stages of All Human Plasmodium Species" 5: 1–5. https://doi.org/10.1186/1475-2875-7-45.

Roberts, David J., Alister G. Craig, Anthony R. Berendt, Robert Pinches, Gerard Nash, Kevin Marsh, and Christopher I. Newbold. 1992. "Rapid Switching to Multiple Antigenic and Adhesive Phenotypes in Malaria." *Nature* 357 (6380): 689–92. https://doi.org/10.1038/357689a0.

Robinson, Bridget A., Teresa L. Welch, and Joseph D. Smith. 2003. "Widespread Functional Specialization of Plasmodium Falciparum Erythrocyte Membrane Protein 1 Family Members to Bind CD36 Analysed across a Parasite Genome." *Molecular Microbiology* 47 (5): 1265–78. https://doi.org/10.1046/j.1365-2958.2003.03378.x.

Rogier, Christophe, Jean-Francois Trape, and Daniel Commenges. 1996. "Evidence for an Age-Dependent Pyrogenic Threshold of Plasmodium Falciparum Parasitemia in Highly Endemic Populations." *The American Journal of Tropical Medicine and Hygiene* 54 (6): 613–19. https://doi.org/10.4269/ajtmh.1996.54.613.

Romer, L H, N V McLean, H C Yan, M Daise, J Sun, and H M DeLisser. 1995. "IFN-Gamma and TNF-Alpha Induce Redistribution of PECAM-1 (CD31) on Human Endothelial Cells." *Journal of Immunology (Baltimore, Md. : 1950)* 154 (12): 6582–92. http://www.ncbi.nlm.nih.gov/pubmed/7759892.

Rottmann, Matthias, Thomas Lavstsen, Joseph Paschal Mugasa, Mirjam Kaestli, Anja T.R. Jensen, Dania Müller, Thor Theander, and Hans Peter Beck. 2006. "Differential Expression of Var Gene Groups Is Associated with Morbidity Caused by Plasmodium Falciparum Infection in Tanzanian Children." *Infection and Immunity* 74 (7): 3904–11. https://doi.org/10.1128/IAI.02073-05.

Rowe, J. Alexandra, Ian G. Handel, Mahamadou A. Thera, Anne Marie Deans, Kirsten E. Lyke, Abdoulaye Koné, Dapa A. Diallo, et al. 2007. "Blood Group O Protects against Severe Plasmodium Falciparum Malaria through the Mechanism of Reduced Rosetting." *Proceedings of the National Academy of Sciences of the United States of America* 104 (44): 17471–76. https://doi.org/10.1073/pnas.0705390104.

RTSS Clinical Trials Partnership. 2015. "Efficacy and Safety of RTS,S/AS01 Malaria Vaccine with or without a Booster Dose in Infants and Children in Africa: Final Results of a Phase 3, Individually Randomised, Controlled Trial." *The Lancet* 386 (9988): 31–45. https://doi.org/10.1016/S0140-6736(15)60721-8.

Rug, Melanie, Marek Cyrklaff, Antti Mikkonen, Leandro Lemgruber, Simone Kuelzer, Cecilia P. Sanchez, Jennifer Thompson, et al. 2014. "Export of Virulence Proteins by Malaria-Infected Erythrocytes Involves Remodeling of Host Actin Cytoskeleton." *Blood* 124 (23): 3459–68. https://doi.org/10.1182/blood-2014-06-583054.

Russo, Ilaria, Shalon Babbitt, Vasant Muralidharan, Tamira Butler, Anna Oksman, and Daniel E. Goldberg. 2010. "Plasmepsin v Licenses Plasmodium Proteins for Export into the Host Erythrocyte." *Nature* 463 (7281): 632–36. https://doi.org/10.1038/nature08726.

Ryan, Sadie J., Catherine A. Lippi, and Fernanda Zermoglio. 2020. "Shifting Transmission Risk for Malaria in Africa with Climate Change: A Framework for Planning and Intervention." *Malaria Journal* 19 (1): 1–14. https://doi.org/10.1186/s12936-020-03224-6.

Safeukui, Innocent, Pierre A. Buffet, Sylvie Perrot, Alain Sauvanet, Beatrice Aussilhou, Safi Dokmak, Anne Couvelard, et al. 2013. "Surface Area Loss and Increased Sphericity Account for the Splenic Entrapment of Subpopulations of Plasmodium Falciparum Ring-Infected Erythrocytes." *PLoS ONE* 8 (3). https://doi.org/10.1371/journal.pone.0060150.

Safeukui, Innocent, Jean Michel Correas, Valentine Brousse, Déborah Hirt, Guillaume Deplaine, Sébastien Mulé, Mickael Lesurtel, et al. 2008. "Retention of Plasmodium Falciparum Ring-Infected Erythrocytes in the Slow, Open Microcirculation of the Human Spleen." *Blood* 112 (6): 2520–28. https://doi.org/10.1182/blood-2008-03-146779.

Saito, Fumiji, Kouyuki Hirayasu, Takeshi Satoh, Christian W Wang, John Lusingu, Takao Arimori, Kyoko Shida, et al. 2017. "Immune Evasion of Plasmodium Falciparum by RIFIN via Inhibitory Receptors." *Nature* 552 (7683): 101–5. https://doi.org/10.1038/nature24994.

Salanti, Ali, Trine Staalsoe, Thomas Lavstsen, Anja T.R. Jensen, M. P.Kordai Sowa, David E. Arnot, Lars Hviid, and Thor G. Theander. 2003. "Selective Upregulation of a Single Distinctly Structured Var Gene in Chondroitin Sulphate A-Adhering Plasmodium Falciparum Involved in Pregnancy-Associated Malaria." *Molecular Microbiology* 49 (1): 179–91. https://doi.org/10.1046/j.1365-2958.2003.03570.x.

Sampaio, Natália G., Samantha J. Emery, Alexandra L. Garnham, Qiao Y. Tan, Xavier Sisquella, Matthew A. Pimentel, Aaron R. Jex, Neta Regev-Rudzki, Louis Schofield, and Emily M. Eriksson. 2018. "Extracellular Vesicles from Early Stage Plasmodium Falciparum-Infected Red Blood Cells Contain PfEMP1 and Induce Transcriptional Changes in Human Monocytes." *Cellular Microbiology* 20 (5): 1–18. https://doi.org/10.1111/cmi.12822.

Sanchez, Cecilia P., Christos Karathanasis, Rodrigo Sanchez, Marek Cyrklaff, Julia Jäger, Bernd Buchholz, Ulrich S. Schwarz, Mike Heilemann, and Michael Lanzer. 2019. "Single-Molecule Imaging and Quantification of the Immune-Variant Adhesin VAR2CSA on Knobs of Plasmodium Falciparum-Infected Erythrocytes." *Communications Biology* 2 (1): 172. https://doi.org/10.1038/s42003-019-0429-z.

Sanyal, Sohini, Stéphane Egeé, Guillaume Bouyer, Sylvie Perrot, Innocent Safeukui, Emmanuel Bischoff, Pierre Buffet, et al. 2012. "Plasmodium Falciparum STEVOR Proteins Impact Erythrocyte Mechanical Properties." *Blood* 119 (2): 1–8. https://doi.org/10.1182/blood-2011-08-370734.

Sargeant, Tobias J., Matthias Marti, Elisabet Caler, Jane M. Carlton, Ken Simpson, Terence P. Speed, and Alan F. Cowman. 2006. "Lineage-Specific Expansion of Proteins Exported to Erythrocytes in Malaria Parasites." *Genome Biology* 7 (2). https://doi.org/10.1186/gb-2006-7-2-r12.

Sattabongkot, Jetsumon, Chayanut Suansomjit, Wang Nguitragool, Jeeraphat Sirichaisinthop, Saradee Warit, Montip Tiensuwan, and Sureemas Buates. 2018. "Prevalence of Asymptomatic Plasmodium Infections with Sub-Microscopic Parasite Densities in the Northwestern Border of Thailand: A Potential Threat to Malaria Elimination." *Malaria Journal* 17 (1): 1–12. https://doi.org/10.1186/s12936-018-2476-1.

Scherf, Arthur, R. Hernandez-Rivas, P. Buffet, E. Bottius, C. Benatar, B. Pouvelle, J. Gysin, and M. Lanzer. 1998. "Antigenic Variation in Malaria: In Situ Switching, Relaxed and Mutually Exclusive Transcription of Var Genes during Intra-Erythrocytic Development in Plasmodium Falciparum." *EMBO Journal* 17 (18): 5418–26. https://doi.org/10.1093/emboj/17.18.5418.

Scheu, Katrin, Ayola Akim Adegnika, Marylyn M. Addo, Daniel Ansong, Jakob P. Cramer, Svenja Fürst, Peter G. Kremsner, et al. 2019. "Determinants of Post-Malarial Anemia in African Children Treated with Parenteral Artesunate." *Scientific Reports* 9 (1): 18134. https://doi.org/10.1038/s41598-019-54639-4.

Schieck, Elise, Judith M. Pfahler, Cecilia P. Sanchez, and Michael Lanzer. 2007. "Nuclear Run-on Analysis of Var Gene Expression in Plasmodium Falciparum." *Molecular and Biochemical Parasitology* 153 (2): 207–12. https://doi.org/10.1016/j.molbiopara.2007.02.004.

Schneider, Petra, J Teun Bousema, Louis C Gouagna, Silas Otieno, Marga van de Vegte-Bolmer, Sabah A Omar, and Robert W Sauerwein. 2007. "Submicroscopic Plasmodium Falciparum Gametocyte Densities Frequently Result in Mosquito Infection." *The American Journal of Tropical Medicine and Hygiene* 76 (3): 470–74. https://doi.org/10.4269/ajtmh.2007.76.470.

Schnitzer, B., T. Sodeman, M. L. Mead, and P. G. Contacos. 1972. "Pitting Function of the Spleen in Malaria: Ultrastructural Observations." *Science* 177 (4044): 175–77. https://doi.org/10.1126/science.177.4044.175.

Schofield, L, S Novakovic, P Gerold, R T Schwarz, M J McConville, and S D Tachado. 1996. "Glycosylphosphatidylinositol Toxin of Plasmodium Up-Regulates Intercellular Adhesion Molecule-1, Vascular Cell Adhesion Molecule-1, and E-Selectin Expression in Vascular Endothelial Cells and Increases Leukocyte and Parasite Cytoadherence via Tyrosine Kin." *Journal of Immunology (Baltimore, Md. : 1950)* 156 (5): 1886–96. http://www.ncbi.nlm.nih.gov/pubmed/8596041.

Schreiber, N., A. Khattab, M. Petter, F. Marks, S. Adjei, R. Kobbe, J. May, and M. Q. Klinkert. 2008. "Expression of Plasmodium Falciparum 3D7 STEVOR Proteins for Evaluation of Antibody Responses Following Malaria Infections in Naïve Infants." *Parasitology* 135 (2): 155–67. https://doi.org/10.1017/S0031182007003794.

Seydel, Karl B., Samuel D. Kampondeni, Clarissa Valim, Michael J. Potchen, Danny A. Milner, Francis W. Muwalo, Gretchen L. Birbeck, et al. 2015. "Brain Swelling and Death in Children with Cerebral Malaria." *New England Journal of Medicine* 372 (12): 1126–37. https://doi.org/10.1056/NEJMoa1400116.

Shaffer, Nathan, Georges E Grau, Katrina Hedberg, Farzin Davachi, Bongo Lyamba, Allen W Hightower, Joel G Breman, and P. Nguyen-Dinh. 1991. "Tumor Necrosis Factor and Severe Malaria." *Journal of Infectious Diseases* 163 (1): 96–101. https://doi.org/10.1093/infdis/163.1.96.

Sharma, Shruti, Rosane B. DeOliveira, Parisa Kalantari, Peggy Parroche, Nadege Goutagny, Zhaozhao Jiang, Jennie Chan, et al. 2011. "Innate

Immune Recognition of an AT-Rich Stem-Loop DNA Motif in the Plasmodium Falciparum Genome." *Immunity* 35 (2): 194–207. https://doi.org/10.1016/j.immuni.2011.05.016.

Siano, James P., Katharine K. Grady, Pascal Millet, and Timothy M. Wick. 1998. "Short Report: Plasmodium Falciparum: Cytoadherence to α(v)B3 on Human Microvascular Endothelial Cells." *American Journal of Tropical Medicine and Hygiene* 59 (1): 77–79. https://doi.org/10.4269/ajtmh.1998.59.77.

Singh, Meghna, Suryanshu, Kanika, Gurmeet Singh, Alok Dubey, and R. K. Chaitanya. 2021. "Plasmodium's Journey through the Anopheles Mosquito: A Comprehensive Review." *Biochimie* 181: 176–90. https://doi.org/10.1016/j.biochi.2020.12.009.

Sinka, Marianne E. 2013. "Global Distribution of the Dominant Vector Species of Malaria." In *Anopheles Mosquitoes - New Insights into Malaria Vectors*. InTech. https://doi.org/10.5772/54163.

Slater, Hannah C, Amanda Ross, Ingrid Felger, Natalie E. Hofmann, Leanne Robinson, Jackie Cook, Bronner P. Gonçalves, et al. 2019. "The Temporal Dynamics and Infectiousness of Subpatent Plasmodium Falciparum Infections in Relation to Parasite Density." *Nature Communications* 10 (1): 1433. https://doi.org/10.1038/s41467-019-09441-1.

Smalley, M. E., S. Abdalla, and J. Brown. 1981. "The Distribution of Plasmodium Falciparum in the Peripheral Blood and Bone Marrow of Gambian Children." *Transactions of the Royal Society of Tropical Medicine and Hygiene* 75 (1): 103–5. https://doi.org/10.1016/0035-9203(81)90019-5.

Smith, Joseph D., Chetan E. Chitnis, Alistar G. Craig, David J. Roberts, Diana E. Hudson-Taylor, David S. Peterson, Robert Pinches, Chris I. Newbold, and Louis H. Miller. 1995. "Switches in Expression of Plasmodium Falciparum Var Genes Correlate with Changes in Antigenic and Cytoadherent Phenotypes of Infected Erythrocytes." *Cell* 82 (1): 101–10. https://doi.org/10.1016/0092-8674(95)90056-X.

Smith, T., I. Felger, M. Tanner, and H. P. Beck. 1999. "The Epidemiology of Multiple Plasmodium Falciparum Infections 11. Premunition in Plasmodium Falciparum Infection: Insights from the Epidemiology of Multiple Infections." *Transactions of the Royal Society of Tropical Medicine and Hygiene* 93 (SUPPL. 1): 59–64. https://doi.org/10.1016/S0035-9203(99)90329-2.

Snounou, Georges, Suganya Viriyakosol, Xin Ping Zhu, William Jarra, Lucilia Pinheiro, Virgilio E. do Rosario, Sodsri Thaithong, and K. Neil Brown. 1993. "High Sensitivity of Detection of Human Malaria Parasites by the Use of Nested Polymerase Chain Reaction." *Molecular and Biochemical Parasitology* 61 (2): 315–20. https://doi.org/10.1016/0166-6851(93)90077-B.

Sonden, Klara, Safiatou Doumbo, Ulf Hammar, Manijeh Vafa Homann, Aissata Ongoiba, Boubacar Traord, Matteo Bottai, Peter D. Crompton, and Anna Färnert. 2015. "Asymptomatic Multiclonal Plasmodium Falciparum Infections Carried Through the Dry Season Predict Protection Against Subsequent Clinical Malaria." *Journal of Infectious Diseases* 212 (4): 608–16. https://doi.org/10.1093/infdis/jiv088.

Spielmann, Tobias, Paula L. Hawthorne, Matthew W.A. Dixon, Mandy Hannemann, Kathleen Klotz, David J. Kemp, Nectarios Klonis, Leann Tilley, Katharine R. Trenholme, and Donald L. Gardiner. 2006. "A Cluster of Ring Stage–Specific Genes Linked to a Locus Implicated in Cytoadherence in Plasmodium Falciparum Codes for PEXEL-Negative and PEXEL-Positive Proteins Exported into the Host Cell." Edited by Ralph Isberg. *Molecular Biology of the Cell* 17 (8): 3613–24. https://doi.org/10.1091/mbc.e06-04-0291.

Spycher, Cornelia, Nectarios Klonis, Tobias Spielmann, Erwin Kump, Sylvia Steiger, Leann Tilley, and Hans Peter Beck. 2003. "MAHRP-1, a Novel Plasmodium Falciparum Histidine-Rich Protein, Binds Ferriprotoporphyrin IX and Localizes to the Maurer's Clefts." *Journal of Biological Chemistry* 278 (37): 35373–83. https://doi.org/10.1074/jbc.M305851200.

Spycher, Cornelia, Melanie Rug, Nectarios Klonis, David J. P. Ferguson, Alan F. Cowman, Hans-Peter Beck, and Leann Tilley. 2006. "Genesis of and Trafficking to the Maurer's Clefts of Plasmodium Falciparum-Infected Erythrocytes." *Molecular and Cellular Biology* 26 (11): 4074–85. https://doi.org/10.1128/MCB.00095-06.

Spycher, Cornelia, Melanie Rug, Esther Pachlatko, Eric Hanssen, David Ferguson, Alan F. Cowman, Leann Tilley, and Hans Peter Beck. 2008. "The Maurer's Cleft Protein MAHRP1 Is Essential for Trafficking of PfEMP1 to the Surface of Plasmodium Falciparum-Infected Erythrocytes." *Molecular Microbiology* 68 (5): 1300–1314. https://doi.org/10.1111/j.1365-2958.2008.06235.x.

Stone, Will, Bronner P. Gonçalves, Teun Bousema, and Chris Drakeley. 2015. "Assessing the Infectious Reservoir of Falciparum Malaria: Past and Future." *Trends in Parasitology* 31 (7): 287–96. https://doi.org/10.1016/j.pt.2015.04.004.

Sturm, Angelika, Rogerio Amino, Claudia Van De Sand, Tommy Regen, Silke Retzlaff, Annika Rennenberg, Andreas Krueger, Jörg Matthias Pollok, Robert Menard, and Volker T. Heussler. 2006. "Manipulation of Host Hepatocytes by the Malaria Parasite for Delivery into Liver Sinusoids." *Science* 313 (5791): 1287–90. https://doi.org/10.1126/science.1129720.

Su, Xin-zhuan, Virginia M. Heatwole, Samuel P. Wertheimer, Frangoise Guinet, Jacqueline A. Herrfeldt, David S. Peterson, Jeffrey A. Ravetch, and Thomas E. Wellems. 1995. "The Large Diverse Gene Family Var Encodes Proteins Involved in Cytoadherence and Antigenic Variation of Plasmodium Falciparum-Infected Erythrocytes." *Cell* 82 (1): 89–100. https://doi.org/10.1016/0092-8674(95)90055-1.

Subramani, Ramesh, Katharina Quadt, Anine E. Jeppesen, Casper Hempel, Jens Emil Vang Petersen, Tue Hassenkam, Lars Hviid, and Lea Barfod. 2015. "Plasmodium Falciparum-Infected Erythrocyte Knob Density Is Linked to the PfEMP1 Variant Expressed." Edited by Louis H. Miller. *MBio* 6 (5): 1–7. https://doi.org/10.1128/mBio.01456-15.

Subramani, Ramesh, Katharina Quadt, Anine E Jeppesen, Casper Hempel, Emil Vang, and Tue Hassenkam. 2015. "Plasmodium Falciparum - Infected Erythrocyte Knob Density Is Linked to the PfEMP1 Variant Expressed" 6 (5): 1–7. https://doi.org/10.1128/mBio.01456-15.Editor.

Swerlick, R A, K H Lee, L J Li, Norbert T Sepp, S Wright Caughman, and Thomas J Lawley. 1992. "Regulation of Vascular Cell Adhesion Molecule 1

on Human Dermal Microvascular Endothelial Cells." *Journal of Immunology (Baltimore, Md. : 1950)* 149 (2): 698–705. http://www.ncbi.nlm.nih.gov/pubmed/1378077.

Tavares, Joana, Pauline Formaglio, Sabine Thiberge, Elodie Mordelet, Nico Van Rooijen, Alexander Medvinsky, Robert Ménard, and Rogerio Amino. 2013. "Role of Host Cell Traversal by the Malaria Sporozoite during Liver Infection." *Journal of Experimental Medicine* 210 (5): 905–15. https://doi.org/10.1084/jem.20121130.

Taylor, Terrie E., Wenjiang J. Fu, Richard A. Carr, Richard O. Whitten, Jeffrey G. Mueller, Nedson G. Fosiko, Susan Lewallen, N. George Liomba, and Malcolm E. Molyneux. 2004. "Differentiating the Pathologies of Cerebral Malaria by Postmortem Parasite Counts." *Nature Medicine* 10 (2): 143–45. https://doi.org/10.1038/nm986.

Tchinda, Viviane H.M., Armand D. Tadem, Ernest A. Tako, Gilbert Tene, Josephine Fogako, Philomina Nyonglema, Grace Sama, Ainong Zhou, and Rose G.F. Leke. 2007. "Severe Malaria in Cameroonian Children: Correlation between Plasma Levels of Three Soluble Inducible Adhesion Molecules and TNF-α." *Acta Tropica* 102 (1): 20–28. https://doi.org/10.1016/j.actatropica.2007.02.011.

Tessema, Sofonias K, Rie Nakajima, Algis Jasinskas, Denise L Doolan, Ivo Mueller, Alyssa E Barry, Sofonias K Tessema, et al. 2019. "Clinical and Translational Report Protective Immunity against Severe Malaria in Children Is Associated with a Limited Repertoire of Antibodies to Conserved PfEMP1 Variants Clinical and Translational Report Protective Immunity against Severe Malaria in Chi." *Cell Host and Microbe* 26 (5): 579-590.e5. https://doi.org/10.1016/j.chom.2019.10.012.

Tibúrcio, Marta, Makhtar Niang, Guillaume Deplaine, Sylvie Perrot, Emmanuel Bischoff, Papa Alioune Ndour, Francesco Silvestrini, et al. 2012. "A Switch in Infected Erythrocyte Deformability at the Maturation and Blood Circulation of Plasmodium Falciparum Transmission Stages." *Blood* 119 (24): 172–80. https://doi.org/10.1182/blood-2012-03-414557.

Tiemi Shio, Marina, Stephanie C. Eisenbarth, Myriam Savaria, Adrien F. Vinet, Marie-Josée Bellemare, Kenneth W. Harder, Fayyaz S. Sutterwala, et al. 2009. "Malarial Hemozoin Activates the NLRP3 Inflammasome through Lyn and Syk Kinases." Edited by James W. Kazura. *PLoS Pathogens* 5 (8): e1000559. https://doi.org/10.1371/journal.ppat.1000559.

Tilley, Leann, Judith Straimer, Nina F. Gnädig, Stuart A. Ralph, and David A. Fidock. 2016. "Artemisinin Action and Resistance in Plasmodium Falciparum." *Trends in Parasitology* 32 (9): 682–96. https://doi.org/10.1016/j.pt.2016.05.010.

Tilly, Ann-Kathrin, Jenny Thiede, Nahla Metwally, Pedro Lubiana, Anna Bachmann, Thomas Roeder, Nichola Rockliffe, et al. 2015. "Type of in Vitro Cultivation Influences Cytoadhesion, Knob Structure, Protein Localization and Transcriptome Profile of Plasmodium Falciparum." *Scientific Reports* 5 (1): 16766. https://doi.org/10.1038/srep16766.

Trager, W, and J. Jensen. 1976. "Human Malaria Parasites in Continuous Culture." *Science* 193 (4254): 673–75. https://doi.org/10.1126/science.781840.

Trager, W, M A Rudzinska, and P C Bradbury. 1966. "The Fine Structure of Plasmodium Falciparum and Its Host Erythrocytes in Natural Malarial Infections in Man." *Bulletin of the World Health Organization* 35 (6): 883–85. https://doi.org/10.1159/000132731.

Tran, Tuan M., Shanping Li, Safiatou Doumbo, Didier Doumtabe, Chiung Yu Huang, Seydou Dia, Aboudramane Bathily, et al. 2013. "An Intensive Longitudinal Cohort Study of Malian Children and Adults Reveals No Evidence of Acquired Immunity to Plasmodium Falciparum Infection." *Clinical Infectious Diseases* 57 (1): 40–47. https://doi.org/10.1093/cid/cit174.

Travassos, Mark A., Amadou Niangaly, Jason A. Bailey, Amed Ouattara, Drissa Coulibaly, Kirsten E. Lyke, Matthew B. Laurens, et al. 2018. "Children with Cerebral Malaria or Severe Malarial Anaemia Lack Immunity to Distinct Variant Surface Antigen Subsets." *Scientific Reports* 8 (1): 1–14. https://doi.org/10.1038/s41598-018-24462-4.

Treutiger, Carl Johan, Andreas Heddini, Victor Fernandez, William A Muller, and Mats Wahlgren. 1997. "PECAM-1/CDS31, an Endothelial Receptor for Binding Plasmodium Falciparum-Infected Erythrocytes." *Nature Medicine* 3 (12): 1405–8. https://doi.org/10.1038/nm1297-1405.

Turner, Gareth D.H., Ly Van Chuong, Nguyen Thi Hoang Mai, Tran Thi Hong Chau, Nguyen Hoan Phu, Delia Bethell, Sarah Wyllie, et al. 1998. "Systemic Endothelial Activation Occurs in Both Mild and Severe Malaria: Correlating Dermal Microvascular Endothelial Cell Phenotype and Soluble Cell Adhesion Molecules with Disease Severity." *American Journal of Pathology* 152 (6): 1477–87.

Turner, Gareth D.H., Heather Morrison, Margaret Jones, Timothy M.E. Davis, Sornchai Looareesuwan, Ian D. Buley, Kevin C. Gatter, et al. 1994. "An Immunohistochemical Study of the Pathology of Fatal Malaria: Evidence for Widespread Endothelial Activation and a Potential Role for Intercellular Adhesion Molecule-1 in Cerebral Sequestration." *American Journal of Pathology* 145 (5): 1057–69.

Turner, Louise, Thomas Lavstsen, Sanne S Berger, Christian W Wang, Jens E. V. Petersen, Marion Avril, Andrew J Brazier, et al. 2013. "Severe Malaria Is Associated with Parasite Binding to Endothelial Protein C Receptor." *Nature* 498 (7455): 502–5. https://doi.org/10.1038/nature12216.

Turner, Louise, Thomas Lavstsen, Bruno P Mmbando, Christian W Wang, Pamela A Magistrado, Lasse S Vestergaard, Deus S Ishengoma, Daniel T R Minja, John P Lusingu, and G Theander. 2015. "IgG Antibodies to Endothelial Protein C Receptor-Binding Cysteine- Rich Interdomain Region Domains of Plasmodium Falciparum Erythrocyte Membrane Protein 1 Are Acquired Early in Life in Individuals Exposed to Malaria" 83 (8): 3096–3103. https://doi.org/10.1128/IAI.00.

Udomsangpetch, R, P H Reinhardt, T Schollaardt, J F Elliott, P Kubes, and M Ho. 1997. "Promiscuity of Clinical Plasmodium Falciparum Isolates for Multiple Adhesion Molecules under Flow Conditions." *Journal of Immunology (Baltimore, Md. : 1950)* 158 (9): 4358–64. http://www.ncbi.nlm.nih.gov/pubmed/9126999.

Venugopal, Kannan, Franziska Hentzschel, Gediminas Valkiūnas, and Matthias Marti. 2020. "Plasmodium Asexual Growth and Sexual Development in the Haematopoietic Niche of the Host." *Nature Reviews Microbiology* 18 (3): 177–89. https://doi.org/10.1038/s41579-019-0306-2.

Viebig, Nicola K, Ulrich Wulbrand, Reinhold Fo, Michael Lanzer, and Percy A Knolle. 2005. "Direct Activation of Human Endothelial Cells by Plasmodium Falciparum-Infected Erythrocytes." *Infection and Immunity* 73 (6): 3271–77. https://doi.org/10.1128/IAI.73.6.3271–3277.

Villaverde, Chandler, Ruth Namazzi, Estela Shabani, Gregory S. Park, Dibyadyuti Datta, Benjamin Hanisch, Robert O. Opoka, and Chandy C. John. 2020. "Retinopathy-Positive Cerebral Malaria Is Associated With Greater Inflammation, Blood-Brain Barrier Breakdown, and Neuronal Damage Than Retinopathy-Negative Cerebral Malaria." *Journal of the Pediatric Infectious Diseases Society* 9 (5): 580–86. https://doi.org/10.1093/jpids/piz082.

Wahlgren, Mats, Suchi Goel, and Reetesh R Akhouri. 2017. "Variant Surface Antigens of Plasmodium Falciparum and Their Roles in Severe Malaria." *Nature Publishing Group* 15 (8): 479–91. https://doi.org/10.1038/nrmicro.2017.47.

Waller, Karena L., Lisa M. Stubberfield, Valentina Dubljevic, Donna W. Buckingham, Narla Mohandas, Ross L. Coppel, and Brian M. Cooke. 2010. "Interaction of the Exported Malaria Protein Pf332 with the Red Blood Cell Membrane Skeleton." *Biochimica et Biophysica Acta - Biomembranes* 1798 (5): 861–71. https://doi.org/10.1016/j.bbamem.2010.01.018.

Wamae, Kevin, Juliana Wambua, George Nyangweso, Gabriel Mwambingu, Faith Osier, Francis Ndung'U, Philip Bejon, and Lynette Isabella Ochola-Oyier. 2019. "Transmission and Age Impact the Risk of Developing Febrile Malaria in Children with Asymptomatic Plasmodium Falciparum Parasitemia." *Journal of Infectious Diseases* 219 (6): 936–44. https://doi.org/10.1093/infdis/jiy591.

Warimwe, George M., Mario Recker, Esther W. Kiragu, Caroline O. Buckee, Juliana Wambua, Jennifer N. Musyoki, Kevin Marsh, and Peter C. Bull. 2013. "Plasmodium Falciparum Var Gene Expression Homogeneity as a Marker of the Host-Parasite Relationship under Different Levels of Naturally Acquired Immunity to Malaria." *PLoS ONE* 8 (7). https://doi.org/10.1371/journal.pone.0070467.

Warncke, Jan D, and Hans-peter Beck. 2019. "Host Cytoskeleton Remodeling throughout the Blood Stages of Plasmodium Falciparum." *Microbiology and Molecular Biology Reviews* 83 (4): 1–21. https://doi.org/10.1128/MMBR.00013-19.

Wassmer, Samuel C, Terrie E Taylor, Pradipsinh K Rathod, Saroj K Mishra, Sanjib Mohanty, Myriam Arevalo-herrera, Manoj T Duraisingh, and Joseph D Smith. 2015. "Investigating the Pathogenesis of Severe Malaria : A Multidisciplinary and Cross-Geographical Approach" 93 (Suppl 3): 42–56. https://doi.org/10.4269/ajtmh.14-0841.

Watermeyer, Jean M, Victoria L Hale, Fiona Hackett, Daniel K Clare, Erin E Cutts, Ioannis Vakonakis, Roland A Fleck, Michael J Blackman, and Helen R Saibil. 2016. "A Spiral Scaffold Underlies Cytoadherent Knobs in Plasmodium Falciparum–Infected Erythrocytes." *Blood* 127 (3): 343–51. https://doi.org/10.1182/blood-2015-10-674002.

White, Nicholas J, Gareth D H Turner, Nicholas P J Day, and Arjen M Dondorp. 2013. "Lethal Malaria : Marchiafava and Bignami Were Right" 208. https://doi.org/10.1093/infdis/jit116.

WHO. 2021. "Who Guidelines for Malaria," no. June: 2019.

Wichers, J. Stephan, Judith A. M. Scholz, Jan Strauss, Susanne Witt, Andrés Lill, Laura-Isabell Ehnold, Niklas Neupert, et al. 2019. "Dissecting the Gene Expression, Localization, Membrane Topology, and Function of the Plasmodium Falciparum STEVOR Protein Family." Edited by John C. Boothroyd. *MBio* 10 (4): 1–20. https://doi.org/10.1128/mBio.01500-19.

World Health Organization. 2020. "World Malaria Report 2020: 20 Years of Global Progress and Challenges."

Zhang, Meng, Pierre Faou, Alexander G. Maier, and Melanie Rug. 2018. "Plasmodium Falciparum Exported Protein PFE60 Influences Maurer's Clefts Architecture and Virulence Complex Composition." *International Journal for Parasitology* 48 (1): 83–95. https://doi.org/10.1016/j.ijpara.2017.09.003.

Zhang, Rou, Rajesh Chandramohanadas, Chwee Teck Lim, and Ming Dao. 2018. "Febrile Temperature Elevates the Expression of Phosphatidylserine on Plasmodium Falciparum (FCR3CSA) Infected Red Blood Cell Surface Leading to Increased Cytoadhesion." *Scientific Reports* 8 (1): 15022. https://doi.org/10.1038/s41598-018-33358-2.

Zhang, Yao, Changjin Huang, Sangtae Kim, Mahdi Golkaram, Matthew W.A. Dixon, Leann Tilley, Ju Li, Sulin Zhang, and Subra Suresh. 2015. "Multiple Stiffening Effects of Nanoscale Knobs on Human Red Blood Cells Infected with Plasmodium Falciparum Malaria Parasite." *Proceedings of the National Academy of Sciences of the United States of America* 112 (19): 6068–73. https://doi.org/10.1073/pnas.1505584112.
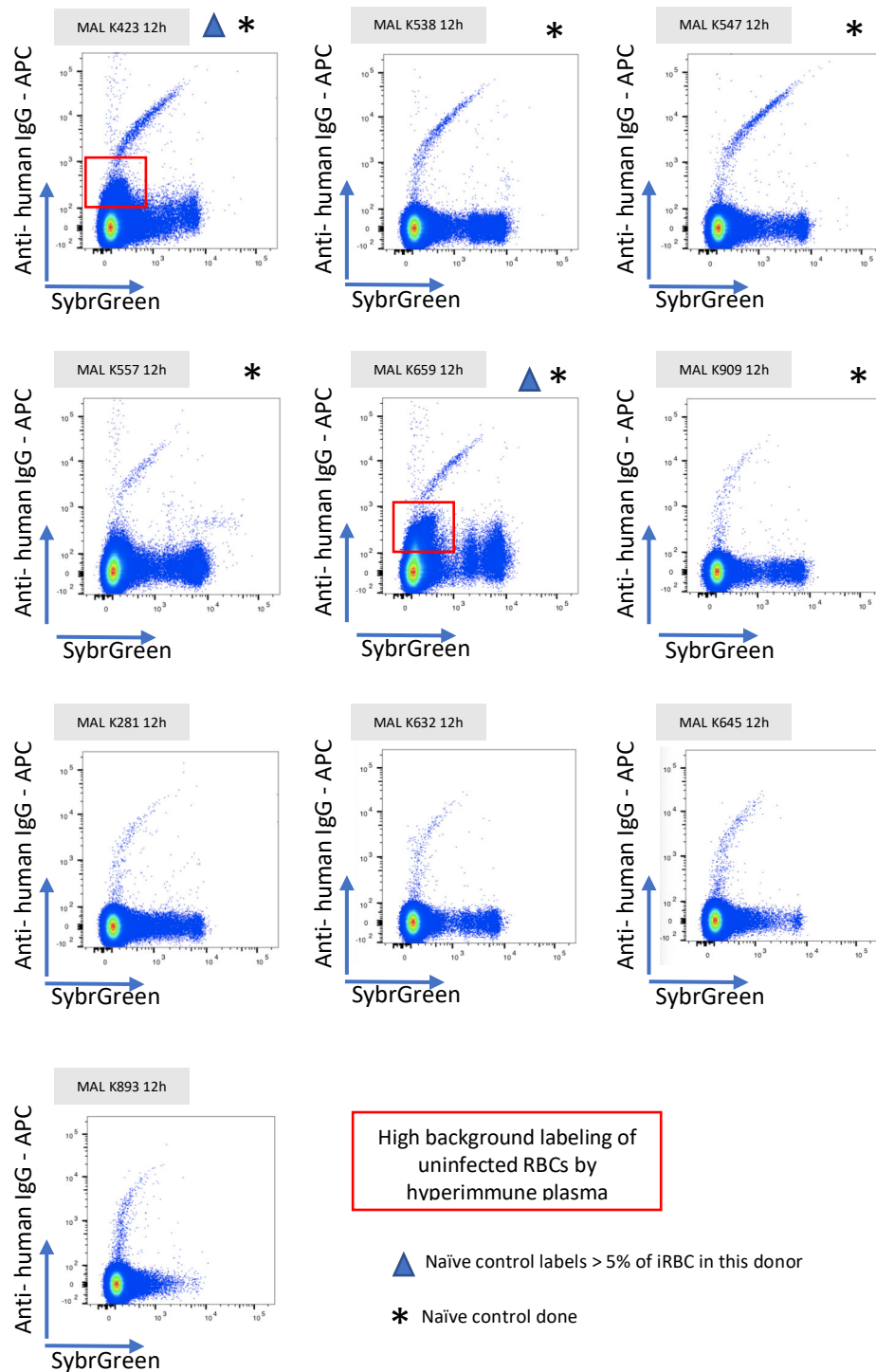
Supplementary data

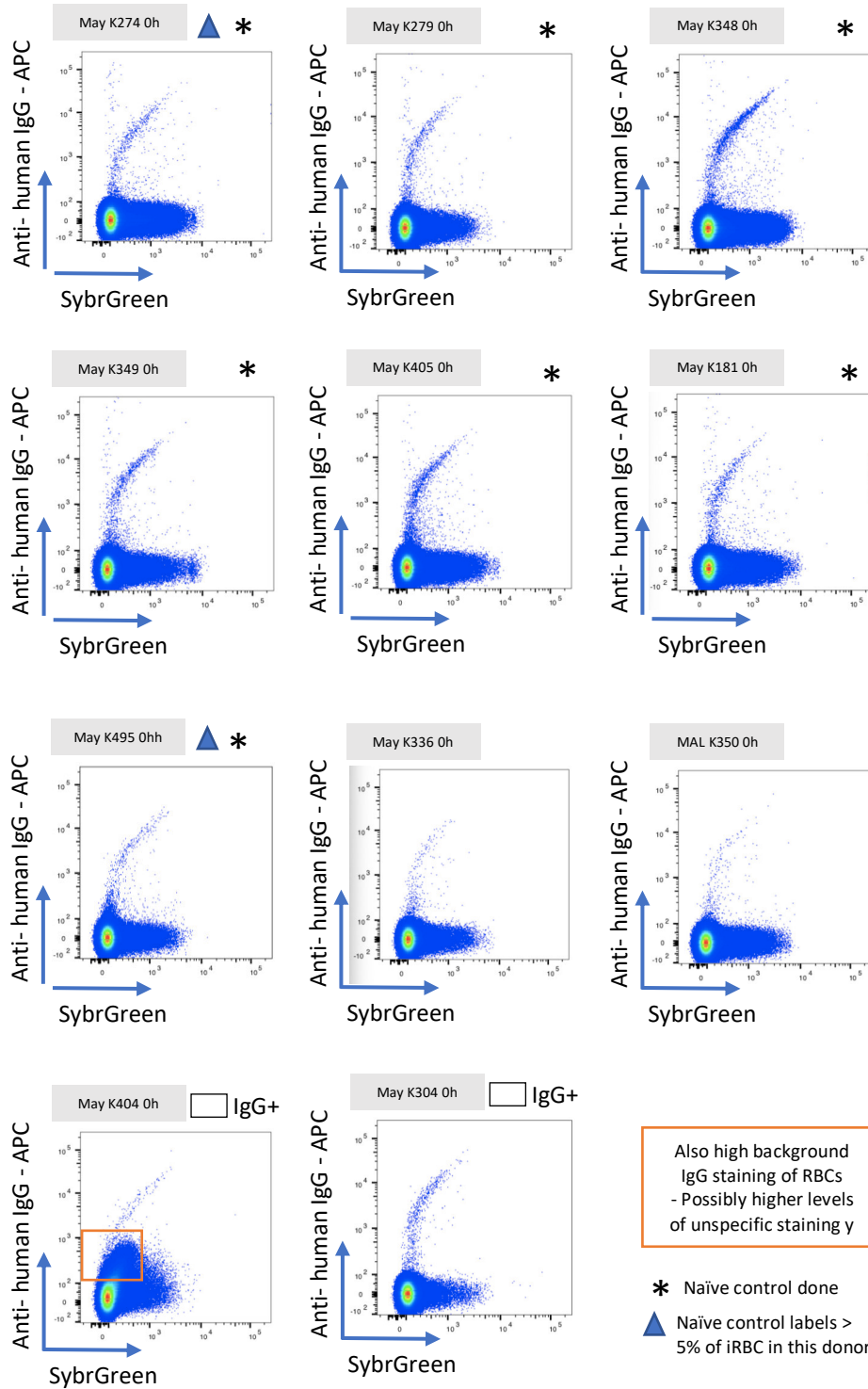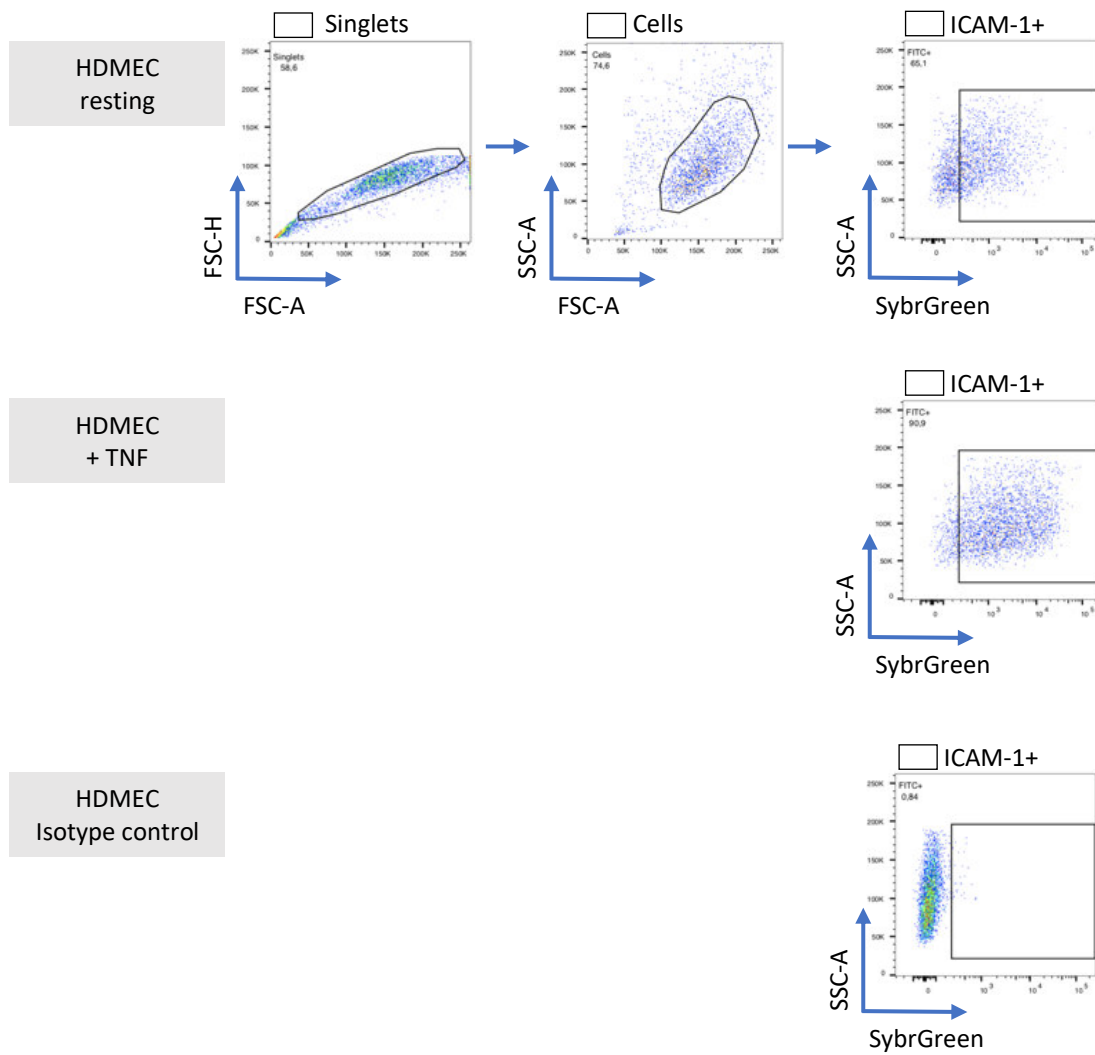*Supplemental figure 1: Gating strategies used in microsphiltration assays*
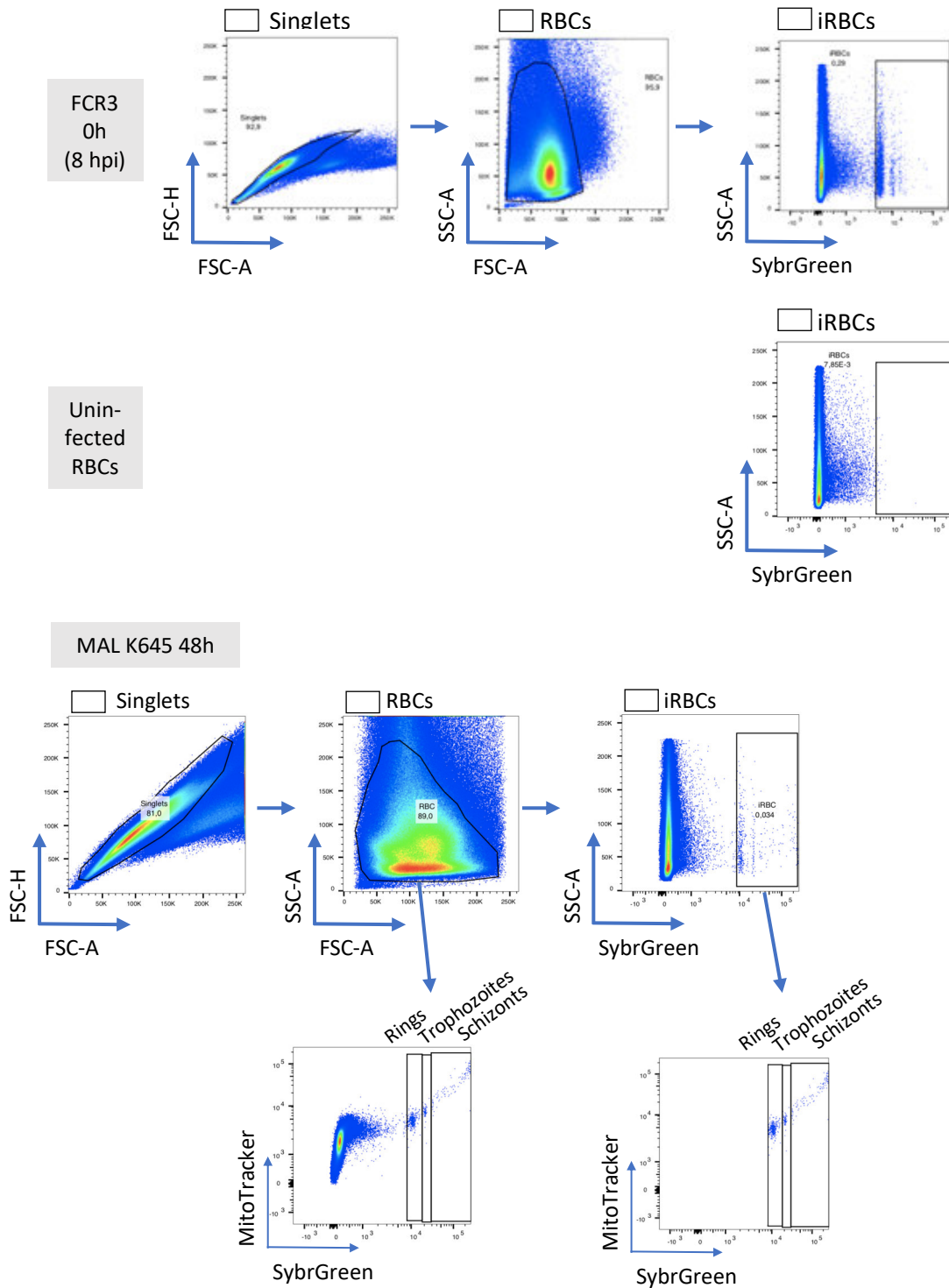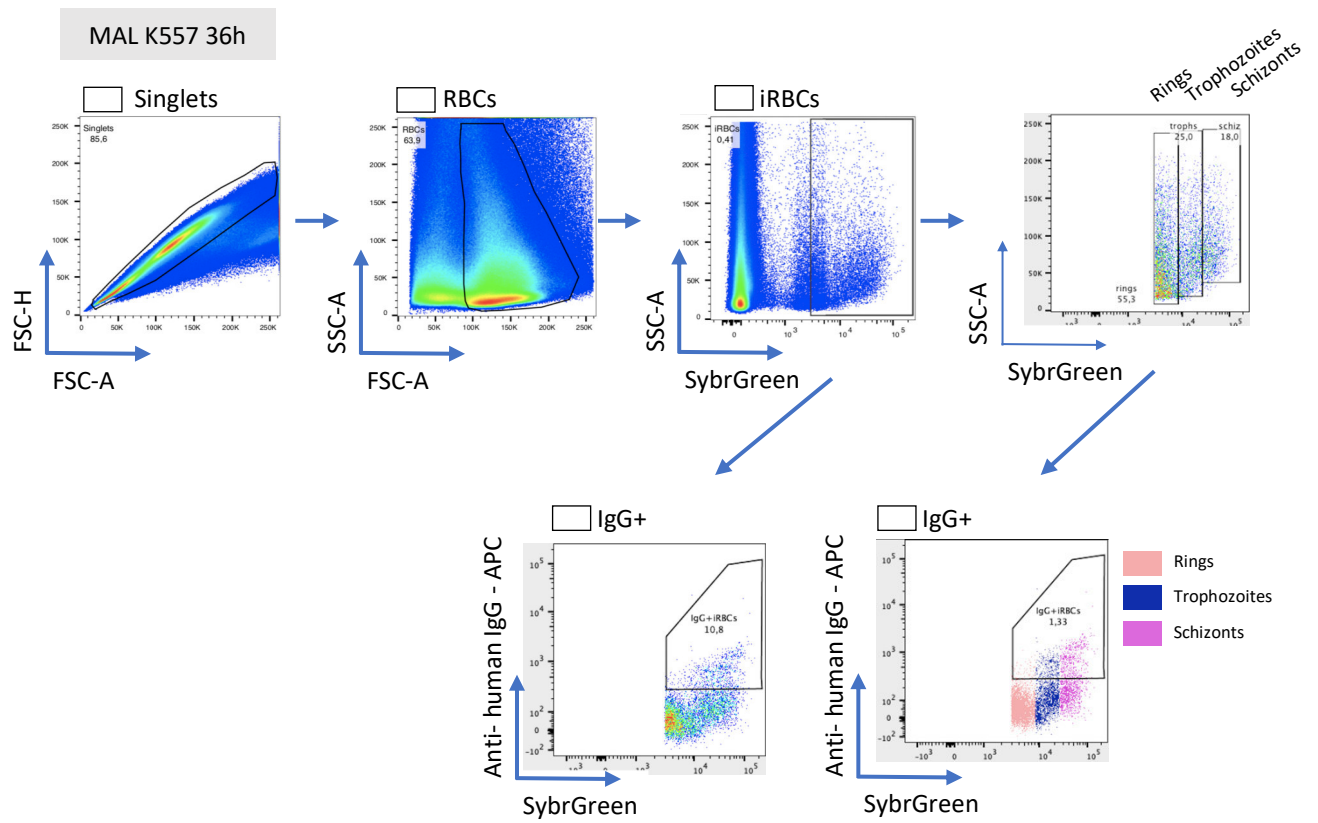
Supplemental figure 2: Gating strategy for surface antigen labeling by a hyperimmune plasma pool

Supplemental figure 3: Unspecific staining by hyperimmune plasma

Plots show RBC population of hyperimmune-plasma labeled blood pellets from donors with clinical malaria (MAL) and asymptomatic malaria. Presence of abnormal RBC population, shifted further up (high ant-igG secondary antibody labeling) indicated by boxes. ((continues on following page).

May K274 0h ▲ *

May K279 0h *

May K348 0h *

May K349 0h *

May K405 0h *

May K181 0h *

May K495 0hh ▲ *

May K336 0h

MAL K350 0h

May K404 0h ☐ IgG+

May K304 0h ☐ IgG+

Also high background
IgG staining of RBCs
- Possibly higher levels
of unspecific staining y

* Naïve control done

▲ Naïve control labels >
5% of iRBC in this donor

Supplemental figure 4: Gating strategy on HDMEC adhesion receptors

ICAM-1+ gate was placed relative to the isotype control staining. Analogous gating strategy was followed for the detection of VCAM-1 and E-Selectin-1

Supplemental table 1: Complete list donors for electron microscopy samples

Visit	Year	Donor ID	Age (years)	Gender	Ethnicity	Hemotype	Time in culture (h)	Parasitemia	Pellet size
May	2018	k0181	17	Male	Bambara	AA	18	5%	M
May	2018	k0209	17	Male	Bambara	AA	18	9%	XS
May	2018	k0269	16	Male	Bambara	AA	18	1%	L
May	2018	k0285	16	Male	Bambara	AA	18	4%	M
May	2018	k0350	15	Male	Bambara	AA	18	3%	S
May	2018	k0405	15	Female	Fulani	AA	18	31%	XS
May	2019	k0181	17	Male	Bambara	AA	12		M
May	2019	k0270	17	Male	Bambara	AA	12		M
May	2019	k0274	17	Female	Fulani	AA	12		M
May	2019	k0348	17	Female	Bambara	AA	12		S
May	2019	k0349	16	Male	Bambara	AA	12		M
May	2019	k0404	16	Male	Bambara	AA	12		M
May	2019	k0405	16	Female	Fulani	AA	12		S
MAL	2018	k0312	16	Female	Bambara	AA	27		L
MAL	2018	k0322	16	Male	Bambara	AA	28		L
MAL	2018	k0421	15	Male	Bambara	AA	26		S
MAL	2018	k0554	11	Male	Bambara	AA	30		L
MAL	2019	k0538	13	Female	Bambara	AA	30	91%	M
MAL	2019	k0538	13	Female	Bambara	AA	42	59%	L
MAL	2019	k0557	12	Female	Bambara	AA	40	5%	L
MAL	2019	k0623	10	Male	Bambara	AA	30	68%	M
MAL	2019	k0670	18	Female	Bambara	AA	42	76%	L
MAL	2019	k0902	5	Male	Fulani	AA	30	91%	L

Supplemental table 2: Complete list of donors for qRT-PCR samples

Visit	Year	Donor ID	Age (years)	Gender	Ethnicity	Hemotype	Data of all timepoints
May	2018	k0209	17	Male	Bambara	AA	yes
May	2018	k0269	16	Male	Bambara	AA	no
May	2018	k0285	16	Male	Bambara	AA	yes
May	2018	k0328	16	Male	Bambara	AA	no
May	2018	k0336	16	Male	Bambara	AA	yes
May	2018	k0348	16	Female	Bambara	AA	no
May	2018	k0352	16	Female	Bambara	AA	no
May	2018	k0373	15	Male	Bambara	AA	yes
May	2018	k0419	15	Male	Fulani	AA	yes
May	2018	k0435	15	Male	Bambara	AA	yes
May	2018	k0452	15	Male	Bambara	AA	yes
May	2018	k0544	13	Male	Bambara	AA	yes
May	2018	k0632	9	Male	Bambara	AA	no
May	2018	k0708	19	Male	Bambara	AA	yes
May	2018	k0724	24	Male	Bambara	AA	yes
MAL	2018	k0265	16	Male	Bambara	AA	yes
MAL	2018	k0286	16	Male	Bambara	AS	no
MAL	2018	k0322	16	Male	Bambara	AA	yes
MAL	2018	k0391	15	Male	Bambara	AA	yes
MAL	2018	k0394	15	Female	Bambara	AA	no
MAL	2018	k0421	15	Male	Bambara	AA	yes
MAL	2018	k0463	14	Female	Bambara	AA	no
MAL	2018	k0495	13	Female	Bambara	AA	yes
MAL	2018	k0535	12	Male	Bambara	AA	no
MAL	2019	k0538	13	Female	Bambara	AA	yes
MAL	2018	k0554	11	Male	Bambara	AA	yes
MAL	2019	k0623	10	Male	Bambara	AA	yes
MAL	2019	k0670	18	Female	Bambara	AA	yes

Macros

CountAdhesion

```
//batch measurements - set type of measurements
setBatchMode("show")
run("Maximize");
setTool("multipoint");
run("Grid...", "grid=Lines area=60 color=Yellow center");

//let user do measurements manually+ overlay measurements
waitForUser( "Measurements","Measure the structures.\nPress OK when you are done");
```

EMimages_scoring

```
#@ File (label = "Input directory", style = "directory") input
#@ File (label = "Output directory", style = "directory") output
#@ String (label = "File suffix", value = ".tif") suffix


num = 0;
// start processing images in folder... assumes no subfolders, only images
processFolder(input);

// function to scan folders/subfolders/files to find files with correct suffix
function processFolder(input) {
        list = getFileList(input);
        list = Array.sort(list);
        for (i = 0; i < list.length; i++) {
                if(endsWith(list[i], suffix)) {
                        processFile(input, output, list[i], num);
                        num++; //increment num
                }
        }
        // save results table with scores...
        saveAs("Results", output + "/Image_Scores.csv");
}

function processFile(input, output, file, num) {
        // open image using Bio-Formats
        run("Bio-Formats", "open=[" + input + "/" + file +"] autoscale color_mode=Default rois_import=[ROI manager]
view=Hyperstack stack_order=XYCZT");
        title = getTitle(); // get image title
        setResult("Image", num, title);

        // ask user for String input on grading... and set the score in the Results Table
        run("Maximize");
        waitForUser( "zoom","Adjust zoom");
        nuclei = getString("How many nuclei are there: ", "0");
        setResult("Nuclei", num, nuclei);
        segmenter = getString("Is the parasite segmented? y or n", "n");
        setResult("Segmenter", num, segmenter);
        rhoptries = getString("Are there rhoptries: y or n", "n");
        setResult("Rhoptries", num, rhoptries);
```

```
                // close image
                selectWindow(title);
                close();
}
```

MeasureAreas

Use Batch_MeasureAreas:

```
        setBatchMode("show")

        //get starting setting
        setTool("freehand");
        run("Maximize");

        //let user do measurements manually+ overlay measurements
        waitForUser( "Measurements","Measure the structures.\nPress OK when you are done");
```

KnobDensity

```
#@ File (label = "Input directory", style = "directory") input
#@ File (label = "Output directory", style = "directory") output
#@ String (label = "File suffix", value = ".tif") suffix


num = 0;
// start processing images in folder... assumes no subfolders, only images
processFolder(input);

// function to scan folders/subfolders/files to find files with correct suffix
function processFolder(input) {
        list = getFileList(input);
        list = Array.sort(list);
        for (i = 0; i < list.length; i++) {
                if(endsWith(list[i], suffix)) {
                        processFile(input, output, list[i], num);
                        num++; //increment num
                }
        }
        // save results table with scores...
        saveAs("Results", output + "/knob_density.csv");
}

function processFile(input, output, file, num) {
        // open image using Bio-Formats
        run("Bio-Formats", "open=[" + input + "/" + file +"] autoscale color_mode=Default rois_import=[ROI manager]
view=Hyperstack stack_order=XYCZT");
        title = getTitle(); // get image title
        //setResult("Image", num, title);

        // Scale Bar
        makeLine(63, 2151, 332, 2151);
        run("To Selection");
        waitForUser("Adjust scale","Adjust length of line. \n Then measure and set scale \nPress OK when you are done");
        getLine(x1, y1, x2, y2, lineWidth);
```

```
        lengthsb = (x2-x1);
        run("Set Scale...", "distance=lengthsb known=1 pixel=1 unit=µm");

        //measure area
        run("Original Scale");
        setTool("freehand");
        waitForUser( "Draw area of interest","Circle the area you want to measure \nPress OK when you are done");
        run("Measure");
        area = getResult("Area", num);
        setResult("Area", num, area);
        run("Add Selection...");

        //Measure knobs
        setTool("multipoint");
        waitForUser( "Knob counting","Click on the knobs \nPress OK when you are done");
        run("Add Selection...");
        knobs = getString("How many knobs are there: ", "0");
        setResult("Knobs", num, knobs);

        //save overlayed image
        name=getTitle;
        name=replace(name, ".tif","_kd");
        path=output+"/"+name;
        saveAs("tif", path);
        title = name+".tif";

        // close image
        selectWindow(title);
        close();
}
```

CropImages

```
//get starting setting
makeRectangle(1107, 1590, 450, 450); #enter custom rectangle size

//let user do measurements manually+ overlay measurements
waitForUser( "Measurements","Place over parasite.\nPress OK when you are done");
run("Crop");

//save overlayed image
name=getTitle
dir=getDirectory("image");
name= replace(name, ".jpg","");
name=name+"_cropped";
path=dir+name;
saveAs("Jpeg", path);
close();
```

Abbreviations

AFM Atomic force microscopy

ATS Acidic terminal segment

BSA Bovine serum albumin

CD Cluster of differentiation

cDNA Complementary DNA

CI Confidence interval

CIDR Cysteine-rich interdomain region

CO2 Carbon dioxide

DBL Duffy-binding like

ddH2O Double distilled water

DNase Deoxyribonuclease

dNTP Deoxyribonucleoside triphosphate

EPCR Endothelial protein C receptor

GA Glutaraldehyde

gDNA Genomic DNA

Hb Hemoglobin

HBSS Hank's Balanced Salt Solution

HDMEC Human dermal microvascular endothelial cells

HEPES 2-[4-(2-hydroxyethyl)piperazin-1-yl] ethanesulfonic acid

hpi Hours post invasion

HUVEC Human umbilical vein endothelial cells

ICAM Intercellular adhesion molecule

IFN Interferon

Ig Immunoglobulin

IL Interleukin

iRBC Infected red blood cell

IQR interquartile range

KO Knock out

MACS Magnetic activated cell sorter

mRNA Messenger RNA

MC Maurer's cleft

NF-κB Nuclear factor kappa B

P. Plasmodium

PBS Phosphate buffered saline

PCR Polymerase chain reaction

PECAM-1 Platelet endothelial cell adhesion molecule 1

PEXEL Protein Export Elements

PFA Paraformaldehyde

PfEMP Plasmodium falciparum erythrocyte membrane protein

pH Power of hydrogen
PNEP Pexel negative exported protein
PV Parasitophorous vacuole
PVM Parasitophorous vacuolar membrane
RBC Red blood cell
RNA Ribonucleic acid
rpm Revolutions per minute
RPMI Roswell Park Memorial Institute
RT Room temperature
SD Standard deviation
SEM Scanning electron microscopy
TEM Transmission electron microscopy
TNF Tumor necrosis factor
uRBC Uninfected red blood cell
v/v Volume-volume
VCAM-1 Vascular cell adhesion molecule 1
w/v Weight-volume

List of figures

List of tables

Acknowledgements

First and foremost, I thank Silvia for this exciting project. I appreciate your guidance, support and encouragement and am grateful for all I have learned from you over the past years, and it will have a great impact on my future scientific career. I'm also thankful for travelling to Mali together, I enjoyed it very much.

I like to thank Prof. Michael Lanzer for the opportunity to work in his department, his input in the TAC meetings and for allowing me to use the lab facilities longer to finish the experiments in Heidelberg.

I am also grateful to Prof. Dr. Jude Przyborski and Dr. Petr Chlanda for valuable input during my TAC meetings, and Prof. Dr. Nina Papavasiliou and Dr. Petr Chlanda for participating in my defense committee.

A big big thank goes you to all the people that formed part of the lab: Silvia, Carrie, Carolina, Richard, Nathalia, Sukai, Usama, Nick, Lasse and the students that joined us, for a friendly, fun and stimulating environment in Heidelberg, input on the project and support in the lab, as well as fun lab outings and all the gatherings with tasty food. It has been a pleasure to work with you. A special thanks also to Carolina for the great teamwork in Mali and for sharing this journey together. I'm also grateful to all the lab members in Berlin, especially Tina for her support with experiments and organization, and virtual encouragements.

Thank you to our Hiwi and rotation student Nick, for his great support with EM sample acquisition and analysis, an eye for the details and enthusiasm to do great work.

I want to thank all the members in the department, for discussions and suggestions during the department seminar, beer hours and Christmas parties. Also especially to the Osier lab for sharing lab space, equipment and lunchtimes in the kitchen. I'm also particularly grateful to Marianne, Severina, Marta, Ardin, Carolina and all the other members of the PhD committee and department representatives, for putting in the work and motivation to support each other.

Especially, I am grateful to Prof. Boubacar Traore and Dr. Peter Crompton for the opportunity to do work in Bamako, Aissata and Kassoum for taking us to visit Kalifabougou, and for the lab team in Bamako, Didier, Leon, Sacko, Hamidou and Doumbia for welcoming me to the lab, support with the experiments and the fun times in Bamako. I also thank the security guards for their continued efforts to teach me Bambara.

My gratitude also goes to the study participants and their families.

I am grateful to Prof. Catherine Lavazec and her team, especially Marie-Esther, for hosting me in Paris and teaching the ins and outs of microsphiltration.